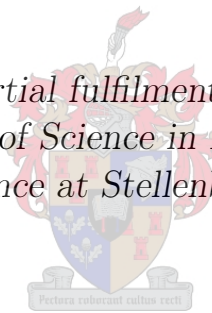


Whole body modelling of glucose metabolism in malaria patients

by

Kathleen Green

*Thesis presented in partial fulfilment of the requirements for
the degree of Master of Science in Biomathematics in the
Faculty of Science at Stellenbosch University*



Department of Mathematical Sciences
University of Stellenbosch,
Private Bag X1, Matieland 7602, South Africa.

Supervisor: Prof. J. L. Snoep
Dr. D. van Niekerk

March 2017

Declaration

By submitting this thesis electronically, I declare that the entirety of the work contained therein is my own, original work, that I am the sole author thereof (save to the extent explicitly otherwise stated), that reproduction and publication thereof by Stellenbosch University will not infringe any third party rights and that I have not previously in its entirety or in part submitted it for obtaining any qualification.

Signature: K. A. Green

Date:March 2017.

Abstract

Whole body modelling of glucose metabolism in malaria patients

K. A. Green

*Department of Mathematical Sciences
University of Stellenbosch,
Private Bag X1, Matieland 7602, South Africa.*

Thesis: MSc BSc (Math Sc)(Bio-math)

March 2017

Diagnosing a patient with a disease is typically done by considering a list of clinical symptoms. For severe malaria two of the key pathophysiological indicators for poor chances of survival are hypoglycemia (blood glucose < 2.2 mmol/L) and lactic acidosis (blood lactate > 5 mmol/L). These could be due to accelerated glycolytic flux (conversion of glucose to lactate) in parasite infected red blood cells, anaemia brought about by the parasites destroying the red blood cells, or reduced perfusion resulting from coagulation of red blood cells (parasites change the red blood cell shape) in the bloodstream. To date, no mathematical models exist that can quantify the relative contribution of increased glycolytic flux to hypoglycemia and lactic acidosis. In this study we constructed a physiologically relevant model of human glucose metabolism that contains the molecular mechanisms of erythrocyte and *Plasmodium* glycolysis. This allows for the investigation of the extent to which hypoglycaemia and lactic acidosis can be explained by the increased metabolic burden of the parasite. This was accomplished by combining three independent models of glucose metabolism in the parasite, red blood cell and the whole body to form a model of glucose metabolism at the level of the whole body that now contained mechanistic detail of reactions at the level of the red blood cell and malaria parasite (the green1 model). Predictions from the green1 model were compared to clinical data which showed that the increased glycolytic flux caused by the presence of the parasites could be sufficient to explain clinical symptoms of hypoglycemia and lactic acidosis seen in malaria patients. It was seen that for the strength of this modelling technique to be tested, better quality data are needed to validate the model

ABSTRACT

predictions. Furthermore with local and global sensitivity analysis it was observed that there are reactions and parameters in the *Plasmodium* glycolysis pathway that could guide the development of possible drug targets that could lead to a reversal of hypoglycemia and lactic acidosis.

Uittreksel

Whole body modelling of glucose metabolism in malaria patients

K. A. Green

*Department of Mathematical Sciences
University of Stellenbosch,
Private Bag X1, Matieland 7602, South Africa.*

Tesis: MSc BSc (Math Sc)(Bio-math)

Maart 2017

Diagnose van 'n pasiënt met 'n siekte word tipies gedoen deur die oorweging van 'n lys kliniese simptome. Vir ernstige malaria is twee van die belangrikste patofisiologiese aanwysers vir swak kanse op oorlewing hipoglukemie (bloedglukose < 2.2 mmol/L) en laktaatversuring (bloed laktaat > 5 mmol/L). Dit kan wees as gevolg van versnelde glikolitiese fluksie (omskakeling van glukose na laktaat) in parasietgeïnfekteerde rooibloedselle, bloedarmoede teweeg gebring word deur die vernietiging van rooibloedselle deur parasiete, verminderde perfusie as gevolg van koagulasie van rooibloedselle (parasiete verander die rooibloedselle se vorm) in die bloedstroom. Tot op datum, bestaan geen wiskundige modelle wat die relatiewe bydrae van verhoogde glikolitiese vloed te hipoglukemie en laktaatversuring kan kwantifiseer. In hierdie studie het ons 'n fisiologies relevante model van menslike glukose metabolisme gebou wat die molekulêre meganismes van direritrosiet en *Plasmodium* glikolise bevat. Dit maak voorsiening vir die ondersoek na die mate waarin hipoglukemie en laktaatversuring verduidelik kan word deur die verhoogde glikolitiese las van die parasiet. Dit is bewerkstellig deur die kombinerings van drie onafhanklike modelle van glukose metabolisme in die parasiet, rooibloedselle en die hele liggaam om 'n model van glukose metabolisme te vorm op die vlak van die hele liggaam wat nou meganistiese besonderhede van reaksies vervat op die vlak van die rooibloedsel en malariaparasiet (die green1 model). Voorspellings van die green1 model is vergelyk met kliniese data wat toon dat die verhoogde glikolitiese fluksie wat veroorsaak word deur die teenwoordigheid van die parasiete voldoende is om kliniese simptome van hipoglukemie en laktaatversuring gesien in malaria pasiënte te verduidelik. Dit

is gesien dat vir die krag van hierdie modelle tegniek om getoets te word, 'n beter gehalte data benodig word om die model voorspellings te versterk. Verder met plaaslike en globale sensitiviteitsanalise is dit opgemerk dat daar reaksies en parameters in die *Plasmodium* glikolitiese pad is wat lig kan werp op die ontwikkeling van moontlike dwelm-teikens en sodoende kan lei tot 'n ommekeer van hipoglukemie en laktaatversuring.

Acknowledgements

I would like to express my sincere gratitude to Prof. Jacky Snoep and Dr. Dawie van Niekerk for their time and encouragement.

I am thankful to the South African Research Chairs Initiative (SARChI) and Thuthuka program for funding this project.

A special thanks to Francois Du Toit for the diagrams and the Molecular Systems Biology research group.

Dedications

Thank you to my family and friends for their love and support.

Let all that you do be done in love

1 Corinthians 16:14

Contents

Declaration	i
Abstract	ii
Uittreksel	iv
Acknowledgements	vi
Dedications	vii
Contents	viii
List of Figures	x
List of Tables	xi
Nomenclature	xii
1 General Introduction	1
2 Literature Review	5
2.1 The biology of whole body glucose metabolism in humans	5
2.2 A mechanism based whole body model	8
2.3 Mechanism based models for pharmacology	9
2.4 Multi-scale and multi-level approaches to modelling	10
2.5 Bottom-up approaches using mechanistic models	11
2.6 Existing mathematical models	11
2.7 Sensitivity analysis	15
3 Model construction and initial validation	17
3.1 Original models and validation of model description	19
3.2 Building the parasitized RBC culture model	31
3.3 Model adaptations, scaling up and linking the models to represent the whole body level	39
4 Model Simulations and Sensitivity Analysis	48
4.1 Initial validation and steady state solutions	48
4.2 Sensitivity, Robustness and Control Analysis	55

5 Discussion and Conclusion	64
5.1 Summary	64
5.2 Shortcomings	67
5.3 Conclusion	68
Appendices	69
A Model description for the green1 model	70
A.1 Naming conventions	70
A.2 Initial Values:	71
A.3 Parameter Values:	75
A.4 Kinetic rates or reaction processes:	88
A.5 Assignment rules:	121
A.6 Ordinary differential equations:	126
B Publication	131
Bibliography	139

List of Figures

2.1	Scheme showing the hierarchical multi-level model for malaria patients.	9
3.1	Flow diagram of Chapter 3	19
3.2	Overview of the <i>Plasmodium falciparum</i> glycolysis model [1].	20
3.3	Validation of the Penkler model.	23
3.4	Schema of the red blood cell model [9–11].	25
3.5	Liver compartment of the Xu model.	26
3.6	Adipose tissue compartment of the Xu model.	27
3.7	Muscle compartment of the Xu model.	28
3.8	The glucose influx rate of the Xu model.	29
3.9	Validation of the coded Xu model.	29
3.10	Reaction scheme for the Potts & Kuchel [60] glucose transporter.	32
3.11	Schema from Du Toit [2] showing the combined <i>Plasmodium falciparum</i> and red blood cell model.	35
3.12	Scheme showing the different volume compartments in the parasitized red blood cell culture model.	36
3.13	Scheme of a moiety cycle.	38
3.14	Scheme of the green1 model which consists of the whole body model [3] combined with the compartment for the red blood cells (namely the parasitized RBC culture model).	40
4.1	Model simulation of the steady state blood glucose concentration with increasing parasitaemia (solid line).	53
4.2	Model simulation of the steady state blood lactate concentration with increasing parasitaemia (solid line).	54
4.3	Effect of a parasite glycolytic inhibitor on whole body glucose and lactate concentrations.	55
4.4	Distribution of blood glucose steady states arising from parameter uncertainty.	62
4.5	Distribution of blood lactate steady states arising from parameter uncertainty.	63

List of Tables

3.1	Validation of the Penkler model.	22
3.2	Validation of the Mulquiney & Kuchel model.	24
3.3	Initial units for components of each model.	42
3.4	Final units for components of each model.	44
4.1	Initial validation of the addition of the red blood cell compartment to the whole body model.	50
4.2	Verification of conservation of mass during the combining of the Xu and parasitized red blood cell culture model.	51
4.3	Steady state results from the green1 model.	52
4.4	Control coefficients from the green1 model.	57
4.5	Response coefficients from the green1 model.	60

Nomenclature

Abbreviations

WB	Whole-body model
RBC	Red Blood Cell
RBCs	Red Blood Cells
MCA	Metabolic Control Analysis
SB	Systems Biology
ODE	Ordinary Differential Equation
ODEs	Ordinary Differential Equations
ADME	Absorption Distribution Metabolism Excretion
PK	Pharmacokinetics
PD	Pharmacodynamics
PF	<i>Plasmodium falciparum</i> model
ATP	Adenosine triphosphate
PPP	Pentose Phosphate Pathway
NPPs	New Permeability Pathways
HCT	Hematocrit
SBML	Systems Biology Markup Language
pRBC	Parasitized Red Blood Cell
ProMoT	Process Modeling Tool

PCI Potential Coupling Interface

Model names

penkler1 Penkler [1] model

penkler2 Steady state Penkler [1] model

dutoit1 Parasitized RBC model (Du Toit [2])

dutoit2 Steady state parasitized RBC model (Du Toit [2])

dutoit3 Parasitized RBC culture model (extended Du Toit [2])

xu Whole body glucose metabolism model (Xu et al. [3])

green1 Merged dutoit3 and xu model

Units

M molar concentration

mM millimolar concentration

L litre

fmol femtomole amount

mmol millimole amount

μ micro

min minute

s second

Chapter 1

General Introduction

Malaria is a mosquito-borne infectious disease that has created major public health concerns particularly in the developing world. While accurate estimates on the precise number of deaths caused by this disease are unreliable [4], we do know it affects many children in sub-Saharan Africa with at least 236 000 deaths in 2015 [5]. In May 2015 the World Health Assembly accepted the Global Technical Strategy for Malaria 2016-2030 which shares goals with the Roll Back Malaria Partnership. This strategy outlines goals and targets for the next few years that are required for reducing and ultimately eliminating malaria incidence. It is outlined that a challenge would be the use of effective antimalarials and innovation to develop vaccines. Currently artemisinin is the most commonly recommended prophylaxis but it is only administered in combinations with other compounds due to the fear of parasite resistance (as was seen with a previously frequently used anti-malarial chloroquine) [6]. Adverse effects of artemisinin include nausea, vomiting, anorexia, and dizziness [7]. Parasite resistance to antimalarials has created a demand for a continued effort to identify new possible drug targets that could lead to more effective treatment (with fewer side-effects).

The malaria parasite has a multi-stage life cycle using both human and mosquito hosts. During the bite from an infected female *Anopheles* mosquito the parasite (in sporozoite form) is transmitted into the bloodstream of the human host. These sporozoites then move to the liver where they infect hepatocytes and begin to divide asexually into merozoites. These merozoites can invade more hepatocytes or can move into the bloodstream where they invade red blood cells, causing the clinical symptoms observed in malaria patients. Merozoites that invade red blood cells then grow into immature trophozoites (ring phase) that can either develop into mature trophozoites or gametocytes. Mature trophozoites divide asexually to form a schizont (multinucleated) which divides further into mononucleated merozoites. This results in the rupturing of the red blood cell and release of merozoites that are free to invade other red blood cells. This releasing of merozoites is the cause for the fevers associated with malaria. If the immature trophozoites form gametocytes, they are taken up from in the blood stream through a blood meal by the *Anopheles* mosquito and move to its gut. Next, the gametocytes fuse and after a number of intermittent phases form sporozoites. These sporozoites move to the salivary glands

of the mosquito and are injected into the human bloodstream during a bite. The life cycle then repeats.

There are five *Plasmodium spp.* that cause malaria in humans but for this work only *Plasmodium falciparum*, the most lethal (responsible for most malaria deaths [8]) of the *Plasmodium* species, is considered (in the trophozoite phase). *Plasmodium falciparum* does not have carbohydrate reserves and relies solely on the human host for glucose. Once it has invaded the erythrocyte it transports glucose across its membrane which undergoes a multiple-step catabolism in a glycolytic pathway that closely resembles that of the human erythrocyte. A by-product of this metabolic pathway is lactate which is transported out of the parasite cell into the red blood cell (RBC). Thereafter the lactate is transported from the red blood cell into the blood stream.

Severe malaria is often accompanied by hypoglycemia (low blood glucose concentrations) and lactic acidosis (high blood lactate concentrations). A number of different factors can contribute to these clinical symptoms: accelerated glycolytic flux (conversion of glucose to lactate) in parasite infected red blood cells, anaemia, or reduced perfusion (blood flow). The anaemia could be caused by the parasites destroying the red blood cells. Infection by *Plasmodium falciparum* causes a change in red blood cell shape that results in the coagulation of RBCs from the bloodstream which reduces perfusion. This leads to less oxygen being transported in the bloodstream to tissues. This creates an anaerobic environment which results in an increase in the production of lactate (rather than oxidative metabolism) by the body itself, amplifying the problem of high blood lactate. Although hypoglycemia and lactic acidosis are clinically diagnosed at the whole body level, they occur due to molecular mechanistic effects of the malaria parasite's interaction with the host.

So too will any effect that a drug has on the disease, clinically manifest at the level of the whole body, but be a result of a molecular effect of the drug. A quantitative understanding of malaria symptoms as they emerge from the complex network of enzyme catalyzed reactions of the parasite and human host could therefore not only facilitate a deeper understanding of the pathophysiology of the malaria disease state but also assist in the identification of possible drug targets. Such a quantitative understanding could be obtained by linking a model that describes the relevant features at the whole body level, to a model that contains the molecular mechanisms of the relevant cells and parasites in the body.

One of the objectives of this project is to link an existing model that describes whole body glucose metabolism in humans with a detailed kinetic model for *Plasmodium* glycolysis and human erythrocyte glycolysis into a multi-level hierarchical framework. This will allow us to test to what extent accelerated glycolytic flux in red blood cells contributes to hypoglycemia and lactic acidosis by considering different levels of parasitemia. Model analyses can further lead to the identification of drug targets and the mechanistic explanation of the effects of pharmaceutical intervention at the whole body level.

The research question is:

Can we merge three existing kinetic models for glucose metabolism in *Plasmodium falciparum*, red blood cell, and whole body *Homo sapiens* and use the resulting model to estimate the contribution of *Plasmodium falciparum* to hypoglycemia and lactic acidosis in malaria patients?

Aims:

1. Construct a multi-level model of human glucose metabolism that contains the molecular mechanisms of erythrocyte and *Plasmodium* glycolysis.
2. Simulate to what extent an increased parasitemia leads to an increased utilisation of glucose and production of lactate, taking into account the homeostatic mechanisms for glucose and lactate at the whole body level.

Objectives:

- Identify existing mathematical models that sufficiently describe the compartments that will be needed
- Combine and make necessary adjustments to existing mathematical models to create a framework that describes whole body glucose metabolism in a hierarchical manner
- Compare predictions from the newly constructed multi-level model with experimentally measured blood glucose and lactate in the disease state
- Identify the reactions that are most crucial in generating the predicted outcome or point at important steps in the model using e.g. Metabolic Control Analysis (MCA)

This thesis is structured in the following way:

A literature review is presented in Chapter 2. Chapter 3 consists of three sections. In the first section, we present the original models for the i) parasite model [1], ii) the red blood cell model [9–11] and iii) the whole body model [3] with initial validations (steady state analysis, plots, etc.). In the second section the linking of the parasite with the red blood cell model (done by Du Toit [2]) to create a model of parasitized red blood cell is presented and extended to describe a parasitized red blood cell culture with varying degrees of parasitemia. The third section of Chapter 3 explains the linking of the extended parasitized red blood cell culture model with the whole body model including a description of changes that were made to combine the two models (called the green1 model). Chapter 4 consists of two sections: In the first section we present the validation of the combined green1 model with available data from the scientific literature; the second section shows the results of sensitivity, robustness and control analysis applied to the green1 model. Lastly, Chapter 5

consists of a discussion of the results and outlines the limitations of the model, concluding remarks and suggestions for future work.

Chapter 2

Literature Review

In this thesis we intend to construct a physiologically relevant model for human glucose metabolism that can describe certain features of the disease state of malaria patients in terms of molecular mechanisms at work in the malaria parasite and its interaction with the human erythrocyte. Diagnosing a patient with a disease is typically done by considering a list of clinical symptoms. For severe malaria two of the key pathophysiological indicators for poor chances of survival are hypoglycemia (blood glucose < 2.2 mmol/L) and lactic acidosis (blood lactate > 5 mmol/L) [12]. Accelerated glycolytic flux in infected red blood cells [2], anaemia [13] and reduced perfusion [14] have been observed experimentally, but to date there are no mathematical models that are able to quantify their relative contributions to hypoglycemia and lactic acidosis. While these metabolic complications are likely to be caused by a combination of factors we intend to investigate the extent to which accelerated glycolytic flux leads to hypoglycemia and lactic acidosis.

In this chapter we give a brief description of the biological processes, including the functions of major organs, that play a crucial role in whole body glucose metabolism. Thereafter different modelling approaches used to study metabolism and disease states are described. These include mechanistic, phenomenological, pharmacokinetic, pharmacodynamic, multi-scale and multi-level modelling techniques. We then present a literature review on the different models available for each of the studied levels, in the construction of the hierarchical framework. Lastly a description of sensitivity analysis that is used to analyse and verify accuracy of model predictions is given.

2.1 The biology of whole body glucose metabolism in humans

Whole body glucose metabolism consists of multiple metabolic pathways interacting with each other in different parts of the body. It is a comprehensive network and can be complex when considering all the biological detail associated with it. Therefore we will provide a brief discussion (that follows from D. Voet & J. Voet [15]) on some of the key tissues and organs, including the metabolic pathways associated

2.1. The biology of whole body glucose metabolism in humans

with each in an attempt to explain human glucose metabolism. A realistic model of whole body glucose metabolism should contain descriptions of as many of these components as possible.

The main source of energy in the **brain** is glucose. Since it is unable to store glucose it depends on a continuous supply to sustain brain functioning [16]. During periods of starvation the brain switches to using ketone bodies. Most of this energy is required for the brain to maintain the sodium potassium membrane potential allowing for nerve pulses to be transmitted [16]. The glucose transporter (GLUT-3) transports glucose into the brain cells where it is metabolised via glycolysis. The brain can not utilise fatty acids as an energy source because they are unable to cross the blood-brain barrier [16]. This results in the brain consuming about 20% of the whole body glucose [16]. In cases of hypoglycaemia, which can be caused by an insulin overdose or, in the context of this study, the increased demand on blood glucose by the malaria parasite, the individual could become comatose, suffer irreversible organ damage or die.

Muscle tissue also relies on glucose and ketone bodies as a fuel source but unlike the brain it can metabolise fatty acids and store excess glucose as glycogen. Glucose is broken down by glycolysis resulting in the formation of pyruvate which can lead to the production of lactate under anaerobic conditions. Muscle tissue can not export glucose; however during the energy deprived states muscle glucose can be converted to alanine which is then transported to the liver. Once at the liver, the alanine is converted back to glucose that is released into the bloodstream. This process is known as the glucose alanine cycle. However, in resting muscle tissue fatty acids are the main source of energy [16]. In particular, the heart muscle (when "resting"), relies mostly on fatty acids for energy but can also metabolise ketone bodies and lactate if needed.

The **liver**, which is about 2-4 % of a persons body weight [16], is responsible for regulating many metabolic activities. After a carbohydrate containing meal, the glucose levels in the blood rise. This glucose is transported into the hepatocytes where it is converted to glucose-6-phosphate after which it stored in the form of glycogen. Importantly, insulin is not required for the uptake of glucose in hepatocytes unlike the insulin dependent muscle cells and adipose tissues. During starvation the glycogen stores in the liver are utilised (via gluconeogenesis) to replenish the glucose concentrations in the blood thereby maintaining homeostasis.

Another function of the liver, when the energy supply is abundant, is to synthesize fatty acids and export them into the blood stream. These fatty acids, in the form of lipoproteins, then move towards the adipose tissue where they are stored. In contrast, during periods of fasting the fatty acids are converted into ketone bodies and exported into the circulatory system.

Muscle tissue and the liver work together to maintain glucose homeostasis in the body. To elaborate on the role of the liver let us consider anaerobic metabolism for muscle cells. The product of glucose metabolism in the absence of oxygen is lactate.

2.1. The biology of whole body glucose metabolism in humans

This metabolite is exported from the muscle tissue into the blood and moves to the liver where it is imported and undergoes gluconeogenesis (to produce glucose) and lipogenesis (formation of fatty acids) as well as oxidative phosphorylation (producing ATP).

In addition to these specialised functions the liver also plays a crucial role in amino acid metabolism however this will not be discussed in the current work.

Even though the liver is the major tissue responsible for fatty acid synthesis, fatty acids are stored in the form of triacylglycerols in **adipose tissue**. Adipose tissue can not take up triacylglycerols and therefore relies on the lipoproteins exported by the liver [16]. The low density lipoproteins are hydrolyzed through stimulation from the hormone insulin releasing free fatty acids. In the adipose cells they reassemble to form triacylglycerols. When energy is in demand triacylglycerols are hydrolyzed to fatty acids and glycerol through regulation by the hormones glucagon, epinephrine and insulin [16]. Glycerol is released and exported to the liver while the product glycerol 3-phosphate, derived from the esterification of a fatty acid, is released into the blood stream [16].

The last organ that will be briefly discussed is the **kidney**. The main function of this organ is to filter out waste products from the blood [16]. Metabolites such as glucose are filtered out of the blood and reabsorbed by the kidney. The kidney excretes excess H^+ ions (in the form of urea) allowing for the pH balance in blood to be maintained. During starvation gluconeogenesis occurs in this organ leading to almost half of the glucose supply in the bloodstream [16].

The balance between different fuel sources, their formation and their excretion by different tissue types, is regulated by a number of metabolites and hormones. For the present study we will briefly describe how the hormones insulin, epinephrine and glucagon regulate glucose levels in the body.

When blood glucose levels are high, beta cells in the pancreas secrete insulin into the blood stream. This hormone causes the uptake of glucose from the blood into the liver, muscle and adipose cells. These tissues are known as insulin dependent tissues while the brain, kidney and red blood cells do not require insulin for glucose uptake and are therefore insulin independent. In constant, when blood glucose levels are low the alpha cells in the pancreas secrete the hormone glucagon. Glucagon stimulates the release of glucose from the liver through the regulation of gluconeogenesis and glycogen degradation. Epinephrine, also known as adrenalin, has a similar role to that of glycagon. It regulates the release of glucose to restore blood glucose levels and it usually activated in "fight or flight" responses which require a sudden burst of energy. These hormones work together to carefully maintain glucose homeostasis in the body.

In the next section we will introduce systems biology models as a tool to integrate multiple components, such as body organs, to analyse overall systems behaviour, such as whole body physiology.

2.2 A mechanism based whole body model

Models of whole body physiological processes are typically not formulated in terms of intra-cellular molecular mechanisms but with phenomenological descriptions of whole-organ or whole-cell level processes. This is usually sufficient to describe clinical features at the whole body or organ levels. Models that use phenomenological functions to describe observables are usually only valid under the conditions for which the model was constructed since model parameters contain no information on how they are dependent on surrounding conditions. Such models are therefore limited in terms of predictive power. Phenomenological models do not contain information at the enzyme level therefore they cannot be used to accurately predict drug effects. In addition, when trying to understand the clinical features of a disease state as an emergent property of complex molecular networks on the sub-cellular level, these models need to be extended to contain the molecular mechanistic detail of the metabolic networks in the organs or compartments of interest. In the context of the current discussion, hypoglycemia and lactic acidosis associated with the malaria disease state are clinically described at the level of the whole body. These conditions are brought about by changes at the level of the enzyme catalyzed reactions in cells related to glycolysis and lactate production. A hierarchical model that links the features of the whole body to these detailed molecular mechanisms would therefore greatly assist in understanding disease causing mechanisms in the malaria parasite and point to possible drug targets.

Our construction of a whole body model that describes glucose metabolism in malaria patients and contains the detailed molecular mechanisms of the most immediately relevant cellular components, will employ three existing models: a *Plasmodium falciparum* parasite glycolytic model, a red blood cell glycolytic model and a model of whole body glucose metabolism. Knowing how much detail each model should have can be challenging: since we are ultimately interested in understanding the molecular reasons for the appearance of the disease state and identifying molecular drug targets, the lower levels that are directly related to the metabolism of the malaria parasite need to be more detailed. Linking models of differing complexity across hierarchical levels requires intensive planning as models are not always created in the same mathematical formalism, computational framework or have the same units. Furthermore detailed kinetic models provide considerable amounts of information and can become complex once the multiple models are linked. Lastly, even if these models can be linked successfully, the computational power required to conduct analyses on these models may be prohibitively high.

An illustration of how this hierarchical concept is going to be utilised to better understand disease states of malaria patients can be seen in Figure 2.1.

2.3. Mechanism based models for pharmacology

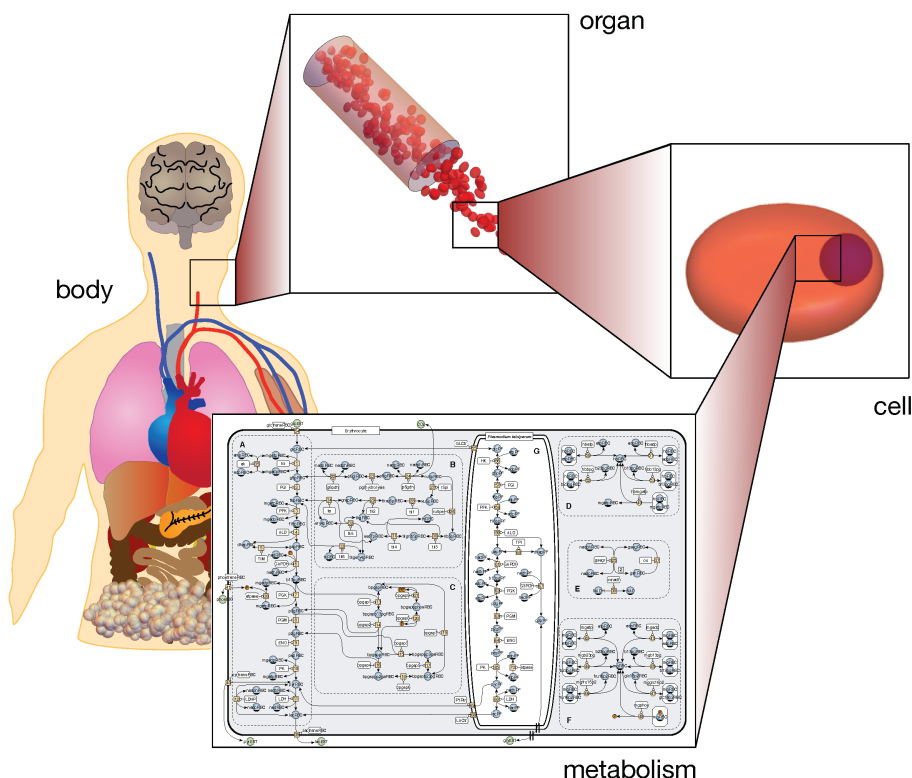


Figure 2.1: **Scheme showing the hierarchical multi-level model for malaria patients.** The whole body model consists of different tissues and organs while the red blood cell and parasite model compartment are modelled at a cellular level. This figure was originally published in [<http://www.biochemsoctrans.org/content/43/6/1157>, Jacky L. Snoep, Kathleen Green, Johann Eicher, Daniel C. Palm, Gerald Penkler, Francois du Toit, Nicolas Walters, Robert Burger, Hans V. Westerhoff, David D. van Niekerk, Biochemical Society Transactions, 2015].

2.3 Mechanism based models for pharmacology

Typical SB models are able to analyze the effects of drugs at the level of molecular mechanisms but usually do not take into account the way a drug is affected by the body (pharmacokinetics). In pharmacology, this process of drug ADME (absorption, distribution, metabolism and excretion) is usually treated in a phenomenological model that describes the change in a drug's concentration over time at different sites in the body. The effect of the drug concentration at the site or organ of interest is also typically described in a phenomenological way using pharmacodynamic models, which gives little to no insight into the drug's molecular mechanism of action or mechanistic reasons for side effects. Inclusion of molecular mechanistic detail of the target of interest and other compartments (cell types) responsible for drug metabolism could, in the end, then also assist in not only understanding a drug's pharmacological properties but also aid in drug design. The concept of integrating SB and PK/PD models (sometimes referred to as Systems Pharmacology) to allow for more accurate pharmacological analyses has been suggested by Swat et al. [17].

2.4 Multi-scale and multi-level approaches to modelling

The recent progress in the fields of genomics, proteomics and metabolomics has resulted in large amounts of data and scientific knowledge on biological phenomena. These are on different levels of biological organisation, such as cell, tissue or organ level. This has required development in computational modelling to include models that are in different forms or structures to describe the respective levels of organisation. As a result multi-level and multi-scale modelling approaches have been developed to combine models in hierarchical manners. Multi-level models have different parts of the model described in different levels of detail, but the whole model uses a single modelling framework (e.g. ODEs). Multi-scale models use different frameworks to deal with the different spatial and temporal scales [18]. Multi-level and multi-scale modelling has allowed for the linking of subcellular processes to physiological processes of the whole system rather than studying sub-systems in isolation [18, 19].

The development of a platform that allows for the study of combined metabolic functions is beneficial as the understanding of complex diseases often requires knowledge of the molecular, cell/tissue and organ level (as well as the interaction between these levels) [20, 21]. The combined description of the whole body level will not only give mechanistic insights into diagnostics but help with drug development [22]. Such a model would aid in identifying adverse side effects that a drug might possibly have on a patient.

An alternative method used to reduce drug side effects include the administration of medication or drugs in combination [21]. Hwang et al. [21] mention that this approach becomes experimentally challenging as determining the effects attributable to individual drugs and their combinations requires expensive and labour intensive medical trials. For this reason multi-scale and multi-level modelling become desirable as it can determine possible predicted outcomes at a very low cost [21].

There are some software packages, specification standards and tools that have been developed which allow for the reuse or automated merging of mathematical models. SemGen [23] is a semantics based model composition software that allows for composite annotations through existing ontologies. This software is an example of support that can be added to Systems Biology Markup Language (SBML) files, one of the most commonly used standards for format exchange [24], to allow for better annotation required when merging sub-models. Models can be merged in SemGen; however currently it does not support initial assignment rules which were essential in our approach, due to moiety cycles that were present (see Section 3.2.4). Process Modeling Tool (ProMoT) [25] is another example of a software tool that has been developed to support the linking of mathematical models. ProMoT provides a framework that allows for the construction, manipulation and visualisation of mathematical models in a modular structured way. Potential Coupling Interface (PCI), developed by Bulatewicz et al. [26], is an example of an interface that allows for the

2.5. Bottom-up approaches using mechanistic models

coupling of models. This tool aims to display models in a visual way that allows for the merging of models to be done without prior knowledge of the of the source code [26]. The CellML language (based on the XML markup language) has been developed to simplify components of different formats allowing for easier multi-scale integration of models [18] (for more detail refer to the Physiome Project [27]).

2.5 Bottom-up approaches using mechanistic models

The Systems Biology (SB) field allows for the understanding of detailed metabolic networks through mathematical models that describe system behaviour in terms of defined molecular mechanisms such as enzyme-catalysed reactions and transport steps. The advantage of using these types of models is that they are often mechanistic and contain many experimentally determined parameters opposed to models in which parameter identifiability is not always possible or accurate. These features make for more realistic interpretation and explanation of causative factors of emergent system behaviour. In SB models, the time-evolution of system state (in terms of, for example, metabolite quantities or concentrations) are often modelled using ordinary differential equations (ODEs) formulated in terms of mechanistic rate equations associated with the different reactions in the system. Living systems are open systems, meaning that there is an import and export of substances. Metabolic pathways of interest are therefore typically modelled as open systems where there is a constant source of substrates and removal of products. These systems tend towards steady state in which the rate of formation and consumption of metabolites are equal therefore keeping their concentrations constant in time. This rate is referred to as the steady state flux. The steady state flux and metabolite concentrations can be computed by finding the roots of the ODEs (i.e. values of the metabolites for which the ODEs are zero). Using software such as Wolfram Mathematica, the ODEs can also be numerically integrated to determine how the metabolites change over time from some initial state or in response to a change in the system. Such models give insights into the appearance of phenomena at the level of the network as a result of (a combination of) individual steps or reactions. The effect that an external modifier such as a drug can have on the network can therefore also be understood in terms of mechanistic effects within the network.

2.6 Existing mathematical models

The construction of a hierarchical model to explain hypoglycemia and lactic acidosis in malaria patients requires the use of models that describe *Plasmodium falciparum* glycolysis, erythrocyte glycolysis and whole body glucose metabolism. Therefore this multi-level model will consist of three different levels. Next, we present a literature review on the available models for each of the levels of organisation that will be required to form the hierarchical model.

2.6.1 Existing *Plasmodium falciparum* models

Penkler et al. [1] described the metabolic pathways for *Plasmodium falciparum* glycolysis using a mechanistic mathematical model. It uses a bottom-up approach with rate equations to describe individual enzyme catalysed reactions in the glycolytic pathway and a glycerol producing branch. Each glycolytic enzyme was characterised by fitting an enzyme mechanistic rate equation to a complete experimental data set. This resulted in a mechanistic kinetic equation for each reaction. Eighteen reaction steps were needed to explain the conversion of glucose into lactate, pyruvate and glycerol and the production of ATP. It is the first of its kind for *Plasmodium falciparum* in the sense that all of the enzymes have been experimentally characterised under the same physiologically relevant conditions. The model has been validated and shows good predictive abilities [1].

2.6.2 Existing erythrocyte models

Moving up one level, an erythrocyte model is required but in contrast to the parasite there are multiple options to choose from. One of the first models that was used to describe glycolysis in red blood cells is that of Rapoport et al. [28]. They describe glycolysis (including ATP synthesis and consumption) using four differential equations and used Michaelis Menten kinetic equations to model the enzyme reaction rates. Another example of a detailed erythrocyte model is that of Schuster et al. [29]. They developed a mathematical model which included reactions for glycolysis, the hexose monophosphate shunt (HMS) and the glutathione system. Schuster et al. [29] included experimental information on kinetic properties of enzymes that are responsible for regulating glycolysis, the oxidative pentose phosphate and the glutathione systems.

Simulation platforms such as the E-Cell System, which allows for the prediction of metabolism under different physiological and pathological conditions, have also been used to model and analyse mathematical models of human erythrocyte metabolism. Kinoshita [30] describes a simulation of human erythrocyte metabolism in this way by focusing on glucose-6-phosphate dehydrogenase (G6PDH) deficiency. Nakayama et al. [31] is another example of an in silico red blood cell model. It is able to describe the glycolytic pathway, the pentose phosphate pathway and the nucleotide metabolic pathway. This type of modelling uses rate equations with a flux-based approach to reduce the number of equations and parameters. In cases where complete sets of data are not always available for parametrization, flux-based approaches can be beneficial. According to Nakayama et al. [31] these E-Cell simulation systems are not always good at predicting what happens during abnormal conditions such as deficiencies because sometimes alternative metabolic pathways are used. This could create problems when studying hypoglycemia and lactic acidosis as these effects are not normally present in a healthy individual.

Friedman & Lungu [32] constructed a model that includes the dynamics of the red blood cells and malaria parasites. They modelled the dynamics using the density of the normal and infected red blood cells as well as the intracellular and extracel-

lular parasites. The model incorporates the effect of adaptive and innate immunity of malaria infected individuals. In contrast, Chiyaka et al. [33] did not include immunity in their model; however they did focus on using mathematical analysis which includes the evaluation of the reproductive number R_0 using three differential equations with compartments for the normal red blood cells, infected red blood cells and merozoites. Both of these studies used mathematics to understand the malaria infection during the erythrocytic stages but neither are detailed enough in terms of erythrocyte or parasite metabolism (i.e. containing individual enzyme catalysed reactions) that would be needed to identify drug targets.

The required level of mechanistic detail is an important consideration when choosing a suitable red blood cell model. Not only does the parasite glycolytic pathway share many features with the red blood cell glycolytic pathway, but in an experimental study by Mehta et al. [34, 35] it was found that only a small percentage of the red blood cells need to be infected to cause the down regulation in the glucose utilisation rate in the uninfected erythrocytes. The glucose flux was considerably higher in the infected red blood cells and showed almost a 100-fold increase in glucose utilization compared to the uninfected red blood cells [1, 34]. The glucose flux was maximal at the trophozoite stage. Mehta et al. [35] suggested that the decrease in the glycolytic flux of the uninfected RBCs is due to the regulation of glycolytic enzymes by some unknown compound related to parasite metabolism. This motivates the investigation of mechanisms of the glycolytic enzymes in order to understand what happens during malaria infection in the erythrocytic stage and should be considered when choosing a model with sufficient detail for the red blood cell.

One such model with a high level of experimentally characterized and validated enzyme kinetic detail, is that of Mulquiney & Kuchel [9–11]. This model contains a high level of metabolic detail and is able to explain erythrocyte metabolism under different physiological and experimental conditions. It includes the glycolytic pathway, the pentose phosphate pathway (PPP), the 2,3-bisphosphoglycerate shunt, the transportation of metabolites, the binding of metabolites to haemoglobin and Mg^{2+} as well as the effect of pH on certain reactions.

2.6.3 Existing whole body models

Lastly the features related to the appearance of the disease state (i.e. blood glucose and lactate) need to be modelled at the level of the whole body. Several mathematical models have been developed to describe glucose metabolism on a whole body level [36, 37]. While some focus on including different organs as compartments [3, 38, 39], others address hormonal regulation and signalling [37, 40, 41]. Model predictions have mainly been studied to be able to understand how glucose homeostasis is maintained when perturbations are made in the glucose-insulin system, such as the effects of diseases like diabetes.

According to Kang et al. [42] one of the first simple whole-body glucose regulation models was that of Bolie [43]; however it has been described as being too simplistic for understanding the complex glucose-insulin system [37, 42]. Another simple

model known as the "minimal model" was developed by Bergman & Cobelli [44]. It explains glucose kinetics with compartments for peripheral tissues and liver that take up glucose in response to secretion of insulin from the remote insulin compartment. Two drawbacks of the minimal model are firstly the assumption that glucose and insulin effects on organs are linear, and secondly the fact that the effects of glucagon on the liver glucose production are ignored. Cobelli et al. [45] addresses these drawbacks with a comprehensive model to include glucagon and non-linear dynamics. It is argued [45] that simple models can not necessarily give the correct description for understanding the behaviour of parameters but poor validation and excessive detail should also be avoided when developing comprehensive models. This more comprehensive model has been validated [45] and many other extensions that follow from the basic minimal model can be found in the literature [46–48].

A disadvantage of using the models described above is that most of them have been developed to better understand how glucose levels return to normal physiological conditions after a perturbation leading to an increase in blood glucose, for example in intravenous glucose tolerance tests. Using an existing model that has only been tested for hyperglycaemic states would be a concern as these models consist of lumped reactions (lacking the mechanistic detail) and might not be representative of a hypoglycaemic individual. These models consider disease states of Type 1 and Type 2 diabetes (specifically models by Wang et al. [49] and Dalla Man et al. [39]) which could be used as proof of concept to show metabolism of different diseases on a whole body level. However they are either not able to describe the hypoglycemic and lactic acidosis state of a malaria-infected individual or lack the necessary details of processes crucial for the understanding of the dynamics under this condition.

An example of a model that includes the Cori-cycle (blood lactate being converted back to glucose by the liver, possibly a very important feature for glucose and lactate homeostasis) is that of Konig et al. [41]. This model provided insights into using a detailed kinetic model for hepatic glucose metabolism using tools such as metabolic control analysis (MCA). The effects of hormonal regulation by insulin, glucagon and epinephrine were also studied. While this model is much more detailed it was not developed to describe different organs in the whole body (e.g. adipose tissue, muscle, etc.) and obtaining a working model description has been difficult.

Kim et al. [38] claim to have developed the first mechanistic model of glucose homeostasis that links cellular metabolism to whole-body responses and includes hormonal control after exercise. This model is a constraint based model and is therefore limited in kinetic description of the enzymes (each rate equation was described by a general irreversible bi-bi substrate to product reaction).

The glycogen regulation model of Xu et al. [3] was constructed to address the role of substrate cycling in maintaining glucose homeostasis (regulated by the liver for feeding and fasting reference states). The model includes blood glucose and blood lactate which are the linking metabolites that are needed between the RBC and whole body levels. Xu et al. [3] suggest compartments for the brain, kidneys and red blood cells could be added to give a more accurate description of the whole body.

The provision for incorporating a red blood cell compartment in the framework is hugely beneficial.

2.7 Sensitivity analysis

One technique that is used to better understand and interpret mathematical models is known as sensitivity analysis. Sensitivity analysis is performed on the results of mathematical models for two main reasons. Firstly it can be used to determine which process e.g. parameter, reaction, etc. are most important in generating a desired outcome. Hill et. al. [50] discuss how this approach of sensitivity analysis can be used to identify important model parameters, parameter interactions and correlations, observation dominance in complex models, and the effect of uncertainty of estimated parameters. The study of uncertainty in model predictions or outputs is the second motivation to perform sensitivity analysis on a model [51]. Essentially it tests how much the model output would differ if the model inputs were slightly different. Therefore sensitivity analysis provides confidence in the accuracy of model predictions.

Sensitivity analysis can be described as local or global. For the purpose of this work we define local sensitivity analysis to be the analysis of the sensitivity of system behaviour to small changes in single inputs (as is done in Metabolic Control Analysis) and global sensitivity analysis to be the analysis of changes in system behaviour due to larger changes in combinations of model inputs [52].

Metabolic Control Analysis, developed by Heinrich & Rapoport [53] and Kacser & Burns [54], quantifies the effect that small perturbations in the biological system would have on steady state behaviour. In system biology, sensitivity analysis tools such as MCA can provide insights into the impact of uncertainty of parameter values and indications of control of processes on system behaviour or responses of system behaviour to changes in a metabolic pathway.

Metabolic Control Analysis defines three coefficients that can be used to describe how a change in local property effects the systemic property[55]. Consider the elasticity coefficient that is given by

$$\epsilon_p^v = \frac{\partial \ln v}{\partial \ln p}$$

where v and p represent an enzyme rate and parameter respectively. This coefficient describes how the activity of an enzyme is altered by making a 1 % perturbation in a parameter. Control coefficients explain how much control a rate has over a systemic property such as the steady state of a metabolite (C_v^X) or flux (C_v^J) therefore we have

$$C_v^X = \frac{\partial \ln X}{\partial \ln v} \quad \text{and} \quad C_v^J = \frac{\partial \ln J}{\partial \ln v}.$$

with X representing a metabolite steady state and J representing a reaction flux. An enzyme will have a high control coefficient, if a 1% perturbation has a large effect on the flux or steady state concentration.

The third coefficient, namely the response coefficient, can be defined in terms of the elasticity and control coefficients. Response coefficients describe the effect that a local property like a parameter has on the steady states in a system. Hence,

$$R_p^X = \frac{\partial \ln X}{\partial \ln p} \quad \text{and} \quad R_p^J = \frac{\partial \ln J}{\partial \ln p}. \quad (2.7.1)$$

or

$$R_p^X = C_v^X \cdot \epsilon_p^v \quad \text{and} \quad R_p^J = C_v^J \cdot \epsilon_p^v. \quad (2.7.2)$$

If the parameter is a multiplier of the rate that is being studied the elasticity coefficient is 1 and as a result the response coefficient will be the same as the control coefficient for the systemic property. Metabolic Control Analysis can be computationally and experimentally evaluated. For example, the effect of an inhibitor could be studied using these response coefficients.

These coefficients are an example of how sensitivity analysis allows for the investigation of the effect of variations in model inputs. An application of control and response coefficients could be drug target identification. A way in which drug targets can be identified is through the analysis of systemic effects after the addition of a reaction effector. Furthermore, Cascante et. al. [56] suggest that Metabolic Control Analysis can be used to understand genotype-phenotype correlations as it provides a mechanism in which to link gene expression with gene products.

In global sensitivity analysis, the combinations of model inputs are changed to give insights into model predictions. This allows for the investigation of predictions based on the uncertainty of parameter spaces.

In the following chapter we elaborate on the existing models that were chosen to represent each level for the construction of a model for human glucose metabolism that can explain the disease state of malaria patients.

Chapter 3

Model construction and initial validation

The construction of a hierarchical model to explain abnormalities in glucose homeostasis in malaria patients requires the use of models that describe *Plasmodium falciparum* glycolysis, erythrocyte glycolysis and whole body glucose metabolism. The modelling approach used in this study consists of detailed bottom-up models for the lower levels (*Plasmodium falciparum* and erythrocyte glycolysis), and a phenomenological model for whole body glucose metabolism.

Penkler et al. [1] described the metabolic pathways for *Plasmodium falciparum* glycolysis using an enzyme mechanistic mathematical model. This model was chosen to represent the parasite compartment, since all of the enzymes have been experimentally characterised and the validation of the model showed good predictive abilities [1]. Similarly, the Mulquiney & Kuchel model [9–11] was chosen for the red blood cell compartment as it contains all the essential details of erythrocyte glycolysis and provides a good structure that can be modified to link to whole body and parasite models.

There is no clear best option for a whole body model of glucose metabolism that can explain disease states in terms of physiological or molecular mechanisms but multiple phenomenological models were investigated (see Chapter 2). It was decided that the Xu et al. [3] model would be the best choice for the linking to the combined RBC and parasite model for several reasons: 1) the inclusion of multiple compartments for various organs involved in glucose metabolism 2) the provision made for incorporating a red blood cell compartment 3) unit compatibility and 4) the ability to obtain a curated and working model description. Most importantly this whole body model was developed to study how glycogen regulates blood glucose levels which is beneficial when studying hypoglycemia as the body tries to maintain glucose homeostasis through the action of glycogen.

This chapter is divided into three main sections. The first section describes the original models for *Plasmodium falciparum* glycolysis (Penkler et al. model [1]), erythrocyte glycolysis (Mulquiney & Kuchel model [9–11]) and the whole body glu-

glucose metabolism (Xu model [3]). The parasite and original red blood cell models were obtained from JWS Online [57]. The whole body model was coded and curated by comparing the model simulations with the published paper results.

The second section in this chapter describes how the changes were made to the units of the red blood cell model for further compatibility with the parasite model. Furthermore, this section includes the description of linking the red blood cell model to the parasite model. While the concept of linking the red blood cell model with the parasite model has been studied by Du Toit et al. [2], in this thesis we include a different equation for the glucose transporter. Note that the original Mulquiney & Kuchel model [9–11] does not have a glucose transporter reaction and we needed to include this reaction step in the red blood cell model. We also extend the red blood cell compartment to include an uninfected red blood cell compartment.

In the third section of this chapter the scaling up of volumes to represent a whole body level and linking of the Xu et al. [3] model to the parasitized RBC culture model is described. Model adaptations that were necessary to be made after or during the linking of the models are also discussed.

Figure 3.1 shows a flow diagram of the process followed in combining the different models (including the model units, their description source and in what sections they can be found in this chapter).

3.1. Original models and validation of model description

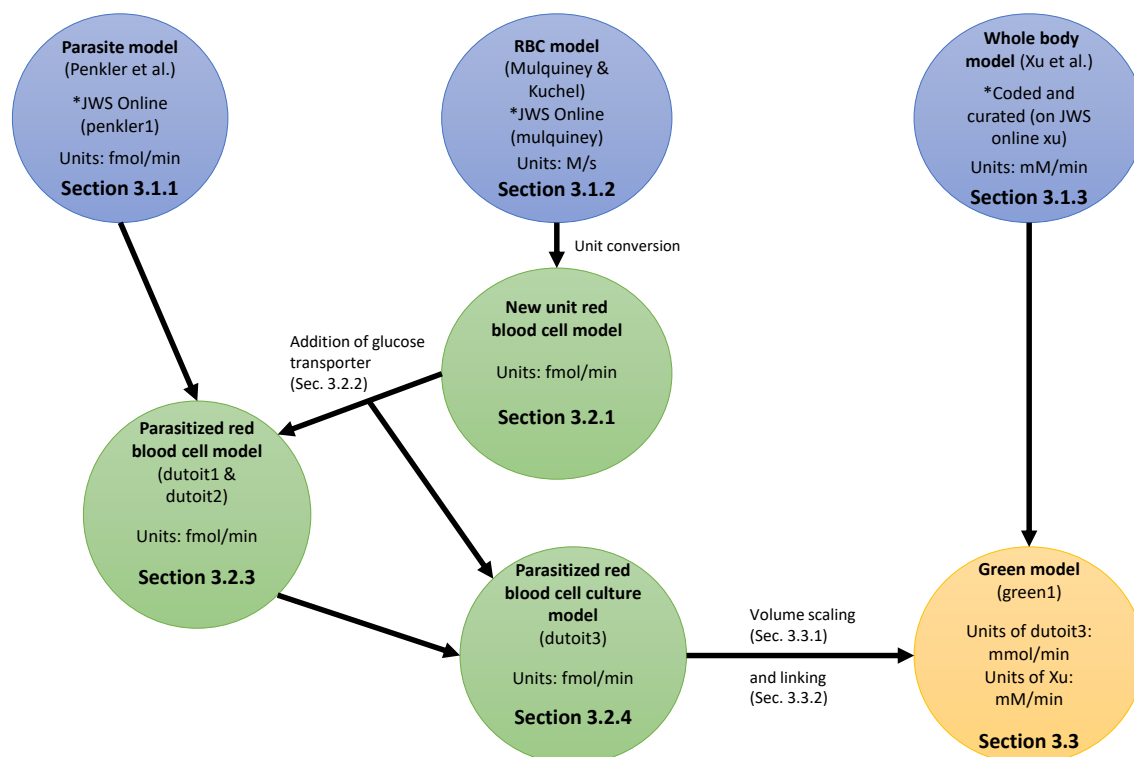


Figure 3.1: **Flow diagram of Chapter 3.** Models in blue circles are discussed in Section 1, models in green circles are discussed in Section 2 and the final green1 model (yellow circle) is described in Section 3. The * indicates where the model was obtained from or can be found. In the case of the whole body model it was coded and curated as "xu" on JWS Online. Text on the arrows indicate changes that were made in the linking process.

3.1 Original models and validation of model description

This section consists of the original models for *Plasmodium falciparum* glycolysis (Penkler et al. model [1]), red blood cell model (Mulquiney & Kuchel model [9–11]) and the whole body model (Xu model [3]). Both the parasite model and red blood cell model were obtained (and are available) on JWS Online. For the whole body model the Matlab files (obtained from the supplementary information of the original manuscript) were used to build the Xu et al. [3] model on JWS Online. Figures in the published paper Xu et al. [3] were compared to confirm that the model is correctly coded.

3.1.1 Parasite model

The detailed kinetic model of *Plasmodium falciparum* describes the glycolytic pathway of the parasite (Embden-Meyerhof-Parnas pathway). A schema of this pathway can be seen in Figure 3.2. Each enzyme in this metabolic pathway was experimen-

3.1. Original models and validation of model description

tally characterised to obtain a parameterized kinetic rate equation [1]. These rate equations were used to generate a system of eighteen ODEs. Independent data sets were used to validate the model which confirmed the accuracy of the model predictions [1]. JWS Online (<http://jjj.bio.vu.nl/database/penkler>) has the two different penkler models (penkler1 represents an open system and penkler2 a closed system).

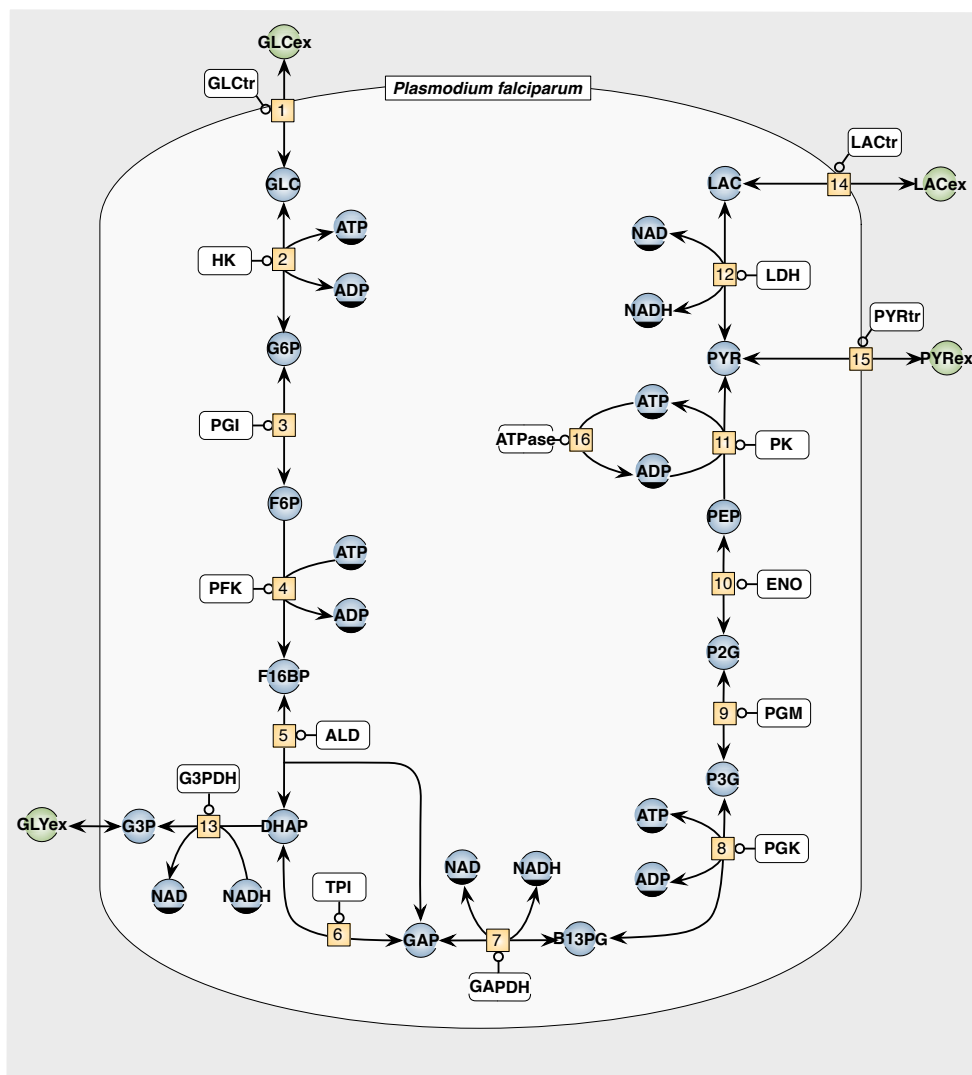


Figure 3.2: Overview of the *Plasmodium falciparum* glycolysis model [1]. Orange blocks show enzymatic reactions, blue circles are the metabolites (each have an ODE) and green circles represent the fixed metabolites in the steady state model.

In the blood form, trophozoite stage, *Plasmodium falciparum* parasites reside inside red blood cells. In a mechanistic model, the transfer of metabolites between these two organisms is typically modelled in terms of concentration dependent reactions (diffusion or concentration dependent transport). Penkler et al. [1] constructed a model in terms of metabolite amounts (fmol) and reaction rates in terms of amount

3.1. Original models and validation of model description

per time (fmol/min) (rather than molar concentrations) to allow for the possibility to model a growing parasite i.e. with variable compartment volumes. Since enzymes and transporters are sensitive to concentrations, this necessitates the inclusion of additional volume factors in an enzyme's rate equation to convert the metabolite quantity to concentration i.e. a metabolite amount will be divided by the volume of the compartment in which it occurs. In addition, if a rate constant is in units of concentration per time it has to be multiplied by the volume of the compartment to generate a differential equation that describes an amount per time change in a metabolite. An example of how this was done in Penkler et al. [1] is shown for a Michealis-Menten equation.

The textbook equation is:

$$v = \frac{V_{\max} \cdot s}{K_m + s}$$

$$v = \frac{V_{\max} \cdot \frac{s}{K_m}}{1 + \frac{s}{K_m}} \quad (3.1.1)$$

where K_m is the substrate concentration at half the maximal velocity (in units of M) and s the substrate concentration (in units of M). The overall unit of v is the same as V_{\max} which for the sake of argument, we assume to be concentration per time (M/min). If we would like to work with S in terms of fmol rather than molar, the equation becomes

$$v = \frac{V \cdot V_{\max} \cdot \frac{S}{V}}{1 + \frac{S}{V K_m}} \quad (3.1.2)$$

If we assume that a compartment volume V is measured in units of fL, then

$$v \text{ units} = \frac{\text{fL} \frac{\text{M}}{\text{min}} \frac{\text{fmol}}{\text{fL} \cdot \text{M}}}{1 + \frac{\text{fmol}}{\text{fL} \cdot \text{M}}} \quad (3.1.3)$$

$$v \text{ units} = \frac{\text{fmol}}{\text{min}} \quad (3.1.4)$$

The maximal velocity (V_{\max}) still has units of concentration per time but Equation (3.1.2) is in amount per time (fmol/minute). This conversion allows the modelling of ordinary differential equations to be in mole amounts per time which generates the variables/metabolites in units of amounts. In the Penkler model the internal metabolites in the *Plasmodium falciparum* glycolysis model were scaled to fmol amounts per 28 fL (volume of a trophozoite [1]) while the metabolites external to the parasite, namely RBC glucose, pyruvate, glycerol and lactate were scaled according to the volume of one RBC (90 fL) [58].

It was necessary to confirm that the model that would be worked with agreed with the results of Penkler et al. [1]. This initial validation consisted of comparing the steady state results (for metabolites and fluxes) with Table 14 in Penkler et al. [1]. Verification of the model required unit conversions using $V_{\text{pf}} = 28 \text{ fL}$, and a conversion factor $4.67 \frac{\mu\text{L cytosol}}{\text{mg total protein}}$). Table 3.1 shows the results.

3.1. Original models and validation of model description

Table 3.1: **Validation of the Penkler model.** Steady state results for metabolites and some fluxes from our parasite model which is identical to Table 14 in the Penkler et al.[1].

Metabolite	Model (mM)
GLC	0.71
G6P	0.79
F6P	0.24
F16BP	1
DHAP	1.1
G3P	0.53
GAP	0.048
B13PG	0.001
3PG	0.5
2PG	0.049
PEP	0.054
PYR	1.1
LAC	2.9
ATP	2.5
ADP	0.5
NADH	0.058
NAD ⁺	2.9
Flux	Model $\left(\frac{\mu\text{mol mg}}{\text{protein min}}\right)$
J_{GLCTR}	0.044
J_{LACTR}	0.081
J_{GLYTR}	0.004
J_{PYRTR}	0.004

Figure 3.3 shows our simulations of the penkler2 model which is identical to the graphs (Figure 16) from Penkler et al. [1]. External glucose and external lactate are plotted over 90 minutes. It is assumed that the external metabolites are unclamped and reach a steady state due to lack of substrate supply (<http://jjj.bio.vu.nl/database/penkler2>). Metabolite amounts (fmol) were divided by the volume of

3.1. Original models and validation of model description

incubation (taking into account 28 fL and 0.0106 cytosolic volume/total volume) and then converted to mM.

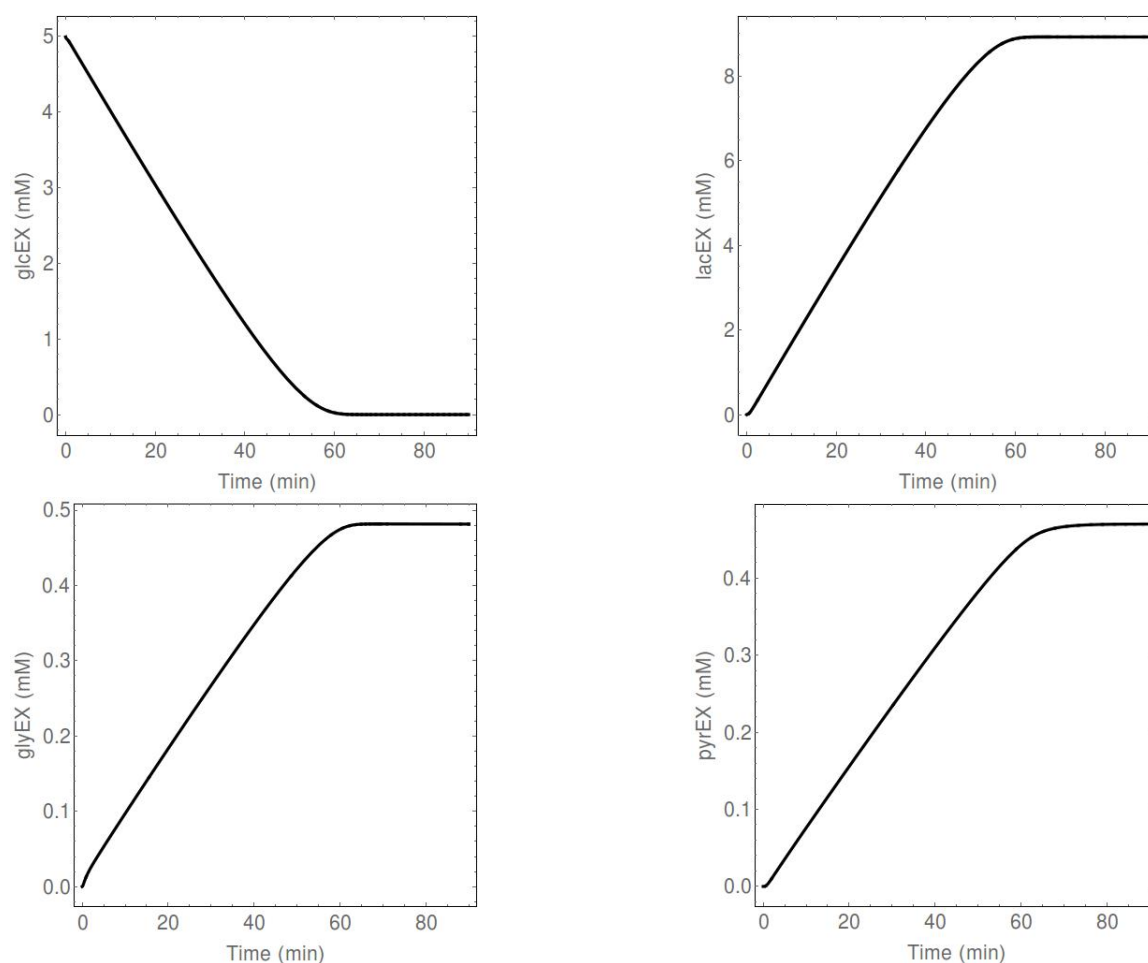


Figure 3.3: **Validation of the Penkler model.** External metabolites in the our parasite model which agrees with the Penkler model (Figure 16 in Penkler et al. [1]). (Excludes experimental data)

For more detail on this model refer to Penkler et al. [1].

3.1.2 Red blood cell model

The red blood cell (Mulquiney & Kuchel [9–11]) model was obtained from JWS Online [57] (<http://jjj.bio.vu.nl/database/mulquiney>). In this model a rate equation was derived for each enzyme catalysed reaction resulting in a system of 108 differential equations leading to a high level of kinetic detail. To account for the accuracy of prediction under a wide range of physiological conditions it was necessary that the parameters had to be identified (through experimentation and simulation); iteratively changed; and further refined (until model validation was acceptable). These physiological conditions included validation of the normal *in*

3.1. Original models and validation of model description

in vivo steady state, and refinement of model parameters by comparison with experimental data considering the response to external effectors such as pH, glucose-1,6-bisphosphate, inorganic phosphate and total magnesium concentrations [10].

Mulquiney & Kuchel [9–11] assumed that only glucose, lactate, pyruvate and inorganic phosphate can cross the cell membrane. External metabolites that were fixed in the Mulquiney & Kuchel model include lactate, glucose, pyruvate, inorganic phosphate and carbon dioxide. All other metabolites were time dependent variables. This model also considers the percentage of volume of blood that consists of erythrocytes (known as the hematocrit) and the total cell volume accessible to the intracellular solute (α). Figure 3.4 shows a simplified scheme of the main metabolic pathways involved in erythrocyte metabolism.

This model was described in units of molar per second. In Section 3.2.1 and Section 3.2.2 a number of changes are introduced to the model to make it compatible with the parasite model, such that the two models can be linked (Section 3.2.3).

The initial model validation for our red blood model showed that the JWS Online results are in close agreement with that of the original Mulquiney & Kuchel model [9–11] (see Table 3.2). Differences can be explained by numerical issues in the model and model changes that occurred after the initial publication which was confirmed with the authors.

Table 3.2: **Validation of the Mulquiney & Kuchel model.** Steady state results for some glycolytic metabolites from Mulquiney & Kuchel [9–11] compared to our red blood cell model ("mulquiney") steady state results from JWS Online.

Metabolite	Mulquiney & Kuchel [9–11] model (mM)	JWS Online output (mM)
G6P	0.0375	0.0403
F6P	0.0122	0.0131
F(1,6)BP	0.00231	0.00220
GraP	0.00531	0.00508
1,3-BPG	0.000369	0.000207
3-PGA	0.0721	0.0713
2-PGA	0.0120	0.0119
PEP	0.0203	0.0199
PYR	0.0586	0.0588
LAC	1.40	1.40

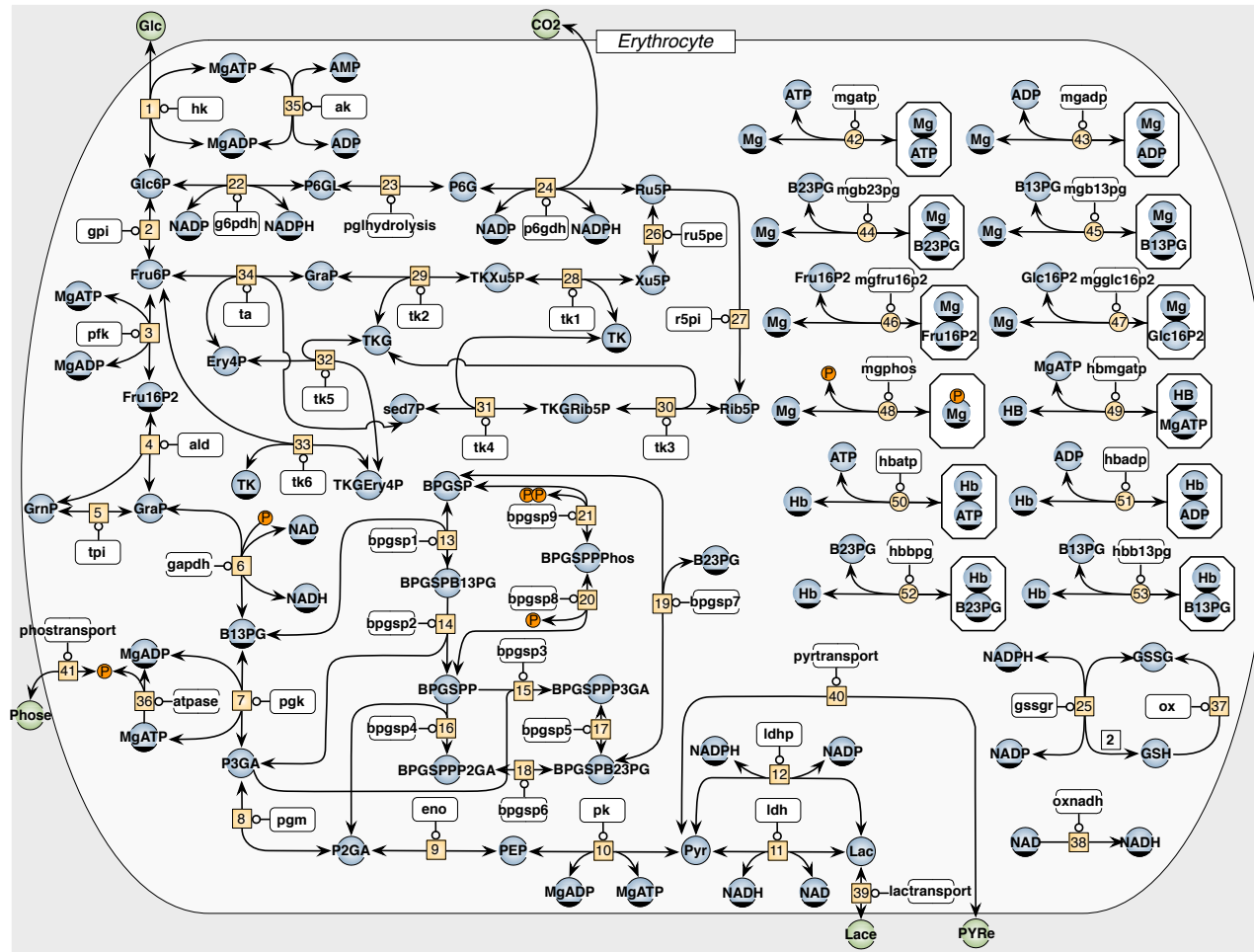


Figure 3.4: **Schema of the red blood cell model [9–11]**. Orange blocks show enzyme catalyzed reactions, blue circles are the metabolites (each have an ODE), green circles represent the fixed metabolites and orange circles represent the release of inorganic phosphate [2].

3.1. Original models and validation of model description

3.1.3 Whole body model

Xu et al. [3] created a whole body model for glycogen regulation to study the role of substrate cycling of glycogen in maintaining blood glucose homeostasis. This physiological model consists of the following compartments: adipose tissue, skeletal muscle, liver and blood. The liver compartment is the most detailed due to the key role that it plays in glycogen regulation. Schema's for the liver, adipose tissue and muscle compartment are shown in Figure 3.5, Figure 3.6, and Figure 3.7 respectively.

We coded this model on JWS Online using the original Matlab files that were published. It was necessary to confirm that the model description that was coded in this project was in agreement with the published results of Xu et al. [3]. This was done by checking that the Figures (for example see Figure 3.9) generated by our model description were identical to that of Xu et al. [3], after which the model was curated and made available on JWS Online (<http://jjj.bio.vu.nl/database/xu>). The translation of code from the Matlab files to SBML was done manually using the model builder of JWS Online. The SBML model was obtained using the JWS Online output facility.

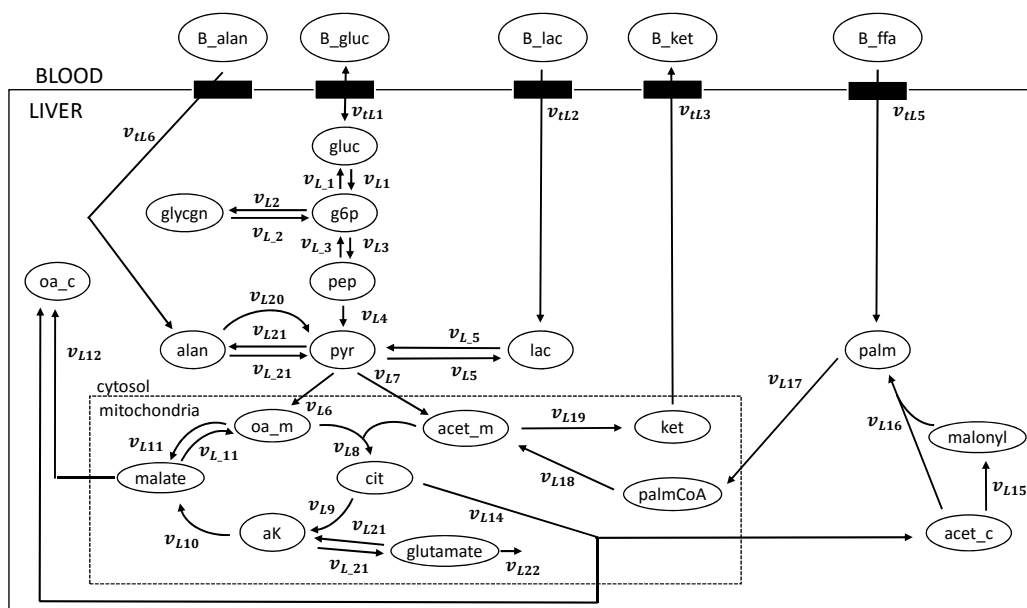


Figure 3.5: **Liver compartment of the Xu model.** Schema showing the metabolites and reaction rates for the liver compartment in the Xu model [3].

3.1. Original models and validation of model description

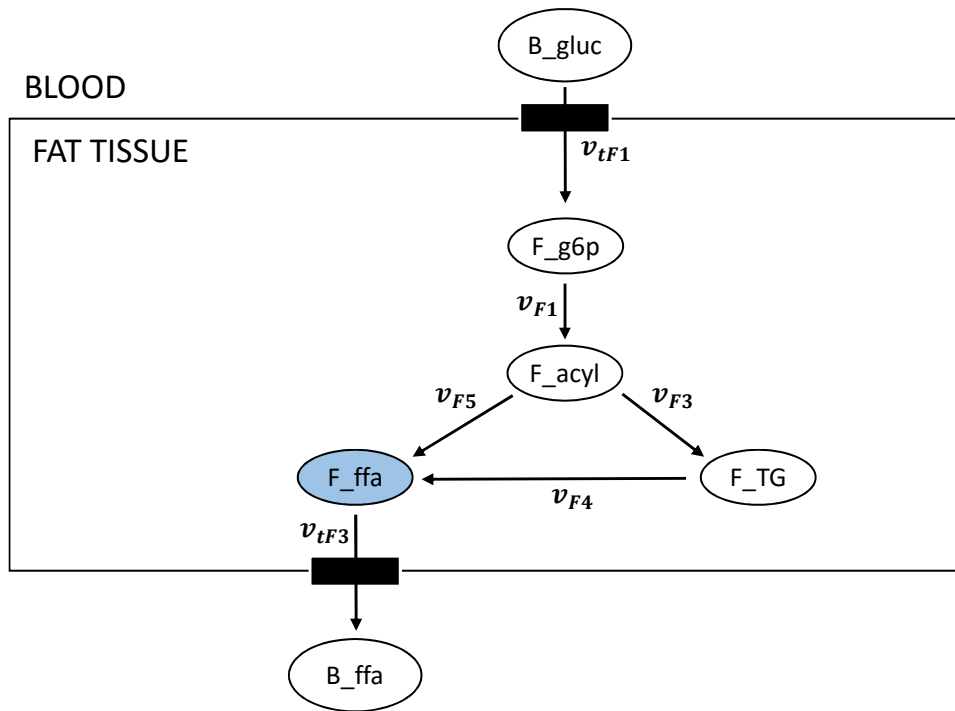


Figure 3.6: **Adipose tissue compartment of the Xu model.** Schema showing the metabolites and reaction rates for the adipose tissue compartment in the Xu model [3]. The blue metabolite for free fatty acids in the adipose tissue (F_{FFA}) is fixed in the model.

3.1. Original models and validation of model description

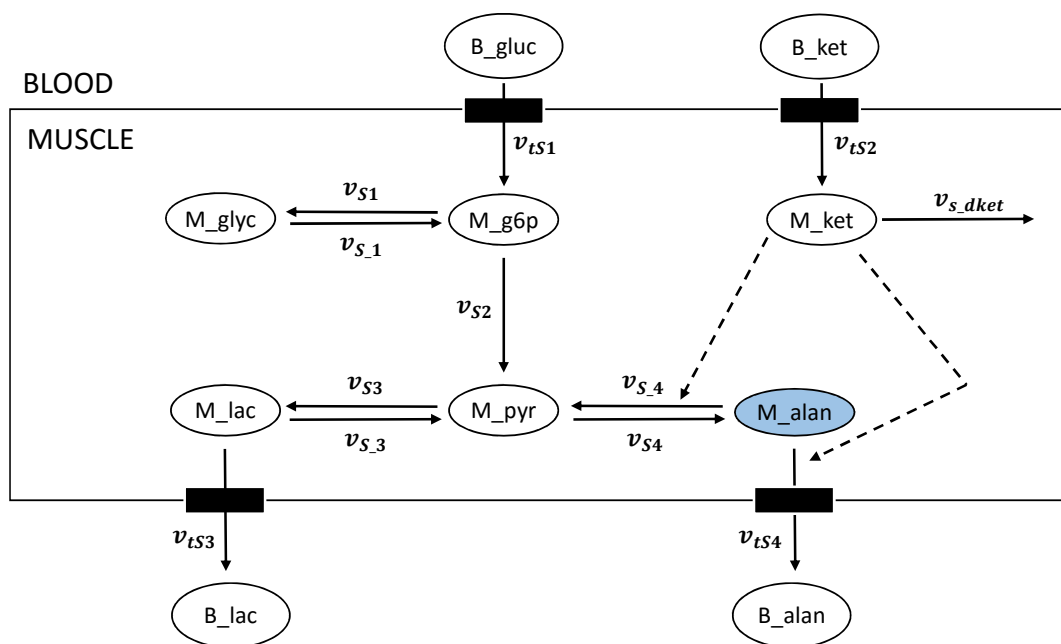


Figure 3.7: **Muscle compartment of the Xu model.** Schema showing the metabolites and reaction rates for the muscle compartment in the Xu model [3]. The blue metabolite for muscle alanine M_{alan} is fixed in the model.

The Xu model incorporates the effects of the two hormones insulin and glucagon on blood glucose. There are two separate scenarios that can be modelled, namely fed and fasting, depending on the glycogen stores in the liver. In the model, the switch between fed and fasting states is controlled by an "injection" of glucose into the blood. The rate of injection is called v_{feed} . A constant v_{feed} leads to a large glycogen pool whereas $v_{feed} = 0$ leads to glycogen depletion. For constant glucose input $v_{feed} = k_f$. In Xu et al. [3], a simulation is shown for the scenario where there is an initial glucose input ($k_f = 0.5$ mM/min), followed by a decay function for 250 minutes, and a final resumed feeding rate of $k_f = 1.4$ mM/min. We successfully reproduced this simulation as shown in Figure 3.8 (see Figure S5 in the supplementary information for Xu et al. [3]).

3.1. Original models and validation of model description

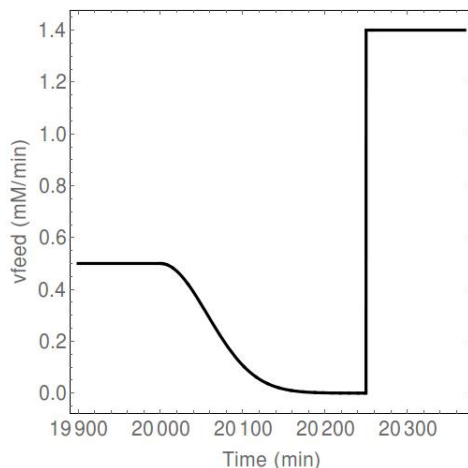


Figure 3.8: **The glucose influx rate of the Xu model.** The three-step glucose influx rate v_{feed} in a fed liver from Xu et al. [3] is shown: first there is constant feeding of 0.5 mM/min for 20000 min, followed by a decay function for 250 min and a resumed feeding of $k_f = 1.4$ mM/min.

Figure 3.9 shows two reproduced plots from Xu et al.[3] for a fed and fasted liver. These results can also be seen on JWS Online (<http://jjj.bio.vu.nl/database/xu>) by plotting the assignment rules GPaPlot and GSaPlot.

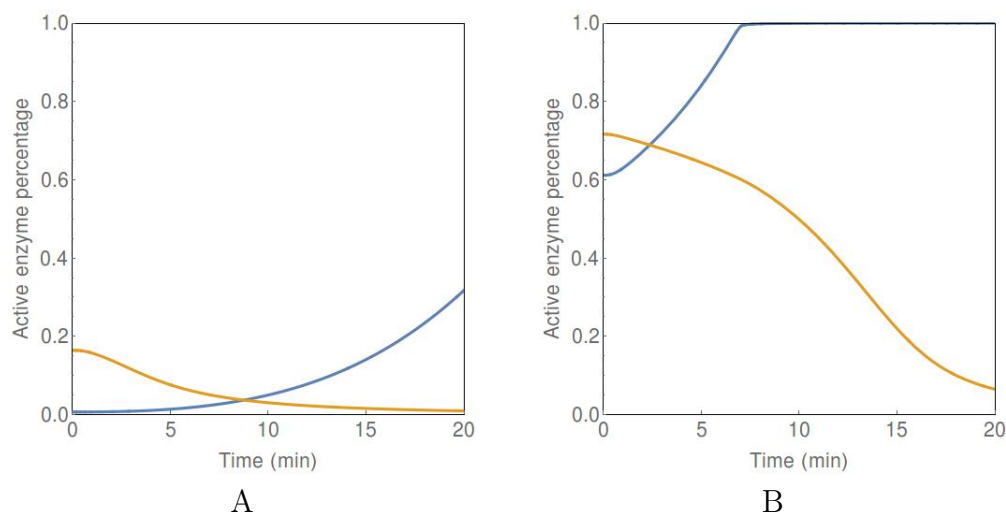


Figure 3.9: **Validation of the coded Xu model.** Verification of two of the plots in our coded model description that are identical to those in Figure 9 of Xu et al.[3]. Glycogen synthase (GSa) activity in blue and glycogen phosphorylase (GPa) activity in orange in a fed liver (A) and fasted liver (B) for $k_f = 1.4$ mM/min.

In this section we presented the three original models that have been chosen for the multi-level whole body glucose metabolism model in malaria patients. Initial validations of our model descriptions for the parasite and red blood cell model are in

3.1. Original models and validation of model description

agreement with the published results for each model. Furthermore we have shown that we were able to successfully code and reproduce figures from the Xu et al. [3] model.

3.2 Building the parasitized RBC culture model

During the erythrocytic stage of malaria, the *Plasmodium falciparum* parasite invades the erythrocyte. In order to model this parasitised red blood cell, the red blood cell and parasite model must be combined. Linking mathematical models is not as simple as combining the species, parameters, differential equations, etc. Challenges occur due to models being in different units, modelling formats and models having different naming conventions. Furthermore, the level of detail of mechanistic models can create computational difficulties.

The Mulquiney & Kuchel model was constructed in units of M/s while the Penkler model is in units of fmol/min. This section describes the changes that had to be made to the red blood cell model to allow for linking with the parasite model. Du Toit et. al. [2] described the fundamentals of building the parasitised RBC model. In this chapter the units of the parasitised RBC model were checked (Section 3.2.1 and Section 3.2.3), a new glucose transporter was added to the red blood cell model (Section 3.2.2) and lastly the parasitised RBC model was extended (Section 3.2.4) to allow for a better description of the parasitised red blood cell culture by including an uninfected red blood cell compartment, which is more representative of blood at the level of the whole body in a malaria infected individual.

3.2.1 Building the red blood cell model (Mulquiney & Kuchel model) with new units

Mathematical models are not always formulated in the same units. Unit consistency is necessary for models to be linked so that the variables in each sub-model are directly relatable. In addition, quantity or concentration units need to be compatible with the units of the parameters or constants in the rate equations. Furthermore, due to the time stepping nature of numerical integration the time scales of the separate models to be merged need to be the same at least at the level of the differential equations. Changing the unit descriptions of a model can be challenging, especially when models are large and contain a great amount of detail.

The rates in the Mulquiney & Kuchel model were modelled in units of concentration per time (molar per second). Mulquiney & Kuchel introduced a volume ratio in the stoichiometry of transport reactions (lactate transporter, pyruvate transporter, phosphate transporter) to account for different volume sizes of intracellular and extracellular compartments. This creates complications if we want to alter volumes dynamically, by for example modelling the growing parasite volume over time, as it changes the stoichiometry. Therefore these volume ratios were removed and all the rate equations converted to amount per time units (fmol/s) as described in Equation (3.1.2). In Du Toit [2] the volumes were explicitly modelled in fL using a volume of 90 fL [58] for a red blood cell, while the externals (pyruvate, lactate and inorganic phosphate) were scaled according to an incubation volume of 129 fL (representative of the incubation volumes used in their study [2]). With this rate unit change, the metabolite unit in the rate equations correspondingly changes to fmol amounts. In addition all initial values were multiplied by 90 fL to convert from

3.2. Building the parasitized RBC culture model

a molar concentration to a fmol amount. The parameter T_{srbc} was also introduced into all the rate equations to convert from seconds to minutes by multiplying by 60 so that the final rate unit was fmol/min. Lastly annotation changes were made to the red blood cell model (names of variables and rate equations) to make different compartments in the merged model more distinguishable.

3.2.2 Adding a glucose transport to the new unit red blood cell model

The original Mulquiney & Kuchel model did not include a kinetic rate equation for the glucose transporter and the reaction was assumed to be in equilibrium. It was essential to add a mechanistic equation for red blood cell glucose transport as it can play an important role in the glycolytic flux of the infected red blood cell. In Du Toit et al. [2] the glucose transport rate equation that was used in the Holzhütter model [59] was chosen to extend the red blood cell model with a glucose transport reaction. However, we discovered the RBC glucose transporter by Potts & Kuchel [60] which we decided to use as it was from the same research group that constructed the glycolytic model and made use of experimentally determined parameters.

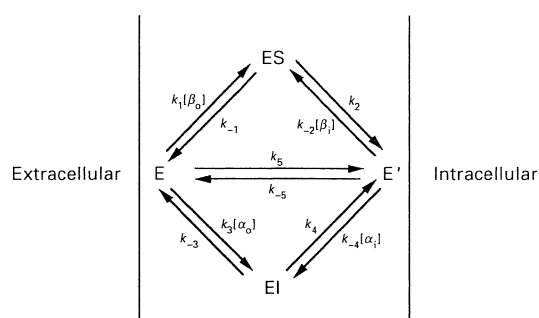


Figure 3.10: **Reaction scheme for the Potts & Kuchel [60] glucose transporter.** Either α or β glucose is transported across the transport membrane. ES and EI represent single carrier-substrate complexes while the forms of the carrier, with binding sites exposed to the extra-cellular and intra-cellular sides of the membrane, are denoted with E and E' respectively.

The Potts & Kuchel [60] rate equation is based on experimental observations and considers the binding of the two different anomers (α and β) of glucose to the integral membrane protein which transports glucose in and out of the red blood cell. Potts & Kuchel derived this rate equation using the King Altman method [61] (a scheme can be seen in Figure 3.10). According to Neuman [62] 36 % of the equilibrium mixture for D-glucose is the α anomer and 64 % consists of the β anomer.

Since most models just include glucose (not the different anomer forms) for this work it was assumed that 0.36 (glc_{α}) of the blood glucose goes via the transport route for α -glucose while the other 0.64 ($1 - glc_{\alpha}$) is transported via the β -glucose route with a different binding affinity. Additionally it was assumed that these two

3.2. Building the parasitized RBC culture model

routes are reversible and symmetrical, with the use of Equation 1 and 2 in Potts & Kuchel [60] the following equations were obtained:

$$v_{\alpha} = \frac{V_{\max\alpha} \cdot \alpha_o}{K_{\alpha} + \frac{K_{\alpha}}{K_{\beta}} \beta_o + \alpha_o} - \frac{V_{\max\alpha} \cdot \alpha_i}{K_{\alpha} + \frac{K_{\alpha}}{K_{\beta}} \beta_i + \alpha_i} \quad (3.2.1)$$

$$v_{\beta} = \frac{V_{\max\beta} \cdot \beta_o}{K_{\beta} + \frac{K_{\beta}}{K_{\alpha}} \alpha_o + \beta_o} - \frac{V_{\max\beta} \cdot \beta_i}{K_{\beta} + \frac{K_{\beta}}{K_{\alpha}} \alpha_i + \beta_i} \quad (3.2.2)$$

where $\beta = 1 - \alpha$ and K_{β} and K_{α} were determined assuming equilibrium conditions. The first term in v_{α} is the rate at which glucose outside of the red blood cell is transported into the red blood cell. The second negative rate in v_{α} is the rate for glucose moving from within the red blood cell back into the blood. The two terms for v_{β} can be explained in the same way. From Potts & Kuchel [60] K_{α} and K_{β} are given as 8.3 mM and 7 mM at 37 °C. The K values were chosen for 37 °C (and not the alternatives at 34 °C) as this temperature is closer to the physiological reference state for body temperature of a healthy individual (usually between 36.5 °C – 37.5 °C [63]). These K values were then converted to molar concentrations by dividing by 1000. Lastly the V_{\max} was assumed to be the same for both the α and β -glucose anomers and was determined by Potts & Kuchel [60] to be 33 mmol/s/litre of RBCs. Since the other Vmax values of the RBC enzymes in the new unit red blood cell model are in M/s, converting the glucose transporter V_{\max} would be beneficial. The Mulquiney & Kuchel model includes a parameter called alpha (called AlphaCellWaterFraction in the new unit red blood cell model) that describes the fraction of volume of cytosol (in litres) to the volume of a red blood cell (in litres), namely 0.7. The parameter Tsrbc is included to convert from seconds to minutes. Therefore multiplying the time-scaling factor Tsrbc with the V_{\max} we have

$$\text{VRBCvGLCTransport} = \text{Tsrbc} \frac{33 \text{ mmol}}{\text{s} \cdot \text{RBC}}$$

resulting in

$$\begin{aligned} &= \frac{\text{Time scaling factor}}{\frac{60 \text{ s}}{\text{min}}} \cdot \frac{\overbrace{33 \text{ mmol}}^{V_{\max}}}{\text{s} \cdot \text{L of RBCs}} \cdot \frac{\overbrace{1 \text{ L of RBCs}}^{1/\text{cytosolic ratio of RBCs}}}{0.7 \text{ L cytosol} \cdot 1000} \\ &= 2.82 \frac{\text{M}}{\text{min}} \end{aligned} \quad (3.2.3)$$

The glucose transporter rate equation was converted from concentration units to amount per time units in a similar way as mentioned above, to be compatible with the rate units of the new unit red blood cell model.

3.2.3 Combining the parasite and new unit RBC model (with glucose transporter)

The parasite (Penkler) and red blood cell (Mulquiney & Kuchel) models were combined in a previous study (Du Toit model [2]) to describe a parasitized RBC. In the

3.2. Building the parasitized RBC culture model

combining of these two models, Du Toit [2] had to make certain changes in order to link them. The two metabolites that provide the linking points are red blood cell glucose and red blood cell lactate. In the Penkler model these two metabolites were external to the parasite cell and modelled as fixed parameters. Since the new unit red blood cell model is in the same units as that of the parasite model, the combining of the models only required a change in the parasite glucose and lactate transporters. These transporters in the parasite model were changed by removing the source (external glucose) and replacing it with red blood cell glucose. Similarly, the external lactate sink in the parasite model was changed to red blood cell lactate from the new unit red blood cell model. This implementation was reproduced on JWS Online, as well as the merging of all the reactions, parameters, initial values, rules, etc. Figure 3.11 shows the combined schema of the parasite and red blood cell model. For the scope of this work it was necessary to confirm the merging of the models done by Du Toit [2] (and add a more appropriate glucose transporter as discussed in Section 3.2.2).

In the combined new unit red blood cell and parasite model glucose, pyruvate, lactate and phosphate can move across the red blood cell membrane. These metabolites that are external to the red blood cell are scaled to a fixed external volume (v_{Bld}). When the red blood cell and parasite models were linked, the parasitized red blood cell lactate flux was too low to explain the experimental data and therefore an additional multiplier was included in the red blood cell lactate transporter. Physiologically this can be explained by the parasite creating new permeability pathways (NPPs) in the red blood cell membrane [2, 64] allowing for lactate to move more freely into the bloodstream. In the parasitized RBC model the external metabolites can either be modelled as constants (model called `dutoit1`), or they can be unclamped to simulate a batch incubation experiment in which glucose is completely consumed (called `dutoit2`). These models were constructed by Du Toit [2] but in this thesis a different glucose transporter was adopted. Through inspection of the code for the transporter steps and analysing the steady states the merging of these models was checked and found to be correct.

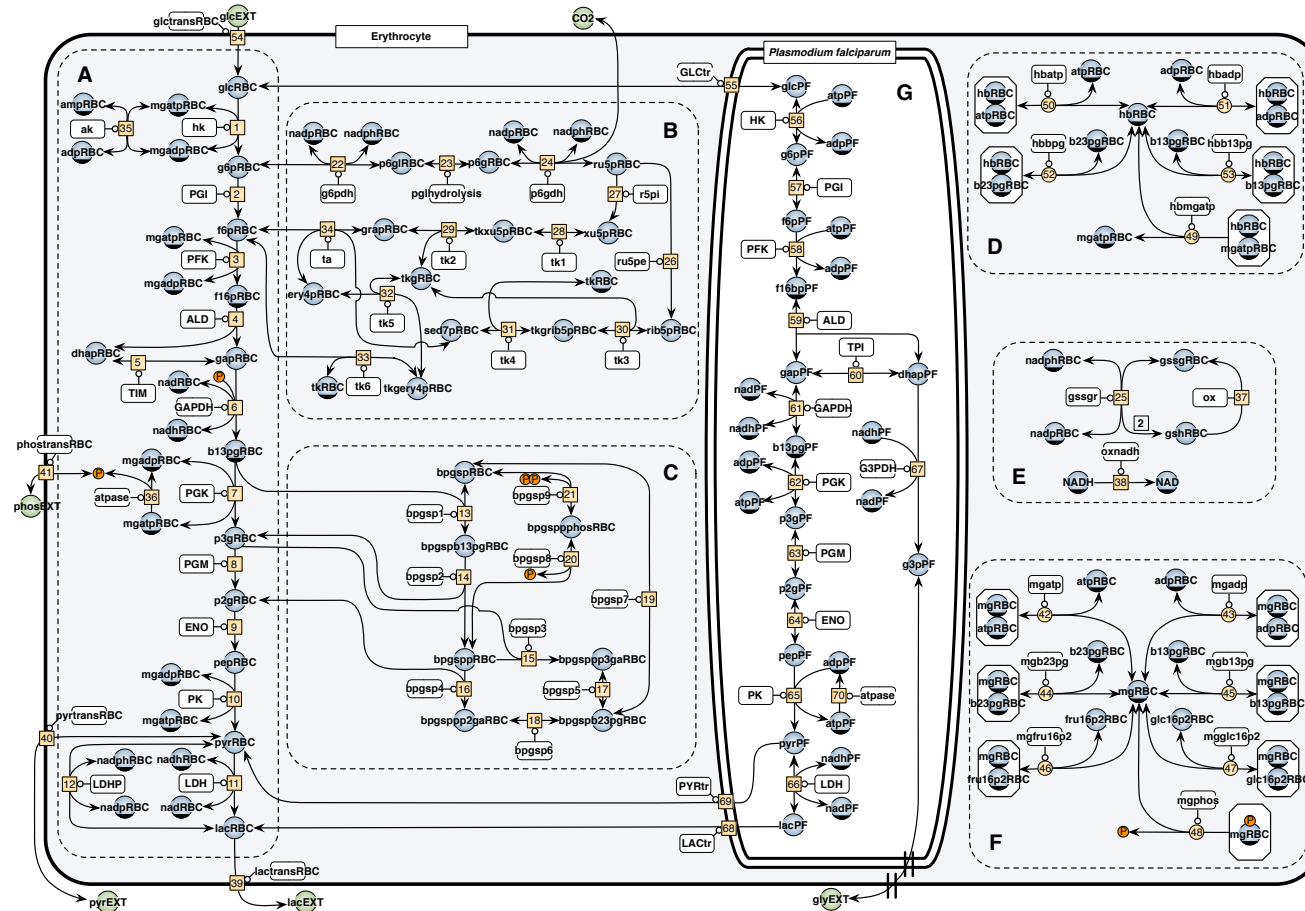


Figure 3.11: Schema from Du Toit [2] showing the combined *Plasmodium falciparum* and red blood cell model. Orange blocks show enzyme catalyzed reactions, blue circles are the metabolites (each have an ODE), green circles represent the fixed metabolites and orange circles represent inorganic phosphate for the steady state version of the model.

3.2.4 Building the parasitized RBC culture model (dutoit3)

Thus far we have confirmed that the merging of the parasite and new unit red blood cell models was correctly implemented. The parasitized RBC model can be used to understand what happens to the red blood cell after invasion by the *Plasmodium falciparum* parasite, however a malaria culture typically includes a mixture of infected and uninfected red blood cells. Also, according to Metha [34] malaria infected red blood cells can down-regulate the glucose flux of uninfected red blood cells. The importance of including uninfected red blood cells in the model was two-fold. Firstly, the incorporation of the uninfected red blood cells would allow for further investigations into understanding the effect that the parasite infected red blood cells have on the uninfected red blood cells. Secondly, with the aim to develop a whole body model it would be more realistic to have a total red blood cell compartment that consists of uninfected and infected red blood cells. Figure 3.12 shows a schema of the two separate red blood cell compartments.

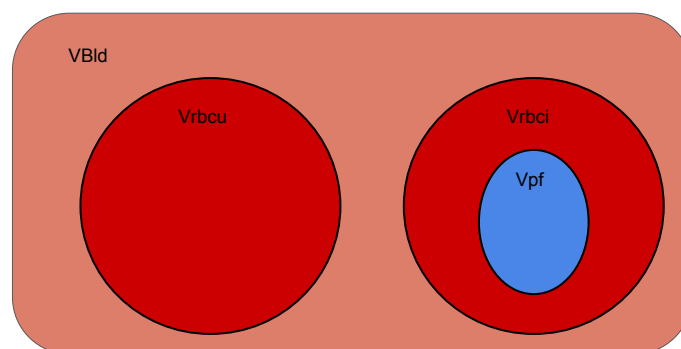


Figure 3.12: **Scheme showing the different volume compartments in the parasitized red blood cell culture model.** The blood volume v_{Bld} , the uninfected RBC volume V_{rbcu} , the infected RBC volume V_{rbci} , and the parasite volume V_{pf} . Each volume compartment can consist of multiple cells, but is simulated as a total volume.

Constructing an infected red blood cell compartment (volume represented by V_{rbci}) and uninfected red blood cell compartment (volume represented by V_{rbcu}) requires the use of the new unit Mulquiney & Kuchel model for the uninfected part and the parasitized RBC model (dutoit2) for the infected part. In the current context, the uninfected and infected red blood cell volumes need to sum up to a total red blood cell volume as expected in the human body. For simplicity the current discussion only considers one uninfected red blood cell and one infected red blood cell. When the red blood cell volume is scaled up to the whole body level (Section 3.3.1) this is changed to represent multiple red blood cells (infected and uninfected) on the whole body level.

The volume of the infected RBC compartment is calculated by using the parasitaemia to determine the infected fraction of the total RBC volume (see Equations 3.2.4). Modelling the total V_{rbc} using these two compartments also makes it easy

3.2. Building the parasitized RBC culture model

to move between the extremes of 0% and 100% parasitaemia (called *par*) with the simple implementation of a parameter called *parMulti* which switches between 0 (healthy individual) or 1 (malaria infected individual). The parasite volume depends on how many red blood cells are infected (*Vrbc_i*) and on the ratio of volumes of one trophozoite parasite (24-40 fL according to Du Toit et al. [2], typically 28 fL) to one red blood cell (90 fL according to McLaren et al. [58]) resulting in the parameter *trophToRBC* equalling 28/90.

$$\left. \begin{aligned} Vrbc &= 90 \text{ fL} \\ Vrbc_u &= Vrbc - \text{parMulti} \cdot Vrbc_i \\ Vrbc_i &= Vrbc \cdot \text{par} \\ V_{pf} &= \text{trophToRBC} \cdot Vrbc_i \end{aligned} \right\} \quad (3.2.4)$$

The rates and metabolites of the new unit red blood cell model were added to the parasitized RBC model to describe the uninfected and infected RBC compartments. The parasitized RBC model includes a number of definitions of parameters in terms of other parameters and variables. As such, these also needed to be duplicated and renamed to correspond to *Vrbc_i* and/or *Vrbc_u* explicitly. For example, the model would now consist of a *glcRBC* (glucose in the uninfected red blood cells) and *glcRBC_i* (glucose in the infected red blood cells). All infected red blood cell rates and parasite rates include an additional parameter *parMulti* resulting in these reactions becoming zero (as well as *Vrbc_i*) when parasitaemia is zero. Similarly a parameter called *unparMulti* was added to the uninfected rate equations that can be set to zero to allow for 100 % parasitaemia to be modelled. The blood *glcEXT*, *lacEXT*, *phosEXT*, *pyrEXT*, *glyEXT* and *Co2RBC* (and *Co2RBC_i*) still remain external and shared between both the infected and uninfected red blood cells. The glucose and lactate transporters for the red blood cell were the linking points of the two models. For example, *glcEXT* (which represents the glucose in the blood) can either move into the uninfected red blood cell compartment or into the infected red blood cell compartment.

The parasitized RBC culture model (*dutoit3*) contains a number of moiety conserved cycles. Mathematically they appear in the linear dependence of metabolite differential equations on one another. Consider the cycle in Figure 3.13 where A is converted to B (by *v1*) and then back to A (by *v2*), then

3.2. Building the parasitized RBC culture model

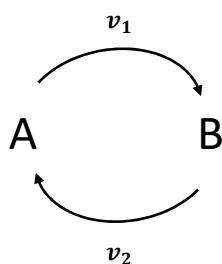


Figure 3.13: **Scheme of a moiety cycle.** The metabolite A is converted to B by v_1 and then back to A by v_2 .

$$\frac{dA}{dt} = v_1 - v_2 \quad (3.2.5)$$

$$\frac{dB}{dt} = -v_1 + v_2 \quad (3.2.6)$$

The initial values for A and B determine $A+B$ for all time in the system. Usually these conservation relations are modelled in terms of concentrations and there is not a general solution to modelling these cycles in terms of amounts (as required by Penkler and Mulquiney & Kuchel models) but here we assume that the amount of a species that is present in a volume should be adjusted with the increased volume size - a larger volume would contain a larger amount of metabolite to ensure the same concentration. We assume that the total moiety concentration is conserved over growing volumes as we do explicitly include biosynthesis moiety concentrations in the model. To account for this in the model description there are initial assignments which scale all the metabolite amounts to their respective compartment volumes.

Adaptations to initial assignments required the uninfected red blood cell metabolites to be scaled to a volume of V_{rbcu} and for the infected RBC scaling by the infected RBC volume V_{rbc_i} to obtain initial values in units of fmol. The initial value for each metabolite consists of a molar concentration which is multiplied by V_{rbcu} or V_{rbc_i} (in fL) to obtain the metabolite in units of fmol amounts in the relevant compartment.

3.3. Model adaptations, scaling up and linking the models to represent the whole body level

3.3 Model adaptations, scaling up and linking the models to represent the whole body level

The description of how the Xu et al. model (in units of mM/min) and parasitized RBC culture model (in units of fmol/min) were combined to explain glucose metabolism in malaria infected individuals will be divided into two sections. First, how the aspects (such as volumes) of the parasitized RBC culture model had to be modified to be representative of a whole body level and second the adaptations that had to be made to the transporters to link the models with consistent units. Figure 3.14 shows a schema of the different compartments of the whole body model including the red blood cell structure that will be added in this section to allow for the modelling of disease states in malaria infected individuals.

3.3. Model adaptations, scaling up and linking the models to represent the whole body level

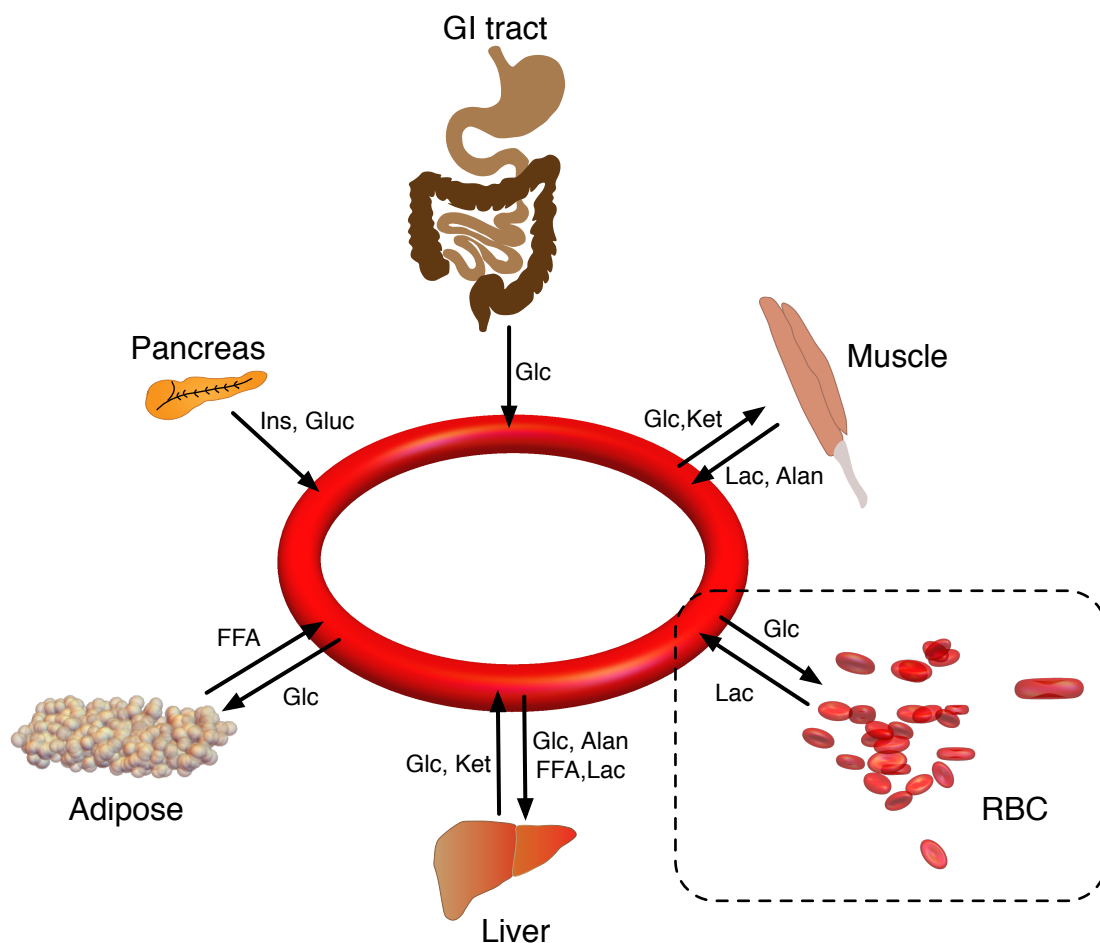


Figure 3.14: Scheme of the green1 model which consists of the whole body model [3] combined with the compartment for the red blood cells (namely the parasitized RBC culture model). This figure was originally published in [<http://www.biochemsoctrans.org/content/43/6/1157>, Jacky L. Snoep, Kathleen Green, Johann Eicher, Daniel C. Palm, Gerald Penkler, Francois du Toit, Nicolas Walters, Robert Burger, Hans V. Westerhoff, David D. van Niekerk, Biochemical Society Transactions, 2015].

3.3.1 Scaling up the parasitized RBC culture model volumes to represent the whole body level

In the parasitized RBC model (Section 3.2.3) only one red blood cell and parasite cell were considered (i.e. one infected red blood cell). An accurate description of the whole body level would require the scaling up from one pRBC to multiple red blood cells infected and uninfected (as seen in the body). In the parasitized RBC culture model (Section 3.2.4) the division of the red blood cell compartment into an infected and uninfected part was modelled in such a way to make provision for scaling up to the number of red blood cells on the whole body level.

There are different ways in which the total red blood cell compartment can be

3.3. Model adaptations, scaling up and linking the models to represent the whole body level

modelled to represent the red blood cell population in an individual. Ideally an accurate description of the mechanistic biological phenomenon would model the red blood cells individually. This would entail having a Mulquiney & Kuchel [10] model for each red blood cell present in the body. The computational power required to model/simulate such a large and complex model would be a restriction. As metabolites inside the red blood cell see the same external environment (the same concentrations of blood glucose and lactate) an alternative is to lump all of the red blood cells into one compartment that is able to represent the total volume of RBCs at the whole body level. One approach to achieve this is to take the average number of red blood cells that can be expected for a human and multiply it by the volume that is expected for one red blood cell (90 fL according to McLaren et al. [58]). Initially this approach was considered but since the average number of RBCs in a human is between $2 - 3 \cdot 10^{13}$ [65] it created a 10^{13} error range for the red blood cell volume. Another option is to follow the same approach that was used in the building of the parasitized RBC culture model by allowing for the grouping of all infected red blood cells to be in the Vrbc_i compartment and the uninfected red blood cells to be in the Vrbc_u compartment (with the incorporation of the hematocrit).

On average a human has 6.24 L of blood, assuming a volume of distribution of 0.08 L/kg [66] and an average body weight of 78 kg [39]. This 6.24 L consists primarily of plasma and red blood cells. The fraction of total blood volume occupied by red blood cells is known as the hematocrit. Mulquiney & Kuchel [10] used a hematocrit of 0.5, therefore by extension our model assumes the same. The parameters for the total blood volume and hematocrit are called v_{totblood} and HCT respectively. The volume of red blood cells is then determined by $v_{\text{totblood}} \cdot \text{HCT}$ and is then converted to fL by multiplying by 10^{15} . To accommodate for the volume of cell organelles a factor called AlphaCellWaterFraction from Mulquiney & Kuchel [10] is included. The total cytosolic red blood cell compartment volume is therefore given by:

$$\text{Vrbc} = v_{\text{totblood}} \cdot \text{HCT} \cdot \text{AlphaCellWaterFraction} \cdot 10^{15} \text{ fL} \quad (3.3.1)$$

The volumes for the parasite infected red blood cell compartment (Vrbc_i) and uninfected red blood cell compartment (Vrbc_u) sum to total red blood cell volume Vrbc. The infected red blood cell compartment is determined by the level of parasitemia while the parasite volume depends on how many red blood cells are infected. These volume equations can be seen in Equation (3.2.4).

The volume of blood in litres that does not consist of red blood cells (considered to be all plasma in this study) can be represented by the expression $v_{\text{totblood}} \cdot (1.0 - \text{HCT})$. This is the volume in which the metabolites external to the red blood cells are dissolved. From this an equation for blood plasma vBld is derived to be

$$\text{vBld} = v_{\text{totblood}} \cdot (1.0 - \text{HCT}) \cdot 10^{15} \text{ fL} \quad (3.3.2)$$

3.3. Model adaptations, scaling up and linking the models to represent the whole body level

3.3.2 Modifications of the glucose and lactate transporters to link the parasitized RBC culture model with the whole body model

Using the parasitized red blood cell culture model to represent all red blood cells in a malaria infected human host not only requires a change in volumes, but also an adjustment of the transport equations that will link to the whole body model. Extracellular glucose and lactate were identified as the species that would link to the whole body model. These two species are equivalent to the blood glucose (B_{gluc}) and blood lactate (B_{lac}) in the whole body model. The combining of these models was done on the JWS Online platform to allow for full SBML (the standard specification format for Systems Biology models) compliance. Furthermore having the final combined model on JWS Online allows for other outputs in languages such as Mathematica and Python. It is advantageous to combine the models in the browser as it is user-friendly and the Xu et al. [3] model was already added the curated JWS Online database earlier in the current study.

A derivative of the parasitized RBC culture model was created on JWS Online and the compartment structures, species, initial assignments, rate equations, parameters, assignment rules and unit definitions from the whole body model were added. The event for reducing glycogen accumulation in the liver present in the Xu et al. [3] model was omitted as the glucose influx was assumed to be a low constant to reduce model complexity.

Table 3.3: Initial units for components of each model.

Model	Rate	Metabolites	Rate constant or V_{max}	Volumes	Km	Typical rate expression
Xu [3]	$\frac{\text{mM}}{\text{min}}$	mM	$\frac{1}{\text{min}}$	-	-	rate \propto rate constant \cdot metabolite
dutoit3	$\frac{\text{fmol}}{\text{min}}$	fmol	$\frac{\text{M}}{\text{min}}$	fL	M	rate $\propto V_{\text{max}} \cdot \text{Volume} \cdot \frac{\frac{\text{metabolite}/\text{Volume}}{\text{Km}}}{(1 + \frac{\text{metabolite}}{\text{Volume} \cdot \text{Km}})}$

When modelling combined systems of differential equations it is possible to have sub-systems in different units provided that the linking species in the rate equations between systems are seen in the correct units consistent with the respective system parameters and that the time units are the same (for numerical integration). The dutoit3 model (parasitized RBC culture model) has rate units of fmol/min but the whole body is in units of mM/min (see Table 3.3). The models were initially linked in this way i.e. separate transport equations were used for RBC and whole body that converted B_{gluc} and B_{lac} to correct units on the fly. This can best be explained by showing the differential equations and transporter rates. The blood glucose and

3.3. Model adaptations, scaling up and linking the models to represent the whole body level

red blood cell glucose differential equations looked as follows

$$\begin{aligned} B'_{\text{gluc}}(t) &= v_{\text{feed}} - v_{\text{tF1}} - v_{\text{tL1}} - v_{\text{tS1}} - v_{\text{d_Bgluc}} - v_{\text{WBvGLCTransport}} \\ \text{glcRBC}'(t) &= v_{\text{RBCvGLCTransport}} - v_{\text{RBCvHK}} \end{aligned}$$

where $v_{\text{RBCvGLCTransport}}$ is the red blood cell glucose transport in units of fmol/min while the duplicated red blood cell glucose transport $v_{\text{WBvGLCTransport}}$ is in mM/min even though they represent exactly the same transport process. Each transport is in the same units as the ODE in which it appears. Expanding on the unit description for the glucose transporters we have

$v_{\text{RBCvGLCTransport}}$:

$$\begin{aligned} &= \text{TsRBC} \cdot \text{Vrbcu} \cdot \left(\frac{\text{glc_alpha} \cdot \text{VRBCvGLCTransport} \cdot \frac{\text{B_gluc}(t)}{1000}}{\left(\frac{(1-\text{glc_alpha}) \cdot \frac{\text{B_gluc}(t)}{1000} \cdot \text{k_alpha}}{\text{k_beta}} + \text{k_alpha} + \text{glc_alpha} \cdot \frac{\text{B_gluc}(t)}{1000} \right)} \right. \\ &\quad \left. - \frac{\text{glc_alpha} \cdot \text{VRBCvGLCTransport} \cdot \text{glcRBC}(t)}{\text{Vrbcu} \cdot \left(\frac{(1-\text{glc_alpha}) \cdot \text{glcRBC}(t) \cdot \text{k_alpha}}{\text{k_beta} \cdot \text{Vrbcu}} + \text{k_alpha} + \frac{\text{glc_alpha} \cdot \text{glcRBC}(t)}{\text{Vrbcu}} \right)} + \dots \right) \end{aligned}$$

Units of $v_{\text{RBCvGLCTransport}}$:

$$\begin{aligned} &= \frac{\text{s}}{\text{min}} \cdot \text{fL} \cdot \left(\frac{1 \cdot \text{M/s} \cdot \frac{\text{mM}}{1000}}{\left(\frac{1 \cdot \frac{\text{mM}}{1000} \cdot \text{M}}{\text{M}} + \text{M} + \frac{\text{mM}}{1000} \right)} - \frac{1 \cdot \text{M/s} \cdot \text{fmol}}{\text{fL} \cdot \left(\frac{1 \cdot \text{fmol} \cdot \text{M}}{\text{M} \cdot \text{fL}} + \text{M} + \frac{1 \cdot \text{fmol}}{\text{fL}} \right)} + \dots \right) \\ &= \frac{\text{s}}{\text{min}} \cdot \text{fL} \cdot \left(\frac{1 \cdot \text{M/s} \cdot \text{M}}{\text{M}} - \frac{1 \cdot \text{M/s} \cdot \text{fmol}}{\text{fL} \cdot (\text{M})} + \dots \right) \\ &= \frac{\text{s}}{\text{min}} \cdot \text{fL} \cdot \left(\frac{\text{M}}{\text{s}} \right) \\ &= \frac{\text{fmol}}{\text{min}} \end{aligned} \tag{3.3.3}$$

and $v_{\text{WBvGLCTransport}}$:

$$\begin{aligned} &= \text{TsRBC} \cdot \text{Vrbcu} \cdot \frac{1000}{\text{vBld}} \cdot \left(\frac{\text{glc_alpha} \cdot \text{VRBCvGLCTransport} \cdot \frac{\text{B_gluc}(t)}{1000}}{\left(\frac{(1-\text{glc_alpha}) \cdot \frac{\text{B_gluc}(t)}{1000} \cdot \text{k_alpha}}{\text{k_beta}} + \text{k_alpha} + \text{glc_alpha} \cdot \frac{\text{B_gluc}(t)}{1000} \right)} \right. \\ &\quad \left. - \frac{\text{glc_alpha} \cdot \text{VRBCvGLCTransport} \cdot \text{glcRBC}(t)}{\text{Vrbcu} \cdot \left(\frac{(1-\text{glc_alpha}) \cdot \text{glcRBC}(t) \cdot \text{k_alpha}}{\text{k_beta} \cdot \text{Vrbcu}} + \text{k_alpha} + \frac{\text{glc_alpha} \cdot \text{glcRBC}(t)}{\text{Vrbcu}} \right)} + \dots \right) \end{aligned}$$

Units of $v_{\text{WBvGLCTransport}}$:

$$\begin{aligned} &= \frac{\text{s}}{\text{min}} \cdot \text{fL} \cdot \frac{1000}{\text{fL}} \cdot \left(\frac{1 \cdot \text{M/s} \cdot \frac{\text{mM}}{1000}}{\left(\frac{1 \cdot \frac{\text{mM}}{1000} \cdot \text{M}}{\text{M}} + \text{M} + \frac{\text{mM}}{1000} \right)} - \frac{1 \cdot \text{M/s} \cdot \text{fmol}}{\text{fL} \cdot \left(\frac{1 \cdot \text{fmol} \cdot \text{M}}{\text{M} \cdot \text{fL}} + \text{M} + \frac{1 \cdot \text{fmol}}{\text{fL}} \right)} + \dots \right) \\ &= \frac{\text{s}}{\text{min}} \cdot \text{fL} \cdot \frac{1000}{\text{fL}} \cdot \left(\frac{1 \cdot \text{M/s} \cdot \text{M}}{\text{M}} - \frac{1 \cdot \text{M/s} \cdot \text{fmol}}{\text{fL} \cdot (\text{M})} + \dots \right) \\ &= \frac{\text{s}}{\text{min}} \cdot \text{fL} \cdot \frac{1000}{\text{fL}} \cdot \left(\frac{\text{M}}{\text{s}} \right) \\ &= \frac{\text{mM}}{\text{min}} \end{aligned} \tag{3.3.4}$$

3.3. Model adaptations, scaling up and linking the models to represent the whole body level

The duplication of the RBC glucose transporter (with units consistent with each respective model) was numerically unstable when the model was simulated on Mathematica 10.3. A possible solution to such numerical problems (such as machine precision errors) is to avoid having a combination of very small and large numbers in expressions that need to be integrated. This led to the conversion of the parasitized RBC culture model from fmol/minute to mmol/minute. Ideally, the whole body model should also be modelled in amounts which led to an unsuccessful initial attempt to convert the units of the whole body model to amounts. After closer inspection, it was found that the volumes in the Xu et al. [3] model were not well described (see Discussion). Since it is beyond the scope of this work to change the content of the Xu et al. [3] model the whole body rates were kept in units of mM/min.

Model descriptions for species, volumes and time units for dutoit3 therefore need to be in mmol, mL and min. Modifying the volumes to be in units of mL rather than fL is a simple adjustment by a factor of 10^{-12} . The initial assignments for the red blood cell and parasite metabolites are determined by a concentration (molar) multiplied by the respective volume compartments now in mL resulting in initial values in units of mmol. In the rate equations for the dutoit3 the species are explicitly divided by the volumes which now have units mL. This results in a reappearance of molar concentration values as required by the model parameters (e.g. Km values are in molar). The differential equations for these metabolites are in mmol per min resulting from the multiplication of V_{\max} values (in M/min) by volumes (in mL). Table 3.4 shows a summary of the converted units for the respective models.

Table 3.4: Final units for components of each model.

Model	Rate	Metabolites	Rate constant or V_{\max}	Volumes	Km	Typical rate expression
Xu [3]	$\frac{\text{mM}}{\text{min}}$	mM	$\frac{1}{\text{min}}$	-	-	rate \propto rate constant \cdot metabolite
dutoit3	$\frac{\text{mmol}}{\text{min}}$	mmol	$\frac{\text{M}}{\text{min}}$	mL	M	rate $\propto V_{\max} \cdot \text{Volume} \cdot \frac{\text{metabolite}/\text{Volume}}{\left(1 + \frac{\text{metabolite}}{\text{Volume} \cdot \text{Km}}\right)}$

To link the Xu and dutoit3 models the transporters (for glucose and lactate) need to be in the same units. A simple solution to overcome unit differences in rate equations (as determined by rate constants (in Xu model) and V_{\max} (in parasitized RBC culture model)) between models is to incorporate a conversion factor as seen in Equation (3.3.4). The conversion factor ω was created to change the whole body model unit descriptions of mM/min to mmol/min and is given by:

$$\omega = \frac{\text{vBld}}{1000}$$

3.3. Model adaptations, scaling up and linking the models to represent the whole body level

where initially vBld was modelled in fL and the division by 1000 was required to convert the rates between fmol and mM per minute. In the context of the changed units of the parasitized RBC culture model rates from fmol to mmol, vBld is modelled in mL.

The description of the conversion factor ω allows for the duplicated transport rates that are in whole body model to be written as

$$\begin{aligned} \text{vWBvGLCTransport} &= \frac{1}{\omega} \cdot \text{vRBCvGLCTransport} \\ &= \frac{1000}{\text{vBld}} \cdot \text{vRBCvGLCTransport} \\ &= \frac{1000}{\text{mL}} \cdot \frac{\text{mmol}}{\text{min}} \\ &= \frac{\text{mM}}{\text{min}} \end{aligned}$$

Similarly this construction was done for blood lactate and red blood cell lactate in the infected and uninfected RBC compartment. The modification of this model to include multiple transport rates required us to confirm that mass balance is still conserved in the system. This is shown in the next chapter (see Table 4.2).

3.3.3 Model adaptations made during the linking of the parasitised RBC and whole body model

Understanding disease states in malaria patients by combining existing mathematical models requires the analysis of model simulations. We are interested in knowing what happens to the steady state values of model variables such as blood glucose, blood lactate (indicative of disturbances in the homeostasis of these metabolites) as well as to the fluxes of transporters (indicative of increased flow of metabolites to and from compartments possibly linked to an increased metabolic burden on an organ). After merging the Xu et al. [3] model with the dutoit3 model (Section 3.3.1 and Section 3.3.2) it was discovered that not all metabolites reached a steady state (even for uninfected individuals). Initially it was thought that a possible reason for this could be that the time required for the combined model to reach a steady state is much longer due to differences in time scales of the separate models. However increasing the time of integration did not show different results. An alternative explanation for this unrealistic physiological behaviour of ever accumulating metabolites (i.e. lactate and glycogen levels in the liver) could be that we were using models, particularly the phenomenological Xu model, to describe physiological conditions for which it has not originally been constructed and validated. To avoid the accumulation of ever accumulating lactate concentration and glycogen stores in the liver two modifications were made.

Blood lactate is transported into the liver, after which it undergoes a multi-step metabolic process called the Cori-cycle that converts lactate back into glucose. The

3.3. Model adaptations, scaling up and linking the models to represent the whole body level

glucose is stored in the liver in the form of glycogen and is transported back into the blood stream as glucose during low blood sugar levels. Xu et al. [3] modelled the transport of blood lactate into the liver with a simple mass action rate law. However, it was noticed that a constant input of v_{feed} resulted in an accumulation of glycogen in the liver due to the lack of reversibility and product sensitivity of the lactate transporter. In an attempt to address the accumulation of both lactate and glycogen stores in the liver, it was decided that the hepatocyte transporter in the whole body model would have to be changed. A literature search on human liver metabolism highlighted a possible solution from the Virtual Liver Project[67].

The lactate hepatocyte transporter was adopted from the Virtual Liver Project, more specifically, Konig et al. [41]. While little is known about the hepatocyte lactate transporter in humans, this reversible Michaelis Menten equation is currently the only available option. In this equation the binding constant K_{mtL2} was described in units consistent with the original Xu model, namely 0.8 mM. The maximal velocity V_{mtL2} was modelled in $\mu\text{mol}/\text{kg}/\text{min}$ and converted to the unit of the other rate constants in Xu using the average kg weight per L of blood in humans as before (see Section 3.3.1). Therefore,

$$\begin{aligned} V_{\text{mtL2}} &= \frac{33 \mu\text{mol}}{\text{kg min}} \cdot \frac{\text{kg}}{0.08 \text{ L}} \cdot 10^3 \\ &= 0.4125 \frac{\text{mM}}{\text{min}}. \end{aligned}$$

The lactate liver transport is

$$\begin{aligned} v_{\text{tL2}} &= \frac{V_{\text{mtL2}} \cdot (B_{\text{lac}}(t) - \text{lac}(t))}{K_{\text{mtL2}} \cdot \left(\frac{B_{\text{lac}}(t)}{K_{\text{mtL2}}} + \frac{\text{lac}(t)}{K_{\text{mtL2}}} + 1 \right)} \\ \text{Units of } v_{\text{tL2}} &= \frac{\frac{\text{mM}}{\text{min}} \cdot (\text{mM} - \text{mM})}{\text{mM} \cdot \left(\frac{\text{mM}}{\text{mM}} + \frac{\text{mM}}{\text{mM}} + 1 \right)} \\ &= \frac{\text{mM}}{\text{min}} \end{aligned}$$

Xu et. al. [3] used a three step function (including a form of a decay function) to model the feeding rate of an individual. Their study was concerned with understanding the differences between fed and fasting states in terms of glycogen stores in the liver. For simplification purposes we assumed a constant feeding rate of 0.5 in the green1 model. Plotting the whole body metabolites over time it was seen that glycogen stores in the liver continued to show a continued accumulation despite the modifications made to the liver lactate transporter. This led to the investigation of the steady state value for blood glucose in the original Xu et al. [3] model. It was discovered that when setting v_{feed} to zero the steady state value for B_{gluc} was around 6.4 mM. The physiological reference state for blood glucose is around 5 mM [68], suggesting that the original whole body model predicts a higher steady state for blood glucose than biologically expected.

3.3. Model adaptations, scaling up and linking the models to represent the whole body level

A simple calculation was done to determine the average glucose consumption for an individual per day. The implementation of this calculated constant value, namely 0.68 mM/min and the inclusion of the parasitised RBC model with the whole body model with this adjusted value for v_{feed} did not solve the behaviour of glycogen seen in the liver.

Further investigation showed that two fixed parameters F_{FFA} (free fatty acids in the fat compartment) and M_{alan} (alanine in the muscle compartment) have a large effect on the blood glucose steady state which prompted the second modification that had to be made. This involved the determination of v_{feed} by manipulating two fixed species F_{ffa} , M_{alan} so that the original Xu model (with the new liver lactate transporter) reaches a blood glucose steady state as close to 5 mM as possible. Despite attempts made to have a more realistic feed rate, through optimisation it was found that by setting v_{feed} to 0.2 mM/min, $F_{\text{ffa}} = 0.029$ mM, and $M_{\text{alan}} = 0.0$ mM the most physiological relevant blood glucose concentration was obtained. Thereafter, these fixed values were adopted in the green1 model leading to steady state solutions for the metabolites allowing for simulation analysis to be done (discussed in the following chapter). It could be suggested that we could have made v_{feed} zero and then adjust F_{ffa} and M_{alan} to obtain a blood glucose steady state of 5 mM; however physiologically we would expect an individual to have a glucose intake therefore we decided to have a low (constant) glucose feeding rate.

In this chapter we were able to reproduce simulations from the original models for each level of description in the green1 model, including coding and reproducing plots from the Xu et al. [3] model. Furthermore these models were modified as required in order to successfully merge them by making changes to units and adaptations that allows for a more physiologically realistic description of whole body glucose metabolism in malaria patients. The full description of the green1 model can be seen in Appendix A. In the next chapter we present simulations and sensitivity analysis results for the green1 model.

Chapter 4

Model Simulations and Sensitivity Analysis

In the previous chapter, a hierarchical model was constructed to describe glucose metabolism in malaria patients (green1), using three existing mathematical models. The first Section (4.1) of this chapter shows initial validations and steady state solutions of blood glucose and blood lactate for the model. The second section describes both local (Section 4.2.1) and global sensitivity analysis (Section 4.2.2).

4.1 Initial validation and steady state solutions

In any type of modelling it is important to validate the model to verify the accuracy of the predictions. Thorough validation of computational simulations requires complete and accurate sets of data which are almost never available. Recall that Xu et al. [3] made provision for the inclusion of a red blood cell compartment in the framework; however they did not explicitly include a red blood cell model. During the construction of the green1 model a red blood cell compartment was added (Section 3.2.4). Since combining models can lead to unexpected outcomes it is good practice to have checks during the linking process so that any unexpected behaviour can be identified. Therefore we needed to confirm that the addition of the red blood cell compartment did not result in unexpected behaviour of the whole body system. Table 4.1 shows the effect of adding the red blood cell compartment to the original whole body model by analysing some of the whole body fluxes. This initial validation is achieved by comparing some of the fluxes of the original whole body model, with the adaptations as described in Section 3.3.3 for F_{ffa} , M_{alan} , v_{feed} and the lactate transporter in the liver, and to the green1 model for zero parasitaemia. Only the rates that influence blood glucose and lactate are shown.

In Table 4.1 it can be seen that with the addition of the red blood cell compartment there was an increase in the fluxes for blood lactate degradation ($v_{\text{d_Blac}}$) and liver lactate transport (v_{tL2}) while the other rates showed a decrease. The incorporation of a red blood cell compartment to the whole body model results in lower blood glucose levels (B_{gluc}) and higher lactate levels (B_{lac}) due to the in-

4.1. Initial validation and steady state solutions

creased metabolism caused by erythrocyte glycolysis. Since both the degradation rates (v_d_Bgluc and v_d_Blac), from the RBC absent Xu et al. [3] model, are of the mass action form, a constant multiplied by a concentration, the decrease in blood glucose leads to a decrease in the degradation rate for glucose while the inverse is true for blood lactate. The rate of glucose transport from the blood into the fat (v_tF1) or muscle compartment (v_tS1) similarly decreases due to the reduced levels of glucose in the blood. The transport of lactate from the muscle tissue into the blood compartment also decreases (v_tS3). This is mostly likely due to increased blood lactate levels inhibiting the muscle lactate transporter.

The rate of transport for glucose in the liver (v_tL1) decreases while the liver lactate transport rate (v_tL2) shows an increase. The increase in blood lactate levels causes the increase in transport of lactate from blood to the liver. Once in the liver, the lactate is converted back to glucose through a multi-step process known as the Cori cycle. The rate of transport for blood glucose into the liver is given by the expression $k(B_{gluc} - gluc)$ where k is a rate constant. Therefore a decrease in the rate v_tL1 , as can be seen in Table 4.1, results in less blood glucose being imported into the liver. This is expected as the addition of the red blood cell compartment leads to lower glucose levels in the blood which would reduce the amount of glucose that can be transported from the blood into the liver. While the rate (v_tL1) decreases, the rate of the liver lactate transport increases in order to accommodate the increased levels of lactate in the blood.

4.1. Initial validation and steady state solutions

Table 4.1: **Initial validation of the addition of the red blood cell compartment to the whole body model.** Comparison of selected steady state metabolite concentrations and some relevant fluxes for the Xu et. al [3] with model adaptations and green1 with zero parasitemia.

Metabolite (mM)	Description	Xu et. al [3] with model adaptations	green1 (with 0 % par)
B_{gluc}	Blood glucose	5.6	5.1
B_{lac}	Blood lactate	0.072	0.79
Flux (mM/min)	Description of rate		
$v_d_B_{\text{gluc}}$	Blood glucose degradation	$8.4 \cdot 10^{-2}$	$7.7 \cdot 10^{-2}$
$v_d_B_{\text{lac}}$	Blood lactate degradation	$1.1 \cdot 10^{-3}$	$1.2 \cdot 10^{-2}$
v_tL1	Liver glucose transporter	$-5.9 \cdot 10^{-4}$	$-5.3 \cdot 10^{-3}$
v_tL2	Liver lactate transporter	$6.7 \cdot 10^{-3}$	$4.2 \cdot 10^{-2}$
v_tF1	Fat tissue glucose transporter	$5.8 \cdot 10^{-2}$	$5.3 \cdot 10^{-2}$
v_tS1	Muscle glucose transporter	$5.8 \cdot 10^{-2}$	$5.3 \cdot 10^{-2}$
v_tS3	Muscle lactate transporter	$7.8 \cdot 10^{-3}$	$7.0 \cdot 10^{-3}$

During the construction of the green1 model the glucose and lactate transporters (from the blood to the red blood cell) had to be duplicated due to unit differences between the dutoit3 and Xu model (see Section 3.3.2). This required the inclusion of a conversion factor (ω) allowing for the whole body transporters to be in units of mM/min and the dutoit3 transporters to be in units of mmol/min. To verify that mass was conserved between the two models during this conversion, the fluxes that link the different models were calculated in their respective units and compared by using the unit conversion factor.

Table 4.2 shows the results for the duplicated transporters for each system along with the dutoit3 transporters to units of mM/min for green1 with 5 % par (using the conversion factor ω). For example, the first entry in the table describes the glucose transport rate `vRBCvGLCTransport` in the red blood cell part of the green1 model in units of mmol per min, followed by its value in mM/min through conversion by division with ω (see Section 3.3.2), and lastly the value for glucose transport in the whole body part of the model (`vWBvGLCTransport`). Since all of the red blood cell transporters (that have been converted to mM/min in Table 4.2) are identical to the whole body transporter rates mass is conserved within the green1 model.

4.1. Initial validation and steady state solutions

Table 4.2: **Verification of conservation of mass during the combining of the Xu and parasitized red blood cell culture model.** Flux results for duplicated transport rates of parasite infected and uninfected RBC transporters in their different units. Conversion between mmol/min and mM/min was done by division with $\omega = \frac{v_{\text{Bld}}}{1000}$ (see Section 3.3.2) for 5% parasitemia.

Transport rate	RBC transporter (mmol/min)	RBC transporter (mM/min)	Whole body RBC transporter (mM/min)
Uninfected glucose flux	$7.0 \cdot 10^{-2}$	$2.2 \cdot 10^{-2}$	$2.2 \cdot 10^{-2}$
Uninfected lactate flux	$1.4 \cdot 10^{-1}$	$4.3 \cdot 10^{-1}$	$4.3 \cdot 10^{-1}$
Infected glucose flux	$3.2 \cdot 10^{-1}$	$1.0 \cdot 10^{-1}$	$1.0 \cdot 10^{-1}$
Infected lactate flux	$5.9 \cdot 10^{-1}$	$1.9 \cdot 10^{-1}$	$1.9 \cdot 10^{-1}$

Another approach to check that mass is conserved is by considering the glucose influx and utilisation rates. In the green1 model the only input for glucose is the feeding rate which was set to 0.2 mM/min. Glucose, in the blood, can be transported into the adipose tissue (v_{tF1}), liver (v_{tL1}), muscle tissue (v_{tS1}), uninfected RBC (vWBvGLCTransport), parasite infected RBC (vWBivGLCTransport) or it can degrade at a rate $v_{\text{d_Bgluc}}$. Therefore, using the fluxes from the green1 model (for 5% parasitemia), we have

$$\begin{aligned}
 \text{Glucose utilisation} &= v_{\text{tF1}} + v_{\text{tL1}} + v_{\text{tS1}} + v_{\text{d_Bgluc}} \\
 &\quad + \text{vWBvGLCTransport} + \text{vWBivGLCTransport} \\
 &= 0.0257 - 0.0133 + 0.0257 + 0.0376 + 0.0223 + 0.102 \\
 &= 0.2 \frac{\text{mM}}{\text{min}} \tag{4.1.1}
 \end{aligned}$$

From equation (4.1.1) it can be seen that the glucose influx is equivalent to the sum of the utilisation rates and therefore mass is conserved within the merged system.

One of the aims of this thesis is to simulate to what extent an increased parasitaemia leads to an increased utilisation of glucose and production of lactate at the whole body level. Table 4.3 shows the important steady states (of metabolites and rates) in the green1 model in two scenarios. The first is the case where there is 0% parasitaemia, namely simulating a healthy individual; while the second shows the steady state results for blood glucose, blood lactate and relevant transporter rates in the green1 model with 5% parasitaemia.

4.1. Initial validation and steady state solutions

Table 4.3: **Steady state results from the green1 model.** Steady state results for selected metabolites and rates in the green1 model under two conditions: firstly 0% parasitaemia and secondly 5% parasitaemia.

Metabolite (mM)	green1 (with 0 % par)	green1 (with 5 % par)
B_{gluc}	5.1	2.5
B_{lac}	0.79	9.9
Flux (mmol/min)		
$J_{\text{vPFvGLCtr}}$	0	$3.1 \cdot 10^{-1}$
$J_{\text{vPFvLACtr}}$	0	$5.8 \cdot 10^{-1}$
$J_{\text{vRBCvGLCTransport}}$	$7.3 \cdot 10^{-2}$	$7.0 \cdot 10^{-2}$
$J_{\text{vRBCivGLCTransport}}$	0	$3.2 \cdot 10^{-1}$
$J_{\text{vRBCvLACTransport}}$	$1.4 \cdot 10^{-1}$	$1.4 \cdot 10^{-1}$
$J_{\text{vRBCivLACTransport}}$	0	$5.9 \cdot 10^{-1}$
$J_{\text{v_tL1}}^*$	$-5.3 \cdot 10^{-3}$	$-1.3 \cdot 10^{-2}$
$J_{\text{v_tL2}}^*$	$4.2 \cdot 10^{-2}$	$8.9 \cdot 10^{-2}$

* v_tL1 represents the liver glucose transporter (transport from glucose in the blood into the liver), v_tL2 represents the liver lactate transporter (transport from lactate in the blood into the liver)

From Table 4.3 it can be seen that the presence of parasites in the green1 model yields a lower blood glucose and a higher blood lactate steady state concentration. This effect is brought about by the metabolism of the *Plasmodium falciparum* parasites. In the 0% parasitaemia green1 model the infected red blood cell transporters for glucose ($J_{\text{vRBCivGLCTransport}}$) and lactate ($J_{\text{vRBCivLACTransport}}$) are zero (the parasitized red blood cell compartment is not active by design). As expected, the fluxes in the green1 model for the uninfected red blood cell transporters do not change much with the addition of the parasite model.

As can be seen in Table 4.3 the parasites cause an increase in the utilisation of glucose and increase in production of lactate in malaria patients. This led us to investigate the effect of varying levels of parasitaemia on blood glucose and blood lactate. Figure 4.1 and Figure 4.2 shows the simulation result. The model illustrates that increasing parasitaemia leads to a decrease in blood glucose and increase in blood lactate (despite the whole body mechanisms for glucose and lactate homeostasis). The data that can be seen in Figure 4.1 and Figure 4.2 are independent data sets/points used to validate the model. Longitudinal data (especially of individuals not on antimalarials) are not readily available and most of the clinical data in literature consists of one or two points related to the admission data collected for malaria

4.1. Initial validation and steady state solutions

patients. Therefore validating the model becomes challenging as it is limited to the available data and the clinical measurements taken. A literature search was conducted to obtain as much data available as possible; however the data is not ideal for model validation, due to large patient variability and absence of longitudinal data.

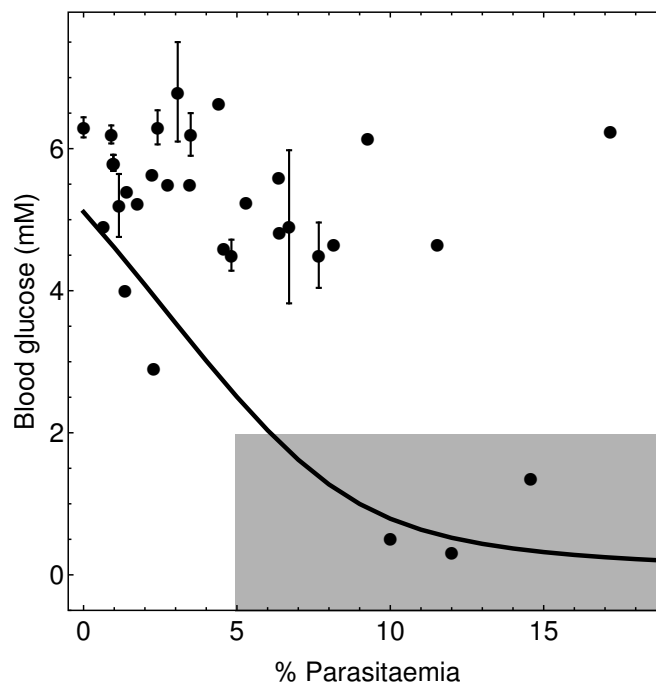


Figure 4.1: **Model simulation of the steady state blood glucose concentration with increasing parasitaemia (solid line).** The grey region denotes clinical diagnostic criteria for hypoglycaemia and severe malaria. Published data for this region has not been found. Data points for malaria patients at admission are from literature [69].

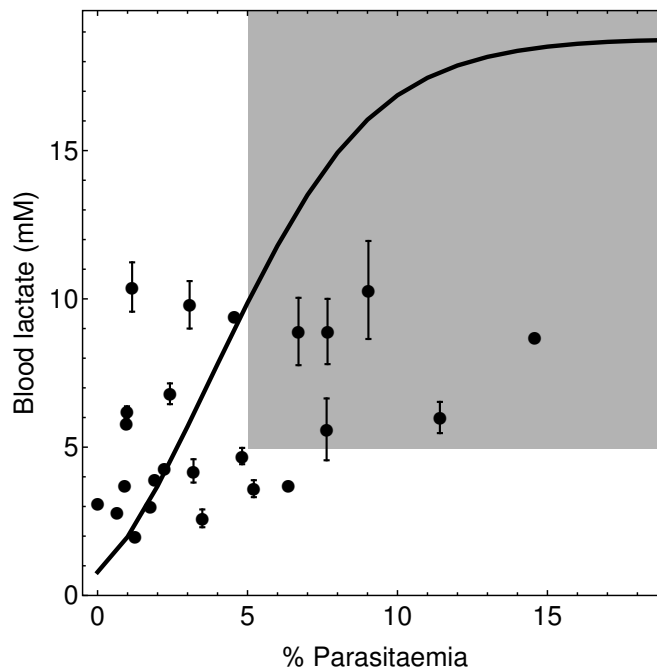


Figure 4.2: **Model simulation of the steady state blood lactate concentration with increasing parasitaemia (solid line).** The grey region denotes clinical diagnostic criteria for lactic acidosis and severe malaria. Published data for this region has not been found. Data points for malaria patients at admission are from literature [69].

4.1.1 Inhibition of the parasites glycolytic flux

Mathematical models are a powerful tool that can be used to predict possible outcomes of biological systems. We have shown that the increased glycolytic flux of the parasites cause a decrease in blood glucose and increase in blood lactate levels. It would be beneficial to know to what extent we could reduce hypoglycaemia and lactic acidosis through the addition of a glycolytic inhibitor. Cytochalasin B is a known inhibitor of the glucose-D-transporters [70, 71]. In a similar way to that of van Niekerk et al. [52] the glucose transporter for the parasite model was altered to include cytochalasin B by assuming competitive inhibition. An objective function was used in Mathematica 10.3 to determine the concentration of the inhibitor cytochalasin that would be required to produce a 50 % inhibition of the parasites' glycolytic flux (by monitoring $v_{PFvLACtr}$). It was calculated that $11.58 \mu\text{M}$ would be necessary to achieve this amount of inhibition. Figure 4.3 shows a simulation from the model with 50 % inhibition of the parasites' glycolytic flux. Here the effect of inhibiting the parasites' glycolysis can be seen on the blood glucose and lactate concentrations.

In Figure 4.3 it can be seen that before the addition of the inhibitor (to the green1 model with 5 % parasitemia) at time zero the blood glucose level is low while the lactate levels are high. The introduction of the inhibitor leads to a rapid decrease in blood lactate and an increase in blood glucose concentrations. This investigation

4.2. Sensitivity, Robustness and Control Analysis

shows the benefit that reducing the glycolytic flux in the parasites would have on a malaria patients' blood glucose and lactate levels.

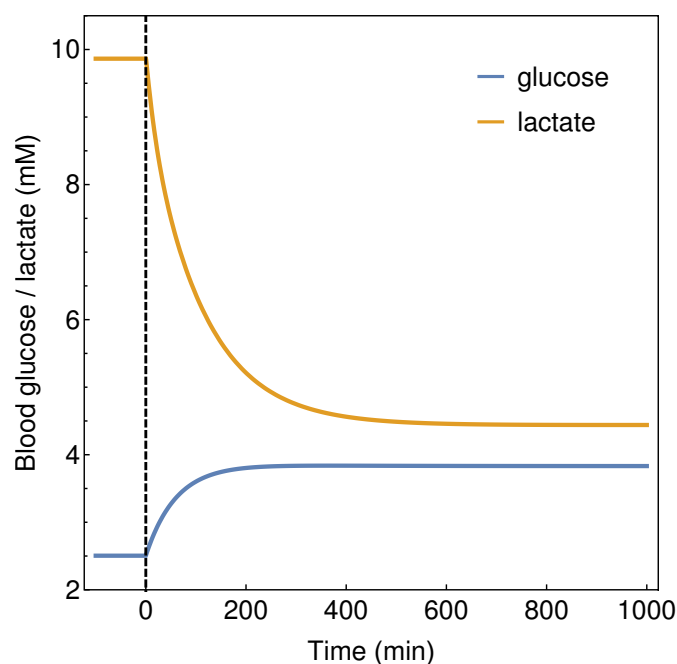


Figure 4.3: **Effect of a parasite glycolytic inhibitor on whole body glucose and lactate concentrations.** Simulation of blood glucose and blood lactate concentrations after the addition of $11.58 \mu\text{M}$ cytochalasin causing 50% reduction in the glycolytic flux of *Plasmodium falciparum* in the green1 model with 5% parasitemia. The inhibitor is administered at time zero and effects only the parasite glycolytic transporter.

4.2 Sensitivity, Robustness and Control Analysis

Sensitivity analysis allows for two main outcomes: firstly it provides insights into the certainty of model predictions in the context of parameter uncertainty. Secondly it can help in determining the vulnerability of a system to changes in specific reactions or parameters. A brief introduction to sensitivity analysis can be found in Chapter 2. In the following section we present results for the local and global sensitivity analysis on the green1 model.

4.2.1 Local sensitivity analysis

In Metabolic Control Analysis there are three different types of coefficients used to give insights into the effects that parameters or reactions have on a system. The green1 model was analysed using control (see Table 4.4) and response coefficients (see Table 4.5). Since the green1 model is so extensive only the rates with the highest positive and negative controls over reactions, relevant to confirm model reliability and predict possible drug targets, are considered here.

4.2.1.1 Control coefficients

Control coefficients show how a perturbation (by 1%) in a rate affects the steady state concentration of a metabolite or a reaction flux. Table 4.4 shows the control coefficient results for the green1 model. While the green1 model is limited in molecular detail (despite the detailed descriptions for the parasite and RBC glycolysis) to accurately predict drug targets, it can give indications or reactions (with control coefficients) that play a crucial role in achieving a desired model outcome on the whole body level. In particular, reactions with high control in the parasite (and low control in the host) are identified as good possibilities for drug targets.

Flux control coefficients

From Table 4.4 it can be seen that the reactions vPFvHK, vPFvPFK and vPFvGLCtr have the most control on the glucose and lactate transporters of the infected red blood cells (vRBCivGLCTransport and vRBCivLACTransport). This result was expected since the parasite is responsible for the increased glycolytic flux after infection and in the isolated parasite model these reactions have the highest control. Since these three parasite rates have the largest control over vRBCivGLCTransport and vRBCivLACTransport they would be good reactions to target i.e. inhibiting vPFvHK, vPFvPFK or vPFvGLCtr would have a dramatic effect on the glucose transport into the parasitized red blood cells and the lactate exported out of the infected red blood cells (see Discussion for reference to previous work done). The homologous enzymes in the RBC have little control on the uninfected red blood cell fluxes for glucose and lactate indicating that side effects on the host would be minimal.

Concentration control coefficients

Metabolic Control Analysis showed that the degradation rates for blood glucose and blood lactate have a negative control on their respective steady state metabolites, namely $C_{v_d_Bgluc}^{B_{gluc}}$ and $C_{v_d_Blac}^{B_{lac}}$. An increase in the rate v_L5r in the liver, responsible for converting lactate to pyruvate, causes a negative effect on blood lactate ($C_{v_{L5r}}^{B_{lac}} = -0.51$) as it feeds blood lactate into the Cori-cycle.

As seen in the control coefficients for the infected transporters the reactions vPFvHK, vPFvPFK or vPFvGLCtr have a relatively large effect (compared to the other reactions) on blood glucose and lactate. The increase in these three parasite enzyme rates have a negative control on blood glucose and a positive control on blood lactate due to the increased glycolytic flux in the parasite.

The glucose intake rate v_feed features in almost all of the control coefficients in Table 4.4 and the fixed value chosen in the model should therefore be carefully considered.

Table 4.4: **Control coefficients from the green1 model.** The highest and lowest control coefficients for relevant metabolites and rates in the green1 model with 5% parasitaemia.

Reaction	$C_v^{B_{\text{gluc}}}$	$C_v^{B_{\text{lac}}}$	$C_v^{J_{\text{vRBCvGLCTRANS}}}$	$C_v^{J_{\text{vRBCivGLCTRANS}}}$	$C_v^{J_{\text{vRBCvLACTRANS}}}$	$C_v^{J_{\text{vRBCivLACTRANS}}}$	$C_v^{J_{\text{vPFvGLCtr}}}$	$C_v^{J_{\text{CJvPFvLACtr}}}$
v_d_Bgluc	-0.37	-	-	-	-	-	-	-
v_d_Bins	-0.13	-	-	-	-	-	-	-
v_d_Blac	-	-0.94	-	-	-	-	-	-
v_L5r	0.15	-0.51	-	-	-	-	-	-
vRBCvHK	-	-	0.10	-	0.12	-	-	-
vRBCvBPGSP9	-	-	0.18	-	0.19	-	-	-
vRBCvATPASE	-	0.14	0.58	-	0.60	-	-	-
v_feed	2.0	0.33	-	0.12	-	0.23	0.24	0.24
vPFvGLCtr	-0.29	0.31	-	0.26	-	0.27	0.26	0.27
vPFvPFK	-0.32	0.35	-	0.29	-	0.30	0.29	0.30
vPFvHK	-0.36	0.39	-	0.32	-	0.33	0.33	0.34

* Values not shown were not significant.

4.2. Sensitivity, Robustness and Control Analysis

4.2.1.2 Response coefficients

Response coefficients indicate the sensitivity of a system property for a change in any system parameter. Therefore these coefficients can be used to describe how perturbing a parameter effects a metabolite concentration or reaction rate at steady state. Table 4.5 shows some of the important response coefficients for relevant metabolites and reactions.

Consider the response coefficients $R_{\text{par}}^{B_{\text{gluc}}}$ and $R_{\text{par}}^{B_{\text{lac}}}$ in Table 4.5. A 1% increase in the parameter par leads to a 1.50% decrease in blood glucose (caused by the parasite utilising glucose for glycolysis) and a 1.6% increase in blood lactate as a result of the increased lactate produced by the parasites. These responses show the direct effect that increasing parasite burden has on blood glucose and lactate concentrations.

The parameter HCT, representative of the hematocrit, has a large effect on many of the relevant reactions and metabolites that are considered in Table 4.5. A slight increase in the hematocrit has a considerable negative effect on blood glucose and a positive effect on blood lactate. These large response coefficients can be explained by considering the changes in red blood cell volume that occurs. An increase in the hematocrit results in a greater fraction of total blood volume consisting of red blood cells. With a greater red blood cell volume (in both the uninfected and infected compartments), more red blood cells are able to utilise glucose and produce lactate causing blood glucose to decrease and blood lactate to increase. This is similar to the effect seen when the red blood cell compartment was added to the Xu model resulting lower glucose levels and higher lactate levels in the blood. While the hematocrit is not likely to change much in humans, Metabolic Control Analysis showed it is an important parameter in the model and therefore its fixed value should be carefully considered.

In Table 4.5 there are three parameters from the whole body model compartment that have significant effects on the rates and metabolite concentrations that were considered. In the liver compartment lactate is converted to pyruvate by the reaction v_L5r. In this reaction v_L5r is directly proportional to k_L5r and inversely proportional to k_mL5r. A 1% increase in k_L5r results in this reaction in the liver to speed up. The increase of conversion of lactate into glucose via the Cori cycle in the liver creates a demand for lactate which is then fulfilled by the import of blood lactate into the liver. This accounts for the negative response coefficient $R_{k_{L5r}}^{B_{lac}}$ (-0.51) and the response of $R_{k_{L5r}}^{J_{v_{tL2}}}$ (0.89) which shows an increase of the flux in v_tL2 that is caused by the increase in the parameter k_L5r. It follows then that the increase in k_mL5r reduces the rate v_L5r leading to a negative response coefficient $R_{k_{mL5r}}^{J_{v_{tL2}}} = -0.10$. The rate constant kd_Blac can be found in the equation for blood lactate degradation described by a simple mass action equation. Therefore an increase in this constant directly causes a decrease in blood lactate.

The binding constant KglcPFvHK can be found in the hexokinase reaction in the parasite model while Kf6pPFvPFK is a binding constant in the phosphofructokinase reaction in the parasite model. In Table 4.5 it can be seen that the responses for

4.2. Sensitivity, Robustness and Control Analysis

an increase in either of these parameters has a negative effect on the flux for vR-BCivGLCTransport. The increase in either of these binding constants causes a decrease in the affinity that each respective enzyme (hexokinase or phosphofructokinase) has for its substrate. For example, a 1% increase in K_{glcPFvHK} results in hexokinase having a lower affinity for glucose (inside the infected red blood cell). As a result, in both of these cases, increasing the binding constants in the parasite results in an inhibitory effect on the glycolytic pathway in the parasite. These lead to the build up of glucose in the parasite, and in turn the build up of blood glucose. This can be seen as the response coefficients $R_{K_{\text{glcPFvHK}}}^{B_{\text{gluc}}}$ and $R_{K_{\text{f6pPFvPFK}}}^{B_{\text{gluc}}}$ are both positive. Typically, pharmaceuticals are developed to target enzymes through inhibitory mechanisms therefore targeting the kinetic constants K_{glcPFvHK} and $K_{\text{f6pPFvPFK}}$ directly does not make sense. However, these response coefficients suggest that a competitive inhibitor that decreases the affinity that hexokinase and phosphofructokinase have for their respective substrates could be a possible drug target solution.

Table 4.5: **Response coefficients from the green1 model.** The highest and lowest response coefficients for relevant metabolites and rates in the green1 model with 5 % parasitaemia.

Parameter	$R_p^{B_{\text{gluc}}}$	$R_p^{B_{\text{lac}}}$	$R_p^{J_{\text{vRBCivGLCTransport}}}$	$R_p^{J_{\text{vRBCvGLCTransport}}}$	$R_p^{J_{\text{vRBCivLACTransport}}}$	$R_p^{J_{\text{vRBCvLACTransport}}}$	$R_p^{J_{\text{v-tL2}}}$
par	-1.5	1.6	1.3	-	1.3	-	-
HCT	-2.7	2.9	1.2	0.22	1.2	0.2	0.32
k_L5r	-	-0.51	-	-	-	-	0.89
k_mL5r	-	-	-	-	-	-	-0.10
kd_Blac	-	-0.94	-	-	-	-	-0.10
Kf6pPFvPFK	0.28	-	-0.25	-	-0.25	-	-
KglcPFvHK	0.30	-	-0.27	-	-0.27	-	-

* Responses of the fluxes and concentrations to the change in reaction rates (i.e. Vmax values) are omitted in this table since $R_v^Y = C_v^Y$ and these values can be found in Table 4.4. Values not shown were not significant.

4.2.2 Global sensitivity analysis

Parameter values play a significant role in the results of model predictions. In some cases they can be experimentally determined while in others they need to be estimated. Sensitivity analysis allows for the estimation of the propagation of parameter uncertainty into model predictions.

Global sensitivity, also known as robustness analysis, was performed on the green1 model (with 5%) parasitaemia. This approach involves sampling of parameter values from the normal distributions with standard deviation of 5% around the mean values of the parameters. The standard deviation is used as an indication to reflect experimental error within the parameters. In reality, the experimental error is most likely higher than the arbitrary chosen 5%, however for our analysis we decided to be more strict in testing the accuracy of our model predictions. This method was used to generate 80 000 different parameters sets. These sets were then used to calculate the frequency of appearance of the blood glucose and blood lactate steady states in this combined parameter space. The precision of this analysis can be refined by increasing the number of bins and parameter sets generated. Although when increasing the number of parameter set simulations from 60000 to 80000 we could not see differences in the distributions, suggesting that the solutions had converged. Figure 4.4 shows the range of steady state values obtained for blood glucose resulting from this procedure. It can be seen that most of the generated parameter sets lead to a steady state of between 2.17 - 2.95 mM for blood glucose (using 6000 parameter sets as the selection criteria for the range). The original value used for parasitaemia was 5 % however during the global sensitivity analysis it can range from 4.75 % to 5.25 %. When parasitaemia was 5 % it was shown in Table 4.3 that green1 had a steady state value of 2.50 mM which is within the range of the solutions for B_{gluc} that most of the parameter sets generated. Therefore model simulations of blood glucose are not overly sensitive to small perturbations in the parameter values which is in agreement with what Xu et al. [3] concluded for the original whole body model.

4.2. Sensitivity, Robustness and Control Analysis

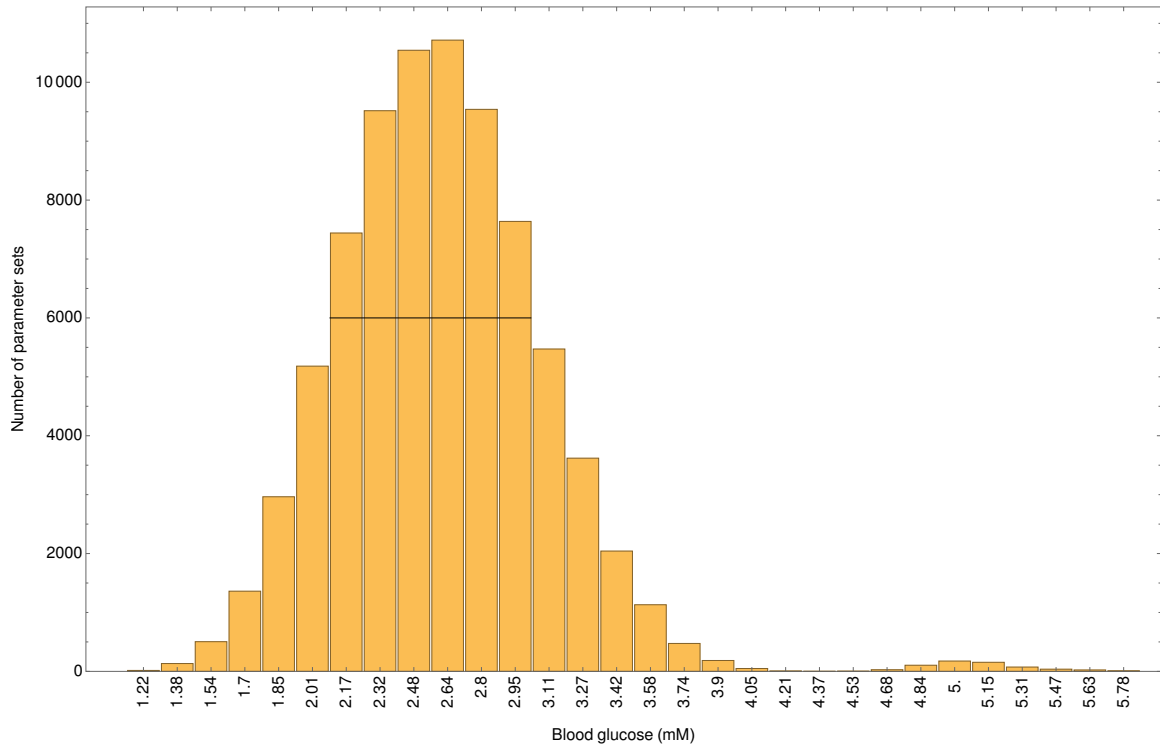


Figure 4.4: **Distribution of blood glucose steady states arising from parameter uncertainty.** Global sensitivity results showing the distribution of blood glucose steady state using 80 000 different parameter sets. Parameter sets were determined by random sampling from a normal distribution centered around the wild type value of the parameters with a 5% standard deviation. Steady states were determined by using a long time integration.

Global sensitivity analysis showed (Figure 4.5) that for blood lactate the uncertainty of parameter values lead to most steady state solutions (more than 6000 parameter sets) being in the range of 7.64 - 10.4 mM. The blood lactate in green1 with 5% parasitaemia led to a steady state solution of 9.86 mM. In Figure 4.5 the range of blood lactate steady state values is the same as that of the global sensitivity analysis for blood glucose in terms of percentage change. This suggests blood lactate, as well as blood glucose, is not sensitive to small perturbations in the parameter set.

4.2. Sensitivity, Robustness and Control Analysis

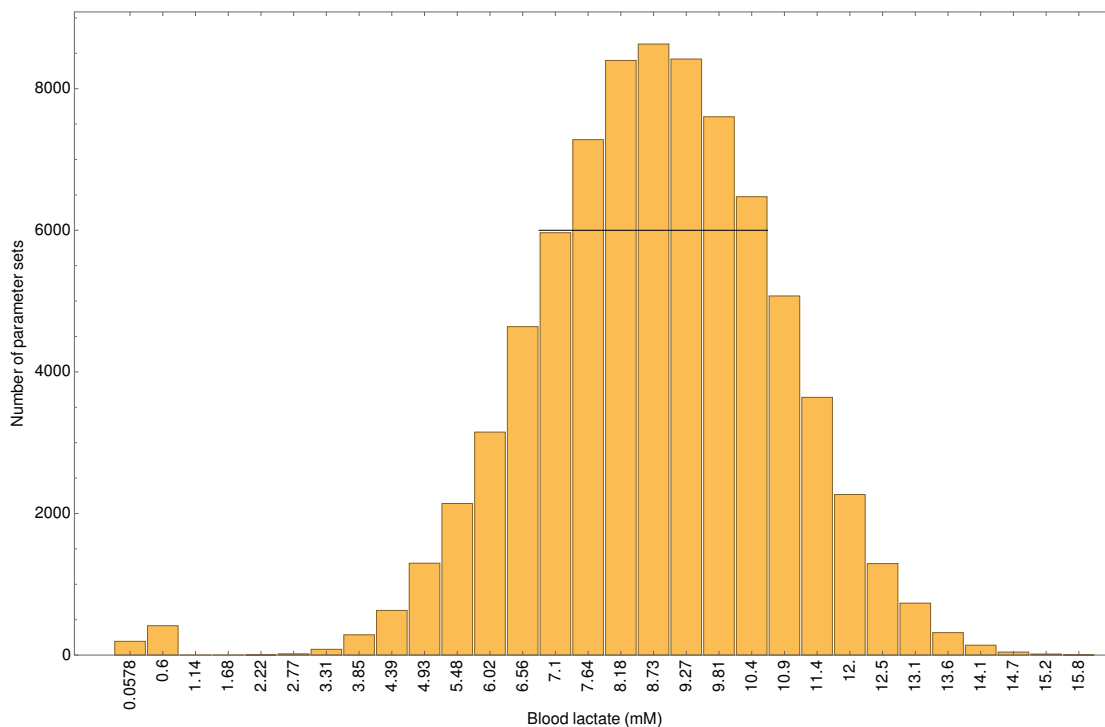


Figure 4.5: **Distribution of blood lactate steady states arising from parameter uncertainty.** Global sensitivity results showing the distribution of blood lactate steady state using 80 000 different parameter sets. Parameter sets were determined by random sampling from a normal distribution centered around the wild type value of the parameters with a 5% standard deviation. Steady states were determined by using a long time integration.

In both histograms, global sensitivity analysis results showed some unexpected behaviour. Some parameter sets lead to steady state blood glucose values ranging between 4.68 - 5.78 mM (Figure 4.4) and lactate levels falling within the range 0.058 - 0.6 mM (Figure 4.5). This could be a result of numerical precision error in Mathematica but most likely it is due to the implementation of calculation of steady state values. To reduce computational power required for the sensitivity analysis, steady states were calculated by running time courses of metabolites for what was thought to be a sufficient amount of time. It is possible that the model had not yet reached steady state for those outlying parameter sets. We investigated one such parameter set and found that the system is very sensitive to changes in the parameter $K_{mPFvATPASE}$ (in the parasite model). Furthermore setting $K_{mPFvATPASE}$ to its wild type value caused blood glucose to change from 5 mM to around 2.7 mM suggesting that the cause of the unexpected behaviour could be parameter sets that impede parasite glycolysis.

Sensitivity analysis has shown that the green1 model is not very sensitive to small perturbations in the parameter sets. In the next chapter we will present a discussion on the summarised results, model limitations and some concluding remarks.

Chapter 5

Discussion and Conclusion

5.1 Summary

An important part of Systems biology is to share and combine existing mathematical models. Models are usually independently constructed to describe particular biological or physical phenomenon, therefore the integration of them would allow for the description of larger complex biological systems. As we illustrated in this thesis, merging models is not a trivial task as they are often constructed in different frameworks and unit descriptions. This can lead to numerical problems or unexpected model behaviour after merging the models. Furthermore it is necessary to validate the merged models to justify the accuracy of model predictions. This has encouraged the development of software packages, specification standards and tools that allow for the reuse or automated merging of mathematical models (see Section 2.4).

In a previous study by Snoep et al. [72] a similar modelling approach, as used in this thesis, was used to combine pathway models for glyoxalase, glycolysis and extending the glycolytic pathway to include a glycerol branch. Their work addresses the importance of integrating the knowledge of individual molecular mechanism-based models to describe larger metabolism effects.

Initiatives such as the Virtual Physiological Human (VPH) [27], Virtual Physiological Rat [73] and Virtual Liver Project [67] have been developed to study organs and tissues through merged mathematical models. The models, at different levels of biological organisation, are integrated through multi-level and multi-scale modelling approaches. While these initiatives employ the same idea of linking models to form hierarchical frameworks by building descriptions of emergent phenomena from underlying mechanisms, we are unaware of any other models that have been merged to explain clinical features of parasite burden in malaria patients.

Ultimately, this study aimed to determine through model simulation to what extent accelerated glycolytic flux in malaria-infected red blood cells contributes to hypoglycemia and lactic acidosis associated with the malaria disease state. This was achieved by linking existing models for whole body glucose metabolism in humans

with detailed kinetic models for *Plasmodium* glycolysis and human erythrocyte glycolysis into a hierarchical framework (green1 model). Our framework allows for the investigation of metabolic pathologies in malaria infected or healthy individuals in whom the presence of malaria parasites could have a dramatic effect on blood glucose and lactate. To our knowledge, to date there are no mathematical models that can describe malaria disease states from the combination of sub-models with varying levels of complexity (see Appendix B for manuscript publication).

In a previous study [2] the red blood cell model (Mulquiney & Kuchel [9–11]) had to be altered to be linked with the parasite model. This involved changing the units of the model and adding a glucose transporter to the red blood cell model. Once the models were compatible in terms of units the parasite model was linked with the red blood cell model. In the current study, the *Plasmodium* infected red blood cell model's glucose transporter was replaced and it was extended with the model for the uninfected red blood cell (Mulquiney & Kuchel [9–11]) to represent a malaria infected red blood cell culture with varying levels of parasitemia (called the dutoit3 model). Splitting the total red blood cell modelling structure into infected and uninfected compartments was required for the subsequent scaling up of the red blood cell volumes to represent the blood compartment (consisting of infected and uninfected red blood cells) of the whole body level. It was decided to use the Xu et al. [3] model to describe whole body glucose metabolism. This model lacks a red blood cell compartment and the dutoit3 model would provide exactly that with a high level of mechanistic detail. To use the Xu model, it was coded from the published Matlab files and curated on JWS Online. After an unsuccessful initial attempt to convert the units of the whole body model to fmol amounts, it was decided to keep the whole body model in units of concentration and link it with the dutoit3 model which was adapted from fmol to mmol amounts. In implementing this unit difference a conversion factor was created and used in duplicated transport rates between the whole body and red blood cell compartment.

During the linking, certain adaptations had to be made to avoid numerical instability and address unexpected behaviour produced by the whole body model that now included a detailed red blood cell compartment. Model adaptations included changing the fixed values for free fatty acids in the fat tissue, alanine in the muscle compartment and the glucose feeding rate such that blood glucose level for a healthy individual was physiologically realistic. Another important adaptation was the changing of the liver lactate transporter to a reversible Michaelis Menten equation to avoid the unrealistic build up of lactate in the liver compartment. Despite the presence of the parasites, physiologically it is unlikely that the liver would be overwhelmed at only 5% parasitaemia. Furthermore for steady state analysis it was essential to change the phenomenologically modelled liver lactate transport of the Xu et al. [3] model. Thereafter the model was numerically stable and showed realistic steady state predictions for physiologically relevant levels of parasitemia.

In Chapter 4 we showed model validations, simulations and sensitivity analysis results. It was necessary to confirm that the addition of the red blood cell compartment did not lead to unexpected behaviour when linked to the whole body model. The

whole body fluxes indicated changes with the added RBC compartment could be physiologically plausible. Verification of duplicated transporters in the same units (using the conversion factor) proved that mass was still conserved within the system. Model predictions showed that the presence of the parasite (5% parasitemia) lead to a blood glucose steady state decrease to 2.5 mM (from 5.1 mM) and an increase in the blood lactate steady state to 9.9 mM (from 0.79 mM).

Further simulations showed good qualitative and quantitative agreement with clinical data of blood glucose and lactate in malaria infected individuals (by increasing parasitaemia). While the trend seen in blood glucose and blood lactate due to accelerated glycolytic flux is promising, a proper validation would require clinical longitudinal data of patients (i.e. data that shows a change in blood glucose and lactate over time in malaria infected hosts). In a model simulation it was shown that with the addition of a known inhibitor of the parasite glucose transporter (and therefore its glycolytic flux), namely cytochalasin, a 50% reduction in the parasite glycolytic flux causes a dramatic partial restoration of blood glucose and lactate.

Results from local sensitivity analysis showed that the rates v_{PFvHK} , v_{PFvPFK} and $v_{PFvGLCtr}$ in the parasite model have a large control over $v_{RBCivGLCTRANS}$ and $v_{RBCivLACTRANS}$ (i.e. the glucose and lactate fluxes across the membrane of the infected red blood cells). We suggest that these enzymes should be considered as good candidates for possible drug targets as an inhibition of these reactions leads to a concomitant decrease in the glycolytic flux of the infected red blood cells and restoration of blood glucose and lactate while having minimal effects in the non-infected red blood cell. In addition, studying the response coefficients in the green1 model showed that increasing either $K_{glcPFvHK}$ or $K_{f6pPFvPFK}$ would lead to a restoration of blood glucose and decrease in blood lactate. A drug acting as a competitive inhibitor for fructose-6-phosphate on the phosphofructokinase enzyme or intracellular glucose on hexokinase, would therefore lead to a rise in blood glucose levels and malaria symptoms such as hypoglycemia and lactic acidosis could be avoided. It has been shown, in a single infected red blood cell, by van Niekerk et al. [52] that the glucose transporter of the parasite might be a good target for competitive inhibition.

Global sensitivity analysis showed that with a normal distribution around the mean value of each parameter (standard deviation of 5%) and considering 80 000 different parameter sets we can expect a steady state value for blood glucose in an infected individual with 5% parasitemia to most likely be between 2.17 - 2.85 mM. Considering that the physiological reference state for glucose in a healthy individual is around 5 mM, the decreased glucose levels would have severe consequences on whole body metabolism in malaria infected individuals. Similarly, most blood lactate steady state solutions were found to be in the range of 7.64 - 10.4 mM. A patient is considered to have lactic acidosis when blood lactate > 5 mmol/L [12] suggesting that the malaria parasite burden contributes significantly to this. Global sensitivity analysis also showed that model simulations are not overly sensitive to small perturbations in the parameter values for blood glucose and blood lactate steady state predictions. Although sensitivity analysis gives insights into parameter uncertainty, the quality

of the prediction is limited to accuracy of the descriptions of biological phenomena in the model.

5.2 Shortcomings

Making assumptions in the modelling of biological systems is essential to reduce the complexity of systems as underlying mechanisms are not always fully understood. In addition it minimizes the computation power required to perform simulations. This creates limitations in the accuracy of predictions and in this study the mechanistic interpretation of the pathophysiology of the disease state in malaria patients. One such limitation is from the Xu et. al. [3] model which by extension can also be found in the green1 model. During this project we discovered that the original whole body model was described in terms of concentration with the assumption that all compartments (e.g. muscle, liver, etc.) are of the same volume. It would be beneficial to have described these separate components with explicit volumes or at least volumes that are proportional to the expected size of each organ which would allow for the combined model to be in units of amount per time. This would allow for more realistic modelling of molecular transport between different compartments. Further investigation into the possible use of allometric equations to scale compartment sizes with respect to absolute body weight should be done (as well as the relationship between body mass and metabolic rate). In the process of combining of the models it was also discovered that the Mulquiney and Kuchel model created many numerical problems. This red blood cell model is very detailed and it is questionable if such level of detail is required for the description of glucose metabolism and pathology in the disease states on the whole body level. A possible solution to reduce the model complexity is to lump pathways, equilibrium reactions, or eliminate reactions and whole branches with low fluxes in a suitable way.

After linking the models it was seen that model adaptations had to be made to the fixed parameters for free fatty acids in the fat tissue compartment and alanine in the muscle compartment in combination with the glucose intake rate in the whole body model. Fixing these parameters places limitations on the accuracy of metabolic prediction as realistically these substances will vary with changing blood glucose concentrations. In addition, model applicability is limited to the values these parameters are fixed at which are not necessary physiologically plausible. For example the feeding rate was fixed at 0.2 mM/min, but a simple calculation on the average calories consumed by an individual in a day equated to 0.63 mM/min if all calories were taken up as glucose.

We suggest more research should also be done on the lactate metabolism in the whole body model. Even though the wildtype prediction for blood lactate is within the frequently occurring range for steady state lactate, it is suggested that the lactate metabolism in the whole body should be further investigated for two main reasons. Firstly, Xu et al. [3] did not conduct a sensitivity analysis (in terms of response coefficients) for blood lactate on the original whole body model and therefore it would be beneficial to know how precise the whole body model is in predicting

lactate metabolism. Secondly, with the change made to the lactate transporter in the liver some validation is required to verify the effect of this model adaptation on lactate metabolism.

Possible causes for hypoglycaemia and lactic acidosis include reduced perfusion, anaemia, or accelerated glycolytic flux caused by the *Plasmodium falciparum* parasite. Increased lactate production is often associated with severe malaria and is correlated to patient death [13]. This model only includes the effect of accelerated glycolytic flux on hypoglycemia and lactic acidosis and in future should be extending to include the other possible causes.

Lastly, this model is limited to only one phase in the erythrocytic stage of malaria in the human host and should be expanded by considering how the parasite grows over time, how its metabolism changes, and how it proliferates in the body as a result of asexual reproduction.

5.3 Conclusion

The aims of this thesis were to: 1) construct a multi-level model of human glucose metabolism that contains the molecular mechanisms of erythrocyte and *Plasmodium* glycolysis and 2) simulate to what extent an increased parasitaemia leads to an increased utilisation of glucose and production of lactate, taking into account the homeostatic mechanisms for glucose and lactate at the whole body level. These aims were achieved by completing the following objectives.

Firstly, three existing mathematical models for the *P. falciparum* metabolism, erythrocyte metabolism and whole body glucose metabolism were identified. These independent models were extended and modified as was necessary to merge them to form the green1 model. Secondly, comparisons of simulations from the green1 model with clinical data showed that increased glycolytic flux, caused by the presence of the parasites, could be sufficient to explain the clinical symptoms of hypoglycemia and lactic acidosis seen in malaria patients. These model predictions should be further validated with sets of longitudinal data. The effect of reducing the glycolytic flux of the parasites with an inhibitor showed a significant improvement to blood glucose and lactate levels. Lastly, local and global sensitivity analysis identified reactions and parameters in the *Plasmodium* glycolysis pathway that could guide the development of possible drug targets. Uncertainty analysis showed model simulations of blood glucose and lactate are not overly sensitive to small perturbations in the parameter values.

In future, we suggest emphasis should be placed on addressing model limitations specifically for the whole body model, made for the simplification of the model construction process, and validating the model simulations with experimental or clinical data. In conclusion, we succeeded in estimating the contribution that *Plasmodium falciparum* activity has on the clinical symptoms hypoglycemia and lactic acidosis associated with malaria patients.

Appendices

Appendix A

Model description for the green1 model

This appendix contains the full model description of the green1 model. This includes the combined extended *P. falciparum* infected erythrocyte model (dutoit3) and the whole body model (Xu et al.[3]) with the modifications made to the respective models to link them (see Section 3.3.3).

A.1 Naming conventions

A parasite metabolite or enzyme reaction is represented with the letters PF e.g. glcPF (parasite glucose). The red blood cell compartment consists of an uninfected and *P. falciparum* infected part. We denote the infected red blood cell metabolites and reactions with the abbreviation RBCi while for the uninfected red blood cell compartment we have RBC. The respective volumes for each compartment are given by V_{rbc_i} (infected RBC volume) and V_{rbc_u} (uninfected RBC volume) with the total red blood cell volume as V_{rbc} . For the dutoit3 model the metabolites are modelled in mmol and reaction rates in mmol/min. Metabolites and rates that do not contain the compartment specification of PF or RBC/RBCi belong to the whole body model (Xu et al.[3]). These variables are present in various compartments of the whole body model as is described in the original model (see Section 3.1.3). The whole body metabolites have units of mM and reactions are modelled in units of mM/min.

A.2 Initial Values:

$B_alan(0) = 0.312$	(A.2.1)
$B_ffa(0) = 0.936$	(A.2.2)
$B_gluc(0) = 12.48$	(A.2.3)
$B_glucgn(0) = 0.$	(A.2.4)
$B_ins(0) = 0.$	(A.2.5)
$B_ket(0) = 0.2496$	(A.2.6)
$B_lac(0) = 0.624$	(A.2.7)
$Cvar(0) = 0.$	(A.2.8)
$F_TG(0) = 0.$	(A.2.9)
$F_acyl(0) = 0.$	(A.2.10)
$F_g6p(0) = 0.$	(A.2.11)
$GPa(0) = 0.1092$	(A.2.12)
$GSa(0) = 0.00468$	(A.2.13)
$M_g6p(0) = 24.96$	(A.2.14)
$M_glycgn(0) = 1.$	(A.2.15)
$M_ket(0) = 0.312$	(A.2.16)
$M_lac(0) = 0.624$	(A.2.17)
$M_pyr(0) = 0.624$	(A.2.18)
$PKa(0) = 0.$	(A.2.19)
$PP1(0) = 0.00078$	(A.2.20)
$PP1_GPa(0) = 0.$	(A.2.21)
$R2C2(0) = 0.00078$	(A.2.22)
$R2_C_cAMP2(0) = 0.$	(A.2.23)
$R2_cAMP4(0) = 0.$	(A.2.24)
$aK(0) = 3.12$	(A.2.25)
$acet_c(0) = 18.72$	(A.2.26)
$acet_m(0) = 21.84$	(A.2.27)
$adpPF(0) = 0.0339733$	(A.2.28)
$adpRBC(0) = 0.643188$	(A.2.29)
$adpRBCi(0) = 0.033852$	(A.2.30)
$alan(0) = 0.312$	(A.2.31)
$ampRBC(0) = 0.062244$	(A.2.32)
$ampRBCi(0) = 0.003276$	(A.2.33)
$atpPF(0) = 0.0679467$	(A.2.34)
$atpRBC(0) = 4.35708$	(A.2.35)
$atpRBCi(0) = 0.22932$	(A.2.36)
$b13pgPF(0) = 0.00339733$	(A.2.37)
$b13pgRBC(0) = 0.00145236$	(A.2.38)
$b13pgRBCi(0) = 0.00007644$	(A.2.39)
$b23pgRBC(0) = 13.9012$	(A.2.40)
$b23pgRBCi(0) = 0.73164$	(A.2.41)
$bpgspRBC(0) = 0.00788424$	(A.2.42)

bpgspRBCi(0) = 0.00041496	(A.2.43)
bpgspb13pgRBC(0) = 0.	(A.2.44)
bpgspb13pgRBCi(0) = 0.	(A.2.45)
bpgspb23pgRBC(0) = 0.	(A.2.46)
bpgspb23pgRBCi(0) = 0.	(A.2.47)
bpgsppRBC(0) = 0.	(A.2.48)
bpgsppRBCi(0) = 0.	(A.2.49)
bpgsppp2gRBC(0) = 0.	(A.2.50)
bpgsppp2gRBCi(0) = 0.	(A.2.51)
bpgsppp3gRBC(0) = 0.	(A.2.52)
bpgsppp3gRBCi(0) = 0.	(A.2.53)
bpgsppphosRBC(0) = 0.	(A.2.54)
bpgsppphosRBCi(0) = 0.	(A.2.55)
cAMP(0) = 0.	(A.2.56)
citrate(0) = 1.56	(A.2.57)
dhapPF(0) = 0.00339733	(A.2.58)
dhapRBC(0) = 0.0394212	(A.2.59)
dhapRBCi(0) = 0.0020748	(A.2.60)
ery4pRBC(0) = 0.020748	(A.2.61)
ery4pRBCi(0) = 0.001092	(A.2.62)
f16bpPF(0) = 0.00339733	(A.2.63)
f16p2RBC(0) = 0.00560196	(A.2.64)
f16p2RBCi(0) = 0.00029484	(A.2.65)
f6pPF(0) = 0.00339733	(A.2.66)
f6pRBC(0) = 0.0269724	(A.2.67)
f6pRBCi(0) = 0.0014196	(A.2.68)
g16p2RBC(0) = 0.253126	(A.2.69)
g16p2RBCi(0) = 0.0133224	(A.2.70)
g3pPF(0) = 0.00339733	(A.2.71)
g6p(0) = 0.624	(A.2.72)
g6pPF(0) = 0.00339733	(A.2.73)
g6pRBC(0) = 0.082992	(A.2.74)
g6pRBCi(0) = 0.004368	(A.2.75)
gapPF(0) = 0.00339733	(A.2.76)
gapRBC(0) = 0.0118264	(A.2.77)
gapRBCi(0) = 0.00062244	(A.2.78)
glcPF(0) = 0.00339733	(A.2.79)
glcRBC(0) = 10.374	(A.2.80)
glcRBCi(0) = 0.546	(A.2.81)
gluc(0) = 15.6	(A.2.82)
glutamate(0) = 0.312	(A.2.83)
glycgn(0) = 31.2	(A.2.84)
gshRBC(0) = 6.63936	(A.2.85)
gshRBCi(0) = 0.34944	(A.2.86)
gssgRBC(0) = 0.000186732	(A.2.87)
gssgRBCi(0) = 9.828×10^{-6}	(A.2.88)
hbRBC(0) = 14.5236	(A.2.89)
hbRBCi(0) = 0.7644	(A.2.90)
hbadpRBC(0) = 0.	(A.2.91)
hbadpRBCi(0) = 0.	(A.2.92)
hbatpRBC(0) = 0.	(A.2.93)
	(A.2.94)

hbatpRBCi(0) = 0.	(A.2.95)
hbb13pgRBC(0) = 0.	(A.2.96)
hbb13pgRBCi(0) = 0.	(A.2.97)
hbb23pgRBC(0) = 0.	(A.2.98)
hbb23pgRBCi(0) = 0.	(A.2.99)
hbm gatpRBC(0) = 0.	(A.2.100)
hbm gatpRBCi(0) = 0.	(A.2.101)
ket(0) = 0.2496	(A.2.102)
lac(0) = 3.12	(A.2.103)
lacPF(0) = 0.00339733	(A.2.104)
lacRBC(0) = 2.90472	(A.2.105)
lacRBCi(0) = 0.15288	(A.2.106)
malate(0) = 9.36	(A.2.107)
malonyl(0) = 0.936	(A.2.108)
mgRBC(0) = 6.2244	(A.2.109)
mgRBCi(0) = 0.3276	(A.2.110)
mgadpRBC(0) = 0.	(A.2.111)
mgadpRBCi(0) = 0.	(A.2.112)
mgatpRBC(0) = 0.	(A.2.113)
mgatpRBCi(0) = 0.	(A.2.114)
mgb13pgRBC(0) = 0.	(A.2.115)
mgb13pgRBCi(0) = 0.	(A.2.116)
mgb23pgRBC(0) = 0.	(A.2.117)
mgb23pgRBCi(0) = 0.	(A.2.118)
mgf16p2RBC(0) = 0.	(A.2.119)
mgf16p2RBCi(0) = 0.	(A.2.120)
mgg16p2RBC(0) = 0.	(A.2.121)
mgg16p2RBCi(0) = 0.	(A.2.122)
mgphosRBC(0) = 0.	(A.2.123)
mgphosRBCi(0) = 0.	(A.2.124)
nadPF(0) = 0.0849333	(A.2.125)
nadRBC(0) = 0.124488	(A.2.126)
nadRBCi(0) = 0.006552	(A.2.127)
nadhPF(0) = 0.0169867	(A.2.128)
nadhRBC(0) = 0.000290472	(A.2.129)
nadhRBCi(0) = 0.000015288	(A.2.130)
nadpRBC(0) = 0.00025935	(A.2.131)
nadpRBCi(0) = 0.00001365	(A.2.132)
nadphRBC(0) = 0.132787	(A.2.133)
nadphRBCi(0) = 0.0069888	(A.2.134)
oa_c(0) = 0.001248	(A.2.135)
oa_m(0) = 0.000624	(A.2.136)
p2gPF(0) = 0.00339733	(A.2.137)
p2gRBC(0) = 0.020748	(A.2.138)
p2gRBCi(0) = 0.001092	(A.2.139)
p3gPF(0) = 0.00339733	(A.2.140)
p3gRBC(0) = 0.132787	(A.2.141)
p3gRBCi(0) = 0.0069888	(A.2.142)
p6gRBC(0) = 0.000290472	(A.2.143)
p6gRBCi(0) = 0.000015288	(A.2.144)
p6glRBC(0) = 2.90472×10^{-7}	(A.2.145)
p6glRBCi(0) = 1.5288×10^{-8}	(A.2.146)
palm(0) = 0.936	(A.2.147)
	(A.2.148)

palmCoA(0) = 0.936	(A.2.149)
pep(0) = 0.00312	(A.2.150)
pepPF(0) = 0.00339733	(A.2.151)
pepRBC(0) = 0.0477204	(A.2.152)
pepRBCi(0) = 0.0025116	(A.2.153)
phosRBC(0) = 2.0748	(A.2.154)
phosRBCi(0) = 0.1092	(A.2.155)
pyr(0) = 9.36	(A.2.156)
pyrPF(0) = 0.00339733	(A.2.157)
pyrRBC(0) = 0.124488	(A.2.158)
pyrRBCi(0) = 0.006552	(A.2.159)
rib5pRBC(0) = 0.020748	(A.2.160)
rib5pRBCi(0) = 0.001092	(A.2.161)
ru5pRBC(0) = 0.020748	(A.2.162)
ru5pRBCi(0) = 0.001092	(A.2.163)
sed7pRBC(0) = 0.020748	(A.2.164)
sed7pRBCi(0) = 0.001092	(A.2.165)
tkRBC(0) = 0.000684684	(A.2.166)
tkRBCi(0) = 0.000036036	(A.2.167)
tkgRBC(0) = 0.	(A.2.168)
tkgRBCi(0) = 0.	(A.2.169)
tkgery4pRBC(0) = 0.	(A.2.170)
tkgery4pRBCi(0) = 0.	(A.2.171)
tkgrib5pRBC(0) = 0.	(A.2.172)
tkgrib5pRBCi(0) = 0.	(A.2.173)
tkxu5pRBC(0) = 0.	(A.2.174)
tkxu5pRBCi(0) = 0.	(A.2.175)
xu5pRBC(0) = 0.0020748	(A.2.176)
xu5pRBCi(0) = 0.0001092	(A.2.177)

A.3 Parameter Values:

AlphaCellWaterFraction = 0.7	(A.3.1)
AlphaRBCvGLCTransport = 0.54	(A.3.2)
CRBCvMGADP = 0.00062	(A.3.3)
CRBCvMGATP = 0.000084	(A.3.4)
CRBCvMGB13PG = 0.0032	(A.3.5)
CRBCvMGB23PG = 0.0032	(A.3.6)
CRBCvMGF16P2 = 0.0083	(A.3.7)
CRBCvMGG16P2 = 0.0083	(A.3.8)
CRBCvMGPHOS = 40800.	(A.3.9)
ConcADPRBC = 0.00031 M	(A.3.10)
ConcAMPRBC = $\frac{3}{100000}$ M	(A.3.11)
ConcATPRBC = 0.0021 M	(A.3.12)
ConcAdpPF = 0.001 M	(A.3.13)
ConcAtpPF = 0.002 M	(A.3.14)
ConcB13PGRBC = $\frac{7}{10000000}$ M	(A.3.15)
ConcB13pgPF = 0.0001 M	(A.3.16)
ConcB23PGRBC = 0.0067 M	(A.3.17)
ConcBPGSPB13PGRBC = 0. M	(A.3.18)
ConcBPGSPB23PGRBC = 0. M	(A.3.19)
ConcBPGSPPP2GRBC = 0. M	(A.3.20)
ConcBPGSPPP3GRBC = 0. M	(A.3.21)
ConcBPGSPPRBC = 0. M	(A.3.22)
ConcBPGSPRBC = 3.8×10^{-6} M	(A.3.23)
ConcBpgspphosRBC = 0. M	(A.3.24)
ConcCo2RBC = 0.0012 M	(A.3.25)
ConcDhapPF = 0.0001 M	(A.3.26)
ConcDhapRBC = 0.000019 M	(A.3.27)
ConcEry4PRBC = $\frac{1}{100000}$ M	(A.3.28)
ConcF16P2RBC = 2.7×10^{-6} M	(A.3.29)
ConcF16bpPF = 0.0001 M	(A.3.30)
ConcF6PRBC = 0.000013 M	(A.3.31)
ConcF6pPF = 0.0001 M	(A.3.32)
ConcG16P2RBC = 0.000122 M	(A.3.33)
ConcG6PRBC = $\frac{1}{25000}$ M	(A.3.34)
ConcG6pPF = 0.0001 M	(A.3.35)
ConcGSHRBC = 0.0032 M	(A.3.36)
ConcGapPF = 0.0001 M	(A.3.37)
ConcGapRBC = 5.7×10^{-6} M	(A.3.38)
ConcGlcEXT = 0.005 M	(A.3.39)
ConcGlcPF = 0.0001 M	(A.3.40)
ConcGlcRBC = 0.001 M	(A.3.41)
ConcGly3pPF = 0.0001 M	(A.3.42)
ConcGssgRBC = $\frac{9}{100000000}$ M	(A.3.43)
ConcHbADPRBC = 0. M	(A.3.44)
ConcHbATPRBC = 0. M	(A.3.45)
ConcHbB13PGRBC = 0. M	(A.3.46)

ConcHbB23PGRBC = 0. M	(A.3.47)
ConcHbRBC = 0.007 M	(A.3.48)
ConcHbmgatpRBC = 0. M	(A.3.49)
ConcLacEXT = 0.00182 M	(A.3.50)
ConcLacPF = 0.0001 M	(A.3.51)
ConcLacRBC = 0.0014 M	(A.3.52)
ConcMgADPRBC = 0. M	(A.3.53)
ConcMgB13PGRBC = 0. M	(A.3.54)
ConcMgB23PGRBC = 0. M	(A.3.55)
ConcMgF16P2RBC = 0. M	(A.3.56)
ConcMgRBC = 0.003 M	(A.3.57)
ConcMgatpRBC = 0. M	(A.3.58)
ConcMgg16p2RBC = 0. M	(A.3.59)
ConcMgphosRBC = 0. M	(A.3.60)
ConcNADPRBC = 1.25×10^{-7} M	(A.3.61)
ConcNADRBC = $\frac{3}{50000}$ M	(A.3.62)
ConcNadPF = 0.0025 M	(A.3.63)
ConcNadhPF = 0.0005 M	(A.3.64)
ConcNadhRBC = 1.4×10^{-7} M	(A.3.65)
ConcNadphRBC = 0.000064 M	(A.3.66)
ConcP2GARBC = $\frac{1}{100000}$ M	(A.3.67)
ConcP2gPF = 0.0001 M	(A.3.68)
ConcP3GARBC = 0.000064 M	(A.3.69)
ConcP3gPF = 0.0001 M	(A.3.70)
ConcP6GLRBC = 1.4×10^{-10} M	(A.3.71)
ConcP6GRBC = 1.4×10^{-7} M	(A.3.72)
ConcPEPRBC = 0.000023 M	(A.3.73)
ConcPepPF = 0.0001 M	(A.3.74)
ConcPhosEXT = 0.00192 M	(A.3.75)
ConcPhosRBC = 0.001 M	(A.3.76)
ConcPyrEXT = 0.000085 M	(A.3.77)
ConcPyrPF = 0.0001 M	(A.3.78)
ConcPyrRBC = $\frac{3}{50000}$ M	(A.3.79)
ConcRib5PRBC = $\frac{1}{100000}$ M	(A.3.80)
ConcRu5PRBC = $\frac{1}{100000}$ M	(A.3.81)
ConcSed7PRBC = $\frac{1}{100000}$ M	(A.3.82)
ConcTKGEry4PRBC = 0. M	(A.3.83)
ConcTKGRBC = 0. M	(A.3.84)
ConcTKGRib5PRBC = 0. M	(A.3.85)
ConcTKRBC = 3.3×10^{-7} M	(A.3.86)
ConcTkxu5pRBC = 0. M	(A.3.87)
ConcXu5PRBC = $\frac{1}{1000000}$ M	(A.3.88)
ConvPF = 0.214133 M	(A.3.89)
ERBCvHK = 2.5×10^{-8} M	(A.3.90)
ERBCvPGI = 2.18×10^{-7} M	(A.3.91)

$$G_{\max} = \frac{1}{20000000} \text{ mM} \quad (\text{A.3.92})$$

$$G_{\min} = \frac{3}{100000000} \text{ mM} \quad (\text{A.3.93})$$

$$\text{HCT} = 0.5 \quad (\text{A.3.94})$$

$$I_{\max} = 1.3 \times 10^{-6} \text{ mM} \quad (\text{A.3.95})$$

$$I_{\min} = \frac{7}{10000000} \text{ mM} \quad (\text{A.3.96})$$

$$K10RBCvBPGSP6 = 1979. \text{ s}^{-1} \quad (\text{A.3.97})$$

$$K10RBCvG6PDH = 1.4 \times 10^9 \text{ M}^{-1}\text{s}^{-1} \quad (\text{A.3.98})$$

$$K10RBCvGSSGR = 5. \times 10^7 \text{ M}^{-1}\text{s}^{-1} \quad (\text{A.3.99})$$

$$K10RBCvP6GDH = 225000. \text{ M}^{-1}\text{s}^{-1} \quad (\text{A.3.100})$$

$$K10RBCvTK5 = 175. \text{ s}^{-1} \quad (\text{A.3.101})$$

$$K11RBCvBPGSP6 = 0.01 \text{ s}^{-1} \quad (\text{A.3.102})$$

$$K11RBCvGSSGR = 7000. \text{ s}^{-1} \quad (\text{A.3.103})$$

$$K11RBCvP6GDH = 300. \text{ s}^{-1} \quad (\text{A.3.104})$$

$$K11RBCvTK6 = 40. \text{ s}^{-1} \quad (\text{A.3.105})$$

$$K12RBCvBPGSP7 = 1000. \text{ s}^{-1} \quad (\text{A.3.106})$$

$$K12RBCvGSSGR = 1. \times 10^8 \text{ M}^{-1}\text{s}^{-1} \quad (\text{A.3.107})$$

$$K12RBCvP6GDH = 4.95 \times 10^6 \text{ M}^{-1}\text{s}^{-1} \quad (\text{A.3.108})$$

$$K12RBCvTK6 = 21300. \text{ M}^{-1}\text{s}^{-1} \quad (\text{A.3.109})$$

$$K13RBCvBPGSP7 = 1.8 \times 10^6 \text{ M}^{-1}\text{s}^{-1} \quad (\text{A.3.110})$$

$$K14RBCvBPGSP8 = 1. \times 10^9 \text{ M}^{-1}\text{s}^{-1} \quad (\text{A.3.111})$$

$$K15RBCvBPGSP8 = 610000. \text{ s}^{-1} \quad (\text{A.3.112})$$

$$K16RBCvBPGSP9 = 0.19 \text{ s}^{-1} \quad (\text{A.3.113})$$

$$K1RBCvAK = 4300. \text{ M}^{-1}\text{s}^{-1} \quad (\text{A.3.114})$$

$$K1RBCvBPGSP1 = 8. \times 10^7 \text{ M}^{-1}\text{s}^{-1} \quad (\text{A.3.115})$$

$$K1RBCvG6PDH = 1.1 \times 10^8 \text{ M}^{-1}\text{s}^{-1} \quad (\text{A.3.116})$$

$$K1RBCvGSSGR = 8.5 \times 10^7 \text{ M}^{-1}\text{s}^{-1} \quad (\text{A.3.117})$$

$$K1RBCvP6GDH = 2.4 \times 10^6 \text{ M}^{-1}\text{s}^{-1} \quad (\text{A.3.118})$$

$$K1RBCvR5PI = 60900. \text{ M}^{-1}\text{s}^{-1} \quad (\text{A.3.119})$$

$$K1RBCvRu5PE = 3.91 \times 10^6 \text{ M}^{-1}\text{s}^{-1} \quad (\text{A.3.120})$$

$$K1RBCvTA = 580000. \text{ M}^{-1}\text{s}^{-1} \quad (\text{A.3.121})$$

$$K1RBCvTK1 = 216000. \text{ M}^{-1}\text{s}^{-1} \quad (\text{A.3.122})$$

$$K2RBCvAK = 1400. \text{ M}^{-1}\text{s}^{-1} \quad (\text{A.3.123})$$

$$K2RBCvBPGSP1 = 400. \text{ s}^{-1} \quad (\text{A.3.124})$$

$$K2RBCvG6PDH = 870. \text{ s}^{-1} \quad (\text{A.3.125})$$

$$K2RBCvGSSGR = 510. \text{ s}^{-1} \quad (\text{A.3.126})$$

$$K2RBCvP6GDH = 410. \text{ s}^{-1} \quad (\text{A.3.127})$$

$$K2RBCvR5PI = 33.3 \text{ s}^{-1} \quad (\text{A.3.128})$$

$$K2RBCvRu5PE = 438. \text{ s}^{-1} \quad (\text{A.3.129})$$

$$K2RBCvTA = 45.3 \text{ s}^{-1} \quad (\text{A.3.130})$$

$$K2RBCvTK1 = 38. \text{ s}^{-1} \quad (\text{A.3.131})$$

$$K3RBCvBPGSP2 = 9.9 \text{ s}^{-1} \quad (\text{A.3.132})$$

$$K3RBCvG6PDH = 2.6 \times 10^7 \text{ M}^{-1}\text{s}^{-1} \quad (\text{A.3.133})$$

$$K3RBCvGSSGR = 1. \times 10^9 \text{ M}^{-1}\text{s}^{-1} \quad (\text{A.3.134})$$

$$K3RBCvP6GDH = 2. \times 10^9 \text{ M}^{-1}\text{s}^{-1} \quad (\text{A.3.135})$$

$$K3RBCvR5PI = 14.2 \text{ s}^{-1} \quad (\text{A.3.136})$$

$$K3RBCvRu5PE = 305. \text{ s}^{-1} \quad (\text{A.3.137})$$

$$K3RBCvTA = 16.3 \text{ s}^{-1} \quad (\text{A.3.138})$$

$$K3RBCvTK2 = 34. \text{ s}^{-1} \quad (\text{A.3.139})$$

$$K4RBCvBPGSP3 = 1.85 \times 10^8 \text{ M}^{-1}\text{s}^{-1} \quad (\text{A.3.140})$$

$K4RBCvG6PDH = 300. s^{-1}$	(A.3.141)
$K4RBCvGSSGR = 72000. s^{-1}$	(A.3.142)
$K4RBCvP6GDH = 26000. s^{-1}$	(A.3.143)
$K4RBCvR5PI = 21600. M^{-1}s^{-1}$	(A.3.144)
$K4RBCvRu5PE = 1.49 \times 10^6 M^{-1}s^{-1}$	(A.3.145)
$K4RBCvTA = 1.01 \times 10^6 M^{-1}s^{-1}$	(A.3.146)
$K4RBCvTK2 = 156000. M^{-1}s^{-1}$	(A.3.147)
$K5RBCvBPGSP3 = 1. \times 10^8 s^{-1}$	(A.3.148)
$K5RBCvG6PDH = 750. s^{-1}$	(A.3.149)
$K5RBCvGSSGR = 810. s^{-1}$	(A.3.150)
$K5RBCvP6GDH = 48. s^{-1}$	(A.3.151)
$K5RBCvTA = 490000. M^{-1}s^{-1}$	(A.3.152)
$K5RBCvTK3 = 329000. M^{-1}s^{-1}$	(A.3.153)
$K6RBCvBPGSP4 = 1000. M^{-1}s^{-1}$	(A.3.154)
$K6RBCvG6PDH = 2000. s^{-1}$	(A.3.155)
$K6RBCvGSSGR = 1000. s^{-1}$	(A.3.156)
$K6RBCvP6GDH = 30. s^{-1}$	(A.3.157)
$K6RBCvTA = 60. s^{-1}$	(A.3.158)
$K6RBCvTK3 = 175. s^{-1}$	(A.3.159)
$K7RBCvBPGSP4 = 1000. s^{-1}$	(A.3.160)
$K7RBCvG6PDH = 220000. s^{-1}$	(A.3.161)
$K7RBCvGSSGR = 1. \times 10^6 s^{-1}$	(A.3.162)
$K7RBCvP6GDH = 630. s^{-1}$	(A.3.163)
$K7RBCvTA = 17. s^{-1}$	(A.3.164)
$K7RBCvTK4 = 40. s^{-1}$	(A.3.165)
$K8RBCvBPGSP5 = 10000. s^{-1}$	(A.3.166)
$K8RBCvG6PDH = 1.1 \times 10^9 M^{-1}s^{-1}$	(A.3.167)
$K8RBCvGSSGR = 5. \times 10^7 M^{-1}s^{-1}$	(A.3.168)
$K8RBCvP6GDH = 36000. M^{-1}s^{-1}$	(A.3.169)
$K8RBCvTA = 79000. M^{-1}s^{-1}$	(A.3.170)
$K8RBCvTK4 = 44800. M^{-1}s^{-1}$	(A.3.171)
$K9RBCvBPGSP5 = 0.55 s^{-1}$	(A.3.172)
$K9RBCvG6PDH = 10000. s^{-1}$	(A.3.173)
$K9RBCvGSSGR = 1. \times 10^6 s^{-1}$	(A.3.174)
$K9RBCvP6GDH = 800. s^{-1}$	(A.3.175)
$K9RBCvTK5 = 2.24 \times 10^6 M^{-1}s^{-1}$	(A.3.176)
$KPFvGLCtr = 0.000213 M$	(A.3.177)
$KRBCvATPASE = 0.000585 s^{-1}$	(A.3.178)
$KRBCvMGADP = 3290. L.mol^{-1}$	(A.3.179)
$KRBCvMGATP = 43200. L.mol^{-1}$	(A.3.180)
$KRBCvMGB13PG = 7410. L.mol^{-1}$	(A.3.181)
$KRBCvMGB23PG = 7410. L.mol^{-1}$	(A.3.182)
$KRBCvMGF16P2 = 363. L.mol^{-1}$	(A.3.183)
$KRBCvMGG16P2 = 363. L.mol^{-1}$	(A.3.184)
$KRBCvOX = 0.000034 s^{-1}$	(A.3.185)
$KRBCvOXNADH = 0.0163 s^{-1}$	(A.3.186)
$KaRBCvHBADP = 300000. M^{-1}s^{-1}$	(A.3.187)
$KaRBCvHBATP = 432000. M^{-1}s^{-1}$	(A.3.188)
$KaRBCvHBB13PG = 380000. M^{-1}s^{-1}$	(A.3.189)
$KaRBCvHBBPG = 300000. M^{-1}s^{-1}$	(A.3.190)
$KaRBCvHBMGATP = 46800. M^{-1}s^{-1}$	(A.3.191)
$KaRBCvMGADP = 2.76 \times 10^6 M^{-1}s^{-1}$	(A.3.192)

$K_{aRBCvMGATP} = 3.12 \times 10^7 \text{ M}^{-1}\text{s}^{-1}$	(A.3.193)
$K_{aRBCvMGB13PG} = 228000. \text{ M}^{-1}\text{s}^{-1}$	(A.3.194)
$K_{aRBCvMGB23PG} = 804000. \text{ M}^{-1}\text{s}^{-1}$	(A.3.195)
$K_{aRBCvMGF16P2} = 480000. \text{ M}^{-1}\text{s}^{-1}$	(A.3.196)
$K_{aRBCvMGG16P2} = 480000. \text{ M}^{-1}\text{s}^{-1}$	(A.3.197)
$K_{aRBCvMGPHOS} = 40800. \text{ M}^{-1}\text{s}^{-1}$	(A.3.198)
$K_{aRBCvPFK} = 8.91251 \times 10^{-8} \text{ M}$	(A.3.199)
$K_{adpPFvHK} = 0.000846735 \text{ M}$	(A.3.200)
$K_{adpPFvPFK} = 0.00074176 \text{ M}$	(A.3.201)
$K_{adpPFvPGK} = 0.00015 \text{ M}$	(A.3.202)
$K_{adpPFvPK} = 0.000317 \text{ M}$	(A.3.203)
$K_{ahbRBC} = 2.51189 \times 10^{-7} \text{ M}$	(A.3.204)
$K_{atpPFvHK} = 0.00069647 \text{ M}$	(A.3.205)
$K_{atpPFvPFK} = 0.0007862 \text{ M}$	(A.3.206)
$K_{atpPFvPGK} = 0.00077 \text{ M}$	(A.3.207)
$K_{b13pgPFvGAPDH} = 0.00002359 \text{ M}$	(A.3.208)
$K_{b13pgPFvPGK} = 0.0000134 \text{ M}$	(A.3.209)
$K_{catfRBCvALD} = 68. \text{ s}^{-1}$	(A.3.210)
$K_{catfRBCvENO} = 190. \text{ s}^{-1}$	(A.3.211)
$K_{catfRBCvGAPDH} = 695.304 \text{ s}^{-1}$	(A.3.212)
$K_{catfRBCvHK} = 299.16 \text{ s}^{-1}$	(A.3.213)
$K_{catfRBCvLDH} = 458. \text{ s}^{-1}$	(A.3.214)
$K_{catfRBCvPFK} = 822. \text{ s}^{-1}$	(A.3.215)
$K_{catfRBCvPGI} = 1470. \text{ s}^{-1}$	(A.3.216)
$K_{catfRBCvPGK} = 2290. \text{ s}^{-1}$	(A.3.217)
$K_{catfRBCvPGM} = 795. \text{ s}^{-1}$	(A.3.218)
$K_{catfRBCvPK} = 1386. \text{ s}^{-1}$	(A.3.219)
$K_{catfRBCvTIM} = 14560. \text{ s}^{-1}$	(A.3.220)
$K_{catrRBCvALD} = 234. \text{ s}^{-1}$	(A.3.221)
$K_{catrRBCvENO} = 50. \text{ s}^{-1}$	(A.3.222)
$K_{catrRBCvGAPDH} = 512.487 \text{ s}^{-1}$	(A.3.223)
$K_{catrRBCvHK} = 1.92792 \text{ s}^{-1}$	(A.3.224)
$K_{catrRBCvLDH} = 115. \text{ s}^{-1}$	(A.3.225)
$K_{catrRBCvPFK} = 36. \text{ s}^{-1}$	(A.3.226)
$K_{catrRBCvPGI} = 1760. \text{ s}^{-1}$	(A.3.227)
$K_{catrRBCvPGK} = 917. \text{ s}^{-1}$	(A.3.228)
$K_{catrRBCvPGM} = 714. \text{ s}^{-1}$	(A.3.229)
$K_{catrRBCvPK} = 3.26 \text{ s}^{-1}$	(A.3.230)
$K_{catrRBCvTIM} = 1280. \text{ s}^{-1}$	(A.3.231)
$K_{dPFvLACtr} = 0.005 \text{ min}^{-1}$	(A.3.232)
$K_{dPFvPYRtr} = 0.0007 \text{ min}^{-1}$	(A.3.233)
$K_{dRBCvHBADP} = 1200. \text{ s}^{-1}$	(A.3.234)
$K_{dRBCvHBATP} = 1200. \text{ s}^{-1}$	(A.3.235)
$K_{dRBCvHBB13PG} = 1200. \text{ s}^{-1}$	(A.3.236)
$K_{dRBCvHBBPG} = 1200. \text{ s}^{-1}$	(A.3.237)
$K_{dRBCvHBMGATP} = 1200. \text{ s}^{-1}$	(A.3.238)
$K_{dRBCvMGADP} = 1200. \text{ s}^{-1}$	(A.3.239)
$K_{dRBCvMGATP} = 1200. \text{ s}^{-1}$	(A.3.240)
$K_{dRBCvMGB13PG} = 1200. \text{ s}^{-1}$	(A.3.241)
$K_{dRBCvMGB23PG} = 1200. \text{ s}^{-1}$	(A.3.242)
$K_{dRBCvMGF16P2} = 1200. \text{ s}^{-1}$	(A.3.243)
$K_{dRBCvMGG16P2} = 1200. \text{ s}^{-1}$	(A.3.244)
$K_{dRBCvMGPHOS} = 1200. \text{ s}^{-1}$	(A.3.245)
$K_{dhapPFvALD} = 0.00011 \text{ M}$	(A.3.246)
$K_{dhapPFvG3PDH} = 0.00034 \text{ M}$	(A.3.247)

$K_{\text{dhapPFvTPI}} = 0.001954 \text{ M}$	(A.3.248)
$K_{\text{dibpgRBCvHK}} = 0.004 \text{ M}$	(A.3.249)
$K_{\text{dig16p2RBCvHK}} = \frac{3}{100000} \text{ M}$	(A.3.250)
$K_{\text{dig6pRBCvHK}} = \frac{1}{100000} \text{ M}$	(A.3.251)
$K_{\text{digshRBCvHK}} = 0.003 \text{ M}$	(A.3.252)
$K_{\text{eqPFvALD}} = \frac{9}{100000} \text{ M}^{-1}$	(A.3.253)
$K_{\text{eqPFvENO}} = 4.6$	(A.3.254)
$K_{\text{eqPFvG3PDH}} = 32600.$	(A.3.255)
$K_{\text{eqPFvHK}} = 1310.$	(A.3.256)
$K_{\text{eqPFvPGI}} = 0.33$	(A.3.257)
$K_{\text{eqPFvPGK}} = 3200.$	(A.3.258)
$K_{\text{eqPFvPGM}} = 0.19$	(A.3.259)
$K_{\text{eqPFvTPI}} = 0.04545$	(A.3.260)
$K_{\text{eqRBCvGLCTRANSPORT}} = 1.$	(A.3.261)
$K_{\text{f16bpPFvALD}} = 0.0000684 \text{ M}$	(A.3.262)
$K_{\text{f16bpPFvPFK}} = 0.003626 \text{ M}$	(A.3.263)
$K_{\text{f6pPFvPFK}} = 0.00109454 \text{ M}$	(A.3.264)
$K_{\text{f6pPFvPGI}} = 0.000096651 \text{ M}$	(A.3.265)
$K_{\text{fRBCvLDHP}} = 0.00346 \text{ s}^{-1}$	(A.3.266)
$K_{\text{g3pPFvG3PDH}} = 0.000398 \text{ M}$	(A.3.267)
$K_{\text{g6pPFvHK}} = 0.000043 \text{ M}$	(A.3.268)
$K_{\text{g6pPFvPGI}} = 0.00100774 \text{ M}$	(A.3.269)
$K_{\text{gapPFvALD}} = 0.000046 \text{ M}$	(A.3.270)
$K_{\text{gapPFvGAPDH}} = 0.000917 \text{ M}$	(A.3.271)
$K_{\text{gapPFvTPI}} = 0.000337 \text{ M}$	(A.3.272)
$K_{\text{glcPFvHK}} = 0.000168613 \text{ M}$	(A.3.273)
$K_{\text{h2bpgRBCvMGB13PG}} = 4.27 \times 10^6 \text{ L.mol}^{-1}$	(A.3.274)
$K_{\text{h2bpgRBCvMGB23PG}} = 4.27 \times 10^6 \text{ L.mol}^{-1}$	(A.3.275)
$K_{\text{h2fRBCvMGF16P2}} = 1.12 \times 10^6 \text{ L.mol}^{-1}$	(A.3.276)
$K_{\text{h2fRBCvMGG16P2}} = 1.12 \times 10^6 \text{ L.mol}^{-1}$	(A.3.277)
$K_{\text{hadpRBCvAK}} = 5.42 \times 10^6 \text{ L.mol}^{-1}$	(A.3.278)
$K_{\text{hadpRBCvMGADP}} = 5.42 \times 10^6 \text{ L.mol}^{-1}$	(A.3.279)
$K_{\text{hampRBCvAK}} = 3.09 \times 10^6 \text{ L.mol}^{-1}$	(A.3.280)
$K_{\text{hatpRBCvMGATP}} = 9.07 \times 10^6 \text{ L.mol}^{-1}$	(A.3.281)
$K_{\text{hbpgRBCvMGB13PG}} = 1.62 \times 10^8 \text{ L.mol}^{-1}$	(A.3.282)
$K_{\text{hbpgRBCvMGB23PG}} = 1.62 \times 10^8 \text{ L.mol}^{-1}$	(A.3.283)
$K_{\text{hfRBCvMGF16P2}} = 7.56 \times 10^6 \text{ L.mol}^{-1}$	(A.3.284)
$K_{\text{hfRBCvMGG16P2}} = 7.56 \times 10^6 \text{ L.mol}^{-1}$	(A.3.285)
$K_{\text{hphosRBCvMGPHOS}} = 5.68 \times 10^6 \text{ L.mol}^{-1}$	(A.3.286)
$K_{\text{hydrolRBCvPGLHYDROLYSIS}} = 0.00071 \text{ L.mol}^{-1}$	(A.3.287)
$K_{\text{iRBCvGLCTRANSPORT}} = 0.0069 \text{ M}$	(A.3.288)
$K_{\text{iRBCvLACTRANSPORT}} = 0.0036 \text{ s}^{-1}$	(A.3.289)
$K_{\text{iRBCvPHOSTRANSPORT}} = 0.00056 \text{ s}^{-1}$	(A.3.290)
$K_{\text{iRBCvPYRTRANSPORT}} = 0.018 \text{ s}^{-1}$	(A.3.291)
$K_{\text{iadpPFvPK}} = 0.002 \text{ M}$	(A.3.292)
$K_{\text{iatpPFvHK}} = 0.026 \text{ M}$	(A.3.293)

KiatpPFvPK = 0.00182 M	(A.3.294)
Kib13pgRBCvGAPDH = 4.55544×10^{-21} M	(A.3.295)
Kib13pgRBCvPGK = 1.6×10^{-6} M	(A.3.296)
Kib23pgRBCvALD = 0.0015 M	(A.3.297)
Kidb13pgRBCvGAPDH = $\frac{1}{1000000}$ M	(A.3.298)
KidgapRBCvGAPDH = 0.000031 M	(A.3.299)
KidhapRBCvALD = 0.000011 M	(A.3.300)
KidpyrRBCvLDH = 0.000101 M	(A.3.301)
Kif16p2RBCvALD = 0.0000198 M	(A.3.302)
Kig6pRBCvHK = 0.000047 M	(A.3.303)
KigapRBCvGAPDH = 4.76523×10^{-19} M	(A.3.304)
KiglcRBCvHK = 0.000047 M	(A.3.305)
KilacPFvPYRtr = 0.000358 M	(A.3.306)
KilacRBCvLDH = 0.00733 M	(A.3.307)
KingRBCvENO = 0.000046 M	(A.3.308)
KingadpRBCvHK = 0.001 M	(A.3.309)
KingadpRBCvPGK = $\frac{1}{12500}$ M	(A.3.310)
KingatpRBCvHK = 0.001 M	(A.3.311)
KingatpRBCvPGK = 0.000186 M	(A.3.312)
KinadRBCvGAPDH = 0.000045 M	(A.3.313)
KinadRBCvLDH = 0.000503 M	(A.3.314)
KinadhRBCvGAPDH = $\frac{1}{100000}$ M	(A.3.315)
KinadhRBCvLDH = 2.45×10^{-6} M	(A.3.316)
Kip2gRBCvENO = 0.00014 M	(A.3.317)
Kip3gRBCvPGK = 0.000205 M	(A.3.318)
KipepPFvPK = 0.00292 M	(A.3.319)
KipepPFvTPI = 0.0000159 M	(A.3.320)
KipepRBCvENO = 0.0001105 M	(A.3.321)
KiphosRBCvGAPDH = 0.00316 M	(A.3.322)
KipyrPFvLACtr = 0.00163 M	(A.3.323)
KipyrPFvPK = 0.105 M	(A.3.324)
KipyrRBCvLDH = 0.000228 M	(A.3.325)
KkadpRBCvAK = 4.8 L.mol ⁻¹	(A.3.326)
KkadpRBCvMGADP = 4.8 L.mol ⁻¹	(A.3.327)
KkampRBCvAK = 1.8 L.mol ⁻¹	(A.3.328)
KkatpRBCvMGATP = 14. L.mol ⁻¹	(A.3.329)
KkbpgrBCvMGB13PG = 85.1 L.mol ⁻¹	(A.3.330)
KkbpgrBCvMGB23PG = 85.1 L.mol ⁻¹	(A.3.331)
KkfrBCvMGF16P2 = 10.7 L.mol ⁻¹	(A.3.332)
KkfrBCvMGG16P2 = 10.7 L.mol ⁻¹	(A.3.333)
KkhhbpgrBCvMGB13PG = 8.9 L.mol ⁻¹	(A.3.334)
KkhhbpgrBCvMGB23PG = 8.9 L.mol ⁻¹	(A.3.335)
KkhfrBCvMGF16P2 = 3.3 L.mol ⁻¹	(A.3.336)
KkhfrBCvMGG16P2 = 3.3 L.mol ⁻¹	(A.3.337)
KkphosRBCvMGPHOS = 3. L.mol ⁻¹	(A.3.338)
KlacPFvLACtr = 0.0038 M	(A.3.339)
KlacPFvLDH = 0.003611 M	(A.3.340)
Klactonase1RBCvPGLHYDROLYSIS = 1.3×10^7 M ⁻¹ s ⁻¹	(A.3.341)
Klactonase2RBCvPGLHYDROLYSIS = 1000. s ⁻¹	(A.3.342)
Klactonase3RBCvPGLHYDROLYSIS = 29. s ⁻¹	(A.3.343)

$K_{mPFvATPASE} = 0.0045 \text{ M}$	(A.3.344)
$K_{mb13pgRBCvGAPDH} = 6.71 \times 10^{-7} \text{ M}$	(A.3.345)
$K_{mb13pgRBCvPGK} = \frac{1}{500000} \text{ M}$	(A.3.346)
$K_{mdhapRBCvALD} = 0.000035 \text{ M}$	(A.3.347)
$K_{mdhapRBCvTIM} = 0.0001624 \text{ M}$	(A.3.348)
$K_{mf16p2RBCvALD} = 7.1 \times 10^{-6} \text{ M}$	(A.3.349)
$K_{mf16p2RBCvPFK} = 0.0005 \text{ M}$	(A.3.350)
$K_{mf6pRBCvPFK} = 0.000075 \text{ M}$	(A.3.351)
$K_{mf6pRBCvPGI} = 0.000071 \text{ M}$	(A.3.352)
$K_{mg6pRBCvPGI} = 0.000181 \text{ M}$	(A.3.353)
$K_{mgapRBCvALD} = 0.000189 \text{ M}$	(A.3.354)
$K_{mgapRBCvGAPDH} = 0.000095 \text{ M}$	(A.3.355)
$K_{mgapRBCvTIM} = 0.000446 \text{ M}$	(A.3.356)
$K_{mgahdpRBCvMGADP} = 107. \text{ L.mol}^{-1}$	(A.3.357)
$K_{mgahdpRBCvMGATP} = 748. \text{ L.mol}^{-1}$	(A.3.358)
$K_{mgbbpgRBCvMGB13PG} = 513. \text{ L.mol}^{-1}$	(A.3.359)
$K_{mgbbpgRBCvMGB23PG} = 513. \text{ L.mol}^{-1}$	(A.3.360)
$K_{mgfRBCvMGF16P2} = 89. \text{ L.mol}^{-1}$	(A.3.361)
$K_{mgfRBCvMGG16P2} = 89. \text{ L.mol}^{-1}$	(A.3.362)
$K_{mlacRBCvLDH} = 0.00107 \text{ M}$	(A.3.363)
$K_{mlacRBCvLDHP} = 0.000414 \text{ M}$	(A.3.364)
$K_{mmgRBCvENO} = 0.000046 \text{ M}$	(A.3.365)
$K_{mmgadpRBCvHK} = 0.001 \text{ M}$	(A.3.366)
$K_{mmgadpRBCvPFK} = 0.00054 \text{ M}$	(A.3.367)
$K_{mmgadpRBCvPGK} = 0.0001 \text{ M}$	(A.3.368)
$K_{mmgatpRBCvHK} = 0.001 \text{ M}$	(A.3.369)
$K_{mmgatpRBCvPFK} = 0.000068 \text{ M}$	(A.3.370)
$K_{mmgatpRBCvPGK} = 0.001 \text{ M}$	(A.3.371)
$K_{mnadRBCvGAPDH} = 0.000045 \text{ M}$	(A.3.372)
$K_{mnadRBCvLDH} = 0.000107 \text{ M}$	(A.3.373)
$K_{mnadhRBCvGAPDH} = 3.3 \times 10^{-6} \text{ M}$	(A.3.374)
$K_{mnadhRBCvLDH} = 8.44 \times 10^{-6} \text{ M}$	(A.3.375)
$K_{mp2gRBCvENO} = 0.00014 \text{ M}$	(A.3.376)
$K_{mp2gRBCvPGM} = 0.0000256 \text{ M}$	(A.3.377)
$K_{mp3gRBCvPGK} = 0.0011 \text{ M}$	(A.3.378)
$K_{mp3gRBCvPGM} = 0.000168 \text{ M}$	(A.3.379)
$K_{mpepRBCvENO} = 0.0001105 \text{ M}$	(A.3.380)
$K_{mphosRBCvGAPDH} = 0.00316 \text{ M}$	(A.3.381)
$K_{mpyrRBCvLDH} = 0.000137 \text{ M}$	(A.3.382)
$K_{mpyrRBCvLDHP} = 0.000414 \text{ M}$	(A.3.383)
$K_{mtL2} = 0.8 \text{ mM}$	(A.3.384)
$K_{nadPFvG3PDH} = 0.00051 \text{ M}$	(A.3.385)
$K_{nadPFvGAPDH} = 0.0000287 \text{ M}$	(A.3.386)
$K_{nadPFvLDH} = 0.000234 \text{ M}$	(A.3.387)
$K_{nadhPFvG3PDH} = \frac{9}{100000} \text{ M}$	(A.3.388)
$K_{nadhPFvGAPDH} = 0.00002719 \text{ M}$	(A.3.389)
$K_{nadhPFvLDH} = 0.000046 \text{ M}$	(A.3.390)
$K_{oRBCvGLCTransport} = 0.0017 \text{ M}$	(A.3.391)

$K_{p2gPFvENO} = 0.000521 \text{ M}$	(A.3.392)
$K_{p2gPFvPGM} = 0.000318 \text{ M}$	(A.3.393)
$K_{p3gPFvPGK} = 0.000267 \text{ M}$	(A.3.394)
$K_{p3gPFvPGM} = 0.00173 \text{ M}$	(A.3.395)
$K_{pepPFvENO} = 0.00129 \text{ M}$	(A.3.396)
$K_{pepPFvPK} = 0.000406 \text{ M}$	(A.3.397)
$K_{pyrPFvLDH} = 0.000133 \text{ M}$	(A.3.398)
$K_{pyrPFvPYRtr} = 0.0157 \text{ M}$	(A.3.399)
$K_{rRBCvLDHP} = 5.43 \times 10^{-7} \text{ s}^{-1}$	(A.3.400)
$K_{rampRBCvPFK} = 0.0003 \text{ M}$	(A.3.401)
$K_{rf16p2RBCvPK} = \frac{1}{200000} \text{ M}$	(A.3.402)
$K_{rg16p2RBCvPFK} = 0.01 \text{ M}$	(A.3.403)
$K_{rg16p2RBCvPK} = 0.0001 \text{ M}$	(A.3.404)
$K_{rmgadpRBCvPK} = 0.000474 \text{ M}$	(A.3.405)
$K_{rmgatpRBCvPK} = 0.003 \text{ M}$	(A.3.406)
$K_{rpepRBCvPK} = 0.000225 \text{ M}$	(A.3.407)
$K_{rphosRBCvPFK} = 0.03 \text{ M}$	(A.3.408)
$K_{rpyrRBCvPK} = 0.002 \text{ M}$	(A.3.409)
$K_{tatpRBCvPFK} = 0.0001 \text{ M}$	(A.3.410)
$K_{tatpRBCvPK} = 0.00339 \text{ M}$	(A.3.411)
$K_{tb23pgRBCvPFK} = 0.005 \text{ M}$	(A.3.412)
$K_{tmgRBCvPFK} = 0.004 \text{ M}$	(A.3.413)
$LPFvPK = 0.255$	(A.3.414)
$PP1t = 0.00025 \text{ mM}$	(A.3.415)
$RtvRBC = 0.69$	(A.3.416)
$TsRBC = 60. \text{ s.min}^{-1}$	(A.3.417)
$VPFvALD = 0.0569593 \text{ M.min}^{-1}$	(A.3.418)
$VPFvATPASE = 0.345 \text{ M.min}^{-1}$	(A.3.419)
$VPFvENO = 0.286296 \text{ M.min}^{-1}$	(A.3.420)
$VPFvGAPDH = 0.656263 \text{ M.min}^{-1}$	(A.3.421)
$VPFvGLCtr = 0.0469 \text{ M.min}^{-1}$	(A.3.422)
$VPFvHK = 0.083 \text{ M.min}^{-1}$	(A.3.423)
$VPFvLACtr = 0.598 \text{ M.min}^{-1}$	(A.3.424)
$VPFvPFK = 0.41 \text{ M.min}^{-1}$	(A.3.425)
$VPFvPGI = 0.800428 \text{ M.min}^{-1}$	(A.3.426)
$VPFvPGM = 0.186938 \text{ M.min}^{-1}$	(A.3.427)
$VPFvPK = 0.762 \text{ M.min}^{-1}$	(A.3.428)
$VPFvPYRtr = 0.216 \text{ M.min}^{-1}$	(A.3.429)
$VPFvTPI = 1.506 \text{ M.min}^{-1}$	(A.3.430)
$VRBCvALD = 3.7 \times 10^{-7} \text{ M}$	(A.3.431)
$VRBCvENO = 2.2 \times 10^{-7} \text{ M}$	(A.3.432)
$VRBCvG6PDH = 9.3 \times 10^{-8} \text{ M}$	(A.3.433)
$VRBCvGAPDH = 7.66 \times 10^{-6} \text{ M}$	(A.3.434)
$VRBCvGLCTRANSPORT = 0.047 \text{ M}$	(A.3.435)
$VRBCvGSSGR = 1.25 \times 10^{-7} \text{ M}$	(A.3.436)
$VRBCvLDH = 3.43 \times 10^{-6} \text{ M}$	(A.3.437)
$VRBCvP6GDH = 2.1 \times 10^{-6} \text{ M}$	(A.3.438)
$VRBCvPFK = 1.1 \times 10^{-7} \text{ M}$	(A.3.439)
$VRBCvPGK = 2.74 \times 10^{-6} \text{ M}$	(A.3.440)
$VRBCvPGLHYDROLYSIS = 0.000014 \text{ M}$	(A.3.441)

$VRBCvPGM = 4.1 \times 10^{-7} \text{ M}$	(A.3.442)
$VRBCvPK = 8.7 \times 10^{-8} \text{ M}$	(A.3.443)
$VRBCvR5PI = 0.0000142 \text{ M}$	(A.3.444)
$VRBCvRu5PE = 4.22 \times 10^{-6} \text{ M}$	(A.3.445)
$VRBCvTA = 6.9 \times 10^{-7} \text{ M}$	(A.3.446)
$VRBCvTIM = 1.14 \times 10^{-6} \text{ M}$	(A.3.447)
$VfPFvG3PDH = 0.012 \text{ M}\cdot\text{min}^{-1}$	(A.3.448)
$VfPFvLDH = 0.542612 \text{ M}\cdot\text{min}^{-1}$	(A.3.449)
$VmtL2 = 0.4125 \text{ mM}\cdot\text{min}^{-1}$	(A.3.450)
$VrPFvGAPDH = 0.243199 \text{ M}\cdot\text{min}^{-1}$	(A.3.451)
$VrPFvLDH = 0.290792 \text{ M}\cdot\text{min}^{-1}$	(A.3.452)
$VrPFvPGK = 0.353533 \text{ M}\cdot\text{min}^{-1}$	(A.3.453)
$\alpha PFvGLCtr = 0.91$	(A.3.454)
$c0 = 5.$	(A.3.455)
$capkt = 0.00025 \text{ mM}$	(A.3.456)
$cmax = 0.0032 \text{ mM}$	(A.3.457)
$cmin = \frac{1}{500000} \text{ mM}$	(A.3.458)
$cyt = 0. \text{ M}$	(A.3.459)
$en1 = 10.$	(A.3.460)
$en10 = 10.$	(A.3.461)
$en11 = 10.$	(A.3.462)
$en12 = 10.$	(A.3.463)
$en2 = 10.$	(A.3.464)
$en3 = 10.$	(A.3.465)
$en4 = 10.$	(A.3.466)
$en5 = 10.$	(A.3.467)
$en6 = 10.$	(A.3.468)
$en7 = 10.$	(A.3.469)
$en8 = 10.$	(A.3.470)
$en9 = 20.$	(A.3.471)
$ep1 = 10.$	(A.3.472)
$ep10 = 10.$	(A.3.473)
$ep11 = 10.$	(A.3.474)
$ep12 = 10.$	(A.3.475)
$ep13 = 10.$	(A.3.476)
$ep14 = 10.$	(A.3.477)
$ep15 = 10.$	(A.3.478)
$ep2 = 10.$	(A.3.479)
$ep3 = 10.$	(A.3.480)
$ep4 = 10.$	(A.3.481)
$ep5 = 10.$	(A.3.482)
$ep6 = 10.$	(A.3.483)
$ep7 = 10.$	(A.3.484)
$ep8 = 10.$	(A.3.485)
$ep9 = 10.$	(A.3.486)
$glc_alpha = 0.36$	(A.3.487)

$h = 4.$	(A.3.488)
$\text{index} = 5.$	(A.3.489)
$k_{11} = 0.000043 \text{ mM}$	(A.3.490)
$k_{22} = 0.0007 \text{ mM}$	(A.3.491)
$k_{\text{PFvGLYtr}} = 2. \text{ min}^{-1}$	(A.3.492)
$k_{\text{RBC}} = 0.15 \text{ M}$	(A.3.493)
$k_{\text{Dglucgn}} = \frac{1}{25000000} \text{ mM}$	(A.3.494)
$k_{\text{Dins}} = \frac{1}{1000000} \text{ mM}$	(A.3.495)
$k_{\text{Dins2}} = 7.5 \times 10^{-7} \text{ mM}$	(A.3.496)
$k_{\text{L10}} = 0.1 \text{ min}^{-1}$	(A.3.497)
$k_{\text{L11f}} = 0.6 \text{ min}^{-1}$	(A.3.498)
$k_{\text{L11r}} = 0.01 \text{ min}^{-1}$	(A.3.499)
$k_{\text{L12}} = 0.6 \text{ min}^{-1}$	(A.3.500)
$k_{\text{L13}} = 0.5 \text{ min}^{-1}$	(A.3.501)
$k_{\text{L14}} = 0.01 \text{ min}^{-1}$	(A.3.502)
$k_{\text{L15}} = 0.01 \text{ min}^{-1}$	(A.3.503)
$k_{\text{L16}} = 0.01 \text{ mM}^{-7} \text{ min}^{-1}$	(A.3.504)
$k_{\text{L17}} = 0.01 \text{ mM} \cdot \text{min}^{-1}$	(A.3.505)
$k_{\text{L18}} = 0.01 \text{ min}^{-1}$	(A.3.506)
$k_{\text{L19}} = 0.01 \text{ mM}^{-1} \text{ min}^{-1}$	(A.3.507)
$k_{\text{L1f}} = 3. \text{ mM} \cdot \text{min}^{-1}$	(A.3.508)
$k_{\text{L1r}} = 4. \text{ mM} \cdot \text{min}^{-1}$	(A.3.509)
$k_{\text{L20}} = 0.2 \text{ min}^{-1}$	(A.3.510)
$k_{\text{L21f}} = 0.001 \text{ mM} \cdot \text{min}^{-1}$	(A.3.511)
$k_{\text{L21r}} = 0.2 \text{ min}^{-1}$	(A.3.512)
$k_{\text{L22}} = 0.01 \text{ min}^{-1}$	(A.3.513)
$k_{\text{L2f}} = 200. \text{ min}^{-1}$	(A.3.514)
$k_{\text{L2r}} = 20. \text{ min}^{-1}$	(A.3.515)
$k_{\text{L3f}} = 0.1 \text{ mM} \cdot \text{min}^{-1}$	(A.3.516)
$k_{\text{L3r}} = 0.3 \text{ mM} \cdot \text{min}^{-1}$	(A.3.517)
$k_{\text{L4}} = 2. \text{ mM} \cdot \text{min}^{-1}$	(A.3.518)
$k_{\text{L5f}} = 0.$	(A.3.519)
$k_{\text{L5r}} = 0.1$	(A.3.520)
$k_{\text{L6}} = 1. \text{ mM} \cdot \text{min}^{-1}$	(A.3.521)
$k_{\text{L7}} = 1. \text{ mM} \cdot \text{min}^{-1}$	(A.3.522)
$k_{\text{L8}} = 0.1 \text{ mM}^{-1} \text{ min}^{-1}$	(A.3.523)
$k_{\text{L9}} = 0.1 \text{ min}^{-1}$	(A.3.524)
$k_{\text{a}} = 60.$	(A.3.525)
$k_{\text{alpha}} = 0.0083 \text{ M}$	(A.3.526)
$k_{\text{beta}} = 0.007 \text{ M}$	(A.3.527)
$k_{\text{dcAMP}} = 3.16227 \times 10^{-6} \text{ mM}$	(A.3.528)
$k_{\text{f1}} = 0.1 \text{ min}^{-1}$	(A.3.529)
$k_{\text{f3}} = 0.2 \text{ min}^{-1}$	(A.3.530)
$k_{\text{f4}} = 0.1 \text{ min}^{-1}$	(A.3.531)
$k_{\text{f5}} = 0.1 \text{ mM}^{-2} \text{ min}^{-1}$	(A.3.532)
$k_{\text{gc1}} = 60000. \text{ mM}^{-2} \text{ min}^{-1}$	(A.3.533)
$k_{\text{gc2}} = 60000. \text{ mM}^2 \text{ min}^{-1}$	(A.3.534)
$k_{\text{i1}} = 0.1 \text{ mM}$	(A.3.535)
$k_{\text{i13}} = 2. \text{ mM}$	(A.3.536)
$k_{\text{i2}} = 1. \text{ mM}$	(A.3.537)

$k_{i4} = 3. \text{ mM}$	(A.3.538)
$k_{i5} = 1. \text{ mM}$	(A.3.539)
$k_{i8} = 2. \text{ mM}$	(A.3.540)
$k_{mGln} = 8. \text{ mM}$	(A.3.541)
$k_{mIns} = 8. \text{ mM}$	(A.3.542)
$k_{mL1f} = 7.7 \text{ mM}$	(A.3.543)
$k_{mL1r} = 1.3 \text{ mM}$	(A.3.544)
$k_{mL21a} = 21. \text{ mM}$	(A.3.545)
$k_{mL21g} = 4.3 \text{ mM}$	(A.3.546)
$k_{mL21k} = 0.22 \text{ mM}$	(A.3.547)
$k_{mL21p} = 0.4 \text{ mM}$	(A.3.548)
$k_{mL2f} = 0.57 \text{ mM}$	(A.3.549)
$k_{mL2r} = 1.4 \text{ mM}$	(A.3.550)
$k_{mL3f} = 0.01 \text{ mM}$	(A.3.551)
$k_{mL3r} = 0.0034 \text{ mM}$	(A.3.552)
$k_{mL4} = 0.18 \text{ mM}$	(A.3.553)
$k_{mL5f} = 0.03 \text{ mM}$	(A.3.554)
$k_{mL5r} = 0.8 \text{ mM}$	(A.3.555)
$k_{mL6} = 0.22 \text{ mM}$	(A.3.556)
$k_{mL7} = 0.0204 \text{ mM}$	(A.3.557)
$k_{p1} = 0.5 \text{ mM}$	(A.3.558)
$k_{p2} = 2. \text{ mM}$	(A.3.559)
$k_{s1f} = 0. \text{ min}^{-1}$	(A.3.560)
$k_{s1r} = 0. \text{ min}^{-1}$	(A.3.561)
$k_{s2} = 0.02 \text{ min}^{-1}$	(A.3.562)
$k_{s3f} = 0.01 \text{ min}^{-1}$	(A.3.563)
$k_{s3r} = 0.01 \text{ min}^{-1}$	(A.3.564)
$k_{s4f} = 0.07 \text{ min}^{-1}$	(A.3.565)
$k_{s4r} = 0. \text{ min}^{-1}$	(A.3.566)
$k_{tF1} = 0.01 \text{ min}^{-1}$	(A.3.567)
$k_{tF3} = 0.008 \text{ mM}^{-2} \text{ min}^{-1}$	(A.3.568)
$k_{tL1} = 100. \text{ min}^{-1}$	(A.3.569)
$k_{tL2} = 0.1 \text{ min}^{-1}$	(A.3.570)
$k_{tL3} = 0.1 \text{ min}^{-1}$	(A.3.571)
$k_{tL5} = 0.1 \text{ min}^{-1}$	(A.3.572)
$k_{tL6} = 1. \text{ min}^{-1}$	(A.3.573)
$k_{tS1} = 0.01 \text{ min}^{-1}$	(A.3.574)
$k_{tS2} = 1. \text{ min}^{-1}$	(A.3.575)
$k_{tS3} = 0.01 \text{ min}^{-1}$	(A.3.576)
$k_{tS4} = 3. \text{ min}^{-1}$	(A.3.577)
$kc1 = 1. \text{ min}^{-1}$	(A.3.578)
$kcm1 = \frac{1}{25000000} \text{ mM}$	(A.3.579)
$kcm2 = \frac{1}{1000000} \text{ mM}$	(A.3.580)
$kd_{Balan} = 0.015 \text{ min}^{-1}$	(A.3.581)
$kd_{Bffa} = 0.015 \text{ min}^{-1}$	(A.3.582)
$kd_{Bgluc} = 0.015 \text{ min}^{-1}$	(A.3.583)
$kd_{Bglucgn} = 0.015 \text{ min}^{-1}$	(A.3.584)
$kd_{Bins} = 0.015 \text{ min}^{-1}$	(A.3.585)
$kd_{Bket} = 0.015 \text{ min}^{-1}$	(A.3.586)
$kd_{Blac} = 0.015 \text{ min}^{-1}$	(A.3.587)
$kf = 0.5 \text{ min}^{-1}$	(A.3.588)

kg2 = 0.5 mM	(A.3.589)
kg3 = 1200. min ⁻¹	(A.3.590)
kg4 = 300. min ⁻¹	(A.3.591)
kg5 = 1200. min ⁻¹	(A.3.592)
kg6 = 300. min ⁻¹	(A.3.593)
kg7 = 1200. min ⁻¹	(A.3.594)
kg8 = 300. min ⁻¹	(A.3.595)
kgi = 10. mM	(A.3.596)
ki1 = 9.26558 × 10 ⁻⁸ M	(A.3.597)
ki2 = 0.0000156304 M	(A.3.598)
kmg3 = 0.0004 mM	(A.3.599)
kmg4 = 0.0011 mM	(A.3.600)
kmg5 = 0.01 mM	(A.3.601)
kmg6 = 0.005 mM	(A.3.602)
kmg7 = 0.015 mM	(A.3.603)
kmg8 = 0.00012 mM	(A.3.604)
kresume = 1.4 mM.min ⁻¹	(A.3.605)
ks_dket = 0.01 min ⁻¹	(A.3.606)
kt = 0.0025 mM	(A.3.607)
nRBCvPFK = 5.	(A.3.608)
ng = 10.	(A.3.609)
ni = 10.	(A.3.610)
p1 = 1.	(A.3.611)
p2 = 1.	(A.3.612)
pHConversionFactor = 1.	(A.3.613)
par = 0.05	(A.3.614)
parMulti = 1.	(A.3.615)
phPF = 7.2	(A.3.616)
phRBC = 7.1	(A.3.617)
pt = 0.07 mM	(A.3.618)
s1 = 100.	(A.3.619)
s2 = 0.001	(A.3.620)
st = 0.003 mM	(A.3.621)
tresume = 20250. min	(A.3.622)
v_totblood = 6.24 L	(A.3.623)
PKb = 0.0078 mM	(A.3.624)

A.4 Kinetic rates or reaction processes:

$$Jg10 = kgc1 \cdot cAMP(t)^2 \cdot R2C2(t) - k_gc1 \cdot Cvar(t) \cdot R2_C_cAMP2(t) \quad (A.4.1)$$

$$Jg11 = kgc2 \cdot cAMP(t)^2 \cdot R2_C_cAMP2(t) - k_gc2 \cdot Cvar(t) \cdot R2_cAMP4(t) \quad (A.4.2)$$

$$Jg3 = \frac{kg3 \cdot Cvar(t) \cdot (kt - PKa(t))}{kmg3 + kt - PKa(t)} \quad (A.4.3)$$

$$Jg4 = \frac{kg4 \cdot PKa(t) \cdot (PP1(t) + PP1_GPa(t))}{kmg4 + PKa(t)} \quad (A.4.4)$$

$$Jg5 = \frac{kg5 \cdot (pt - GPa(t)) \cdot PKa(t)}{kmg5s + pt - GPa(t)} \quad (A.4.5)$$

$$Jg6 = \frac{kg6 \cdot GPa(t) \cdot (PP1(t) + PP1_GPa(t))}{kmg6s + GPa(t)} \quad (A.4.6)$$

$$Jg7 = \frac{kg7 \cdot GSa(t) \cdot (Cvar(t) + PKa(t))}{kmg7s + GSa(t)} \quad (A.4.7)$$

$$Jg8 = \frac{kg8 \cdot (st - GSa(t)) \cdot PP1(t)}{kmg8s + st - GSa(t)} \quad (A.4.8)$$

$$Jg9 = ka \cdot GPa(t) \cdot PP1(t) - k_a \cdot PP1_GPa(t) \quad (A.4.9)$$

$$vPFvALD = \frac{\text{parMulti} \cdot VPFvALD \cdot f16bpPF(t) \cdot \left(1 - \frac{\text{dhapPF}(t) \cdot \text{gapPF}(t)}{\text{KeqPFvALD} \cdot Vpf \cdot f16bpPF(t)}\right)}{Kf16bpPFvALD \cdot \left(\frac{\text{gapPF}(t) \cdot \text{dhapPF}(t)}{K\text{dhapPFvALD} \cdot K\text{gapPFvALD} \cdot Vpf^2} + \frac{\text{dhapPF}(t)}{K\text{dhapPFvALD} \cdot Vpf} + \frac{f16bpPF(t)}{Kf16bpPFvALD \cdot Vpf} + \frac{\text{gapPF}(t)}{K\text{gapPFvALD} \cdot Vpf} + 1\right)} \quad (A.4.10)$$

$$vPFvATPASE = \frac{\text{parMulti} \cdot VPFvATPASE \cdot \text{atpPF}(t)^5}{K\text{mPFvATPASE}^5 \cdot Vpf^4 \cdot \left(\frac{\text{atpPF}(t)^5}{K\text{mPFvATPASE}^5 \cdot Vpf^5} + 1\right)} \quad (A.4.11)$$

$$vPFvENO = \frac{\text{parMulti} \cdot VPFvENO \cdot p2gPF(t) \cdot \left(1 - \frac{\text{pepPF}(t)}{\text{KeqPFvENO} \cdot p2gPF(t)}\right)}{Kp2gPFvENO \cdot \left(\frac{p2gPF(t)}{Kp2gPFvENO \cdot Vpf} + \frac{\text{pepPF}(t)}{K\text{pepPFvENO} \cdot Vpf} + 1\right)} \quad (A.4.12)$$

$$vPFvG3PDH = \frac{\text{parMulti} \cdot VPFvG3PDH \cdot \text{dhapPF}(t) \cdot \text{nadhPF}(t) \cdot \left(1 - \frac{g3pPF(t) \cdot \text{nadhPF}(t)}{\text{KeqPFvG3PDH} \cdot \text{dhapPF}(t) \cdot \text{nadhPF}(t)}\right)}{K\text{dhapPFvG3PDH} \cdot K\text{nadhPFvG3PDH} \cdot Vpf \cdot \left(\frac{\text{dhapPF}(t)}{K\text{dhapPFvG3PDH} \cdot Vpf} + \frac{g3pPF(t)}{Kg3pPFvG3PDH \cdot Vpf} + 1\right) \cdot \left(\frac{\text{nadhPF}(t)}{K\text{nadhPFvG3PDH} \cdot Vpf} + \frac{\text{nadhPF}(t)}{K\text{nadPFvG3PDH} \cdot Vpf} + 1\right)} \quad (A.4.13)$$

$$vPFvGAPDH = \frac{\text{parMulti} \cdot \left(\frac{VPFvGAPDH \cdot \text{gapPF}(t) \cdot \text{nadPF}(t)}{K_{\text{gapPFvGAPDH}} \cdot K_{\text{nadPFvGAPDH}} \cdot V_{\text{pf}}} - \frac{VrPFvGAPDH \cdot \text{b13pgPF}(t) \cdot \text{nadhPF}(t)}{K_{\text{b13pgPFvGAPDH}} \cdot K_{\text{nadhPFvGAPDH}} \cdot V_{\text{pf}}} \right)}{\left(\frac{\text{b13pgPF}(t)}{K_{\text{b13pgPFvGAPDH}} \cdot V_{\text{pf}}} + \frac{\text{gapPF}(t)}{K_{\text{gapPFvGAPDH}} \cdot V_{\text{pf}}} + 1 \right) \cdot \left(\frac{\text{nadhPF}(t)}{K_{\text{nadhPFvGAPDH}} \cdot V_{\text{pf}}} + \frac{\text{nadPF}(t)}{K_{\text{nadPFvGAPDH}} \cdot V_{\text{pf}}} + 1 \right)} \quad (\text{A.4.14})$$

$$vPFvGLCtr = \frac{\text{parMulti} \cdot \left(\frac{V_{\text{pf}} \cdot VPFvGLCtr \cdot \text{glcRBCi}(t)}{\left(\frac{c_{\text{yt}}}{k_{\text{t1}}} + 1 \right) \cdot KPFvGLCtr \cdot V_{\text{rbci}}} - \frac{VPFvGLCtr \cdot \text{glcPF}(t)}{\left(\frac{c_{\text{yt}}}{k_{\text{t1}}} + 1 \right) \cdot KPFvGLCtr} \right)}{\frac{\text{alphaPFvGLCtr} \cdot \text{glcRBCi}(t) \cdot \text{glcPF}(t)}{\left(\frac{c_{\text{yt}}}{k_{\text{t1}}} + 1 \right) \cdot KPFvGLCtr^2 \cdot V_{\text{pf}} \cdot V_{\text{rbci}}} + \frac{\left(\frac{c_{\text{yt}}}{k_{\text{t2}}} + 1 \right) \cdot \text{glcPF}(t)}{\left(\frac{c_{\text{yt}}}{k_{\text{t1}}} + 1 \right) \cdot KPFvGLCtr \cdot V_{\text{pf}}} + \frac{\left(\frac{c_{\text{yt}}}{k_{\text{t2}}} + 1 \right) \cdot \text{glcRBCi}(t)}{\left(\frac{c_{\text{yt}}}{k_{\text{t1}}} + 1 \right) \cdot KPFvGLCtr \cdot V_{\text{rbci}}} + 1} \quad (\text{A.4.15})$$

$$vPFvGLYtr = kPFvGLYtr \cdot \text{parMulti} \cdot V_{\text{pf}} \cdot \left(\frac{\text{g3pPF}(t)}{V_{\text{pf}}} - \frac{\text{glyEXT}}{v_{\text{Bld}}} \right) \quad (\text{A.4.16})$$

$$vPFvHK = \frac{\text{parMulti} \cdot VPFvHK \cdot \text{atpPF}(t) \cdot \left(1 - \frac{\text{adpPF}(t) \cdot \text{g6pPF}(t)}{K_{\text{eqPFvHK}} \cdot \text{atpPF}(t) \cdot \text{glcPF}(t)} \right) \cdot \text{glcPF}(t)}{\text{KatpPFvHK} \cdot K_{\text{glcPFvHK}} \cdot V_{\text{pf}} \cdot \left(\frac{\text{adpPF}(t)}{K_{\text{adpPFvHK}} \cdot V_{\text{pf}}} + \frac{\text{atpPF}(t)}{\text{KatpPFvHK} \cdot V_{\text{pf}}} + 1 \right) \cdot \left(\frac{\text{atpPF}(t)}{K_{\text{iatpPFvHK}} \cdot V_{\text{pf}}} + 1 \right) \cdot \left(\frac{\text{g6pPF}(t)}{K_{\text{g6pPFvHK}} \cdot V_{\text{pf}}} + \frac{\text{glcPF}(t)}{K_{\text{glcPFvHK}} \cdot V_{\text{pf}}} + 1 \right)} \quad (\text{A.4.17})$$

$$vPFvLACtr = KdPFvLACtr \cdot \text{parMulti} \cdot \text{lacPF}(t) \cdot \left(1 - \frac{\text{hRBC} \cdot V_{\text{pf}} \cdot \text{lacRBCi}(t)}{\text{hPF} \cdot V_{\text{rbci}} \cdot \text{lacPF}(t)} \right) \quad (\text{A.4.18})$$

$$+ \frac{VPFvLACtr \cdot \text{lacPF}(t) \cdot \left(1 - \frac{\text{hRBC} \cdot V_{\text{pf}} \cdot \text{lacRBCi}(t)}{\text{hPF} \cdot V_{\text{rbci}} \cdot \text{lacPF}(t)} \right)}{K_{\text{lacPFvLACtr}} \cdot \left(\frac{\text{lacPF}(t)}{K_{\text{lacPFvLACtr}} \cdot V_{\text{pf}}} + \frac{\text{lacRBCi}(t)}{K_{\text{lacPFvLACtr}} \cdot V_{\text{rbci}}} + \frac{\text{pyrPF}(t)}{K_{\text{pyrPFvLACtr}} \cdot V_{\text{pf}}} + \frac{\text{pyrRBCi}(t)}{K_{\text{pyrPFvLACtr}} \cdot V_{\text{rbci}}} + 1 \right)} \quad (\text{A.4.19})$$

$$vPFvLDH = \frac{\text{parMulti} \cdot \left(\frac{VPFvLDH \cdot \text{nadhPF}(t) \cdot \text{pyrPF}(t)}{K_{\text{nadhPFvLDH}} \cdot K_{\text{pyrPFvLDH}} \cdot V_{\text{pf}}} - \frac{VrPFvLDH \cdot \text{lacPF}(t) \cdot \text{nadPF}(t)}{K_{\text{lacPFvLDH}} \cdot K_{\text{nadPFvLDH}} \cdot V_{\text{pf}}} \right)}{\left(\frac{\text{nadhPF}(t)}{K_{\text{nadhPFvLDH}} \cdot V_{\text{pf}}} + \frac{\text{nadPF}(t)}{K_{\text{nadPFvLDH}} \cdot V_{\text{pf}}} + 1 \right) \cdot \left(\frac{\text{lacPF}(t)}{K_{\text{lacPFvLDH}} \cdot V_{\text{pf}}} + \frac{\text{pyrPF}(t)}{K_{\text{pyrPFvLDH}} \cdot V_{\text{pf}}} + 1 \right)} \quad (\text{A.4.20})$$

$$vPFvPFK = \frac{\text{parMulti} \cdot VPFvPFK \cdot \text{atpPF}(t) \cdot \text{f6pPF}(t)}{\text{KatpPFvPFK} \cdot K_{\text{f6pPFvPFK}} \cdot V_{\text{pf}} \cdot \left(\frac{\text{atpPF}(t)}{\text{KatpPFvPFK} \cdot V_{\text{pf}}} + 1 \right) \cdot \left(\frac{\text{adpPF}(t)}{K_{\text{adpPFvPFK}} \cdot V_{\text{pf}}} + \frac{\text{atpPF}(t)}{\text{KatpPFvPFK} \cdot V_{\text{pf}}} + 1 \right) \cdot \left(\frac{\text{f16bpPF}(t)}{K_{\text{f16bpPFvPFK}} \cdot V_{\text{pf}}} + \frac{\text{f6pPF}(t)}{K_{\text{f6pPFvPFK}} \cdot V_{\text{pf}}} + 1 \right)} \quad (\text{A.4.21})$$

$$vPFvPGI = \frac{\text{parMulti} \cdot VPFvPGI \cdot \left(1 - \frac{\text{f6pPF}(t)}{K_{\text{eqPFvPGI}} \cdot \text{g6pPF}(t)} \right) \cdot \text{g6pPF}(t)}{K_{\text{g6pPFvPGI}} \cdot \left(\frac{\text{f6pPF}(t)}{K_{\text{f6pPFvPGI}} \cdot V_{\text{pf}}} + \frac{\text{g6pPF}(t)}{K_{\text{g6pPFvPGI}} \cdot V_{\text{pf}}} + 1 \right)} \quad (\text{A.4.22})$$

$$vPFvPGK = \frac{K_{\text{adpPFvPGK}} \cdot K_{\text{b13pgPFvPGK}} \cdot K_{\text{eqPFvPGK}} \cdot \text{parMulti} \cdot V_{\text{rPFvPGK}} \cdot \text{atpPF}(t) \cdot \left(\frac{K_{\text{eqPFvPGK}} \cdot \text{adpPF}(t) \cdot \text{b13pgPF}(t)}{\text{atpPF}(t) \cdot \text{p3gPF}(t)} - 1 \right) \cdot \text{p3gPF}(t)}{\text{KatpPFvPGK}^2 \cdot K_{\text{p3gPFvPGK}}^2 \cdot V_{\text{pf}} \cdot \left(\frac{\text{adpPF}(t)}{K_{\text{adpPFvPGK}} \cdot V_{\text{pf}}} + \frac{\text{atpPF}(t)}{\text{KatpPFvPGK} \cdot V_{\text{pf}}} + 1 \right) \cdot \left(\frac{\text{b13pgPF}(t)}{K_{\text{b13pgPFvPGK}} \cdot V_{\text{pf}}} + \frac{\text{p3gPF}(t)}{K_{\text{p3gPFvPGK}} \cdot V_{\text{pf}}} + 1 \right)} \quad (\text{A.4.23})$$

$$vPFvPGM = \frac{\text{parMulti} \cdot VPFvPGM \cdot \left(1 - \frac{\text{p2gPF}(t)}{K_{\text{eqPFvPGM}} \cdot \text{p3gPF}(t)} \right) \cdot \text{p3gPF}(t)}{K_{\text{p3gPFvPGM}} \cdot \left(\frac{\text{p2gPF}(t)}{K_{\text{p2gPFvPGM}} \cdot V_{\text{pf}}} + \frac{\text{p3gPF}(t)}{K_{\text{p3gPFvPGM}} \cdot V_{\text{pf}}} + 1 \right)} \quad (\text{A.4.24})$$

$$vPFvPK = \frac{\text{parMulti} \cdot \text{VPFvPK} \cdot \text{adpPF}(t) \cdot \text{pepPF}(t)}{\text{KadpPFvPK} \cdot \text{KpepPFvPK} \cdot \text{Vpf} \cdot \left(\frac{\text{adpPF}(t)}{\text{KadpPFvPK} \cdot \text{Vpf}} + 1 \right) \cdot \left(\frac{\text{pepPF}(t)}{\text{KpepPFvPK} \cdot \text{Vpf}} + 1 \right) \cdot \left(\text{LPFvPK} \cdot \left(\left(\frac{\text{adpPF}(t)}{\text{KiadpPFvPK} \cdot \text{Vpf}} + \frac{\text{atpPF}(t)}{\text{KiatpPFvPK} \cdot \text{Vpf}} \right)^h + 1 \right) \cdot \left(\left(\frac{\text{pepPF}(t)}{\text{KipepPFvPK} \cdot \text{Vpf}} + \frac{\text{pyrPF}(t)}{\text{KipyrPFvPK} \cdot \text{Vpf}} \right)^h + 1 \right) + 1 \right)} \quad (\text{A.4.25})$$

$$vPFvPYRtr = \text{KdPFvPYRtr} \cdot \text{parMulti} \cdot \text{pyrPF}(t) \cdot \left(1 - \frac{\text{hRBC} \cdot \text{Vpf} \cdot \text{pyrRBCi}(t)}{\text{hPF} \cdot \text{Vrbci} \cdot \text{pyrPF}(t)} \right) \quad (\text{A.4.26})$$

$$+ \frac{\text{VPFvPYRtr} \cdot \text{pyrPF}(t) \cdot \left(1 - \frac{\text{hRBC} \cdot \text{Vpf} \cdot \text{pyrRBCi}(t)}{\text{hPF} \cdot \text{Vrbci} \cdot \text{pyrPF}(t)} \right)}{\text{KpyrPFvPYRtr} \cdot \left(\frac{\text{lacPF}(t)}{\text{KilacPFvPYRtr} \cdot \text{Vpf}} + \frac{\text{lacRBCi}(t)}{\text{KilacPFvPYRtr} \cdot \text{Vrbci}} + \frac{\text{pyrPF}(t)}{\text{KpyrPFvPYRtr} \cdot \text{Vpf}} + \frac{\text{pyrRBCi}(t)}{\text{KpyrPFvPYRtr} \cdot \text{Vrbci}} + 1 \right)} \quad (\text{A.4.27})$$

$$vPFvTPI = \frac{\text{parMulti} \cdot \text{VPFvTPI} \cdot \text{dhapPF}(t) \cdot \left(1 - \frac{\text{gapPF}(t)}{\text{KeqPFvTPI} \cdot \text{dhapPF}(t)} \right)}{\text{KdhapPFvTPI} \cdot \left(\frac{\text{dhapPF}(t)}{\text{KdhapPFvTPI} \cdot \text{Vpf}} + \frac{\text{gapPF}(t)}{\text{KgapPFvTPI} \cdot \text{Vpf}} + \frac{\text{pepPF}(t)}{\text{KipepPFvTPI} \cdot \text{Vpf}} + 1 \right)} \quad (\text{A.4.28})$$

$$vRBCivAK = \text{parMulti} \cdot \text{TsRBC} \cdot \text{Vrbci} \cdot \left(\frac{\text{K1appRBCvAK} \cdot \text{adpRBCi}(t) \cdot \text{mgadpRBCi}(t)}{\text{Vrbci}^2} - \frac{\text{K2appRBCvAK} \cdot \text{ampRBCi}(t) \cdot \text{mgatpRBCi}(t)}{\text{Vrbci}^2} \right) \quad (\text{A.4.29})$$

$$vRBCivALD = \frac{\text{parMulti} \cdot \text{TsRBC} \cdot \text{Vrbci} \cdot \text{VRBCvALD} \cdot \left(\frac{\text{KcatfRBCvALD} \cdot \text{f16p2RBCi}(t)}{\text{Kmf16p2RBCvALD} \cdot \text{Vrbci}} - \frac{\text{KcatrRBCvALD} \cdot \text{dhapRBCi}(t) \cdot \text{gapRBCi}(t)}{\text{KidhapRBCvALD} \cdot \text{KmgapRBCvALD} \cdot \text{Vrbci}^2} \right)}{\frac{\text{gapRBCi}(t) \cdot \text{dhapRBCi}(t)}{\text{KidhapRBCvALD} \cdot \text{KmgapRBCvALD} \cdot \text{Vrbci}^2} + \frac{\text{dhapRBCi}(t)}{\text{KidhapRBCvALD} \cdot \text{Vrbci}} + \frac{\text{f16p2RBCi}(t)}{\text{Kmf16p2RBCvALD} \cdot \text{Vrbci}} + \frac{\text{KmdhapRBCvALD} \cdot \text{f16p2RBCi}(t) \cdot \text{gapRBCi}(t)}{\text{KidhapRBCvALD} \cdot \text{Kif16p2RBCvALD} \cdot \text{KmgapRBCvALD} \cdot \text{Vrbci}^2} + 1} + \frac{\frac{\text{b23pgRBCi}(t)}{\text{Vrbci}} + \frac{\text{mgb23pgRBCi}(t)}{\text{Vrbci}}}{\text{Kib23pgRBCvALD}} + \frac{\text{KmdhapRBCvALD} \cdot \text{gapRBCi}(t) \cdot \left(\frac{\frac{\text{b23pgRBCi}(t)}{\text{Vrbci}} + \frac{\text{mgb23pgRBCi}(t)}{\text{Vrbci}}}{\text{Kib23pgRBCvALD}} + 1 \right)}{\text{KidhapRBCvALD} \cdot \text{KmgapRBCvALD} \cdot \text{Vrbci}} + 1} \quad (\text{A.4.30})$$

$$vRBCivATPASE = \text{KRBCvATPASE} \cdot \text{parMulti} \cdot \text{TsRBC} \cdot \text{mgatpRBCi}(t) \quad (\text{A.4.31})$$

$$vRBCivBPGSP1 = \text{parMulti} \cdot \text{TsRBC} \cdot \text{Vrbci} \cdot \left(\frac{\text{K1appRBCvBPGSP1} \cdot \text{b13pgRBCi}(t) \cdot \text{bpgspRBCi}(t)}{\text{Vrbci}^2} - \frac{\text{K2RBCvBPGSP1} \cdot \text{bpgspb13pgRBCi}(t)}{\text{Vrbci}} \right) \quad (\text{A.4.32})$$

$$vRBCivBPGSP2 = \text{K3appRBCvBPGSP2} \cdot \text{parMulti} \cdot \text{TsRBC} \cdot \text{bpgspb13pgRBCi}(t) \quad (\text{A.4.33})$$

$$vRBCivBPGSP3 = \text{parMulti} \cdot \text{TsRBC} \cdot \text{Vrbci} \cdot \left(\frac{\text{K4appRBCvBPGSP3} \cdot \text{bpgsppRBCi}(t) \cdot \text{p3gRBCi}(t)}{\text{Vrbci}^2} - \frac{\text{K5RBCvBPGSP3} \cdot \text{bpgsppp3gRBCi}(t)}{\text{Vrbci}} \right) \quad (\text{A.4.34})$$

$$vRBCivBPGSP4 = \text{parMulti} \cdot \text{TsRBC} \cdot \text{Vrbci} \cdot \left(\frac{\text{K6appRBCvBPGSP4} \cdot \text{bpgsppRBCi}(t) \cdot \text{p2gRBCi}(t)}{\text{Vrbci}^2} - \frac{\text{K7RBCvBPGSP4} \cdot \text{bpgsppp2gRBCi}(t)}{\text{Vrbci}} \right) \quad (\text{A.4.35})$$

$$vRBCivBPGSP5 = \text{parMulti} \cdot \text{TsRBC} \cdot \text{Vrbci} \cdot \left(\frac{\text{K8RBCvBPGSP5} \cdot \text{bpgsppp3gRBCi}(t)}{\text{Vrbci}} - \frac{\text{K9RBCvBPGSP5} \cdot \text{bpgspb23pgRBCi}(t)}{\text{Vrbci}} \right) \quad (\text{A.4.36})$$

$$vRBCivBPGSP6 = \text{parMulti} \cdot \text{TsRBC} \cdot \text{Vrbci} \cdot \left(\frac{\text{K10RBCvBPGSP6} \cdot \text{bpgsppp2gRBCi}(t)}{\text{Vrbci}} - \frac{\text{K11RBCvBPGSP6} \cdot \text{bpgspb23pgRBCi}(t)}{\text{Vrbci}} \right) \quad (\text{A.4.37})$$

$$vRBCivBPGSP7 = \text{parMulti} \cdot \text{TsRBC} \cdot \text{Vrbc}i \cdot \left(\frac{K12RBCvBPGSP7 \cdot \text{bpgspb23pgRBC}i(t)}{\text{Vrbc}i} - \frac{K13appRBCvBPGSP7 \cdot \text{b23pgRBC}i(t) \cdot \text{bpgspRBC}i(t)}{\text{Vrbc}i^2} \right) \quad (\text{A.4.38})$$

$$vRBCivBPGSP8 = \text{parMulti} \cdot \text{TsRBC} \cdot \text{Vrbc}i \cdot \left(\frac{K14RBCvBPGSP8 \cdot \text{bpgsppRBC}i(t) \cdot \text{phosRBC}i(t)}{\text{Vrbc}i^2} - \frac{K15RBCvBPGSP8 \cdot \text{bpgsppphosRBC}i(t)}{\text{Vrbc}i} \right) \quad (\text{A.4.39})$$

$$vRBCivBPGSP9 = K16RBCvBPGSP9 \cdot \text{parMulti} \cdot \text{TsRBC} \cdot \text{bpgsppphosRBC}i(t) \quad (\text{A.4.40})$$

$$vRBCivENO = \frac{\text{parMulti} \cdot \text{TsRBC} \cdot \text{Vrbc}i \cdot \text{VRBCvENO} \cdot \left(\frac{K\text{catfRBCvENO} \cdot \text{mgRBC}i(t) \cdot \text{p2gRBC}i(t)}{K\text{imgRBCvENO} \cdot K\text{mp2gRBCvENO} \cdot \text{Vrbc}i^2} - \frac{K\text{catrRBCvENO} \cdot \text{mgRBC}i(t) \cdot \text{pepRBC}i(t)}{K\text{ipepRBCvENO} \cdot K\text{mmgRBCvENO} \cdot \text{Vrbc}i^2} \right)}{\frac{\text{p2gRBC}i(t) \cdot \text{mgRBC}i(t)}{K\text{imgRBCvENO} \cdot K\text{mp2gRBCvENO} \cdot \text{Vrbc}i^2} + \frac{\text{pepRBC}i(t) \cdot \text{mgRBC}i(t)}{K\text{ipepRBCvENO} \cdot K\text{mmgRBCvENO} \cdot \text{Vrbc}i^2} + \frac{\text{mgRBC}i(t)}{K\text{imgRBCvENO} \cdot \text{Vrbc}i} + \frac{\text{p2gRBC}i(t)}{K\text{ip2gRBCvENO} \cdot \text{Vrbc}i} + \frac{\text{pepRBC}i(t)}{K\text{ipepRBCvENO} \cdot \text{Vrbc}i} + 1} \quad (\text{A.4.41})$$

$$vRBCivG6PDH = [\text{parMulti} \cdot \text{TsRBC} \cdot \text{Vrbc}i \cdot \text{VRBCvG6PDH} \cdot \quad (\text{A.4.42})$$

$$\left(\frac{K1RBCvG6PDH \cdot K3RBCvG6PDH \cdot K5RBCvG6PDH \cdot K7RBCvG6PDH \cdot K9RBCvG6PDH \cdot \text{g6pRBC}i(t) \cdot \text{nadpRBC}i(t)}{\text{Vrbc}i^2} \quad (\text{A.4.43})$$

$$- \frac{K10RBCvG6PDH \cdot K2RBCvG6PDH \cdot K4RBCvG6PDH \cdot K6RBCvG6PDH \cdot K8RBCvG6PDH \cdot \text{nadphRBC}i(t) \cdot \text{p6glRBC}i(t)}{\text{Vrbc}i^2} \right) / \quad (\text{A.4.44})$$

$$[K2RBCvG6PDH \cdot K9RBCvG6PDH \quad (\text{A.4.45})$$

$$\cdot (K4RBCvG6PDH \cdot K6RBCvG6PDH + K4RBCvG6PDH \cdot K7RBCvG6PDH + K5RBCvG6PDH \cdot K7RBCvG6PDH) \quad (\text{A.4.46})$$

$$+ \frac{K3RBCvG6PDH \cdot K5RBCvG6PDH \cdot K7RBCvG6PDH \cdot \text{g6pRBC}i(t) \cdot K9RBCvG6PDH}{\text{Vrbc}i} \quad (\text{A.4.47})$$

$$+ \frac{K1RBCvG6PDH \cdot \text{nadpRBC}i(t) \cdot K9RBCvG6PDH}{1 \cdot (K4RBCvG6PDH \cdot K6RBCvG6PDH + K4RBCvG6PDH \cdot K7RBCvG6PDH + K5RBCvG6PDH \cdot K7RBCvG6PDH)} \quad (\text{A.4.48})$$

$$+ \frac{K10RBCvG6PDH \cdot K3RBCvG6PDH \cdot K5RBCvG6PDH \cdot K7RBCvG6PDH \cdot \text{g6pRBC}i(t) \cdot \text{nadphRBC}i(t)}{\text{Vrbc}i^2} \quad (\text{A.4.49})$$

$$+ \frac{K10RBCvG6PDH \cdot K2RBCvG6PDH \cdot (K4RBCvG6PDH \cdot K6RBCvG6PDH}{1 + K5RBCvG6PDH \cdot K6RBCvG6PDH + K5RBCvG6PDH \cdot K7RBCvG6PDH) \cdot \text{nadphRBC}i(t)}{\text{Vrbc}i} \quad (\text{A.4.50})$$

$$\quad (\text{A.4.51})$$

$$+ \frac{K1RBCvG6PDH \cdot K3RBCvG6PDH \cdot (K5RBCvG6PDH \cdot K7RBCvG6PDH + K9RBCvG6PDH \cdot K7RBCvG6PDH + K5RBCvG6PDH \cdot K9RBCvG6PDH + K6RBCvG6PDH \cdot K9RBCvG6PDH) \cdot g6pRBCi(t) \cdot nadpRBCi(t)}{Vrbci^2} \quad (A.4.52)$$

$$+ \frac{K10RBCvG6PDH \cdot K3RBCvG6PDH \cdot (K5RBCvG6PDH + K6RBCvG6PDH) \cdot K8RBCvG6PDH \cdot g6pRBCi(t) \cdot nadphRBCi(t) \cdot p6glRBCi(t)}{Vrbci^3} \quad (A.4.53)$$

$$+ \frac{K10RBCvG6PDH \cdot (K2RBCvG6PDH \cdot K4RBCvG6PDH + K6RBCvG6PDH \cdot K4RBCvG6PDH + K2RBCvG6PDH \cdot K6RBCvG6PDH) \cdot K8RBCvG6PDH \cdot nadphRBCi(t) \cdot p6glRBCi(t)}{Vrbci^2} \quad (A.4.54)$$

$$+ \frac{K1RBCvG6PDH \cdot K3RBCvG6PDH \cdot (K5RBCvG6PDH + K6RBCvG6PDH) \cdot K8RBCvG6PDH \cdot g6pRBCi(t) \cdot nadpRBCi(t) \cdot p6glRBCi(t)}{Vrbci^3} \quad (A.4.55)$$

$$+ \frac{K1RBCvG6PDH \cdot K4RBCvG6PDH \cdot K6RBCvG6PDH \cdot K8RBCvG6PDH \cdot nadpRBCi(t) \cdot p6glRBCi(t)}{Vrbci^2} \quad (A.4.56)$$

$$+ \left. \frac{K2RBCvG6PDH \cdot K4RBCvG6PDH \cdot K6RBCvG6PDH \cdot K8RBCvG6PDH \cdot p6glRBCi(t)}{Vrbci} \right] \quad (A.4.57)$$

$$vRBCivGAPDH = \left[parMulti \cdot TsRBC \cdot Vrbci \cdot VRBCvGAPDH \cdot \left(\frac{KcatfappRBCvGAPDH \cdot gapRBCi(t) \cdot nadRBCi(t) \cdot phosRBCi(t)}{KiappgapRBCvGAPDH \cdot KiphosRBCvGAPDH \cdot KmnadRBCvGAPDH \cdot Vrbci^3} \right) \right. \quad (A.4.58)$$

$$\left. - \frac{KcatrappRBCvGAPDH \cdot b13pgRBCi(t) \cdot nadhRBCi(t)}{Kiappb13pgRBCvGAPDH \cdot KmappnadhRBCvGAPDH \cdot Vrbci^2} \right] / \quad (A.4.59)$$

$$\left[\frac{b13pgRBCi(t) \cdot \left(\frac{gapRBCi(t)}{KidgapRBCvGAPDH \cdot Vrbci} + 1 \right)}{Kiappb13pgRBCvGAPDH \cdot Vrbci} + \frac{gapRBCi(t) \cdot \left(\frac{gapRBCi(t)}{KidgapRBCvGAPDH \cdot Vrbci} + 1 \right)}{KiappgapRBCvGAPDH \cdot Vrbci} \right. \quad (A.4.60)$$

$$+ \frac{gapRBCi(t) \cdot phosRBCi(t) \cdot \left(\frac{gapRBCi(t)}{KidgapRBCvGAPDH \cdot Vrbci} + 1 \right)}{KiappgapRBCvGAPDH \cdot KiphosRBCvGAPDH \cdot Vrbci^2} + \frac{b13pgRBCi(t) \cdot nadhRBCi(t)}{Kiappb13pgRBCvGAPDH \cdot KmappnadhRBCvGAPDH \cdot Vrbci^2} \quad (A.4.61)$$

$$+ \frac{gapRBCi(t) \cdot nadhRBCi(t)}{KiappgapRBCvGAPDH \cdot KiappnadhRBCvGAPDH \cdot Vrbci^2} + \frac{Kmb13pgRBCvGAPDH \cdot nadhRBCi(t)}{Kiappb13pgRBCvGAPDH \cdot KmappnadhRBCvGAPDH \cdot Vrbci} \quad (A.4.62)$$

$$+ \frac{b13pgRBCi(t) \cdot nadRBCi(t)}{Kiappb13pgRBCvGAPDH \cdot KinadRBCvGAPDH \cdot Vrbci^2} + \frac{gapRBCi(t) \cdot nadRBCi(t)}{KiappgapRBCvGAPDH \cdot KinadRBCvGAPDH \cdot Vrbci^2} \quad (A.4.63)$$

$$+ \frac{Kmb13pgRBCvGAPDH \cdot b13pgRBCi(t) \cdot nadhRBCi(t) \cdot phosRBCi(t)}{Kiappb13pgRBCvGAPDH \cdot Kidb13pgRBCvGAPDH \cdot KiphosRBCvGAPDH \cdot KmappnadhRBCvGAPDH \cdot Vrbci^3} \quad (A.4.64)$$

$$(A.4.65)$$

$$+ \frac{\text{gapRBCi}(t) \cdot \text{nadhRBCi}(t) \cdot \text{phosRBCi}(t)}{\text{KiappgapRBCvGAPDH} \cdot \text{KiappnadhRBCvGAPDH} \cdot \text{KiphosRBCvGAPDH} \cdot \text{Vrbci}^3} \quad (\text{A.4.66})$$

$$+ \frac{\text{Kmb13pgRBCvGAPDH} \cdot \text{nadhRBCi}(t) \cdot \text{phosRBCi}(t)}{\text{Kiappb13pgRBCvGAPDH} \cdot \text{KiphosRBCvGAPDH} \cdot \text{KmappnadhRBCvGAPDH} \cdot \text{Vrbci}^2} \quad (\text{A.4.67})$$

$$+ \frac{\text{KmgapRBCvGAPDH} \cdot \text{b13pgRBCi}(t) \cdot \text{nadRBCi}(t) \cdot \text{phosRBCi}(t)}{\text{KiappgapRBCvGAPDH} \cdot \text{Kidb13pgRBCvGAPDH} \cdot \text{KiphosRBCvGAPDH} \cdot \text{KmnadRBCvGAPDH} \cdot \text{Vrbci}^3} \quad (\text{A.4.68})$$

$$+ \frac{\text{gapRBCi}(t) \cdot \text{nadRBCi}(t) \cdot \text{phosRBCi}(t)}{\text{KiappgapRBCvGAPDH} \cdot \text{KiphosRBCvGAPDH} \cdot \text{KmnadRBCvGAPDH} \cdot \text{Vrbci}^3} \quad (\text{A.4.69})$$

$$+ \left. \frac{\text{KmgapRBCvGAPDH} \cdot \text{nadRBCi}(t) \cdot \text{phosRBCi}(t)}{\text{KiappgapRBCvGAPDH} \cdot \text{KiphosRBCvGAPDH} \cdot \text{KmnadRBCvGAPDH} \cdot \text{Vrbci}^2} \right] \quad (\text{A.4.70})$$

$$\text{vRBCivGLCTRANSPORT} = \text{parMulti} \cdot \text{TsRBC} \cdot \text{Vrbci} \cdot \left(\frac{\text{glc_alpha} \cdot \text{VRBCvGLCTRANSPORT} \cdot \text{B_gluc}(t)}{1000 \cdot \left(\frac{(1-\text{glc_alpha}) \cdot \text{B_gluc}(t) \cdot \text{k_alpha}}{1000 \cdot \text{k_beta}} + \text{k_alpha} + \frac{\text{glc_alpha} \cdot \text{B_gluc}(t)}{1000} \right)} \right) \quad (\text{A.4.71})$$

$$+ \frac{(1 - \text{glc_alpha}) \cdot \text{VRBCvGLCTRANSPORT} \cdot \text{B_gluc}(t)}{1000 \cdot \left(\frac{\text{glc_alpha} \cdot \text{B_gluc}(t) \cdot \text{k_beta}}{1000 \cdot \text{k_alpha}} + \text{k_beta} + \frac{(1-\text{glc_alpha}) \cdot \text{B_gluc}(t)}{1000} \right)} \quad (\text{A.4.72})$$

$$- \frac{\text{glc_alpha} \cdot \text{VRBCvGLCTRANSPORT} \cdot \text{glcRBCi}(t)}{\text{Vrbci} \cdot \left(\frac{(1-\text{glc_alpha}) \cdot \text{glcRBCi}(t) \cdot \text{k_alpha}}{\text{k_beta} \cdot \text{Vrbci}} + \text{k_alpha} + \frac{\text{glc_alpha} \cdot \text{glcRBCi}(t)}{\text{Vrbci}} \right)} \quad (\text{A.4.73})$$

$$- \left. \frac{(1 - \text{glc_alpha}) \cdot \text{VRBCvGLCTRANSPORT} \cdot \text{glcRBCi}(t)}{\text{Vrbci} \cdot \left(\frac{\text{glc_alpha} \cdot \text{glcRBCi}(t) \cdot \text{k_beta}}{\text{k_alpha} \cdot \text{Vrbci}} + \text{k_beta} + \frac{(1-\text{glc_alpha}) \cdot \text{glcRBCi}(t)}{\text{Vrbci}} \right)} \right) \quad (\text{A.4.74})$$

$$\text{vRBCivGSSGR} = [\text{parMulti} \cdot \text{TsRBC} \cdot \text{Vrbci} \cdot \text{VRBCvGSSGR} \cdot \quad (\text{A.4.75})$$

$$\left(\frac{\text{K11RBCvGSSGR} \cdot \text{K1RBCvGSSGR} \cdot \text{K3RBCvGSSGR} \cdot \text{K5RBCvGSSGR} \cdot \text{K7RBCvGSSGR}}{\text{K9RBCvGSSGR} \cdot \text{gssgRBCi}(t) \cdot \text{nadphRBCi}(t)} \cdot \text{Vrbci}^2 \right) \quad (\text{A.4.76})$$

$$- \left. \frac{\text{K10RBCvGSSGR} \cdot \text{K12RBCvGSSGR} \cdot \text{K2RBCvGSSGR} \cdot \text{K4RBCvGSSGR} \cdot \text{K6RBCvGSSGR}}{\text{K8RBCvGSSGR} \cdot \text{gshRBCi}(t)^2 \cdot \text{nadpRBCi}(t)} \cdot \text{Vrbci}^3 \right) / \quad (\text{A.4.77})$$

$$\left[\frac{\text{K10RBCvGSSGR} \cdot \text{K1RBCvGSSGR} \cdot \text{K3RBCvGSSGR} \cdot (\text{K5RBCvGSSGR} + \text{K6RBCvGSSGR})}{\text{K8RBCvGSSGR} \cdot \text{gssgRBCi}(t) \cdot \text{nadphRBCi}(t) \cdot \text{gshRBCi}(t)^2} \cdot \text{Vrbci}^4 \right] \quad (\text{A.4.78})$$

$$+ \frac{K_{10}RBCvGSSGR \cdot K_{1}RBCvGSSGR \cdot K_{4}RBCvGSSGR \cdot K_{6}RBCvGSSGR \cdot K_{8}RBCvGSSGR \cdot \text{nadphRBCi}(t) \cdot \text{gshRBCi}(t)^2}{Vrbci^3} \quad (\text{A.4.79})$$

$$+ \frac{K_{10}RBCvGSSGR \cdot K_{12}RBCvGSSGR \cdot K_{3}RBCvGSSGR \cdot (K_{5}RBCvGSSGR + K_{6}RBCvGSSGR) \cdot K_{8}RBCvGSSGR \cdot \text{gssgRBCi}(t) \cdot \text{nadpRBCi}(t) \cdot \text{gshRBCi}(t)^2}{Vrbci^4} \quad (\text{A.4.80})$$

$$+ \frac{1}{Vrbci^3} \frac{K_{10}RBCvGSSGR \cdot K_{12}RBCvGSSGR \cdot (K_{2}RBCvGSSGR \cdot K_{4}RBCvGSSGR + K_{6}RBCvGSSGR \cdot K_{4}RBCvGSSGR + K_{2}RBCvGSSGR \cdot K_{5}RBCvGSSGR + K_{2}RBCvGSSGR \cdot K_{6}RBCvGSSGR) \cdot K_{8}RBCvGSSGR \cdot \text{nadpRBCi}(t) \cdot \text{gshRBCi}(t)^2}{Vrbci^3} \quad (\text{A.4.81})$$

$$+ \frac{K_{10}RBCvGSSGR \cdot K_{2}RBCvGSSGR \cdot K_{4}RBCvGSSGR \cdot K_{6}RBCvGSSGR \cdot K_{8}RBCvGSSGR \cdot \text{gshRBCi}(t)^2}{Vrbci^2} \quad (\text{A.4.82})$$

$$+ \frac{K_{10}RBCvGSSGR \cdot K_{1}RBCvGSSGR \cdot K_{3}RBCvGSSGR \cdot K_{5}RBCvGSSGR \cdot K_{7}RBCvGSSGR \cdot \text{gssgRBCi}(t) \cdot \text{nadphRBCi}(t) \cdot \text{gshRBCi}(t)}{Vrbci^3} \quad (\text{A.4.83})$$

$$+ \frac{K_{11}RBCvGSSGR \cdot K_{1}RBCvGSSGR \cdot K_{3}RBCvGSSGR \cdot (K_{5}RBCvGSSGR + K_{6}RBCvGSSGR) \cdot K_{8}RBCvGSSGR \cdot \text{gssgRBCi}(t) \cdot \text{nadphRBCi}(t) \cdot \text{gshRBCi}(t)}{Vrbci^3} \quad (\text{A.4.84})$$

$$+ \frac{K_{11}RBCvGSSGR \cdot K_{1}RBCvGSSGR \cdot K_{4}RBCvGSSGR \cdot K_{6}RBCvGSSGR \cdot K_{8}RBCvGSSGR \cdot \text{nadphRBCi}(t) \cdot \text{gshRBCi}(t)}{Vrbci^2} \quad (\text{A.4.85})$$

$$+ \frac{K_{10}RBCvGSSGR \cdot K_{12}RBCvGSSGR \cdot K_{3}RBCvGSSGR \cdot K_{5}RBCvGSSGR \cdot K_{7}RBCvGSSGR \cdot \text{gssgRBCi}(t) \cdot \text{nadpRBCi}(t) \cdot \text{gshRBCi}(t)}{Vrbci^3} \quad (\text{A.4.86})$$

$$+ \frac{1}{Vrbci^2} \frac{K_{10}RBCvGSSGR \cdot K_{12}RBCvGSSGR \cdot K_{2}RBCvGSSGR \cdot (K_{4}RBCvGSSGR \cdot K_{6}RBCvGSSGR + K_{4}RBCvGSSGR \cdot K_{7}RBCvGSSGR + K_{5}RBCvGSSGR \cdot K_{7}RBCvGSSGR) \cdot \text{nadpRBCi}(t) \cdot \text{gshRBCi}(t)}{Vrbci^2} \quad (\text{A.4.87})$$

$$+ \frac{K_{12}RBCvGSSGR \cdot K_{2}RBCvGSSGR \cdot K_{4}RBCvGSSGR \cdot K_{6}RBCvGSSGR \cdot K_{8}RBCvGSSGR \cdot \text{nadpRBCi}(t) \cdot \text{gshRBCi}(t)}{Vrbci^2} \quad (\text{A.4.88})$$

$$+ \frac{K_{11}RBCvGSSGR \cdot K_{2}RBCvGSSGR \cdot K_{4}RBCvGSSGR \cdot K_{6}RBCvGSSGR \cdot K_{8}RBCvGSSGR \cdot \text{gshRBCi}(t)}{Vrbci} \quad (\text{A.4.89})$$

$$+ K_{11}RBCvGSSGR \cdot K_{2}RBCvGSSGR \cdot K_{9}RBCvGSSGR \quad (\text{A.4.90})$$

$$\cdot (K_{4}RBCvGSSGR \cdot K_{6}RBCvGSSGR + K_{4}RBCvGSSGR \cdot K_{7}RBCvGSSGR + K_{5}RBCvGSSGR \cdot K_{7}RBCvGSSGR) \quad (\text{A.4.91})$$

$$+ \frac{K_{11}RBCvGSSGR \cdot K_{3}RBCvGSSGR \cdot K_{5}RBCvGSSGR \cdot K_{7}RBCvGSSGR \cdot K_{9}RBCvGSSGR \cdot gssgRBCi(t)}{Vrbc_i} \quad (A.4.92)$$

$$+ \frac{\frac{K_{1}RBCvGSSGR \cdot K_{3}RBCvGSSGR \cdot (K_{11}RBCvGSSGR \cdot K_{5}RBCvGSSGR \cdot K_{7}RBCvGSSGR + K_{11}RBCvGSSGR \cdot K_{9}RBCvGSSGR \cdot K_{7}RBCvGSSGR + K_{5}RBCvGSSGR \cdot K_{9}RBCvGSSGR \cdot K_{7}RBCvGSSGR + K_{11}RBCvGSSGR \cdot K_{5}RBCvGSSGR \cdot K_{9}RBCvGSSGR + K_{11}RBCvGSSGR \cdot K_{6}RBCvGSSGR \cdot K_{9}RBCvGSSGR) \cdot gssgRBCi(t) \cdot nadphRBCi(t)}{1}}{Vrbc_i^2} \quad (A.4.93)$$

$$+ \frac{\frac{K_{11}RBCvGSSGR \cdot K_{1}RBCvGSSGR \cdot (K_{4}RBCvGSSGR \cdot K_{6}RBCvGSSGR + K_{4}RBCvGSSGR \cdot K_{7}RBCvGSSGR + K_{5}RBCvGSSGR \cdot K_{7}RBCvGSSGR) \cdot K_{9}RBCvGSSGR \cdot nadphRBCi(t)}{1}}{Vrbc_i} \quad (A.4.94)$$

$$+ \frac{K_{12}RBCvGSSGR \cdot K_{3}RBCvGSSGR \cdot K_{5}RBCvGSSGR \cdot K_{7}RBCvGSSGR \cdot K_{9}RBCvGSSGR \cdot gssgRBCi(t) \cdot nadpRBCi(t)}{Vrbc_i^2} \quad (A.4.95)$$

$$+ \frac{\frac{K_{12}RBCvGSSGR \cdot K_{2}RBCvGSSGR \cdot (K_{4}RBCvGSSGR \cdot K_{6}RBCvGSSGR + K_{4}RBCvGSSGR \cdot K_{7}RBCvGSSGR + K_{5}RBCvGSSGR \cdot K_{7}RBCvGSSGR) \cdot K_{9}RBCvGSSGR \cdot nadpRBCi(t)}{1}}{Vrbc_i} \quad (A.4.96)$$

$$vRBCivHBADP = \text{parMulti} \cdot \text{TsRBC} \cdot \text{Vrbci} \cdot \left(\frac{\text{KaappRBCvHBADP} \cdot \text{adpRBCi}(t) \cdot \text{hbRBCi}(t)}{\text{Vrbci}^2} - \frac{\text{KdRBCvHBADP} \cdot \text{hbadpRBCi}(t)}{\text{Vrbci}} \right) \quad (\text{A.4.97})$$

$$vRBCivHBATP = \text{parMulti} \cdot \text{TsRBC} \cdot \text{Vrbci} \cdot \left(\frac{\text{KaappRBCvHBATP} \cdot \text{atpRBCi}(t) \cdot \text{hbRBCi}(t)}{\text{Vrbci}^2} - \frac{\text{KdRBCvHBATP} \cdot \text{hbatpRBCi}(t)}{\text{Vrbci}} \right) \quad (\text{A.4.98})$$

$$vRBCivHBB13PG = \text{parMulti} \cdot \text{TsRBC} \cdot \text{Vrbci} \cdot \left(\frac{\text{KaappRBCvHBB13PG} \cdot \text{b13pgRBCi}(t) \cdot \text{hbRBCi}(t)}{\text{Vrbci}^2} - \frac{\text{KdRBCvHBB13PG} \cdot \text{hbb13pgRBCi}(t)}{\text{Vrbci}} \right) \quad (\text{A.4.99})$$

$$vRBCivHBB23PG = \text{parMulti} \cdot \text{TsRBC} \cdot \text{Vrbci} \cdot \left(\frac{\text{KaappRBCvHBB23PG} \cdot \text{b23pgRBCi}(t) \cdot \text{hbRBCi}(t)}{\text{Vrbci}^2} - \frac{\text{KdRBCvHBB23PG} \cdot \text{hbb23pgRBCi}(t)}{\text{Vrbci}} \right) \quad (\text{A.4.100})$$

$$vRBCivHBMGATP = \text{parMulti} \cdot \text{TsRBC} \cdot \text{Vrbci} \cdot \left(\frac{\text{KaappRBCvHBMGATP} \cdot \text{hgatpRBCi}(t) \cdot \text{hbRBCi}(t)}{\text{Vrbci}^2} - \frac{\text{KdRBCvHBMGATP} \cdot \text{hbm gatpRBCi}(t)}{\text{Vrbci}} \right) \quad (\text{A.4.101})$$

$$vRBCivHK = \left[\text{parMulti} \cdot \text{TsRBC} \cdot \text{Vrbci} \cdot \left(\frac{\text{ERBCvHK} \cdot \text{KcatfappRBCvHK} \cdot \text{glcRBCi}(t) \cdot \text{mgatpRBCi}(t)}{\text{KiglcRBCvHK} \cdot \text{KmmgatpRBCvHK} \cdot \text{Vrbci}^2} \right. \right. \quad (\text{A.4.102})$$

$$\left. \left. - \frac{\text{ERBCvHK} \cdot \text{KcatrappRBCvHK} \cdot \text{g6pRBCi}(t) \cdot \text{mgadpRBCi}(t)}{\text{Kig6pRBCvHK} \cdot \text{KmmgadpRBCvHK} \cdot \text{Vrbci}^2} \right) \right] / \quad (\text{A.4.103})$$

$$\left[\frac{\text{glcRBCi}(t) \cdot \text{g6pRBCi}(t)}{\text{Kdig6pRBCvHK} \cdot \text{KiglcRBCvHK} \cdot \text{Vrbci}^2} + \frac{\text{mgadpRBCi}(t) \cdot \text{g6pRBCi}(t)}{\text{Kig6pRBCvHK} \cdot \text{KmmgadpRBCvHK} \cdot \text{Vrbci}^2} + \frac{\text{g6pRBCi}(t)}{\text{Kig6pRBCvHK} \cdot \text{Vrbci}} \right. \quad (\text{A.4.104})$$

$$\left. + \frac{\text{b23pgRBCi}(t) \cdot \text{glcRBCi}(t)}{\text{KdibpgRBCvHK} \cdot \text{KiglcRBCvHK} \cdot \text{Vrbci}^2} + \frac{\text{g16p2RBCi}(t) \cdot \text{glcRBCi}(t)}{\text{Kdig16p2RBCvHK} \cdot \text{KiglcRBCvHK} \cdot \text{Vrbci}^2} + \frac{\text{glcRBCi}(t)}{\text{KiglcRBCvHK} \cdot \text{Vrbci}} \right. \quad (\text{A.4.105})$$

$$\left. + \frac{\text{glcRBCi}(t) \cdot \text{gshRBCi}(t)}{\text{KdigshRBCvHK} \cdot \text{KiglcRBCvHK} \cdot \text{Vrbci}^2} + \frac{\text{mgadpRBCi}(t)}{\text{KimgadpRBCvHK} \cdot \text{Vrbci}} + \frac{\text{glcRBCi}(t) \cdot \text{mgatpRBCi}(t)}{\text{KiglcRBCvHK} \cdot \text{KmmgatpRBCvHK} \cdot \text{Vrbci}^2} \right. \quad (\text{A.4.106})$$

$$\left. + \frac{\text{mgatpRBCi}(t)}{\text{KimgatpRBCvHK} \cdot \text{Vrbci}} + 1 \right] \quad (\text{A.4.107})$$

$$vRBCivLACTRANSPORT = 20 \cdot \text{parMulti} \cdot \text{TsRBC} \cdot \text{Vrbci} \cdot \left(\frac{\text{KoRBCvLACTRANSPORT} \cdot \text{lacRBCi}(t)}{\text{Vrbci}} - \frac{\text{KiRBCvLACTRANSPORT} \cdot \text{B_lac}(t)}{1000} \right) \quad (\text{A.4.108})$$

$$vRBCivLDH = \left[\text{parMulti} \cdot \text{TsRBC} \cdot \text{Vrbc} \cdot \text{VRBCvLDH} \cdot \left(\frac{\text{KcatfRBCvLDH} \cdot \text{nadhRBCi}(t) \cdot \text{pyrRBCi}(t)}{\text{KinadhRBCvLDH} \cdot \text{KmapppyrRBCvLDH} \cdot \text{Vrbc}^2} \right. \right. \quad (\text{A.4.109})$$

$$\left. \left. - \frac{\text{KcatrRBCvLDH} \cdot \text{lacRBCi}(t) \cdot \text{nadRBCi}(t)}{\text{KinadRBCvLDH} \cdot \text{KmapplacRBCvLDH} \cdot \text{Vrbc}^2} \right) \right] / \quad (\text{A.4.110})$$

$$\left[\frac{\text{KmnadRBCvLDH} \cdot \text{lacRBCi}(t) \cdot \text{nadhRBCi}(t)}{\text{KinadhRBCvLDH} \cdot \text{KinadRBCvLDH} \cdot \text{KmapplacRBCvLDH} \cdot \text{Vrbc}^2} + \frac{\text{lacRBCi}(t) \cdot \text{pyrRBCi}(t) \cdot \text{nadhRBCi}(t)}{\text{KiapplacRBCvLDH} \cdot \text{KinadhRBCvLDH} \cdot \text{KmapppyrRBCvLDH} \cdot \text{Vrbc}^3} \right. \quad (\text{A.4.111})$$

$$\left. + \frac{\text{pyrRBCi}(t) \cdot \text{nadhRBCi}(t)}{\text{KinadhRBCvLDH} \cdot \text{KmapppyrRBCvLDH} \cdot \text{Vrbc}^2} + \frac{\text{nadhRBCi}(t)}{\text{KinadhRBCvLDH} \cdot \text{Vrbc}} + \frac{\text{lacRBCi}(t) \cdot \text{nadRBCi}(t)}{\text{KinadRBCvLDH} \cdot \text{KmapplacRBCvLDH} \cdot \text{Vrbc}^2} \right. \quad (\text{A.4.112})$$

$$\left. + \frac{\text{nadRBCi}(t)}{\text{KinadRBCvLDH} \cdot \text{Vrbc}} + \frac{\text{lacRBCi}(t) \cdot \text{nadRBCi}(t) \cdot \text{pyrRBCi}(t)}{\text{KiapppyrRBCvLDH} \cdot \text{KinadRBCvLDH} \cdot \text{KmapplacRBCvLDH} \cdot \text{Vrbc}^3} \right. \quad (\text{A.4.113})$$

$$\left. + \frac{\text{KmnadhRBCvLDH} \cdot \text{nadRBCi}(t) \cdot \text{pyrRBCi}(t)}{\text{KinadhRBCvLDH} \cdot \text{KinadRBCvLDH} \cdot \text{KmapppyrRBCvLDH} \cdot \text{Vrbc}^2} \right. \quad (\text{A.4.114})$$

$$\left. + \left(\frac{\text{pyrRBCi}(t)}{\text{KidpyrRBCvLDH} \cdot \text{Vrbc}} + 1 \right) \cdot \left(\frac{\text{KmnadRBCvLDH} \cdot \text{lacRBCi}(t)}{\text{KinadRBCvLDH} \cdot \text{KmapplacRBCvLDH} \cdot \text{Vrbc}} + \frac{\text{KmnadhRBCvLDH} \cdot \text{pyrRBCi}(t)}{\text{KinadhRBCvLDH} \cdot \text{KmapppyrRBCvLDH} \cdot \text{Vrbc}} + 1 \right) \right] \quad (\text{A.4.115})$$

$$vRBCivLDHP = \frac{\text{parMulti} \cdot \text{TsRBC} \cdot \text{Vrbc} \cdot \left(\frac{\text{KfRBCvLDHP} \cdot \text{nadpRBCi}(t) \cdot \text{pyrRBCi}(t)}{\text{KmpyrRBCvLDHP} \cdot \text{Vrbc}^2} - \frac{\text{KrRBCvLDHP} \cdot \text{lacRBCi}(t) \cdot \text{nadpRBCi}(t)}{\text{KmlacRBCvLDHP} \cdot \text{Vrbc}^2} \right)}{\frac{\text{lacRBCi}(t)}{\text{KmlacRBCvLDHP} \cdot \text{Vrbc}} + \frac{\text{pyrRBCi}(t)}{\text{KmpyrRBCvLDHP} \cdot \text{Vrbc}} + 1} \quad (\text{A.4.116})$$

$$vRBCivMGADP = \text{parMulti} \cdot \text{TsRBC} \cdot \text{Vrbc} \cdot \left(\frac{\text{KaappRBCvMGADP} \cdot \text{adpRBCi}(t) \cdot \text{mgRBCi}(t)}{\text{Vrbc}^2} - \frac{\text{KdRBCvMGADP} \cdot \text{mgadpRBCi}(t)}{\text{Vrbc}} \right) \quad (\text{A.4.117})$$

$$vRBCivMGATP = \text{parMulti} \cdot \text{TsRBC} \cdot \text{Vrbc} \cdot \left(\frac{\text{KaappRBCvMGATP} \cdot \text{atpRBCi}(t) \cdot \text{mgRBCi}(t)}{\text{Vrbc}^2} - \frac{\text{KdRBCvMGATP} \cdot \text{mgatpRBCi}(t)}{\text{Vrbc}} \right) \quad (\text{A.4.118})$$

$$vRBCivMGB13PG = \text{parMulti} \cdot \text{TsRBC} \cdot \text{Vrbc} \cdot \left(\frac{\text{KaappRBCvMGB13PG} \cdot \text{b13pgRBCi}(t) \cdot \text{mgRBCi}(t)}{\text{Vrbc}^2} - \frac{\text{KdRBCvMGB13PG} \cdot \text{mgb13pgRBCi}(t)}{\text{Vrbc}} \right) \quad (\text{A.4.119})$$

$$vRBCivMGB23PG = \text{parMulti} \cdot \text{TsRBC} \cdot \text{Vrbc} \cdot \left(\frac{\text{KaappRBCvMGB23PG} \cdot \text{b23pgRBCi}(t) \cdot \text{mgRBCi}(t)}{\text{Vrbc}^2} - \frac{\text{KdRBCvMGB23PG} \cdot \text{mgb23pgRBCi}(t)}{\text{Vrbc}} \right) \quad (\text{A.4.120})$$

$$vRBCivMGF16P2 = \text{parMulti} \cdot \text{TsRBC} \cdot \text{Vrbc} \cdot \left(\frac{\text{KaappRBCvMGF16P2} \cdot \text{f16p2RBCi}(t) \cdot \text{mgRBCi}(t)}{\text{Vrbc}^2} - \frac{\text{KdRBCvMGF16P2} \cdot \text{mgf16p2RBCi}(t)}{\text{Vrbc}} \right) \quad (\text{A.4.121})$$

$$vRBCivMGG16P2 = \text{parMulti} \cdot \text{TsRBC} \cdot \text{Vrbci} \cdot \left(\frac{\text{KaappRBCvMGG16P2} \cdot \text{g16p2RBCi}(t) \cdot \text{mgRBCi}(t)}{\text{Vrbci}^2} - \frac{\text{KdRBCvMGG16P2} \cdot \text{mgg16p2RBCi}(t)}{\text{Vrbci}} \right) \quad (\text{A.4.122})$$

$$vRBCivMGPHOS = \text{parMulti} \cdot \text{TsRBC} \cdot \text{Vrbci} \cdot \left(\frac{\text{KaappRBCvMGPHOS} \cdot \text{mgRBCi}(t) \cdot \text{phosRBCi}(t)}{\text{Vrbci}^2} - \frac{\text{KdRBCvMGPHOS} \cdot \text{mgphosRBCi}(t)}{\text{Vrbci}} \right) \quad (\text{A.4.123})$$

$$vRBCivOX = \text{KRBCvOX} \cdot \text{parMulti} \cdot \text{TsRBC} \cdot \text{gshRBCi}(t) \quad (\text{A.4.124})$$

$$vRBCivOXNADH = \text{KRBCvOXNADH} \cdot \text{parMulti} \cdot \text{TsRBC} \cdot \text{nadhRBCi}(t) \quad (\text{A.4.125})$$

$$vRBCivP6GDH = [\text{parMulti} \cdot \text{TsRBC} \cdot \text{Vrbci} \cdot \text{VRBCvP6GDH} \quad (\text{A.4.126})$$

$$\cdot \left(\frac{\text{K11RBCvP6GDH} \cdot \text{K1RBCvP6GDH} \cdot \text{K3RBCvP6GDH} \cdot \text{K5RBCvP6GDH} \cdot \text{K7RBCvP6GDH} \cdot \text{K9RBCvP6GDH}}{\text{Vrbci}^2} \cdot \text{nadpRBCi}(t) \cdot \text{p6gRBCi}(t) \right) \quad (\text{A.4.127})$$

$$- \frac{1}{\text{Vrbci}^3} \cdot \left(\text{co2RBCi} \cdot \text{K10RBCvP6GDH} \cdot \text{K12RBCvP6GDH} \cdot \text{K2RBCvP6GDH} \cdot \text{K4RBCvP6GDH} \cdot \text{K6RBCvP6GDH} \cdot \text{K8RBCvP6GDH} \cdot \text{nadphRBCi}(t) \cdot \text{ru5pRBCi}(t) \right) \Big] / \quad (\text{A.4.128})$$

$$\left[\frac{\text{co2RBCi} \cdot \text{K12RBCvP6GDH} \cdot \text{K2RBCvP6GDH} \cdot \text{K4RBCvP6GDH} \cdot \text{K6RBCvP6GDH} \cdot \text{nadphRBCi}(t) \cdot \text{K8RBCvP6GDH}}{\text{Vrbci}^2} \right] \quad (\text{A.4.129})$$

$$+ \frac{\text{co2RBCi} \cdot \text{K11RBCvP6GDH} \cdot \text{K1RBCvP6GDH} \cdot \text{K4RBCvP6GDH} \cdot \text{K6RBCvP6GDH} \cdot \text{nadpRBCi}(t) \cdot \text{K8RBCvP6GDH}}{\text{Vrbci}^2} \quad (\text{A.4.130})$$

$$+ \frac{\text{co2RBCi} \cdot \text{K11RBCvP6GDH} \cdot \text{K1RBCvP6GDH} \cdot \text{K3RBCvP6GDH} \cdot (\text{K5RBCvP6GDH} + \text{K6RBCvP6GDH}) \cdot \text{nadpRBCi}(t) \cdot \text{p6gRBCi}(t) \cdot \text{K8RBCvP6GDH}}{\text{Vrbci}^3} \quad (\text{A.4.131})$$

$$+ \frac{\text{co2RBCi} \cdot \text{K10RBCvP6GDH} \cdot \text{K12RBCvP6GDH} \cdot (\text{K2RBCvP6GDH} \cdot \text{K4RBCvP6GDH} + \text{K6RBCvP6GDH} \cdot \text{K4RBCvP6GDH} + \text{K2RBCvP6GDH} \cdot \text{K5RBCvP6GDH} + \text{K2RBCvP6GDH} \cdot \text{K6RBCvP6GDH}) \cdot \text{nadphRBCi}(t) \cdot \text{ru5pRBCi}(t) \cdot \text{K8RBCvP6GDH}}{\text{Vrbci}^3} \quad (\text{A.4.132})$$

$$+ \frac{\text{co2RBCi} \cdot \text{K10RBCvP6GDH} \cdot \text{K1RBCvP6GDH} \cdot \text{K4RBCvP6GDH} \cdot \text{K6RBCvP6GDH} \cdot \text{nadpRBCi}(t) \cdot \text{ru5pRBCi}(t) \cdot \text{K8RBCvP6GDH}}{\text{Vrbci}^3} \quad (\text{A.4.133})$$

$$+ \frac{\text{co2RBCi} \cdot \text{K10RBCvP6GDH} \cdot \text{K12RBCvP6GDH} \cdot \text{K3RBCvP6GDH} \cdot (\text{K5RBCvP6GDH} + \text{K6RBCvP6GDH}) \cdot \text{nadphRBCi}(t) \cdot \text{p6gRBCi}(t) \cdot \text{ru5pRBCi}(t) \cdot \text{K8RBCvP6GDH}}{\text{Vrbci}^4} \quad (\text{A.4.134})$$

$$+ \frac{\text{co2RBCi} \cdot \text{K10RBCvP6GDH} \cdot \text{K1RBCvP6GDH} \cdot \text{K3RBCvP6GDH} \cdot (\text{K5RBCvP6GDH} + \text{K6RBCvP6GDH}) \cdot \text{nadpRBCi}(t) \cdot \text{p6gRBCi}(t) \cdot \text{ru5pRBCi}(t) \cdot \text{K8RBCvP6GDH}}{\text{Vrbci}^4} \quad (\text{A.4.135})$$

$$+ \frac{\text{co2RBCi} \cdot \text{K10RBCvP6GDH} \cdot \text{K2RBCvP6GDH} \cdot \text{K4RBCvP6GDH} \cdot \text{K6RBCvP6GDH} \cdot \text{ru5pRBCi}(t) \cdot \text{K8RBCvP6GDH}}{\text{Vrbci}^2} \quad (\text{A.4.136})$$

$$+ \frac{\text{co2RBCi} \cdot \text{K11RBCvP6GDH} \cdot \text{K2RBCvP6GDH} \cdot \text{K4RBCvP6GDH} \cdot \text{K6RBCvP6GDH} \cdot \text{K8RBCvP6GDH}}{\text{Vrbci}} \quad (\text{A.4.137})$$

$$+ \text{K11RBCvP6GDH} \cdot \text{K2RBCvP6GDH} \cdot (\text{K4RBCvP6GDH} \cdot \text{K6RBCvP6GDH} + \text{K4RBCvP6GDH} \cdot \text{K7RBCvP6GDH}) \quad (\text{A.4.138})$$

$$+ \text{K5RBCvP6GDH} \cdot \text{K7RBCvP6GDH}) \cdot \text{K9RBCvP6GDH} \quad (\text{A.4.139})$$

$$+ \frac{\text{K12RBCvP6GDH} \cdot \text{K2RBCvP6GDH} \cdot (\text{K4RBCvP6GDH} \cdot \text{K6RBCvP6GDH} + \text{K4RBCvP6GDH} \cdot \text{K7RBCvP6GDH} + \text{K5RBCvP6GDH} \cdot \text{K7RBCvP6GDH}) \cdot \text{K9RBCvP6GDH} \cdot \text{nadphRBCi}(t)}{\text{Vrbci}} \quad (\text{A.4.140})$$

$$+ \frac{\text{K11RBCvP6GDH} \cdot \text{K1RBCvP6GDH} \cdot (\text{K4RBCvP6GDH} \cdot \text{K6RBCvP6GDH} + \text{K4RBCvP6GDH} \cdot \text{K7RBCvP6GDH} + \text{K5RBCvP6GDH} \cdot \text{K7RBCvP6GDH}) \cdot \text{K9RBCvP6GDH} \cdot \text{nadpRBCi}(t)}{\text{Vrbci}} \quad (\text{A.4.141})$$

$$+ \frac{\text{K12RBCvP6GDH} \cdot \text{K3RBCvP6GDH} \cdot \text{K5RBCvP6GDH} \cdot \text{K7RBCvP6GDH} \cdot \text{K9RBCvP6GDH} \cdot \text{nadphRBCi}(t) \cdot \text{p6gRBCi}(t)}{\text{Vrbci}^2} \quad (\text{A.4.142})$$

$$+ \frac{\text{K1RBCvP6GDH} \cdot \text{K3RBCvP6GDH} \cdot (\text{K11RBCvP6GDH} \cdot \text{K5RBCvP6GDH} \cdot \text{K7RBCvP6GDH} + \text{K11RBCvP6GDH} \cdot \text{K9RBCvP6GDH} \cdot \text{K7RBCvP6GDH} + \text{K5RBCvP6GDH} \cdot \text{K9RBCvP6GDH} \cdot \text{K7RBCvP6GDH} + \text{K11RBCvP6GDH} \cdot \text{K5RBCvP6GDH} \cdot \text{K9RBCvP6GDH} \cdot \text{K7RBCvP6GDH}) \cdot \text{nadpRBCi}(t) \cdot \text{p6gRBCi}(t)}{\text{Vrbci}^2} \quad (\text{A.4.143})$$

$$+ \frac{\text{K11RBCvP6GDH} \cdot \text{K3RBCvP6GDH} \cdot \text{K5RBCvP6GDH} \cdot \text{K7RBCvP6GDH} \cdot \text{K9RBCvP6GDH} \cdot \text{p6gRBCi}(t)}{\text{Vrbci}} \quad (\text{A.4.144})$$

$$+ \frac{\text{K10RBCvP6GDH} \cdot \text{K12RBCvP6GDH} \cdot \text{K2RBCvP6GDH} \cdot (\text{K4RBCvP6GDH} \cdot \text{K6RBCvP6GDH} + \text{K4RBCvP6GDH} \cdot \text{K7RBCvP6GDH} + \text{K5RBCvP6GDH} \cdot \text{K7RBCvP6GDH}) \cdot \text{nadphRBCi}(t) \cdot \text{ru5pRBCi}(t)}{\text{Vrbci}^2} \quad (\text{A.4.145})$$

$$+ \frac{\text{K10RBCvP6GDH} \cdot \text{K12RBCvP6GDH} \cdot \text{K3RBCvP6GDH} \cdot \text{K5RBCvP6GDH} \cdot \text{K7RBCvP6GDH} \cdot \text{nadphRBCi}(t) \cdot \text{p6gRBCi}(t) \cdot \text{ru5pRBCi}(t)}{\text{Vrbci}^3} \quad (\text{A.4.146})$$

$$+ \frac{\text{K10RBCvP6GDH} \cdot \text{K1RBCvP6GDH} \cdot \text{K3RBCvP6GDH} \cdot \text{K5RBCvP6GDH} \cdot \text{K7RBCvP6GDH} \cdot \text{nadpRBCi}(t) \cdot \text{p6gRBCi}(t) \cdot \text{ru5pRBCi}(t)}{\text{Vrbci}^3} \quad (\text{A.4.147})$$

$$(\text{A.4.148})$$

$$vRBCivPFK = \left[\text{parMulti} \cdot \text{TsRBC} \cdot \text{Vrbci} \cdot \text{VRBCvPFK} \cdot \left(\frac{\text{KcatfRBCvPFK} \cdot \text{f6pRBCi}(t) \cdot \text{mgatpRBCi}(t)}{\text{Kmf6pRBCvPFK} \cdot \text{KmmgatpRBCvPFK} \cdot \text{Vrbci}^2} \right. \right. \quad (\text{A.4.149})$$

$$\left. \left. - \frac{\text{KcatfRBCvPFK} \cdot \text{f16p2RBCi}(t) \cdot \text{mgadpRBCi}(t)}{\text{Kmf16p2RBCvPFK} \cdot \text{KmmgadpRBCvPFK} \cdot \text{Vrbci}^2} \right) \right] / \quad (\text{A.4.150})$$

$$\left[\left(\frac{\text{mgadpRBCi}(t) \cdot \text{f16p2RBCi}(t)}{\text{Kmf16p2RBCvPFK} \cdot \text{KmmgadpRBCvPFK} \cdot \text{Vrbci}^2} + \frac{\text{f16p2RBCi}(t)}{\text{Kmf16p2RBCvPFK} \cdot \text{Vrbci}} + \frac{\text{f6pRBCi}(t)}{\text{Kmf6pRBCvPFK} \cdot \text{Vrbci}} \right. \right. \quad (\text{A.4.151})$$

$$\left. \left. + \frac{\text{mgadpRBCi}(t)}{\text{KmmgadpRBCvPFK} \cdot \text{Vrbci}} + \frac{\text{f6pRBCi}(t) \cdot \text{mgatpRBCi}(t)}{\text{Kmf6pRBCvPFK} \cdot \text{KmmgatpRBCvPFK} \cdot \text{Vrbci}^2} + \frac{\text{mgatpRBCi}(t)}{\text{KmmgatpRBCvPFK} \cdot \text{Vrbci}} + 1 \right) \right] \quad (\text{A.4.152})$$

$$\cdot \left(\frac{\left(\frac{\text{atpRBCi}(t)}{\text{KtatpRBCvPFK} \cdot \text{Vrbci}} + 1 \right)^4 \cdot \left(\frac{\text{b23pgRBCi}(t)}{\text{Ktb23pgRBCvPFK} \cdot \text{Vrbci}} + 1 \right)^4 \cdot \left(\frac{\text{mgRBCi}(t)}{\text{KtmgRBCvPFK} \cdot \text{Vrbci}} + 1 \right)^4 \cdot \left(\frac{\text{hRBC}}{\text{KaRBCvPFK}} \right)^{\text{nRBCvPFK}}}{\left(\frac{\text{ampRBCi}(t)}{\text{KrampRBCvPFK} \cdot \text{Vrbci}} + 1 \right)^4 \cdot \left(\frac{\text{f16p2RBCi}(t)}{\text{Kmf16p2RBCvPFK} \cdot \text{Vrbci}} + \frac{\text{f6pRBCi}(t)}{\text{Kmf6pRBCvPFK} \cdot \text{Vrbci}} + 1 \right)^4 \cdot \left(\frac{\text{g16p2RBCi}(t)}{\text{Krg16p2RBCvPFK} \cdot \text{Vrbci}} + 1 \right)^4 \cdot \left(\frac{\text{phosRBCi}(t)}{\text{KrpHosRBCvPFK} \cdot \text{Vrbci}} + 1 \right)^4} + 1 \right) \right] \quad (\text{A.4.153})$$

$$vRBCivPGI = \frac{ERBCvPGI \cdot parMulti \cdot TsRBC \cdot Vrbc_i \cdot \left(\frac{KcatfRBCvPGI \cdot g6pRBCi(t)}{Kmg6pRBCvPGI \cdot Vrbc_i} - \frac{KcatrRBCvPGI \cdot f6pRBCi(t)}{Kmf6pRBCvPGI \cdot Vrbc_i} \right)}{\frac{f6pRBCi(t)}{Kmf6pRBCvPGI \cdot Vrbc_i} + \frac{g6pRBCi(t)}{Kmg6pRBCvPGI \cdot Vrbc_i} + 1} \quad (A.4.154)$$

$$vRBCivPGK = \frac{1}{\frac{mgadpRBCi(t) \cdot b13pgRBCi(t)}{KimgadpRBCvPGK \cdot Kmb13pgRBCvPGK \cdot Vrbc_i^2} + \frac{b13pgRBCi(t)}{Kib13pgRBCvPGK \cdot Vrbc_i} + \frac{mgadpRBCi(t)}{KimgadpRBCvPGK \cdot Vrbc_i} + \frac{mgatpRBCi(t)}{KimgatpRBCvPGK \cdot Vrbc_i} + \frac{1}{\frac{mgatpRBCi(t) \cdot p3gRBCi(t)}{KimgatpRBCvPGK \cdot Kmp3gRBCvPGK \cdot Vrbc_i^2} + \frac{p3gRBCi(t)}{Kip3gRBCvPGK \cdot Vrbc_i} + 1}}{parMulti \cdot TsRBC \cdot Vrbc_i \cdot VRBCvPGK \cdot \left(\frac{KcatfRBCvPGK \cdot b13pgRBCi(t) \cdot mgadpRBCi(t)}{KimgadpRBCvPGK \cdot Kmb13pgRBCvPGK \cdot Vrbc_i^2} - \frac{KcatrRBCvPGK \cdot mgatpRBCi(t) \cdot p3gRBCi(t)}{KimgatpRBCvPGK \cdot Kmp3gRBCvPGK \cdot Vrbc_i^2} \right)} \quad (A.4.155)$$

$$vRBCivPGLHYDROLYSIS = parMulti \cdot TsRBC \cdot Vrbc_i \cdot \left(\frac{KhydrolRBCvPGLHYDROLYSIS \cdot p6glRBCi(t)}{Vrbc_i} \right) \quad (A.4.156)$$

$$+ \frac{Klactonase3RBCvPGLHYDROLYSIS \cdot VRBCvPGLHYDROLYSIS \cdot p6glRBCi(t)}{Vrbc_i \cdot \left(\frac{Klactonase2RBCvPGLHYDROLYSIS + Klactonase3RBCvPGLHYDROLYSIS}{Klactonase1RBCvPGLHYDROLYSIS} + \frac{p6glRBCi(t)}{Vrbc_i} \right)} \quad (A.4.157)$$

$$vRBCivPGM = \frac{parMulti \cdot TsRBC \cdot Vrbc_i \cdot VRBCvPGM \cdot \left(\frac{KcatfRBCvPGM \cdot p3gRBCi(t)}{Kmp3gRBCvPGM \cdot Vrbc_i} - \frac{KcatrRBCvPGM \cdot p2gRBCi(t)}{Kmp2gRBCvPGM \cdot Vrbc_i} \right)}{\frac{p2gRBCi(t)}{Kmp2gRBCvPGM \cdot Vrbc_i} + \frac{p3gRBCi(t)}{Kmp3gRBCvPGM \cdot Vrbc_i} + 1} \quad (A.4.158)$$

$$vRBCivPHOSTRANSPORT = parMulti \cdot TsRBC \cdot Vrbc_i \cdot \left(\frac{KoRBCvPHOSTRANSPORT \cdot phosRBCi(t)}{Vrbc_i} - \frac{KiRBCvPHOSTRANSPORT \cdot phosEXT}{vBld} \right) \quad (A.4.159)$$

$$(A.4.160)$$

$$vRBCivPK = \left[\text{parMulti} \cdot \text{TsRBC} \cdot \text{Vrbci} \cdot \text{VRBCvPK} \cdot \left(\frac{\text{KcatfRBCvPK} \cdot \text{mgadpRBCi}(t) \cdot \text{pepRBCi}(t)}{\text{KrmgadpRBCvPK} \cdot \text{KrpepRBCvPK} \cdot \text{Vrbci}^2} - \frac{\text{KcatrRBCvPK} \cdot \text{mgatpRBCi}(t) \cdot \text{pyrRBCi}(t)}{\text{KrmgatpRBCvPK} \cdot \text{KrpypRBCvPK} \cdot \text{Vrbci}^2} \right) \right] / \quad (\text{A.4.161})$$

$$\left[(\text{LRBCivPK} + 1) \cdot \left(\frac{\text{pepRBCi}(t) \cdot \text{mgadpRBCi}(t)}{\text{KrmgadpRBCvPK} \cdot \text{KrpepRBCvPK} \cdot \text{Vrbci}^2} + \frac{\text{mgadpRBCi}(t)}{\text{KrmgadpRBCvPK} \cdot \text{Vrbci}} + \frac{\text{mgatpRBCi}(t)}{\text{KrmgatpRBCvPK} \cdot \text{Vrbci}} \right) \right] \quad (\text{A.4.162})$$

$$+ \frac{\text{pepRBCi}(t)}{\text{KrpepRBCvPK} \cdot \text{Vrbci}} + \frac{\text{mgatpRBCi}(t) \cdot \text{pyrRBCi}(t)}{\text{KrmgatpRBCvPK} \cdot \text{KrpypRBCvPK} \cdot \text{Vrbci}^2} + \frac{\text{pyrRBCi}(t)}{\text{KrpypRBCvPK} \cdot \text{Vrbci}} + 1 \quad (\text{A.4.163})$$

$$vRBCivPYRTRANSPORT = \text{parMulti} \cdot \text{TsRBC} \cdot \text{Vrbci} \cdot \left(\frac{\text{KoRBCvPYRTRANSPORT} \cdot \text{pyrRBCi}(t)}{\text{Vrbci}} - \frac{\text{KiRBCvPYRTRANSPORT} \cdot \text{pyrEXT}}{\text{vBld}} \right) \quad (\text{A.4.164})$$

$$vRBCivR5PI = \frac{\text{parMulti} \cdot \text{TsRBC} \cdot \text{Vrbci} \cdot \text{VRBCvR5PI} \cdot \left(\frac{\text{K1RBCvR5PI} \cdot \text{K3RBCvR5PI} \cdot \text{ru5pRBCi}(t)}{(\text{K2RBCvR5PI} + \text{K3RBCvR5PI}) \cdot \text{Vrbci}} - \frac{\text{K2RBCvR5PI} \cdot \text{K4RBCvR5PI} \cdot \text{rib5pRBCi}(t)}{(\text{K2RBCvR5PI} + \text{K3RBCvR5PI}) \cdot \text{Vrbci}} \right)}{\frac{\text{K1RBCvR5PI} \cdot \text{ru5pRBCi}(t)}{(\text{K2RBCvR5PI} + \text{K3RBCvR5PI}) \cdot \text{Vrbci}} + \frac{\text{K4RBCvR5PI} \cdot \text{xu5pRBCi}(t)}{(\text{K2RBCvR5PI} + \text{K3RBCvR5PI}) \cdot \text{Vrbci}} + 1} \quad (\text{A.4.165})$$

$$vRBCivRu5PE = \frac{\text{parMulti} \cdot \text{TsRBC} \cdot \text{Vrbci} \cdot \text{VRBCvRu5PE} \cdot \left(\frac{\text{K1RBCvRu5PE} \cdot \text{K3RBCvRu5PE} \cdot \text{ru5pRBCi}(t)}{(\text{K2RBCvRu5PE} + \text{K3RBCvRu5PE}) \cdot \text{Vrbci}} - \frac{\text{K2RBCvRu5PE} \cdot \text{K4RBCvRu5PE} \cdot \text{xu5pRBCi}(t)}{(\text{K2RBCvRu5PE} + \text{K3RBCvRu5PE}) \cdot \text{Vrbci}} \right)}{\frac{\text{K1RBCvRu5PE} \cdot \text{ru5pRBCi}(t)}{(\text{K2RBCvRu5PE} + \text{K3RBCvRu5PE}) \cdot \text{Vrbci}} + \frac{\text{K4RBCvRu5PE} \cdot \text{xu5pRBCi}(t)}{(\text{K2RBCvRu5PE} + \text{K3RBCvRu5PE}) \cdot \text{Vrbci}} + 1} \quad (\text{A.4.166})$$

$$vRBCivTA = \left[\text{parMulti} \cdot \text{TsRBC} \cdot \text{Vrbci} \cdot \text{VRBCvTA} \cdot \left(\frac{\text{K1RBCvTA} \cdot \text{K3RBCvTA} \cdot \text{K5RBCvTA} \cdot \text{K7RBCvTA} \cdot \text{gapRBCi}(t) \cdot \text{sed7pRBCi}(t)}{\text{Vrbci}^2} \right) \right] \quad (\text{A.4.167})$$

$$- \frac{\text{K2RBCvTA} \cdot \text{K4RBCvTA} \cdot \text{K6RBCvTA} \cdot \text{K8RBCvTA} \cdot \text{ery4pRBCi}(t) \cdot \text{f6pRBCi}(t)}{\text{Vrbci}^2} \quad (\text{A.4.168})$$

$$\left[\frac{\text{K4RBCvTA} \cdot (\text{K2RBCvTA} + \text{K6RBCvTA}) \cdot \text{K8RBCvTA} \cdot \text{f6pRBCi}(t) \cdot \text{ery4pRBCi}(t)}{\text{Vrbci}^2} \right] \quad (\text{A.4.169})$$

$$+ \frac{\text{K1RBCvTA} \cdot \text{K4RBCvTA} \cdot (\text{K6RBCvTA} + \text{K7RBCvTA}) \cdot \text{sed7pRBCi}(t) \cdot \text{ery4pRBCi}(t)}{\text{Vrbci}^2} \quad (\text{A.4.170})$$

$$+ \frac{\text{K2RBCvTA} \cdot \text{K4RBCvTA} \cdot (\text{K6RBCvTA} + \text{K7RBCvTA}) \cdot \text{ery4pRBCi}(t)}{\text{Vrbci}} \quad (\text{A.4.171})$$

$$+ \frac{(\text{K2RBCvTA} + \text{K3RBCvTA}) \cdot \text{K6RBCvTA} \cdot \text{K8RBCvTA} \cdot \text{f6pRBCi}(t)}{\text{Vrbci}} \quad (\text{A.4.172})$$

$$+ \frac{(\text{K2RBCvTA} + \text{K3RBCvTA}) \cdot \text{K5RBCvTA} \cdot \text{K8RBCvTA} \cdot \text{f6pRBCi}(t) \cdot \text{gapRBCi}(t)}{\text{Vrbci}^2} \quad (\text{A.4.173})$$

$$+ \frac{(\text{K2RBCvTA} + \text{K3RBCvTA}) \cdot \text{K5RBCvTA} \cdot \text{K7RBCvTA} \cdot \text{gapRBCi}(t)}{\text{Vrbci}} \quad (\text{A.4.174})$$

$$+ \frac{K1RBCvTA \cdot K5RBCvTA \cdot (K3RBCvTA + K7RBCvTA) \cdot gapRBCi(t) \cdot sed7pRBCi(t)}{Vrbci^2} \quad (A.4.175)$$

$$+ \left. \frac{K1RBCvTA \cdot K3RBCvTA \cdot (K6RBCvTA + K7RBCvTA) \cdot sed7pRBCi(t)}{Vrbci} \right] \quad (A.4.176)$$

$$vRBCivTIM = \frac{parMulti \cdot TsRBC \cdot Vrbci \cdot VRBCvTIM \cdot \left(\frac{KcatfRBCvTIM \cdot gapRBCi(t)}{KmgapRBCvTIM \cdot Vrbci} - \frac{KcatrRBCvTIM \cdot dhapRBCi(t)}{KmdhapRBCvTIM \cdot Vrbci} \right)}{\frac{dhapRBCi(t)}{KmdhapRBCvTIM \cdot Vrbci} + \frac{gapRBCi(t)}{KmgapRBCvTIM \cdot Vrbci} + 1} \quad (A.4.177)$$

$$vRBCivTK1 = parMulti \cdot TsRBC \cdot Vrbci \cdot \left(\frac{K1RBCvTK1 \cdot tkRBCi(t) \cdot xu5pRBCi(t)}{Vrbci^2} - \frac{K2RBCvTK1 \cdot tkxu5pRBCi(t)}{Vrbci} \right) \quad (A.4.178)$$

$$vRBCivTK2 = parMulti \cdot TsRBC \cdot Vrbci \cdot \left(\frac{K3RBCvTK2 \cdot tkxu5pRBCi(t)}{Vrbci} - \frac{K4RBCvTK2 \cdot gapRBCi(t) \cdot tkgRBCi(t)}{Vrbci^2} \right) \quad (A.4.179)$$

$$vRBCivTK3 = parMulti \cdot TsRBC \cdot Vrbci \cdot \left(\frac{K5RBCvTK3 \cdot rib5pRBCi(t) \cdot tkgRBCi(t)}{Vrbci^2} - \frac{K6RBCvTK3 \cdot tkgrib5pRBCi(t)}{Vrbci} \right) \quad (A.4.180)$$

$$vRBCivTK4 = parMulti \cdot TsRBC \cdot Vrbci \cdot \left(\frac{K7RBCvTK4 \cdot tkgrib5pRBCi(t)}{Vrbci} - \frac{K8RBCvTK4 \cdot sed7pRBCi(t) \cdot tkRBCi(t)}{Vrbci^2} \right) \quad (A.4.181)$$

$$vRBCivTK5 = parMulti \cdot TsRBC \cdot Vrbci \cdot \left(\frac{K9RBCvTK5 \cdot ery4pRBCi(t) \cdot tkgRBCi(t)}{Vrbci^2} - \frac{K10RBCvTK5 \cdot tkgery4pRBCi(t)}{Vrbci} \right) \quad (A.4.182)$$

$$vRBCivTK6 = parMulti \cdot TsRBC \cdot Vrbci \cdot \left(\frac{K11RBCvTK6 \cdot tkgery4pRBCi(t)}{Vrbci} - \frac{K12RBCvTK6 \cdot f6pRBCi(t) \cdot tkRBCi(t)}{Vrbci^2} \right) \quad (A.4.183)$$

$$vRBCvAK = TsRBC \cdot Vrbcu \cdot \left(\frac{K1appRBCvAK \cdot adpRBC(t) \cdot mgadpRBC(t)}{Vrbcu^2} - \frac{K2appRBCvAK \cdot ampRBC(t) \cdot mgatpRBC(t)}{Vrbcu^2} \right) \quad (A.4.184)$$

$$(A.4.185)$$

$$vRBCvALD = \left[TsRBC \cdot Vrbcu \cdot VRBCvALD \cdot \left(\frac{KcatfRBCvALD \cdot f16p2RBC(t)}{Kmf16p2RBCvALD \cdot Vrbcu} - \frac{KcatrRBCvALD \cdot dhapRBC(t) \cdot gapRBC(t)}{KidhapRBCvALD \cdot KmgapRBCvALD \cdot Vrbcu^2} \right) \right] / \quad (A.4.186)$$

$$\left[\frac{gapRBC(t) \cdot dhapRBC(t)}{KidhapRBCvALD \cdot KmgapRBCvALD \cdot Vrbcu^2} + \frac{dhapRBC(t)}{KidhapRBCvALD \cdot Vrbcu} + \frac{f16p2RBC(t)}{Kmf16p2RBCvALD \cdot Vrbcu} \right] \quad (A.4.187)$$

$$+ \frac{KmdhapRBCvALD \cdot f16p2RBC(t) \cdot gapRBC(t)}{KidhapRBCvALD \cdot Kif16p2RBCvALD \cdot KmgapRBCvALD \cdot Vrbcu^2} + \frac{\frac{b23pgRBC(t)}{Vrbcu} + \frac{mgb23pgRBC(t)}{Vrbcu}}{Kib23pgRBCvALD} \quad (A.4.188)$$

$$\left. + \frac{KmdhapRBCvALD \cdot gapRBC(t) \cdot \left(\frac{\frac{b23pgRBC(t)}{Vrbcu} + \frac{mgb23pgRBC(t)}{Vrbcu}}{Kib23pgRBCvALD} + 1 \right)}{KidhapRBCvALD \cdot KmgapRBCvALD \cdot Vrbcu} + 1 \right] \quad (A.4.189)$$

$$vRBCvATPASE = KRBCvATPASE \cdot TsRBC \cdot mgatpRBC(t) \quad (A.4.190)$$

$$vRBCvBPGSP1 = TsRBC \cdot Vrbcu \cdot \left(\frac{K1appRBCvBPGSP1 \cdot b13pgRBC(t) \cdot bpgspRBC(t)}{Vrbcu^2} - \frac{K2RBCvBPGSP1 \cdot bpgspb13pgRBC(t)}{Vrbcu} \right) \quad (A.4.191)$$

$$vRBCvBPGSP2 = K3appRBCvBPGSP2 \cdot TsRBC \cdot bpgspb13pgRBC(t) \quad (A.4.192)$$

$$vRBCvBPGSP3 = TsRBC \cdot Vrbcu \cdot \left(\frac{K4appRBCvBPGSP3 \cdot bpgsppRBC(t) \cdot p3gRBC(t)}{Vrbcu^2} - \frac{K5RBCvBPGSP3 \cdot bpgsppp3gRBC(t)}{Vrbcu} \right) \quad (A.4.193)$$

$$vRBCvBPGSP4 = TsRBC \cdot Vrbcu \cdot \left(\frac{K6appRBCvBPGSP4 \cdot bpgsppRBC(t) \cdot p2gRBC(t)}{Vrbcu^2} - \frac{K7RBCvBPGSP4 \cdot bpgsppp2gRBC(t)}{Vrbcu} \right) \quad (A.4.194)$$

$$vRBCvBPGSP5 = TsRBC \cdot Vrbcu \cdot \left(\frac{K8RBCvBPGSP5 \cdot bpgsppp3gRBC(t)}{Vrbcu} - \frac{K9RBCvBPGSP5 \cdot bpgspb23pgRBC(t)}{Vrbcu} \right) \quad (A.4.195)$$

$$vRBCvBPGSP6 = TsRBC \cdot Vrbcu \cdot \left(\frac{K10RBCvBPGSP6 \cdot bpgsppp2gRBC(t)}{Vrbcu} - \frac{K11RBCvBPGSP6 \cdot bpgspb23pgRBC(t)}{Vrbcu} \right) \quad (A.4.196)$$

$$vRBCvBPGSP7 = TsRBC \cdot Vrbcu \cdot \left(\frac{K12RBCvBPGSP7 \cdot bpgspb23pgRBC(t)}{Vrbcu} - \frac{K13appRBCvBPGSP7 \cdot b23pgRBC(t) \cdot bpgspRBC(t)}{Vrbcu^2} \right) \quad (A.4.197)$$

$$vRBCvBPGSP8 = TsRBC \cdot Vrbcu \cdot \left(\frac{K14RBCvBPGSP8 \cdot bpgsppRBC(t) \cdot phosRBC(t)}{Vrbcu^2} - \frac{K15RBCvBPGSP8 \cdot bpgsppphosRBC(t)}{Vrbcu} \right) \quad (A.4.198)$$

$$vRBCvBPGSP9 = K16RBCvBPGSP9 \cdot TsRBC \cdot bpgsppphosRBC(t) \quad (A.4.199)$$

$$vRBCvENO = \frac{TsRBC \cdot Vrbcu \cdot VRBCvENO \cdot \left(\frac{KcatfRBCvENO \cdot mgRBC(t) \cdot p2gRBC(t)}{KimgRBCvENO \cdot Kmp2gRBCvENO \cdot Vrbcu^2} - \frac{KcatrRBCvENO \cdot mgRBC(t) \cdot pepRBC(t)}{KipepRBCvENO \cdot KmmgRBCvENO \cdot Vrbcu^2} \right)}{\frac{p2gRBC(t) \cdot mgRBC(t)}{KimgRBCvENO \cdot Kmp2gRBCvENO \cdot Vrbcu^2} + \frac{pepRBC(t) \cdot mgRBC(t)}{KipepRBCvENO \cdot KmmgRBCvENO \cdot Vrbcu^2} + \frac{mgRBC(t)}{KimgRBCvENO \cdot Vrbcu} + \frac{p2gRBC(t)}{Kip2gRBCvENO \cdot Vrbcu} + \frac{pepRBC(t)}{KipepRBCvENO \cdot Vrbcu} + 1} \quad (A.4.200)$$

$$vRBCvG6PDH = [TsRBC \cdot Vrbcu \cdot VRBCvG6PDH \cdot \quad (A.4.201)$$

$$\left(\frac{K1RBCvG6PDH \cdot K3RBCvG6PDH \cdot K5RBCvG6PDH \cdot K7RBCvG6PDH \cdot K9RBCvG6PDH \cdot g6pRBC(t) \cdot nadpRBC(t)}{Vrbcu^2} \quad (A.4.202)$$

$$- \frac{K10RBCvG6PDH \cdot K2RBCvG6PDH \cdot K4RBCvG6PDH \cdot K6RBCvG6PDH \cdot K8RBCvG6PDH \cdot nadphRBC(t) \cdot p6glRBC(t)}{Vrbcu^2} \right) / \quad (A.4.203)$$

$$[K2RBCvG6PDH \cdot K9RBCvG6PDH \quad (A.4.204)$$

$$\cdot (K4RBCvG6PDH \cdot K6RBCvG6PDH + K4RBCvG6PDH \cdot K7RBCvG6PDH + K5RBCvG6PDH \cdot K7RBCvG6PDH) \quad (A.4.205)$$

$$+ \frac{K3RBCvG6PDH \cdot K5RBCvG6PDH \cdot K7RBCvG6PDH \cdot g6pRBC(t) \cdot K9RBCvG6PDH}{Vrbcu} \quad (A.4.206)$$

$$+ \frac{K1RBCvG6PDH \cdot nadpRBC(t) \cdot K9RBCvG6PDH}{Vrbcu \cdot (K4RBCvG6PDH \cdot K6RBCvG6PDH + K4RBCvG6PDH \cdot K7RBCvG6PDH + K5RBCvG6PDH \cdot K7RBCvG6PDH)} \quad (A.4.207)$$

$$+ \frac{K10RBCvG6PDH \cdot K3RBCvG6PDH \cdot K5RBCvG6PDH \cdot K7RBCvG6PDH \cdot g6pRBC(t) \cdot nadphRBC(t)}{Vrbcu^2} \quad (A.4.208)$$

$$+ \frac{K10RBCvG6PDH \cdot K2RBCvG6PDH \cdot (K4RBCvG6PDH \cdot K6RBCvG6PDH + K5RBCvG6PDH \cdot K7RBCvG6PDH) \cdot nadphRBC(t)}{Vrbcu} \quad (A.4.209)$$

$$+ \frac{K1RBCvG6PDH \cdot K3RBCvG6PDH \cdot (K5RBCvG6PDH \cdot K7RBCvG6PDH + K9RBCvG6PDH \cdot K7RBCvG6PDH + K5RBCvG6PDH \cdot K9RBCvG6PDH + K6RBCvG6PDH \cdot K9RBCvG6PDH) \cdot g6pRBC(t) \cdot nadpRBC(t)}{Vrbcu^2} \quad (A.4.210)$$

$$+ \frac{K10RBCvG6PDH \cdot K3RBCvG6PDH \cdot (K5RBCvG6PDH + K6RBCvG6PDH) \cdot K8RBCvG6PDH \cdot g6pRBC(t) \cdot nadphRBC(t) \cdot p6glRBC(t)}{Vrbcu^3} \quad (A.4.211)$$

$$+ \frac{K10RBCvG6PDH \cdot (K2RBCvG6PDH \cdot K4RBCvG6PDH + K6RBCvG6PDH \cdot K4RBCvG6PDH + K2RBCvG6PDH \cdot K5RBCvG6PDH + K2RBCvG6PDH \cdot K6RBCvG6PDH) \cdot K8RBCvG6PDH \cdot nadphRBC(t) \cdot p6glRBC(t)}{Vrbcu^2} \quad (A.4.212)$$

$$+ \frac{K1RBCvG6PDH \cdot K3RBCvG6PDH \cdot (K5RBCvG6PDH + K6RBCvG6PDH) \cdot K8RBCvG6PDH \cdot g6pRBC(t) \cdot nadpRBC(t) \cdot p6glRBC(t)}{Vrbcu^3} \quad (A.4.213)$$

$$+ \frac{K1RBCvG6PDH \cdot K4RBCvG6PDH \cdot K6RBCvG6PDH \cdot K8RBCvG6PDH \cdot nadpRBC(t) \cdot p6glRBC(t)}{Vrbcu^2} \quad (A.4.214)$$

$$+ \frac{K2RBCvG6PDH \cdot K4RBCvG6PDH \cdot K6RBCvG6PDH \cdot K8RBCvG6PDH \cdot p6glRBC(t)}{Vrbcu} \quad (A.4.215)$$

$$vRBCvGAPDH = \left[TsRBC \cdot Vrbcu \cdot VRBCvGAPDH \cdot \left(\frac{KcatfappRBCvGAPDH \cdot gapRBC(t) \cdot nadRBC(t) \cdot phosRBC(t)}{KiappgapRBCvGAPDH \cdot KiphosRBCvGAPDH \cdot KmnadRBCvGAPDH \cdot Vrbcu^3} \right. \right. \quad (A.4.216)$$

$$\left. - \frac{KcatrappRBCvGAPDH \cdot b13pgRBC(t) \cdot nadhRBC(t)}{Kiappb13pgRBCvGAPDH \cdot KmappnadhRBCvGAPDH \cdot Vrbcu^2} \right) \Big] / \quad (A.4.217)$$

$$\left[\frac{b13pgRBC(t) \cdot \left(\frac{gapRBC(t)}{KidgapRBCvGAPDH \cdot Vrbcu} + 1 \right)}{Kiappb13pgRBCvGAPDH \cdot Vrbcu} + \frac{gapRBC(t) \cdot \left(\frac{gapRBC(t)}{KidgapRBCvGAPDH \cdot Vrbcu} + 1 \right)}{KiappgapRBCvGAPDH \cdot Vrbcu} \right. \quad (A.4.218)$$

$$\left. + \frac{gapRBC(t) \cdot phosRBC(t) \cdot \left(\frac{gapRBC(t)}{KidgapRBCvGAPDH \cdot Vrbcu} + 1 \right)}{KiappgapRBCvGAPDH \cdot KiphosRBCvGAPDH \cdot Vrbcu^2} + \frac{b13pgRBC(t) \cdot nadhRBC(t)}{Kiappb13pgRBCvGAPDH \cdot KmappnadhRBCvGAPDH \cdot Vrbcu^2} \right. \quad (A.4.219)$$

$$\left. + \frac{gapRBC(t) \cdot nadhRBC(t)}{KiappgapRBCvGAPDH \cdot KiappnadhRBCvGAPDH \cdot Vrbcu^2} + \frac{Kmb13pgRBCvGAPDH \cdot nadhRBC(t)}{Kiappb13pgRBCvGAPDH \cdot KmappnadhRBCvGAPDH \cdot Vrbcu} \right. \quad (A.4.220)$$

$$\left. + \frac{b13pgRBC(t) \cdot nadRBC(t)}{Kiappb13pgRBCvGAPDH \cdot KinadRBCvGAPDH \cdot Vrbcu^2} + \frac{gapRBC(t) \cdot nadRBC(t)}{KiappgapRBCvGAPDH \cdot KinadRBCvGAPDH \cdot Vrbcu^2} \right. \quad (A.4.221)$$

$$\left. + \frac{Kmb13pgRBCvGAPDH \cdot b13pgRBC(t) \cdot nadhRBC(t) \cdot phosRBC(t)}{Kiappb13pgRBCvGAPDH \cdot Kidb13pgRBCvGAPDH \cdot KiphosRBCvGAPDH \cdot KmappnadhRBCvGAPDH \cdot Vrbcu^3} \right. \quad (A.4.222)$$

$$\left. + \frac{gapRBC(t) \cdot nadhRBC(t) \cdot phosRBC(t)}{KiappgapRBCvGAPDH \cdot KiappnadhRBCvGAPDH \cdot KiphosRBCvGAPDH \cdot Vrbcu^3} \right. \quad (A.4.223)$$

$$\left. + \frac{Kmb13pgRBCvGAPDH \cdot nadhRBC(t) \cdot phosRBC(t)}{Kiappb13pgRBCvGAPDH \cdot KiphosRBCvGAPDH \cdot KmappnadhRBCvGAPDH \cdot Vrbcu^2} \right. \quad (A.4.224)$$

$$\left. + \frac{KmgapRBCvGAPDH \cdot b13pgRBC(t) \cdot nadRBC(t) \cdot phosRBC(t)}{KiappgapRBCvGAPDH \cdot Kidb13pgRBCvGAPDH \cdot KiphosRBCvGAPDH \cdot KmnadRBCvGAPDH \cdot Vrbcu^3} \right. \quad (A.4.225)$$

$$\left. + \frac{gapRBC(t) \cdot nadRBC(t) \cdot phosRBC(t)}{KiappgapRBCvGAPDH \cdot KiphosRBCvGAPDH \cdot KmnadRBCvGAPDH \cdot Vrbcu^3} \right. \quad (A.4.226)$$

$$\left. + \frac{KmgapRBCvGAPDH \cdot nadRBC(t) \cdot phosRBC(t)}{KiappgapRBCvGAPDH \cdot KiphosRBCvGAPDH \cdot KmnadRBCvGAPDH \cdot Vrbcu^2} \right] \quad (A.4.227)$$

$$vRBCvGLCTransport = TsRBC \cdot Vrbcu \cdot \left(\frac{glc_alpha \cdot VRBCvGLCTransport \cdot B_gluc(t)}{1000 \cdot \left(\frac{(1-gluc_alpha) \cdot B_gluc(t) \cdot k_beta}{1000 \cdot k_beta} + k_alpha + \frac{glc_alpha \cdot B_gluc(t)}{1000} \right)} \right. \quad (A.4.228)$$

$$\left. + \frac{(1-gluc_alpha) \cdot VRBCvGLCTransport \cdot B_gluc(t)}{1000 \cdot \left(\frac{glc_alpha \cdot B_gluc(t) \cdot k_beta}{1000 \cdot k_alpha} + k_beta + \frac{(1-gluc_alpha) \cdot B_gluc(t)}{1000} \right)} \right) \quad (A.4.229)$$

$$\frac{\text{glc_alpha} \cdot \text{VRBCvGLCTRANSPORT} \cdot \text{glcRBC}(t)}{\text{Vrbcu} \cdot \left(\frac{(1-\text{glc_alpha}) \cdot \text{glcRBC}(t) \cdot \text{k_alpha}}{\text{k_beta} \cdot \text{Vrbcu}} + \text{k_alpha} + \frac{\text{glc_alpha} \cdot \text{glcRBC}(t)}{\text{Vrbcu}} \right)} \quad (\text{A.4.230})$$

$$\frac{(1 - \text{glc_alpha}) \cdot \text{VRBCvGLCTRANSPORT} \cdot \text{glcRBC}(t)}{\text{Vrbcu} \cdot \left(\frac{\text{glc_alpha} \cdot \text{glcRBC}(t) \cdot \text{k_beta}}{\text{k_alpha} \cdot \text{Vrbcu}} + \text{k_beta} + \frac{(1-\text{glc_alpha}) \cdot \text{glcRBC}(t)}{\text{Vrbcu}} \right)} \quad (\text{A.4.231})$$

$$\text{vRBCvGSSGR} = [\text{TsRBC} \cdot \text{Vrbcu} \cdot \text{VRBCvGSSGR}] \quad (\text{A.4.232})$$

$$\left(\frac{\text{K11RBCvGSSGR} \cdot \text{K1RBCvGSSGR} \cdot \text{K3RBCvGSSGR} \cdot \text{K5RBCvGSSGR} \cdot \text{K7RBCvGSSGR}}{\text{Vrbcu}^2} \cdot \text{K9RBCvGSSGR} \cdot \text{gssgRBC}(t) \cdot \text{nadpRBC}(t)} \right) \quad (\text{A.4.233})$$

$$\left. - \frac{\text{K10RBCvGSSGR} \cdot \text{K12RBCvGSSGR} \cdot \text{K2RBCvGSSGR} \cdot \text{K4RBCvGSSGR} \cdot \text{K6RBCvGSSGR}}{\text{Vrbcu}^3} \cdot \text{K8RBCvGSSGR} \cdot \text{gshRBC}(t)^2 \cdot \text{nadpRBC}(t) \right) \Bigg] / \quad (\text{A.4.234})$$

$$\left[\frac{\text{K10RBCvGSSGR} \cdot \text{K1RBCvGSSGR} \cdot \text{K3RBCvGSSGR} \cdot (\text{K5RBCvGSSGR} + \text{K6RBCvGSSGR})}{\text{Vrbcu}^4} \cdot \text{K8RBCvGSSGR} \cdot \text{gssgRBC}(t) \cdot \text{nadpRBC}(t) \cdot \text{gshRBC}(t)^2 \right] \quad (\text{A.4.235})$$

$$+ \frac{\text{K10RBCvGSSGR} \cdot \text{K1RBCvGSSGR} \cdot \text{K4RBCvGSSGR} \cdot \text{K6RBCvGSSGR} \cdot \text{K8RBCvGSSGR} \cdot \text{nadpRBC}(t) \cdot \text{gshRBC}(t)^2}{\text{Vrbcu}^3} \quad (\text{A.4.236})$$

$$+ \frac{\text{K10RBCvGSSGR} \cdot \text{K12RBCvGSSGR} \cdot \text{K3RBCvGSSGR} \cdot (\text{K5RBCvGSSGR} + \text{K6RBCvGSSGR}) \cdot \text{K8RBCvGSSGR} \cdot \text{gssgRBC}(t) \cdot \text{nadpRBC}(t) \cdot \text{gshRBC}(t)^2}{\text{Vrbcu}^4} \quad (\text{A.4.237})$$

$$+ \frac{\text{K10RBCvGSSGR} \cdot \text{K12RBCvGSSGR} \cdot (\text{K2RBCvGSSGR} \cdot \text{K4RBCvGSSGR} + \text{K6RBCvGSSGR} \cdot \text{K4RBCvGSSGR} + \text{K2RBCvGSSGR} \cdot \text{K5RBCvGSSGR} + \text{K2RBCvGSSGR} \cdot \text{K6RBCvGSSGR}) \cdot \text{K8RBCvGSSGR} \cdot \text{nadpRBC}(t) \cdot \text{gshRBC}(t)^2}{\text{Vrbcu}^3} \quad (\text{A.4.238})$$

$$+ \frac{\text{K10RBCvGSSGR} \cdot \text{K2RBCvGSSGR} \cdot \text{K4RBCvGSSGR} \cdot \text{K6RBCvGSSGR} \cdot \text{K8RBCvGSSGR} \cdot \text{gshRBC}(t)^2}{\text{Vrbcu}^2} \quad (\text{A.4.239})$$

$$+ \frac{\text{K10RBCvGSSGR} \cdot \text{K1RBCvGSSGR} \cdot \text{K3RBCvGSSGR} \cdot \text{K5RBCvGSSGR} \cdot \text{K7RBCvGSSGR} \cdot \text{gssgRBC}(t) \cdot \text{nadpRBC}(t) \cdot \text{gshRBC}(t)}{\text{Vrbcu}^3} \quad (\text{A.4.240})$$

$$+ \frac{\text{K11RBCvGSSGR} \cdot \text{K1RBCvGSSGR} \cdot \text{K3RBCvGSSGR} \cdot (\text{K5RBCvGSSGR} + \text{K6RBCvGSSGR}) \cdot \text{K8RBCvGSSGR} \cdot \text{gssgRBC}(t) \cdot \text{nadpRBC}(t) \cdot \text{gshRBC}(t)}{\text{Vrbcu}^3} \quad (\text{A.4.241})$$

$$+ \frac{K11RBCvGSSGR \cdot K1RBCvGSSGR \cdot K4RBCvGSSGR \cdot K6RBCvGSSGR \cdot K8RBCvGSSGR \cdot \text{nadpRBC}(t) \cdot \text{gshRBC}(t)}{Vrbcu^2} \quad (\text{A.4.242})$$

$$+ \frac{K10RBCvGSSGR \cdot K12RBCvGSSGR \cdot K3RBCvGSSGR \cdot K5RBCvGSSGR \cdot K7RBCvGSSGR \cdot \text{gssgRBC}(t) \cdot \text{nadpRBC}(t) \cdot \text{gshRBC}(t)}{Vrbcu^3} \quad (\text{A.4.243})$$

$$+ \frac{K10RBCvGSSGR \cdot K12RBCvGSSGR \cdot K2RBCvGSSGR \cdot (K4RBCvGSSGR \cdot K6RBCvGSSGR + K4RBCvGSSGR \cdot K7RBCvGSSGR + K5RBCvGSSGR \cdot K7RBCvGSSGR) \cdot \text{nadpRBC}(t) \cdot \text{gshRBC}(t)}{Vrbcu^2} \quad (\text{A.4.244})$$

$$+ \frac{K12RBCvGSSGR \cdot K2RBCvGSSGR \cdot K4RBCvGSSGR \cdot K6RBCvGSSGR \cdot K8RBCvGSSGR \cdot \text{nadpRBC}(t) \cdot \text{gshRBC}(t)}{Vrbcu^2} \quad (\text{A.4.245})$$

$$+ \frac{K11RBCvGSSGR \cdot K2RBCvGSSGR \cdot K4RBCvGSSGR \cdot K6RBCvGSSGR \cdot K8RBCvGSSGR \cdot \text{gshRBC}(t)}{Vrbcu} \quad (\text{A.4.246})$$

$$+ K11RBCvGSSGR \cdot K2RBCvGSSGR \cdot K9RBCvGSSGR \quad (\text{A.4.247})$$

$$\cdot (K4RBCvGSSGR \cdot K6RBCvGSSGR + K4RBCvGSSGR \cdot K7RBCvGSSGR + K5RBCvGSSGR \cdot K7RBCvGSSGR) \quad (\text{A.4.248})$$

$$+ \frac{K11RBCvGSSGR \cdot K3RBCvGSSGR \cdot K5RBCvGSSGR \cdot K7RBCvGSSGR \cdot K9RBCvGSSGR \cdot \text{gssgRBC}(t)}{Vrbcu} \quad (\text{A.4.249})$$

$$+ \frac{K1RBCvGSSGR \cdot K3RBCvGSSGR \cdot (K11RBCvGSSGR \cdot K5RBCvGSSGR \cdot K7RBCvGSSGR + K11RBCvGSSGR \cdot K9RBCvGSSGR \cdot K7RBCvGSSGR + K5RBCvGSSGR \cdot K9RBCvGSSGR \cdot K7RBCvGSSGR + K11RBCvGSSGR \cdot K6RBCvGSSGR \cdot K9RBCvGSSGR) \cdot \text{gssgRBC}(t) \cdot \text{nadpRBC}(t)}{Vrbcu^2} \quad (\text{A.4.250})$$

$$+ \frac{K11RBCvGSSGR \cdot K1RBCvGSSGR \cdot (K4RBCvGSSGR \cdot K6RBCvGSSGR + K4RBCvGSSGR \cdot K7RBCvGSSGR + K5RBCvGSSGR \cdot K7RBCvGSSGR) \cdot K9RBCvGSSGR \cdot \text{nadpRBC}(t)}{Vrbcu} \quad (\text{A.4.251})$$

$$+ \frac{K12RBCvGSSGR \cdot K3RBCvGSSGR \cdot K5RBCvGSSGR \cdot K7RBCvGSSGR \cdot K9RBCvGSSGR \cdot \text{gssgRBC}(t) \cdot \text{nadpRBC}(t)}{Vrbcu^2} \quad (\text{A.4.252})$$

$$+ \frac{K12RBCvGSSGR \cdot K2RBCvGSSGR \cdot (K4RBCvGSSGR \cdot K6RBCvGSSGR + K4RBCvGSSGR \cdot K7RBCvGSSGR + K5RBCvGSSGR \cdot K7RBCvGSSGR) \cdot K9RBCvGSSGR \cdot \text{nadpRBC}(t)}{Vrbcu} \quad (\text{A.4.253})$$

$$vRBCvHBADP = T_{sRBC} \cdot Vrbcu \cdot \left(\frac{K_{aappRBCvHBADP} \cdot \text{adpRBC}(t) \cdot \text{hbRBC}(t)}{Vrbcu^2} - \frac{K_{dRBCvHBADP} \cdot \text{hbadpRBC}(t)}{Vrbcu} \right) \quad (\text{A.4.254})$$

$$vRBCvHBATP = T_{sRBC} \cdot Vrbcu \cdot \left(\frac{K_{aappRBCvHBATP} \cdot \text{atpRBC}(t) \cdot \text{hbRBC}(t)}{Vrbcu^2} - \frac{K_{dRBCvHBATP} \cdot \text{hbatpRBC}(t)}{Vrbcu} \right) \quad (\text{A.4.255})$$

$$vRBCvHBB13PG = TsRBC \cdot Vrbcu \cdot \left(\frac{KaappRBCvHBB13PG \cdot b13pgRBC(t) \cdot hbRBC(t)}{Vrbcu^2} - \frac{KdRBCvHBB13PG \cdot hbb13pgRBC(t)}{Vrbcu} \right) \quad (A.4.256)$$

$$vRBCvHBB23PG = TsRBC \cdot Vrbcu \cdot \left(\frac{KaappRBCvHBBPG \cdot b23pgRBC(t) \cdot hbRBC(t)}{Vrbcu^2} - \frac{KdRBCvHBBPG \cdot hbb23pgRBC(t)}{Vrbcu} \right) \quad (A.4.257)$$

$$vRBCvHBMGATP = TsRBC \cdot Vrbcu \cdot \left(\frac{KaappRBCvHBMGATP \cdot hbRBC(t) \cdot mgatpRBC(t)}{Vrbcu^2} - \frac{KdRBCvHBMGATP \cdot hbm gatpRBC(t)}{Vrbcu} \right) \quad (A.4.258)$$

$$vRBCvHK = \left[\mathit{TsRBC} \cdot Vrbcu \cdot \left(\frac{ERBCvHK \cdot KcatfappRBCvHK \cdot glcRBC(t) \cdot mgatpRBC(t)}{KiglcRBCvHK \cdot KmmgatpRBCvHK \cdot Vrbcu^2} \right. \right. \quad (A.4.259)$$

$$\left. - \frac{ERBCvHK \cdot KcatrappRBCvHK \cdot g6pRBC(t) \cdot mgadpRBC(t)}{Kig6pRBCvHK \cdot KmmgadpRBCvHK \cdot Vrbcu^2} \right) / \quad (A.4.260)$$

$$\left[\frac{glcRBC(t) \cdot g6pRBC(t)}{Kdig6pRBCvHK \cdot KiglcRBCvHK \cdot Vrbcu^2} + \frac{mgadpRBC(t) \cdot g6pRBC(t)}{Kig6pRBCvHK \cdot KmmgadpRBCvHK \cdot Vrbcu^2} + \frac{g6pRBC(t)}{Kig6pRBCvHK \cdot Vrbcu} \right. \quad (A.4.261)$$

$$\left. + \frac{b23pgRBC(t) \cdot glcRBC(t)}{KdibpgRBCvHK \cdot KiglcRBCvHK \cdot Vrbcu^2} + \frac{g16p2RBC(t) \cdot glcRBC(t)}{Kdig16p2RBCvHK \cdot KiglcRBCvHK \cdot Vrbcu^2} + \frac{glcRBC(t)}{KiglcRBCvHK \cdot Vrbcu} \right. \quad (A.4.262)$$

$$\left. + \frac{glcRBC(t) \cdot gshRBC(t)}{KdigshRBCvHK \cdot KiglcRBCvHK \cdot Vrbcu^2} + \frac{mgadpRBC(t)}{KimgadpRBCvHK \cdot Vrbcu} + \frac{glcRBC(t) \cdot mgatpRBC(t)}{KiglcRBCvHK \cdot KmmgatpRBCvHK \cdot Vrbcu^2} \right. \quad (A.4.263)$$

$$\left. + \frac{mgatpRBC(t)}{KimgatpRBCvHK \cdot Vrbcu} + 1 \right] \quad (A.4.264)$$

$$vRBCvLACTRANSPORT = 20 \cdot TsRBC \cdot Vrbcu \cdot \left(\frac{KoRBCvLACTRANSPORT \cdot lacRBC(t)}{Vrbcu} - \frac{KiRBCvLACTRANSPORT \cdot B_lac(t)}{1000} \right) \quad (A.4.265)$$

$$vRBCvLDH = \left[TsRBC \cdot Vrbcu \cdot VRBCvLDH \cdot \left(\frac{KcatfRBCvLDH \cdot nadhRBC(t) \cdot pyrRBC(t)}{KinadhRBCvLDH \cdot KmapppyrRBCvLDH \cdot Vrbcu^2} \right. \right. \quad (A.4.266)$$

$$\left. - \frac{KcatrRBCvLDH \cdot lacRBC(t) \cdot nadRBC(t)}{KinadRBCvLDH \cdot KmapplacRBCvLDH \cdot Vrbcu^2} \right) / \quad (A.4.267)$$

$$\left[\frac{KmnadRBCvLDH \cdot lacRBC(t) \cdot nadhRBC(t)}{KinadhRBCvLDH \cdot KinadRBCvLDH \cdot KmapplacRBCvLDH \cdot Vrbcu^2} + \frac{lacRBC(t) \cdot pyrRBC(t) \cdot nadhRBC(t)}{KiapplacRBCvLDH \cdot KinadhRBCvLDH \cdot KmapppyrRBCvLDH \cdot Vrbcu^3} \right. \quad (A.4.268)$$

$$\left. + \frac{pyrRBC(t) \cdot nadhRBC(t)}{KinadhRBCvLDH \cdot KmapppyrRBCvLDH \cdot Vrbcu^2} + \frac{nadhRBC(t)}{KinadhRBCvLDH \cdot Vrbcu} + \frac{lacRBC(t) \cdot nadRBC(t)}{KinadRBCvLDH \cdot KmapplacRBCvLDH \cdot Vrbcu^2} \right. \quad (A.4.269)$$

$$\left. \right) \quad (A.4.270)$$

$$+ \frac{\text{nadRBC}(t)}{\text{KinadRBCvLDH} \cdot \text{Vrbcu}} + \frac{\text{lacRBC}(t) \cdot \text{nadRBC}(t) \cdot \text{pyrRBC}(t)}{\text{KiapppyrRBCvLDH} \cdot \text{KinadRBCvLDH} \cdot \text{KmapplacRBCvLDH} \cdot \text{Vrbcu}^3} \quad (\text{A.4.271})$$

$$+ \frac{\text{KmnadhRBCvLDH} \cdot \text{nadRBC}(t) \cdot \text{pyrRBC}(t)}{\text{KinadhRBCvLDH} \cdot \text{KinadRBCvLDH} \cdot \text{KmapppyrRBCvLDH} \cdot \text{Vrbcu}^2} \quad (\text{A.4.272})$$

$$+ \left(\frac{\text{pyrRBC}(t)}{\text{KidpyrRBCvLDH} \cdot \text{Vrbcu}} + 1 \right) \cdot \left(\frac{\text{KmnadRBCvLDH} \cdot \text{lacRBC}(t)}{\text{KinadRBCvLDH} \cdot \text{KmapplacRBCvLDH} \cdot \text{Vrbcu}} + \frac{\text{KmnadhRBCvLDH} \cdot \text{pyrRBC}(t)}{\text{KinadhRBCvLDH} \cdot \text{KmapppyrRBCvLDH} \cdot \text{Vrbcu}} + 1 \right) \quad (\text{A.4.273})$$

$$\text{vRBCvLDHP} = \frac{\text{TsRBC} \cdot \text{Vrbcu} \cdot \left(\frac{\text{KfRBCvLDHP} \cdot \text{nadphRBC}(t) \cdot \text{pyrRBC}(t)}{\text{KmpyrRBCvLDHP} \cdot \text{Vrbcu}^2} - \frac{\text{KrRBCvLDHP} \cdot \text{lacRBC}(t) \cdot \text{nadpRBC}(t)}{\text{KmlacRBCvLDHP} \cdot \text{Vrbcu}^2} \right)}{\frac{\text{lacRBC}(t)}{\text{KmlacRBCvLDHP} \cdot \text{Vrbcu}} + \frac{\text{pyrRBC}(t)}{\text{KmpyrRBCvLDHP} \cdot \text{Vrbcu}} + 1} \quad (\text{A.4.274})$$

$$\text{vRBCvMGADP} = \text{TsRBC} \cdot \text{Vrbcu} \cdot \left(\frac{\text{KaappRBCvMGADP} \cdot \text{adpRBC}(t) \cdot \text{mgRBC}(t)}{\text{Vrbcu}^2} - \frac{\text{KdRBCvMGADP} \cdot \text{mgadpRBC}(t)}{\text{Vrbcu}} \right) \quad (\text{A.4.275})$$

$$\text{vRBCvMGATP} = \text{TsRBC} \cdot \text{Vrbcu} \cdot \left(\frac{\text{KaappRBCvMGATP} \cdot \text{atpRBC}(t) \cdot \text{mgRBC}(t)}{\text{Vrbcu}^2} - \frac{\text{KdRBCvMGATP} \cdot \text{mgatpRBC}(t)}{\text{Vrbcu}} \right) \quad (\text{A.4.276})$$

$$\text{vRBCvMGB13PG} = \text{TsRBC} \cdot \text{Vrbcu} \cdot \left(\frac{\text{KaappRBCvMGB13PG} \cdot \text{b13pgRBC}(t) \cdot \text{mgRBC}(t)}{\text{Vrbcu}^2} - \frac{\text{KdRBCvMGB13PG} \cdot \text{mgb13pgRBC}(t)}{\text{Vrbcu}} \right) \quad (\text{A.4.277})$$

$$\text{vRBCvMGB23PG} = \text{TsRBC} \cdot \text{Vrbcu} \cdot \left(\frac{\text{KaappRBCvMGB23PG} \cdot \text{b23pgRBC}(t) \cdot \text{mgRBC}(t)}{\text{Vrbcu}^2} - \frac{\text{KdRBCvMGB23PG} \cdot \text{mgb23pgRBC}(t)}{\text{Vrbcu}} \right) \quad (\text{A.4.278})$$

$$\text{vRBCvMGF16P2} = \text{TsRBC} \cdot \text{Vrbcu} \cdot \left(\frac{\text{KaappRBCvMGF16P2} \cdot \text{f16p2RBC}(t) \cdot \text{mgRBC}(t)}{\text{Vrbcu}^2} - \frac{\text{KdRBCvMGF16P2} \cdot \text{mgf16p2RBC}(t)}{\text{Vrbcu}} \right) \quad (\text{A.4.279})$$

$$\text{vRBCvMGG16P2} = \text{TsRBC} \cdot \text{Vrbcu} \cdot \left(\frac{\text{KaappRBCvMGG16P2} \cdot \text{g16p2RBC}(t) \cdot \text{mgRBC}(t)}{\text{Vrbcu}^2} - \frac{\text{KdRBCvMGG16P2} \cdot \text{mgg16p2RBC}(t)}{\text{Vrbcu}} \right) \quad (\text{A.4.280})$$

$$\text{vRBCvMGPHOS} = \text{TsRBC} \cdot \text{Vrbcu} \cdot \left(\frac{\text{KaappRBCvMGPHOS} \cdot \text{mgRBC}(t) \cdot \text{phosRBC}(t)}{\text{Vrbcu}^2} - \frac{\text{KdRBCvMGPHOS} \cdot \text{mgphosRBC}(t)}{\text{Vrbcu}} \right) \quad (\text{A.4.281})$$

$$\text{vRBCvOX} = \text{KRBCvOX} \cdot \text{TsRBC} \cdot \text{gshRBC}(t) \quad (\text{A.4.282})$$

$$\text{vRBCvOXNADH} = \text{KRBCvOXNADH} \cdot \text{TsRBC} \cdot \text{nadhRBC}(t) \quad (\text{A.4.283})$$

$$(\text{A.4.284})$$

$$vRBCvP6GDH = [TsRBC \cdot Vrbcu \cdot VRBCvP6GDH \quad (A.4.285)$$

$$\cdot \left(\frac{K11RBCvP6GDH \cdot K1RBCvP6GDH \cdot K3RBCvP6GDH \cdot K5RBCvP6GDH \cdot K7RBCvP6GDH \cdot K9RBCvP6GDH}{Vrbcu^2} \cdot \frac{nadpRBC(t) \cdot p6gRBC(t)}{1} \right) \quad (A.4.286)$$

$$- \frac{co2RBC \cdot K10RBCvP6GDH \cdot K12RBCvP6GDH \cdot K2RBCvP6GDH \cdot K4RBCvP6GDH \cdot K6RBCvP6GDH \cdot K8RBCvP6GDH}{Vrbcu^3} \cdot \frac{nadphRBC(t) \cdot ru5pRBC(t)}{1} \Bigg] / \quad (A.4.287)$$

$$\left[\frac{co2RBC \cdot K12RBCvP6GDH \cdot K2RBCvP6GDH \cdot K4RBCvP6GDH \cdot K6RBCvP6GDH \cdot nadphRBC(t) \cdot K8RBCvP6GDH}{Vrbcu^2} \quad (A.4.288)$$

$$+ \frac{co2RBC \cdot K11RBCvP6GDH \cdot K1RBCvP6GDH \cdot K4RBCvP6GDH \cdot K6RBCvP6GDH \cdot nadpRBC(t) \cdot K8RBCvP6GDH}{Vrbcu^2} \quad (A.4.289)$$

$$+ \frac{co2RBC \cdot K11RBCvP6GDH \cdot K1RBCvP6GDH \cdot K3RBCvP6GDH \cdot (K5RBCvP6GDH + K6RBCvP6GDH) \cdot nadpRBC(t)}{Vrbcu^3} \cdot \frac{p6gRBC(t) \cdot K8RBCvP6GDH}{1} \quad (A.4.290)$$

$$+ \frac{co2RBC \cdot K10RBCvP6GDH \cdot K12RBCvP6GDH \cdot (K2RBCvP6GDH \cdot K4RBCvP6GDH + K6RBCvP6GDH \cdot K4RBCvP6GDH}{Vrbcu^3} + \frac{K2RBCvP6GDH \cdot K5RBCvP6GDH + K2RBCvP6GDH \cdot K6RBCvP6GDH) \cdot nadphRBC(t) \cdot ru5pRBC(t) \cdot K8RBCvP6GDH}{1} \quad (A.4.291)$$

$$+ \frac{co2RBC \cdot K10RBCvP6GDH \cdot K1RBCvP6GDH \cdot K4RBCvP6GDH \cdot K6RBCvP6GDH \cdot nadpRBC(t) \cdot ru5pRBC(t) \cdot K8RBCvP6GDH}{Vrbcu^3} \quad (A.4.292)$$

$$+ \frac{co2RBC \cdot K10RBCvP6GDH \cdot K12RBCvP6GDH \cdot K3RBCvP6GDH \cdot (K5RBCvP6GDH}{Vrbcu^4} + \frac{K6RBCvP6GDH) \cdot nadphRBC(t) \cdot p6gRBC(t) \cdot ru5pRBC(t) \cdot K8RBCvP6GDH}{1} \quad (A.4.293)$$

$$+ \frac{co2RBC \cdot K10RBCvP6GDH \cdot K1RBCvP6GDH \cdot K3RBCvP6GDH \cdot (K5RBCvP6GDH}{Vrbcu^4} + \frac{K6RBCvP6GDH) \cdot nadpRBC(t) \cdot p6gRBC(t) \cdot ru5pRBC(t) \cdot K8RBCvP6GDH}{1} \quad (A.4.294)$$

$$+ \frac{co2RBC \cdot K10RBCvP6GDH \cdot K2RBCvP6GDH \cdot K4RBCvP6GDH \cdot K6RBCvP6GDH \cdot ru5pRBC(t) \cdot K8RBCvP6GDH}{Vrbcu^2} \quad (A.4.295)$$

$$+ \frac{co2RBC \cdot K11RBCvP6GDH \cdot K2RBCvP6GDH \cdot K4RBCvP6GDH \cdot K6RBCvP6GDH \cdot K8RBCvP6GDH}{Vrbcu} \quad (A.4.296)$$

$$+ K11RBCvP6GDH \cdot K2RBCvP6GDH \cdot (K4RBCvP6GDH \cdot K6RBCvP6GDH + K4RBCvP6GDH \cdot K7RBCvP6GDH \quad (A.4.297)$$

$$+ K5RBCvP6GDH \cdot K7RBCvP6GDH) \cdot K9RBCvP6GDH \quad (A.4.298)$$

$$+ \frac{K12RBCvP6GDH \cdot K2RBCvP6GDH \cdot (K4RBCvP6GDH \cdot K6RBCvP6GDH + K4RBCvP6GDH \cdot K7RBCvP6GDH}{Vrbcu} + \frac{K5RBCvP6GDH \cdot K7RBCvP6GDH) \cdot K9RBCvP6GDH \cdot nadphRBC(t)}{1} \quad (A.4.299)$$

$$(A.4.300)$$

$$+ \frac{K_{11}RBCvP6GDH \cdot K_1RBCvP6GDH \cdot (K_4RBCvP6GDH \cdot K_6RBCvP6GDH + K_4RBCvP6GDH \cdot K_7RBCvP6GDH + K_5RBCvP6GDH \cdot K_7RBCvP6GDH) \cdot K_9RBCvP6GDH \cdot nadpRBC(t)}{Vrbcu} \quad (A.4.301)$$

$$+ \frac{K_{12}RBCvP6GDH \cdot K_3RBCvP6GDH \cdot K_5RBCvP6GDH \cdot K_7RBCvP6GDH \cdot K_9RBCvP6GDH \cdot nadpRBC(t) \cdot p6gRBC(t)}{Vrbcu^2} \quad (A.4.302)$$

$$+ \frac{K_1RBCvP6GDH \cdot K_3RBCvP6GDH \cdot (K_{11}RBCvP6GDH \cdot K_5RBCvP6GDH \cdot K_7RBCvP6GDH + K_{11}RBCvP6GDH \cdot K_9RBCvP6GDH \cdot K_7RBCvP6GDH + K_5RBCvP6GDH \cdot K_9RBCvP6GDH \cdot K_7RBCvP6GDH + K_{11}RBCvP6GDH \cdot K_5RBCvP6GDH \cdot K_9RBCvP6GDH + K_{11}RBCvP6GDH \cdot K_6RBCvP6GDH \cdot K_9RBCvP6GDH) \cdot nadpRBC(t) \cdot p6gRBC(t)}{Vrbcu^2} \quad (A.4.303)$$

$$+ \frac{K_{11}RBCvP6GDH \cdot K_3RBCvP6GDH \cdot K_5RBCvP6GDH \cdot K_7RBCvP6GDH \cdot K_9RBCvP6GDH \cdot p6gRBC(t)}{Vrbcu} \quad (A.4.304)$$

$$+ \frac{K_{10}RBCvP6GDH \cdot K_{12}RBCvP6GDH \cdot K_2RBCvP6GDH \cdot (K_4RBCvP6GDH \cdot K_6RBCvP6GDH + K_4RBCvP6GDH \cdot K_7RBCvP6GDH + K_5RBCvP6GDH \cdot K_7RBCvP6GDH) \cdot nadpRBC(t) \cdot ru5pRBC(t)}{Vrbcu^2} \quad (A.4.305)$$

$$+ \frac{K_{10}RBCvP6GDH \cdot K_{12}RBCvP6GDH \cdot K_3RBCvP6GDH \cdot K_5RBCvP6GDH \cdot K_7RBCvP6GDH \cdot nadpRBC(t) \cdot p6gRBC(t) \cdot ru5pRBC(t)}{Vrbcu^3} \quad (A.4.306)$$

$$+ \left. \frac{K_{10}RBCvP6GDH \cdot K_1RBCvP6GDH \cdot K_3RBCvP6GDH \cdot K_5RBCvP6GDH \cdot K_7RBCvP6GDH \cdot nadpRBC(t) \cdot p6gRBC(t) \cdot ru5pRBC(t)}{Vrbcu^3} \right] \quad (A.4.307)$$

$$vRBCvPFK = \left[TsRBC \cdot Vrbcu \cdot VRBCvPFK \cdot \left(\frac{K_{cat}fRBCvPFK \cdot f6pRBC(t) \cdot mgatpRBC(t)}{K_{mf}f6pRBCvPFK \cdot K_{mm}gatpRBCvPFK \cdot Vrbcu^2} \right) \right] \quad (A.4.308)$$

$$- \left. \frac{K_{cat}fRBCvPFK \cdot f16p2RBC(t) \cdot mgadpRBC(t)}{K_{mf}f16p2RBCvPFK \cdot K_{mm}gadpRBCvPFK \cdot Vrbcu^2} \right] / \quad (A.4.309)$$

$$\left[\left(\frac{mgadpRBC(t) \cdot f16p2RBC(t)}{K_{mf}f16p2RBCvPFK \cdot K_{mm}gadpRBCvPFK \cdot Vrbcu^2} + \frac{f16p2RBC(t)}{K_{mf}f16p2RBCvPFK \cdot Vrbcu} + \frac{f6pRBC(t)}{K_{mf}f6pRBCvPFK \cdot Vrbcu} \right) \right] \quad (A.4.310)$$

$$+ \frac{mgadpRBC(t)}{K_{mm}gadpRBCvPFK \cdot Vrbcu} + \frac{f6pRBC(t) \cdot mgatpRBC(t)}{K_{mf}f6pRBCvPFK \cdot K_{mm}gatpRBCvPFK \cdot Vrbcu^2} + \frac{mgatpRBC(t)}{K_{mm}gatpRBCvPFK \cdot Vrbcu} + 1 \quad (A.4.311)$$

$$\cdot \left(\frac{\left(\frac{atpRBC(t)}{K_{tatp}RBCvPFK \cdot Vrbcu} + 1 \right)^4 \cdot \left(\frac{b23pgRBC(t)}{K_{tb23pg}RBCvPFK \cdot Vrbcu} + 1 \right)^4 \cdot \left(\frac{mgRBC(t)}{K_{tmg}RBCvPFK \cdot Vrbcu} + 1 \right)^4 \cdot \left(\frac{hRBC}{K_aRBCvPFK} \right)^{nRBCvPFK}}{\left(\frac{ampRBC(t)}{K_{ramp}RBCvPFK \cdot Vrbcu} + 1 \right)^4 \cdot \left(\frac{f16p2RBC(t)}{K_{mf}f16p2RBCvPFK \cdot Vrbcu} + \frac{f6pRBC(t)}{K_{mf}f6pRBCvPFK \cdot Vrbcu} + 1 \right)^4 \cdot \left(\frac{g16p2RBC(t)}{K_{rg16p2}RBCvPFK \cdot Vrbcu} + 1 \right)^4 \cdot \left(\frac{phosRBC(t)}{K_{rphos}RBCvPFK \cdot Vrbcu} + 1 \right)^4} + 1 \right) \quad (A.4.312)$$

$$vRBCvPGI = \frac{ERBCvPGI \cdot TsRBC \cdot Vrbcu \cdot \left(\frac{KcatfRBCvPGI \cdot g6pRBC(t)}{Kmg6pRBCvPGI \cdot Vrbcu} - \frac{KcatrRBCvPGI \cdot f6pRBC(t)}{Kmf6pRBCvPGI \cdot Vrbcu} \right)}{\frac{f6pRBC(t)}{Kmf6pRBCvPGI \cdot Vrbcu} + \frac{g6pRBC(t)}{Kmg6pRBCvPGI \cdot Vrbcu} + 1} \quad (A.4.313)$$

$$vRBCvPGK = \left[TsRBC \cdot Vrbcu \cdot VRBCvPGK \cdot \left(\frac{KcatfRBCvPGK \cdot b13pgRBC(t) \cdot mgadpRBC(t)}{KimgadpRBCvPGK \cdot Kmb13pgRBCvPGK \cdot Vrbcu^2} \right. \right. \quad (A.4.314)$$

$$\left. \left. - \frac{KcatrRBCvPGK \cdot mgatpRBC(t) \cdot p3gRBC(t)}{KimgatpRBCvPGK \cdot Kmp3gRBCvPGK \cdot Vrbcu^2} \right) \right] / \quad (A.4.315)$$

$$\left[\frac{mgadpRBC(t) \cdot b13pgRBC(t)}{KimgadpRBCvPGK \cdot Kmb13pgRBCvPGK \cdot Vrbcu^2} + \frac{b13pgRBC(t)}{Kib13pgRBCvPGK \cdot Vrbcu} + \frac{mgadpRBC(t)}{KimgadpRBCvPGK \cdot Vrbcu} \right. \quad (A.4.316)$$

$$\left. + \frac{mgatpRBC(t)}{KimgatpRBCvPGK \cdot Vrbcu} + \frac{mgatpRBC(t) \cdot p3gRBC(t)}{KimgatpRBCvPGK \cdot Kmp3gRBCvPGK \cdot Vrbcu^2} + \frac{p3gRBC(t)}{Kip3gRBCvPGK \cdot Vrbcu} + 1 \right] \quad (A.4.317)$$

$$vRBCvPGLHYDROLYSIS = TsRBC \cdot Vrbcu \cdot \left(\frac{KhydrolRBCvPGLHYDROLYSIS \cdot p6glRBC(t)}{Vrbcu} \right) \quad (A.4.318)$$

$$+ \frac{Klactonase3RBCvPGLHYDROLYSIS \cdot VRBCvPGLHYDROLYSIS \cdot p6glRBC(t)}{Vrbcu \cdot \left(\frac{Klactonase2RBCvPGLHYDROLYSIS + Klactonase3RBCvPGLHYDROLYSIS}{Klactonase1RBCvPGLHYDROLYSIS} + \frac{p6glRBC(t)}{Vrbcu} \right)} \quad (A.4.319)$$

$$vRBCvPGM = \frac{TsRBC \cdot Vrbcu \cdot VRBCvPGM \cdot \left(\frac{KcatfRBCvPGM \cdot p3gRBC(t)}{Kmp3gRBCvPGM \cdot Vrbcu} - \frac{KcatrRBCvPGM \cdot p2gRBC(t)}{Kmp2gRBCvPGM \cdot Vrbcu} \right)}{\frac{p2gRBC(t)}{Kmp2gRBCvPGM \cdot Vrbcu} + \frac{p3gRBC(t)}{Kmp3gRBCvPGM \cdot Vrbcu} + 1} \quad (A.4.320)$$

$$vRBCvPHOSTRANSPORT = TsRBC \cdot Vrbcu \cdot \left(\frac{KoRBCvPHOSTRANSPORT \cdot phosRBC(t)}{Vrbcu} - \frac{KiRBCvPHOSTRANSPORT \cdot phosEXT}{vBld} \right) \quad (A.4.321)$$

$$vRBCvPK = \left[TsRBC \cdot Vrbcu \cdot VRBCvPK \cdot \left(\frac{KcatfRBCvPK \cdot mgadpRBC(t) \cdot pepRBC(t)}{KrmgadpRBCvPK \cdot KrpepRBCvPK \cdot Vrbcu^2} - \frac{KcatrRBCvPK \cdot mgatpRBC(t) \cdot pyrRBC(t)}{KrmgatpRBCvPK \cdot KrpyrRBCvPK \cdot Vrbcu^2} \right) \right] / \quad (A.4.322)$$

$$\left[(LRBCvPK + 1) \cdot \left(\frac{pepRBC(t) \cdot mgadpRBC(t)}{KrmgadpRBCvPK \cdot KrpepRBCvPK \cdot Vrbcu^2} + \frac{mgadpRBC(t)}{KrmgadpRBCvPK \cdot Vrbcu} + \frac{mgatpRBC(t)}{KrmgatpRBCvPK \cdot Vrbcu} \right. \right. \quad (A.4.323)$$

$$\left. \left. + \frac{pepRBC(t)}{KrpepRBCvPK \cdot Vrbcu} + \frac{mgatpRBC(t) \cdot pyrRBC(t)}{KrmgatpRBCvPK \cdot KrpyrRBCvPK \cdot Vrbcu^2} + \frac{pyrRBC(t)}{KrpyrRBCvPK \cdot Vrbcu} + 1 \right) \right] \quad (A.4.324)$$

$$vRBCvPYRTRANSPORT = TsRBC \cdot Vrbcu \cdot \left(\frac{KoRBCvPYRTRANSPORT \cdot pyrRBC(t)}{Vrbcu} - \frac{KiRBCvPYRTRANSPORT \cdot pyrEXT}{vBld} \right) \quad (A.4.325)$$

$$vRBCvR5PI = \frac{TsRBC \cdot Vrbcu \cdot VRBCvR5PI \cdot \left(\frac{K1RBCvR5PI \cdot K3RBCvR5PI \cdot ru5pRBC(t)}{(K2RBCvR5PI + K3RBCvR5PI) \cdot Vrbcu} - \frac{K2RBCvR5PI \cdot K4RBCvR5PI \cdot rib5pRBC(t)}{(K2RBCvR5PI + K3RBCvR5PI) \cdot Vrbcu} \right)}{\frac{K1RBCvR5PI \cdot ru5pRBC(t)}{(K2RBCvR5PI + K3RBCvR5PI) \cdot Vrbcu} + \frac{K4RBCvR5PI \cdot xu5pRBC(t)}{(K2RBCvR5PI + K3RBCvR5PI) \cdot Vrbcu} + 1} \quad (A.4.326)$$

$$vRBCvRu5PE = \frac{TsRBC \cdot Vrbcu \cdot VRBCvRu5PE \cdot \left(\frac{K1RBCvRu5PE \cdot K3RBCvRu5PE \cdot ru5pRBC(t)}{(K2RBCvRu5PE + K3RBCvRu5PE) \cdot Vrbcu} - \frac{K2RBCvRu5PE \cdot K4RBCvRu5PE \cdot xu5pRBC(t)}{(K2RBCvRu5PE + K3RBCvRu5PE) \cdot Vrbcu} \right)}{\frac{K1RBCvRu5PE \cdot ru5pRBC(t)}{(K2RBCvRu5PE + K3RBCvRu5PE) \cdot Vrbcu} + \frac{K4RBCvRu5PE \cdot xu5pRBC(t)}{(K2RBCvRu5PE + K3RBCvRu5PE) \cdot Vrbcu} + 1} \quad (A.4.327)$$

$$vRBCvTA = \left[TsRBC \cdot Vrbcu \cdot VRBCvTA \cdot \left(\frac{K1RBCvTA \cdot K3RBCvTA \cdot K5RBCvTA \cdot K7RBCvTA \cdot gapRBC(t) \cdot sed7pRBC(t)}{Vrbcu^2} \right. \right. \quad (A.4.328)$$

$$\left. \left. - \frac{K2RBCvTA \cdot K4RBCvTA \cdot K6RBCvTA \cdot K8RBCvTA \cdot ery4pRBC(t) \cdot f6pRBC(t)}{Vrbcu^2} \right) \right] / \quad (A.4.329)$$

$$\left[\frac{K4RBCvTA \cdot (K2RBCvTA + K6RBCvTA) \cdot K8RBCvTA \cdot f6pRBC(t) \cdot ery4pRBC(t)}{Vrbcu^2} \right. \quad (A.4.330)$$

$$\left. + \frac{K1RBCvTA \cdot K4RBCvTA \cdot (K6RBCvTA + K7RBCvTA) \cdot sed7pRBC(t) \cdot ery4pRBC(t)}{Vrbcu^2} \right. \quad (A.4.331)$$

$$\left. + \frac{K2RBCvTA \cdot K4RBCvTA \cdot (K6RBCvTA + K7RBCvTA) \cdot ery4pRBC(t)}{Vrbcu} \right. \quad (A.4.332)$$

$$\left. + \frac{(K2RBCvTA + K3RBCvTA) \cdot K6RBCvTA \cdot K8RBCvTA \cdot f6pRBC(t)}{Vrbcu} \right. \quad (A.4.333)$$

$$\left. + \frac{(K2RBCvTA + K3RBCvTA) \cdot K5RBCvTA \cdot K8RBCvTA \cdot f6pRBC(t) \cdot gapRBC(t)}{Vrbcu^2} \right. \quad (A.4.334)$$

$$\left. + \frac{(K2RBCvTA + K3RBCvTA) \cdot K5RBCvTA \cdot K7RBCvTA \cdot gapRBC(t)}{Vrbcu} \right. \quad (A.4.335)$$

$$\left. + \frac{K1RBCvTA \cdot K5RBCvTA \cdot (K3RBCvTA + K7RBCvTA) \cdot gapRBC(t) \cdot sed7pRBC(t)}{Vrbcu^2} \right. \quad (A.4.336)$$

$$\left. + \frac{K1RBCvTA \cdot K3RBCvTA \cdot (K6RBCvTA + K7RBCvTA) \cdot sed7pRBC(t)}{Vrbcu} \right] \quad (A.4.337)$$

$$vRBCvTIM = \frac{TsRBC \cdot Vrbcu \cdot VRBCvTIM \cdot \left(\frac{KcatfRBCvTIM \cdot gapRBC(t)}{KmgapRBCvTIM \cdot Vrbcu} - \frac{KcatrRBCvTIM \cdot dhapRBC(t)}{KmdhapRBCvTIM \cdot Vrbcu} \right)}{\frac{dhapRBC(t)}{KmdhapRBCvTIM \cdot Vrbcu} + \frac{gapRBC(t)}{KmgapRBCvTIM \cdot Vrbcu} + 1} \quad (A.4.338)$$

$$vRBCvTK1 = TsRBC \cdot Vrbcu \cdot \left(\frac{K1RBCvTK1 \cdot tkRBC(t) \cdot xu5pRBC(t)}{Vrbcu^2} - \frac{K2RBCvTK1 \cdot tkxu5pRBC(t)}{Vrbcu} \right) \quad (A.4.339)$$

$$vRBCvTK2 = TsRBC \cdot Vrbcu \cdot \left(\frac{K3RBCvTK2 \cdot tkxu5pRBC(t)}{Vrbcu} - \frac{K4RBCvTK2 \cdot gapRBC(t) \cdot tkgRBC(t)}{Vrbcu^2} \right) \quad (A.4.340)$$

$$vRBCvTK3 = TsRBC \cdot Vrbcu \cdot \left(\frac{K5RBCvTK3 \cdot rib5pRBC(t) \cdot tkgRBC(t)}{Vrbcu^2} - \frac{K6RBCvTK3 \cdot tkgrib5pRBC(t)}{Vrbcu} \right) \quad (A.4.341)$$

$$vRBCvTK4 = TsRBC \cdot Vrbcu \cdot \left(\frac{K7RBCvTK4 \cdot tkgrib5pRBC(t)}{Vrbcu} - \frac{K8RBCvTK4 \cdot sed7pRBC(t) \cdot tkRBC(t)}{Vrbcu^2} \right) \quad (A.4.342)$$

$$vRBCvTK5 = TsRBC \cdot Vrbcu \cdot \left(\frac{K9RBCvTK5 \cdot ery4pRBC(t) \cdot tkgRBC(t)}{Vrbcu^2} - \frac{K10RBCvTK5 \cdot tkgery4pRBC(t)}{Vrbcu} \right) \quad (A.4.343)$$

$$vRBCvTK6 = TsRBC \cdot Vrbcu \cdot \left(\frac{K11RBCvTK6 \cdot tkgery4pRBC(t)}{Vrbcu} - \frac{K12RBCvTK6 \cdot f6pRBC(t) \cdot tkRBC(t)}{Vrbcu^2} \right) \quad (A.4.344)$$

$$vWBivGLCTRANSPORT = \frac{1}{\omega} \left[parMulti \cdot TsRBC \cdot Vrbcu \cdot \left(\frac{glc_alpha \cdot VRBCvGLCTRANSPORT \cdot B_gluc(t)}{1000 \cdot \left(\frac{(1-glc_alpha) \cdot B_gluc(t) \cdot k_alpha}{1000 \cdot k_beta} + k_alpha + \frac{glc_alpha \cdot B_gluc(t)}{1000} \right)} \right) \right] \quad (A.4.345)$$

$$+ \frac{(1-glc_alpha) \cdot VRBCvGLCTRANSPORT \cdot B_gluc(t)}{1000 \cdot \left(\frac{glc_alpha \cdot B_gluc(t) \cdot k_beta}{1000 \cdot k_alpha} + k_beta + \frac{(1-glc_alpha) \cdot B_gluc(t)}{1000} \right)} \quad (A.4.346)$$

$$- \frac{glc_alpha \cdot VRBCvGLCTRANSPORT \cdot glcRBCi(t)}{Vrbcu \cdot \left(\frac{(1-glc_alpha) \cdot glcRBCi(t) \cdot k_alpha}{k_beta \cdot Vrbcu} + k_alpha + \frac{glc_alpha \cdot glcRBCi(t)}{Vrbcu} \right)} \quad (A.4.347)$$

$$- \frac{(1-glc_alpha) \cdot VRBCvGLCTRANSPORT \cdot glcRBCi(t)}{Vrbcu \cdot \left(\frac{glc_alpha \cdot glcRBCi(t) \cdot k_beta}{k_alpha \cdot Vrbcu} + k_beta + \frac{(1-glc_alpha) \cdot glcRBCi(t)}{Vrbcu} \right)} \quad (A.4.348)$$

$$vWBivLACTRANSPORT = \frac{1}{\omega} \left[20 \cdot parMulti \cdot TsRBC \cdot Vrbcu \cdot \left(\frac{KoRBCvLACTRANSPORT \cdot lacRBCi(t)}{Vrbcu} - \frac{KiRBCvLACTRANSPORT \cdot B_lac(t)}{1000} \right) \right] \quad (A.4.349)$$

$$(A.4.350)$$

$$v_{WBvGLCTransport} = \frac{1}{\omega} \left[Ts_{RBC} \cdot V_{rbcu} \cdot \left(\frac{glc_alpha \cdot VRBCvGLCTransport \cdot B_gluc(t)}{1000 \cdot \left(\frac{(1-gl_alpha) \cdot B_gluc(t) \cdot k_alpha}{1000 \cdot k_beta} + k_alpha + \frac{glc_alpha \cdot B_gluc(t)}{1000} \right)} \right) \right. \quad (A.4.351)$$

$$+ \frac{(1 - glc_alpha) \cdot VRBCvGLCTransport \cdot B_gluc(t)}{1000 \cdot \left(\frac{glc_alpha \cdot B_gluc(t) \cdot k_beta}{1000 \cdot k_alpha} + k_beta + \frac{(1-gl_alpha) \cdot B_gluc(t)}{1000} \right)} \quad (A.4.352)$$

$$- \frac{glc_alpha \cdot VRBCvGLCTransport \cdot glcRBC(t)}{V_{rbcu} \cdot \left(\frac{(1-gl_alpha) \cdot glcRBC(t) \cdot k_alpha}{k_beta \cdot V_{rbcu}} + k_alpha + \frac{glc_alpha \cdot glcRBC(t)}{V_{rbcu}} \right)} \quad (A.4.353)$$

$$\left. - \frac{(1 - glc_alpha) \cdot VRBCvGLCTransport \cdot glcRBC(t)}{V_{rbcu} \cdot \left(\frac{glc_alpha \cdot glcRBC(t) \cdot k_beta}{k_alpha \cdot V_{rbcu}} + k_beta + \frac{(1-gl_alpha) \cdot glcRBC(t)}{V_{rbcu}} \right)} \right] \quad (A.4.354)$$

$$v_{WBvLACTransport} = \frac{1}{\omega} \left[20 \cdot Ts_{RBC} \cdot V_{rbcu} \cdot \left(\frac{KoRBCvLACTransport \cdot lacRBC(t)}{V_{rbcu}} - \frac{KiRBCvLACTransport \cdot B_lac(t)}{1000} \right) \right] \quad (A.4.355)$$

$$(A.4.356)$$

$$v_{F1} = k_{f1} \cdot \left(\frac{B_ins(t)^{ep14}}{k_Dins^{ep14} + B_ins(t)^{ep14}} + 1 \right) \cdot F_g6p(t) \quad (A.4.357)$$

$$v_{F3} = k_{f3} \cdot \left(\frac{B_ins(t)^{ep15}}{k_Dins^{ep15} + B_ins(t)^{ep15}} + 1 \right) \cdot F_acyl(t) \quad (A.4.358)$$

$$v_{F4} = \frac{k_Dins^{en12} \cdot k_{f4} \cdot F_TG(t)}{k_Dins^{en12} + B_ins(t)^{en12}} \quad (A.4.359)$$

$$v_{F5} = F_ffa^3 \cdot k_{f5} \quad (A.4.360)$$

$$v_{Ggluc} = \frac{k1glucgn \cdot B_gluc(t)^{ng}}{k_mG1gn^{ng} + B_gluc(t)^{ng}} \quad (A.4.361)$$

$$v_{Igluc} = \frac{k1ins \cdot B_gluc(t)^{ni}}{k_mIns^{ni} + B_gluc(t)^{ni}} \quad (A.4.362)$$

$$v_{L10} = k_{L10} \cdot aK(t) \quad (A.4.363)$$

$$v_{L11f} = k_{L11f} \cdot \left(\frac{B_glucgn(t)^{ep5}}{k_Dglucgn^{ep5} + B_glucgn(t)^{ep5}} + 1 \right) \cdot oa_m(t) \quad (A.4.364)$$

$$v_{L11r} = k_{L11r} \cdot malate(t) \quad (A.4.365)$$

$$v_L12 = \frac{k_Dins^{en4} \cdot k_L12 \cdot \left(\frac{B_glucgn(t)^{ep6}}{k_Dglucgn^{ep6} + B_glucgn(t)^{ep6}} + 1 \right) \cdot malate(t)}{k_Dins^{en4} + B_ins(t)^{en4}} \quad (A.4.366)$$

$$v_L13 = \frac{k_Dins^{en5} \cdot k_L13 \cdot \left(\frac{B_glucgn(t)^{ep7}}{k_Dglucgn^{ep7} + B_glucgn(t)^{ep7}} + 1 \right) \cdot oa_c(t)}{k_Dins^{en5} + B_ins(t)^{en5}} \quad (A.4.367)$$

$$v_L14 = \frac{k_Dglucgn^{en7} \cdot k_L14 \cdot \left(\frac{B_ins(t)^{ep10}}{k_Dins^{ep10} + B_ins(t)^{ep10}} + 1 \right) \cdot citrate(t)}{k_Dglucgn^{en7} + B_glucgn(t)^{en7}} \quad (A.4.368)$$

$$v_L15 = \frac{k_i5 \cdot k_L15 \cdot acet_c(t) \cdot \left(\frac{p1 \cdot citrate(t)}{k_p1 + citrate(t)} + 1 \right)}{k_i5 + palmCoA(t)} \quad (A.4.369)$$

$$v_L16 = k_L16 \cdot acet_c(t) \cdot malonyl(t)^7 \quad (A.4.370)$$

$$v_L17 = \frac{k_i1 \cdot k_L17 \cdot palm(t)}{k_i1 + malonyl(t)} \quad (A.4.371)$$

$$v_L18 = \frac{k_i2 \cdot k_L18 \cdot palmCoA(t)}{k_i2 + malonyl(t)} \quad (A.4.372)$$

$$v_L19 = \frac{k_Dins^{en8} \cdot k_L19 \cdot acet_m(t)^2 \cdot \left(\frac{cAMP(t)^{ep11}}{k_dcAMP^{ep11} + cAMP(t)^{ep11}} + 1 \right)}{k_Dins^{en8} + B_ins(t)^{en8}} \quad (A.4.373)$$

$$v_L1f = \frac{k_L1f \cdot \left(\frac{B_ins(t)^{ep1}}{k_Dins^{ep1} + B_ins(t)^{ep1}} + 1 \right) \cdot gluc(t)}{k_mL1f + gluc(t)} \quad (A.4.374)$$

$$v_L1r = \frac{k_L1r \cdot \left(\frac{B_glucgn(t)^{ep9}}{k_Dglucgn^{ep9} + B_glucgn(t)^{ep9}} + 1 \right) \cdot g6p(t)}{k_mL1r + g6p(t)} \quad (A.4.375)$$

$$v_L20 = \frac{k_Dins2^{en3} \cdot k_L20 \cdot alan(t)}{k_Dins2^{en3} + B_ins(t)^{en3}} \quad (A.4.376)$$

$$v_L21f = \frac{k_Dins^{en3} \cdot k_L21f \cdot glutamate(t) \cdot pyr(t)}{(k_Dins^{en3} + B_ins(t)^{en3}) \cdot (k_mL21g + glutamate(t)) \cdot (k_mL21p + pyr(t))} \quad (A.4.377)$$

$$v_L21r = \frac{k_Dins^{en3} \cdot k_L21r \cdot acet_m(t) \cdot aK(t) \cdot alan(t)}{(k_mL21k + aK(t)) \cdot (k_mL21a + alan(t)) \cdot (k_Dins^{en3} + B_ins(t)^{en3})} \quad (A.4.378)$$

$$v_L22 = k_L22 \cdot glutamate(t) \quad (A.4.379)$$

$$v_L2f = \frac{k_L2f \cdot g6p(t) \cdot GSa(t)}{k_mL2f + g6p(t)} \quad (A.4.380)$$

$$v_L2r = \frac{k_L2r \cdot glycgn(t) \cdot GPa(t)}{k_mL2r + glycgn(t)} \quad (A.4.381)$$

$$v_L3f = \frac{k_Dglucgn^{en1} \cdot k_L3f \cdot \left(\frac{B_ins(t)^{ep2}}{k_Dins^{ep2} + B_ins(t)^{ep2}} + 1 \right) \cdot g6p(t)}{(k_Dglucgn^{en1} + B_glucgn(t)^{en1}) \cdot (k_mL3f + g6p(t))} \quad (A.4.382)$$

$$v_L3r = \frac{k_Dins2^{en6} \cdot k_L3r \cdot \left(\frac{B_glucgn(t)^{ep8}}{k_Dglucgn^{ep8} + B_glucgn(t)^{ep8}} + 1 \right) \cdot pep(t)}{(k_Dins2^{en6} + B_ins(t)^{en6}) \cdot (k_mL3r + pep(t))} \quad (A.4.383)$$

$$v_L4 = \frac{k_Dglucgn^{en2} \cdot k_i13 \cdot k_L4 \cdot \left(\frac{B_ins(t)^{ep3}}{k_Dins^{ep3} + B_ins(t)^{ep3}} + 1 \right) \cdot pep(t)}{(k_i13 + alan(t)) \cdot (k_Dglucgn^{en2} + B_glucgn(t)^{en2}) \cdot (k_mL4 + pep(t))} \quad (A.4.384)$$

$$v_L5f = \frac{k_L5f \cdot pyr(t)}{k_mL5f + pyr(t)} \quad (A.4.385)$$

$$v_L5r = \frac{k_L5r \cdot lac(t)}{k_mL5r + lac(t)} \quad (A.4.386)$$

$$v_L6 = \frac{k_L6 \cdot \left(\frac{p2 \cdot acet_m(t)}{k_p2 + acet_m(t)} + 1 \right) \cdot \left(\frac{B_glucgn(t)^{ep4}}{k_Dglucgn^{ep4} + B_glucgn(t)^{ep4}} + 1 \right) \cdot pyr(t)}{k_mL6 + pyr(t)} \quad (A.4.387)$$

$$v_L7 = \frac{k_i8 \cdot k_L7 \cdot pyr(t)}{(k_i8 + acet_m(t)) \cdot (k_mL7 + pyr(t))} \quad (A.4.388)$$

$$v_L8 = \frac{k_i4 \cdot k_L8 \cdot acet_m(t) \cdot oa_m(t)}{k_i4 + palmCoA(t)} \quad (A.4.389)$$

$$v_L9 = k_L9 \cdot citrate(t) \quad (A.4.390)$$

$$v_S1f = k_s1f \cdot M_g6p(t) \quad (A.4.391)$$

$$v_S1r = k_s1r \cdot M_glycgn(t) \quad (A.4.392)$$

$$v_S2 = k_s2 \cdot M_g6p(t) \quad (A.4.393)$$

$$v_S3f = k_s3f \cdot M_pyr(t) \quad (\text{A.4.394})$$

$$v_S3r = k_s3r \cdot M_lac(t) \quad (\text{A.4.395})$$

$$v_S4f = k_s4f \cdot M_pyr(t) \quad (\text{A.4.396})$$

$$v_S4r = k_s4r \cdot M_alan \cdot M_ket(t) \quad (\text{A.4.397})$$

$$v_c1cAMP = \frac{kc1 \cdot B_glucgn(t)^{ng}}{kcm1^{ng} + B_glucgn(t)^{ng}} \quad (\text{A.4.398})$$

$$v_c2cAMP = \frac{kc2 \cdot B_ins(t)^{ni} \cdot cAMP(t)}{kcm2^{ni} + B_ins(t)^{ni}} \quad (\text{A.4.399})$$

$$v_d_Balan = kd_Balan \cdot B_alan(t) \quad (\text{A.4.400})$$

$$v_d_Bffa = kd_Bffa \cdot B_ffa(t) \quad (\text{A.4.401})$$

$$v_d_Bgluc = kd_Bgluc \cdot B_gluc(t) \quad (\text{A.4.402})$$

$$v_d_Bglucgn = kd_Bglucgn \cdot B_glucgn(t) \quad (\text{A.4.403})$$

$$v_d_Bins = kd_Bins \cdot B_ins(t) \quad (\text{A.4.404})$$

$$v_d_Bket = kd_Bket \cdot B_ket(t) \quad (\text{A.4.405})$$

$$v_d_Blac = kd_Blac \cdot B_lac(t) \quad (\text{A.4.406})$$

$$v_feed = 2 \cdot \times \cdot 10^{-1} \quad (\text{A.4.407})$$

$$v_glucgn = k_glucgn \quad (\text{A.4.408})$$

$$v_ins = k_ins \quad (\text{A.4.409})$$

$$v_s_dket = ks_dket \cdot M_ket(t) \quad (\text{A.4.410})$$

$$v_tF1 = k_tF1 \cdot B_gluc(t) \cdot \left(\frac{B_ins(t)^{ep12}}{k_Dins^{ep12} + B_ins(t)^{ep12}} + 1 \right) \quad (\text{A.4.411})$$

$$v_tF3 = \frac{F_ffa^8 \cdot k_Dins2^{en9} \cdot k_tF3}{k_Dins2^{en9} + B_ins(t)^{en9}} \quad (\text{A.4.412})$$

$$v_tL1 = k_tL1 \cdot (B_gluc(t) - gluc(t)) \quad (\text{A.4.413})$$

$$v_tL2 = \frac{VmtL2 \cdot (B_lac(t) - lac(t))}{KmtL2 \cdot \left(\frac{B_lac(t)}{KmtL2} + \frac{lac(t)}{KmtL2} + 1 \right)} \quad (\text{A.4.414})$$

$$v_{tL3} = k_{tL3} \cdot \text{ket}(t) \quad (\text{A.4.415})$$

$$v_{tL5} = k_{tL5} \cdot B_{ffa}(t) \quad (\text{A.4.416})$$

$$v_{tL6} = \frac{k_{Dins2}^{en10} \cdot k_{tL6} \cdot B_{alan}(t)}{k_{Dins2}^{en10} + B_{ins}(t)^{en10}} \quad (\text{A.4.417})$$

$$v_{tS1} = k_{tS1} \cdot B_{gluc}(t) \cdot \left(\frac{B_{ins}(t)^{ep13}}{k_{Dins}^{ep13} + B_{ins}(t)^{ep13}} + 1 \right) \quad (\text{A.4.418})$$

$$v_{tS2} = k_{tS2} \cdot B_{ket}(t) \quad (\text{A.4.419})$$

$$v_{tS3} = k_{tS3} \cdot M_{lac}(t) \quad (\text{A.4.420})$$

$$v_{tS4} = \frac{k_{Dins2}^{en11} \cdot k_{tS4} \cdot M_{alan}}{k_{Dins2}^{en11} + B_{ins}(t)^{en11}} \quad (\text{A.4.421})$$

A.5 Assignment rules:

$$\text{LRBCivPK} = \frac{(1.58489 \times 10^{-7}) \cdot \text{pHConversionFactor} \cdot \left(\frac{\text{atpRBCi}(t)}{\text{KtatpRBCvPK} \cdot \text{Vrbc}_i} + 1 \right)^4}{\text{hRBC} \cdot \left(\frac{\text{f16p2RBCi}(t)}{\text{Krf16p2RBCvPK} \cdot \text{Vrbc}_i} + \frac{\text{g16p2RBCi}(t)}{\text{Krg16p2RBCvPK} \cdot \text{Vrbc}_i} + 1 \right)^4 \cdot \left(\frac{\text{pepRBCi}(t)}{\text{KrppepRBCvPK} \cdot \text{Vrbc}_i} + \frac{\text{pyrRBCi}(t)}{\text{KrpypRBCvPK} \cdot \text{Vrbc}_i} + 1 \right)^4} \quad (\text{A.5.1})$$

$$\text{KaappRBCvMGG16P2} = \frac{\text{CRBCvMGG16P2} \cdot \text{KaRBCvMGG16P2} \cdot (\text{hRBC} \cdot \text{KhfRBCvMGG16P2} \cdot \text{KmgfRBCvMGG16P2} + \text{KRBCvMGG16P2})}{\text{Kh2fRBCvMGG16P2} \cdot \text{KhfRBCvMGG16P2} \cdot \text{hRBC}^2 + \text{KhfRBCvMGG16P2} \cdot \text{hRBC} + \text{KhfRBCvMGG16P2} \cdot \text{KkhfRBCvMGG16P2} \cdot \text{kRBC} \cdot \text{hRBC} + \text{KkfRBCvMGG16P2} \cdot \text{kRBC} + 1} \quad (\text{A.5.2})$$

$$\text{KaappRBCvMGATP} = \frac{\text{CRBCvMGATP} \cdot \text{KaRBCvMGATP} \cdot (\text{hRBC} \cdot \text{KhatpRBCvMGATP} \cdot \text{KmgatpRBCvMGATP} + \text{KRBCvMGATP})}{\frac{10^{-\text{pHrBC}} \cdot \text{KhatpRBCvMGATP}}{\text{pHConversionFactor}} + \text{KkatpRBCvMGATP} \cdot \text{kRBC} + 1} \quad (\text{A.5.3})$$

$$\text{LRBCvPK} = \frac{(1.58489 \times 10^{-7}) \cdot \text{pHConversionFactor} \cdot \left(\frac{\text{atpRBC}(t)}{\text{KtatpRBCvPK} \cdot \text{Vrbc}_u} + 1 \right)^4}{\text{hRBC} \cdot \left(\frac{\text{f16p2RBC}(t)}{\text{Krf16p2RBCvPK} \cdot \text{Vrbc}_u} + \frac{\text{g16p2RBC}(t)}{\text{Krg16p2RBCvPK} \cdot \text{Vrbc}_u} + 1 \right)^4 \cdot \left(\frac{\text{pepRBC}(t)}{\text{KrppepRBCvPK} \cdot \text{Vrbc}_u} + \frac{\text{pyrRBC}(t)}{\text{KrpypRBCvPK} \cdot \text{Vrbc}_u} + 1 \right)^4} \quad (\text{A.5.4})$$

$$\text{KeqRBCvPHOSTRANSPORT} = \frac{1 + 10^{\text{pHrBC} - 6.75}}{\frac{1}{\text{RtvRBC}} + \frac{10^{\text{pHrBC} - 6.75}}{\text{RtvRBC}^2}} \quad (\text{A.5.5})$$

$$\text{KiapppyrRBCvLDH} = (2.84747 \times 10^{-1}) \cdot \left(1 + (1.58489 \times 10^{-7}) \cdot 10^{\text{pHrBC}} \right) \cdot \text{KipyrRBCvLDH} \quad (\text{A.5.6})$$

$$\text{KaappRBCvMGB13PG} = \frac{\text{CRBCvMGB13PG} \cdot \text{KaRBCvMGB13PG} \cdot (\text{hRBC} \cdot \text{KhbpgrRBCvMGB13PG} \cdot \text{KmgbpgrRBCvMGB13PG} + \text{KRBCvMGB13PG})}{\text{Kh2bpgrRBCvMGB13PG} \cdot \text{KhbpgrRBCvMGB13PG} \cdot \text{hRBC}^2 + \text{KhbpgrRBCvMGB13PG} \cdot \text{hRBC} + \text{KhbpgrRBCvMGB13PG} \cdot \text{KkhbpgrRBCvMGB13PG} \cdot \text{kRBC} \cdot \text{hRBC} + \text{KkbpgrRBCvMGB13PG} \cdot \text{kRBC} + 1} \quad (\text{A.5.7})$$

$$\text{KcatrappRBCvHK} = \frac{\text{KcatrRBCvHK}}{1 + (1.04713 \times 10^7) \cdot 10^{-\text{pHrBC}} + (2.81838 \times 10^{-10}) \cdot 10^{\text{pHrBC}}} \quad (\text{A.5.8})$$

$$\text{Kiappb13pgRBCvGAPDH} = \frac{\text{Kib13pgRBCvGAPDH}}{1 + 10^{\text{pHrBC} - 10} + (3.16228 \times 10^7) \cdot 10^{-\text{pHrBC}}} \quad (\text{A.5.9})$$

$$\text{KcatfappRBCvHK} = \frac{\text{KcatfRBCvHK}}{1 + (1.04713 \times 10^7) \cdot 10^{-\text{pHrBC}} + (2.81838 \times 10^{-10}) \cdot 10^{\text{pHrBC}}} \quad (\text{A.5.10})$$

$$\text{Vrbc} = 1000 \cdot \text{AlphaCellWaterFraction} \cdot \text{HCT} \cdot \text{v_totblood} \quad (\text{A.5.11})$$

$$\text{K1appRBCvAK} = \text{K1RBCvAK} \cdot \left(\text{KkadpRBCvAK} \cdot \text{kRBC} + 10^{-\text{pHrBC}} \cdot \text{KhadpRBCvAK} \cdot \text{pHConversionFactor} + 1 \right) \quad (\text{A.5.12})$$

$$k_a = \frac{k_a}{k_d} \quad (\text{A.5.13})$$

$$K_{m\text{appyrRBCvLDH}} = (2.84747 \times 10^{-1}) \cdot \left(1 + (1.58489 \times 10^{-7}) \cdot 10^{\text{phRBC}}\right) \cdot K_{m\text{pyrRBCvLDH}} \quad (\text{A.5.14})$$

$$\text{pyrEXT} = \text{ConcPyrEXT} \cdot v_{\text{Bld}} \quad (\text{A.5.15})$$

$$h_{\text{PF}} = 10^{-\text{phPF}} \cdot \text{pHConversionFactor} \quad (\text{A.5.16})$$

$$k_d = \frac{(c_{\text{max}} - c_{\text{min}}) \cdot c_0^{\text{index}}}{c_0^{\text{index}} + \text{glycgn}(t)^{\text{index}}} + c_{\text{min}} \quad (\text{A.5.17})$$

$$K_{a\text{appRBCvMGPHOS}} = \frac{K_{a\text{RBCvMGPHOS}} \cdot (K_{k\text{phosRBCvMGPHOS}} \cdot k_{\text{RBC}} + (6.30957 \times 10^{-8}) \cdot K_{h\text{phosRBCvMGPHOS}} \cdot \text{pHConversionFactor} + 1)}{h_{\text{RBC}} \cdot K_{h\text{phosRBCvMGPHOS}} + K_{k\text{phosRBCvMGPHOS}} \cdot k_{\text{RBC}} + 1} \quad (\text{A.5.18})$$

$$k_{\text{mg6s}} = \frac{k_{\text{mg6}}}{\frac{s_2 \cdot \text{gluc}(t)}{k_{\text{gi}}} + 1} \quad (\text{A.5.19})$$

$$k_{c2} = (3.16228 \times 10^5) \cdot k_{c1} \quad (\text{A.5.20})$$

$$K_{e\text{qRBCvLACTRANSPORT}} = \frac{1 + 10^{\text{phRBC}-3.73}}{1 + \frac{10^{\text{phRBC}-3.73}}{R_{\text{tvRBC}}}} \quad (\text{A.5.21})$$

$$K_{a\text{appRBCvHBMGATP}} = H_{\text{bpHRBC}} \cdot K_{a\text{RBCvHBMGATP}} \quad (\text{A.5.22})$$

$$K_{c\text{atfappRBCvGAPDH}} = \frac{K_{c\text{atfRBCvGAPDH}}}{1 + 10^{\text{phRBC}-10} + (3.16228 \times 10^7) \cdot 10^{-\text{phRBC}}} \quad (\text{A.5.23})$$

$$k_{\text{lins}} = (I_{\text{max}} - I_{\text{min}}) \cdot k_{d_B\text{ins}} \quad (\text{A.5.24})$$

$$K_{i\text{appgapRBCvGAPDH}} = \frac{K_{i\text{gapRBCvGAPDH}}}{1 + 10^{\text{phRBC}-10} + (3.16228 \times 10^7) \cdot 10^{-\text{phRBC}}} \quad (\text{A.5.25})$$

$$K_{6\text{appRBCvBPGSP4}} = \frac{1.75858 \cdot K_{6\text{RBCvBPGSP4}}}{1 + (4.7863 \times 10^{28}) \cdot 10^{-4 \cdot \text{phRBC}}} \quad (\text{A.5.26})$$

$$k_{\text{gc1}} = \frac{k_{\text{gc1}}}{k_{11}} \quad (\text{A.5.27})$$

$$K_{a\text{appRBCvHBADP}} = H_{\text{bpHRBC}} \cdot K_{a\text{RBCvHBADP}} \quad (\text{A.5.28})$$

$$K_{o\text{RBCvLACTRANSPORT}} = \frac{K_{i\text{RBCvLACTRANSPORT}}}{K_{e\text{qRBCvLACTRANSPORT}}} \quad (\text{A.5.29})$$

$$k_{_ins} = I_{\text{min}} \cdot k_{d_B\text{ins}} \quad (\text{A.5.30})$$

$$\text{KmappnadhRBCvGAPDH} = (6.30957 \times 10^{-8}) \cdot 10^{\text{phRBC}} \cdot \text{KmnadhRBCvGAPDH} \quad (\text{A.5.31})$$

$$\text{KiapplacRBCvLDH} = (7.15253 \times 10^{-1}) \cdot \left(1 + (6.30957 \times 10^6) \cdot 10^{-\text{phRBC}}\right) \cdot \text{KilacRBCvLDH} \quad (\text{A.5.32})$$

$$\text{co2RBCi} = \text{ConcCo2RBC} \cdot \text{Vrbci} \quad (\text{A.5.33})$$

$$\text{K13appRBCvBPGSP7} = \frac{1.75858 \cdot \text{K13RBCvBPGSP7}}{1 + (4.7863 \times 10^{28}) \cdot 10^{-4 \cdot \text{phRBC}}} \quad (\text{A.5.34})$$

$$\text{hRBC} = 10^{-\text{phRBC}} \cdot \text{pHConversionFactor} \quad (\text{A.5.35})$$

$$\text{Vrbcu} = \text{Vrbc} - \text{parMulti} \cdot \text{Vrbci} \quad (\text{A.5.36})$$

$$\text{Vrbci} = \begin{cases} \cdot \text{par} \cdot \text{Vrbc} \cdot \cdot \text{par} > 0 \cdot \\ \cdot 1 \cdot \cdot \text{True} \end{cases} \quad (\text{A.5.37})$$

$$\text{KoRBCvPYRTRANSPORT} = \frac{\text{KiRBCvPYRTRANSPORT}}{\text{RtvRBC}} \quad (\text{A.5.38})$$

$$\text{KaappRBCvHBATP} = \text{HbpHRBC} \cdot \text{KaRBCvHBATP} \quad (\text{A.5.39})$$

$$\text{KaappRBCvHBB13PG} = \text{HbpHRBC} \cdot \text{KaRBCvHBB13PG} \quad (\text{A.5.40})$$

$$\text{kmg5s} = \text{kmg5} \cdot \left(\frac{\text{s1} \cdot \text{g6p}(t)}{\text{kg2}} + 1 \right) \quad (\text{A.5.41})$$

$$\text{KoRBCvPHOSTRANSPORT} = \frac{\text{KiRBCvPHOSTRANSPORT}}{\text{KeqRBCvPHOSTRANSPORT}} \quad (\text{A.5.42})$$

$$\text{kmg7s} = \text{kmg7} \cdot \left(\frac{\text{s1} \cdot \text{g6p}(t)}{\text{kg2}} + 1 \right) \quad (\text{A.5.43})$$

$$\text{phosEXT} = \text{ConcPhosEXT} \cdot \text{vBld} \quad (\text{A.5.44})$$

$$\text{co2RBC} = \text{ConcCo2RBC} \cdot \text{Vrbcu} \quad (\text{A.5.45})$$

$$\text{GPaPlot} = (1.42857 \times 10^1) \cdot \text{GPa}(t) \quad (\text{A.5.46})$$

$$\text{k_glucgn} = \text{Gmax} \cdot \text{kd_Bglucgn} \quad (\text{A.5.47})$$

$$\text{Vpf} = \begin{cases} \cdot \text{trophToRBC} \cdot \text{Vrbci} \cdot \cdot \text{par} > 0 \cdot \\ \cdot 1 \cdot \cdot \text{True} \end{cases} \quad (\text{A.5.48})$$

$$\text{trophToRBC} = \frac{14}{45} \quad (\text{A.5.49})$$

$$\omega = (1 - \text{HCT}) \cdot v_{\text{totblood}} \quad (\text{A.5.50})$$

$$k1\text{glucgn} = (\text{Gmax} - \text{Gmin}) \cdot kd_{\text{Bglucgn}} \quad (\text{A.5.51})$$

$$\text{GSaPlot} = (3.33333 \times 10^2) \cdot \text{GSa}(t) \quad (\text{A.5.52})$$

$$k_{gc2} = \frac{k_{gc2}}{k22} \quad (\text{A.5.53})$$

$$K2\text{appRBCvAK} = K2\text{RBCvAK} \cdot (\text{hRBC} \cdot K\text{hampRBCvAK} + K\text{kampRBCvAK} \cdot k\text{RBC} + 1) \quad (\text{A.5.54})$$

$$K\text{iappnadhRBCvGAPDH} = (6.30957 \times 10^{-8}) \cdot 10^{\text{phRBC}} \cdot K\text{inadhRBCvGAPDH} \quad (\text{A.5.55})$$

$$K\text{aappRBCvMGADP} = \frac{\text{CRBCvMGADP} \cdot K\text{aRBCvMGADP} \cdot (\text{hRBC} \cdot K\text{hadpRBCvMGADP} \cdot K\text{mghadpRBCvMGADP} + K\text{RBCvMGADP})}{\text{hRBC} \cdot K\text{hadpRBCvMGADP} + K\text{kadpRBCvMGADP} \cdot k\text{RBC} + 1} \quad (\text{A.5.56})$$

$$F_{\text{ffa}} = 2.85138 \times 10^{-2} \quad (\text{A.5.57})$$

$$M_{\text{alan}} = 0 \quad (\text{A.5.58})$$

$$K\text{catrappRBCvGAPDH} = \frac{K\text{catrRBCvGAPDH}}{1 + 10^{\text{phRBC}-10} + (3.16228 \times 10^7) \cdot 10^{-\text{phRBC}}} \quad (\text{A.5.59})$$

$$K\text{mapplacRBCvLDH} = (7.15253 \times 10^{-1}) \cdot \left(1 + (6.30957 \times 10^6) \cdot 10^{-\text{phRBC}}\right) \cdot K\text{mlacRBCvLDH} \quad (\text{A.5.60})$$

$$K1\text{appRBCvBPGSP1} = \frac{3.51189 \cdot K1\text{RBCvBPGSP1}}{1 + (1.58489 \times 10^{-7}) \cdot 10^{\text{phRBC}}} \quad (\text{A.5.61})$$

$$K\text{aappRBCvHBBPG} = \text{HbpHRBC} \cdot K\text{aRBCvHBBPG} \quad (\text{A.5.62})$$

$$v\text{bld} = 1000 \cdot (1 - \text{HCT}) \cdot v_{\text{totblood}} \quad (\text{A.5.63})$$

$$K3\text{appRBCvBPGSP2} = \frac{1.75858 \cdot K3\text{RBCvBPGSP2}}{1 + (4.7863 \times 10^{28}) \cdot 10^{-4 \cdot \text{phRBC}}} \quad (\text{A.5.64})$$

$$k\text{mg8s} = \frac{k\text{mg8}}{\frac{s1.g6p(t)}{k2} + 1} \quad (\text{A.5.65})$$

$$K4\text{appRBCvBPGSP3} = \frac{1.75858 \cdot K4\text{RBCvBPGSP3}}{1 + (4.7863 \times 10^{28}) \cdot 10^{-4 \cdot \text{phRBC}}} \quad (\text{A.5.66})$$

$$\text{HbpHRBC} = \frac{\frac{(2.51189 \times 10^{14}) \cdot \text{KahbRBC}^2}{\text{pHConversionFactor}^2} + \frac{(3.16979 \times 10^7) \cdot \text{KahbRBC}}{\text{pHConversionFactor}} + 1}{\frac{\text{KahbRBC}^2}{\text{hRBC}^2} + \frac{2 \cdot \text{KahbRBC}}{\text{hRBC}} + 1} \quad (\text{A.5.67})$$

$$\text{KaappRBCvMGB23PG} = \frac{\text{CRBCvMGB23PG} \cdot \text{KaRBCvMGB23PG}}{1 \cdot (\text{hRBC} \cdot \text{KhbpgrBCvMGB23PG} \cdot \text{KmgpbpgRBCvMGB23PG} + \text{KRBCvMGB23PG})}{\text{Kh2bpgRBCvMGB23PG} \cdot \text{KhbpgrBCvMGB23PG} \cdot \text{hRBC}^2 + \text{KhbpgrBCvMGB23PG} \cdot \text{hRBC} + \text{KhbpgrBCvMGB23PG} \cdot \text{KkbpgrBCvMGB23PG} \cdot \text{KRBC} \cdot \text{hRBC} + \text{KkbpgrBCvMGB23PG} \cdot \text{KRBC} + 1} \quad (\text{A.5.68})$$

$$\text{KaappRBCvMGF16P2} = \frac{\text{CRBCvMGF16P2} \cdot \text{KaRBCvMGF16P2}}{1 \cdot (\text{hRBC} \cdot \text{KhfrBCvMGF16P2} \cdot \text{KmgfRBCvMGF16P2} + \text{KRBCvMGF16P2})}{\text{Kh2frBCvMGF16P2} \cdot \text{KhfrBCvMGF16P2} \cdot \text{hRBC}^2 + \text{KhfrBCvMGF16P2} \cdot \text{hRBC} + \text{KhfrBCvMGF16P2} \cdot \text{KkfrBCvMGF16P2} \cdot \text{KRBC} \cdot \text{hRBC} + \text{KkfrBCvMGF16P2} \cdot \text{KRBC} + 1} \quad (\text{A.5.69})$$

$$\text{parMulti} = \begin{cases} \cdot 1 \cdot & \cdot \text{par} > 0 \cdot \\ \cdot 0 \cdot & \cdot \text{True} \end{cases} \quad (\text{A.5.70})$$

A.6 Ordinary differential equations:

$$B_alan'(t) = -1.v_d_Balan - 1.v_tL6 + 1.v_tS4 \quad (A.6.1)$$

$$B_ffa'(t) = -1.v_d_Bffa + 1.v_tF3 - 1.v_tL5 \quad (A.6.2)$$

$$B_gluc'(t) = -1.vRBCivGLCTransport - 1.vRBCvGLCTransport - 1.v_d_Bgluc + 1.v_feed - 1.v_tF1 - 1.v_tL1 - 1.v_tS1 \quad (A.6.3)$$

$$B_glucgn'(t) = -1.v_d_Bglucgn - 1.v_Ggluc + 1.v_glucgn \quad (A.6.4)$$

$$B_ins'(t) = -1.v_d_Bins + 1.v_Igluc + 1.v_ins \quad (A.6.5)$$

$$B_ket'(t) = -1.v_d_Bket + 1.v_tL3 - 1.v_tS2 \quad (A.6.6)$$

$$B_lac'(t) = 1.vRBCivLACTransport + 1.vRBCvLACTransport - 1.v_d_Blac - 1.v_tL2 + 1.v_tS3 \quad (A.6.7)$$

$$Cvar'(t) = 1.Jg10 + 1.Jg11 \quad (A.6.8)$$

$$F_TG'(t) = 1.v_F3 - 1.v_F4 \quad (A.6.9)$$

$$F_acyl'(t) = 1.v_F1 - 1.v_F3 + 1.v_F5 \quad (A.6.10)$$

$$F_g6p'(t) = 1.v_tF1 - 1.v_F1 \quad (A.6.11)$$

$$GPa'(t) = 1.Jg5 - 1.Jg6 - 1.Jg9 \quad (A.6.12)$$

$$GSa'(t) = 1.Jg8 - 1.Jg7 \quad (A.6.13)$$

$$M_g6p'(t) = -1.v_S1f + 1.v_S1r - 1.v_S2 + 1.v_tS1 \quad (A.6.14)$$

$$M_glycgn'(t) = 1.v_S1f - 1.v_S1r \quad (A.6.15)$$

$$M_ket'(t) = 1.v_tS2 - 1.v_s_dket \quad (A.6.16)$$

$$M_lac'(t) = 1.v_S3f - 1.v_S3r - 1.v_tS3 \quad (A.6.17)$$

$$M_pyr'(t) = 2.v_S2 - 1.v_S3f + 1.v_S3r - 1.v_S4f + 1.v_S4r \quad (A.6.18)$$

$$PKa'(t) = 1.Jg3 - 1.Jg4 \quad (A.6.19)$$

$$PP1'(t) = -1.Jg9 \quad (A.6.20)$$

$$PP1_GPa'(t) = 1.Jg9 \quad (A.6.21)$$

$$R2C2'(t) = -1.Jg10 \quad (A.6.22)$$

$$R2_C_cAMP2'(t) = 1.Jg10 - 1.Jg11 \quad (A.6.23)$$

$$R2_cAMP4'(t) = 1.Jg11 \quad (A.6.24)$$

$$aK'(t) = -1.v_L10 + 1.v_L21f - 1.v_L21r + 1.v_L9 \quad (A.6.25)$$

$$acet_c'(t) = 1.v_L14 - 1.v_L15 - 1.v_L16 \quad (A.6.26)$$

$$acet_m'(t) = 8.v_L18 - 2.v_L19 + 1.v_L7 - 1.v_L8 \quad (A.6.27)$$

$$adpPF'(t) = 1.vPFvATPase + 1.vPFvHK + 1.vPFvPFK - 1.vPFvPGK - 1.vPFvPK \quad (A.6.28)$$

$$adpRBC'(t) = -1.vRBCvAK - 1.vRBCvHBADP - 1.vRBCvMGADP \quad (A.6.29)$$

$$adpRBCi'(t) = -1.vRBCivAK - 1.vRBCivHBADP - 1.vRBCivMGADP \quad (A.6.30)$$

$$alan'(t) = -1.v_L20 + 1.v_L21f - 1.v_L21r + 1.v_tL6 \quad (A.6.31)$$

$$ampRBC'(t) = 1.vRBCvAK \quad (A.6.32)$$

$$ampRBCi'(t) = 1.vRBCivAK \quad (A.6.33)$$

$$atpPF'(t) = -1.vPFvATPase - 1.vPFvHK - 1.vPFvPFK + 1.vPFvPGK + 1.vPFvPK \quad (A.6.34)$$

$$atpRBC'(t) = -1.vRBCvHBATP - 1.vRBCvMGATP \quad (A.6.35)$$

$$atpRBCi'(t) = -1.vRBCivHBATP - 1.vRBCivMGATP \quad (A.6.36)$$

$$b13pgPF'(t) = 1.vPFvGAPDH - 1.vPFvPGK \quad (A.6.37)$$

$$b13pgRBC'(t) = -1.vRBCvBPGSP1 + 1.vRBCvGAPDH - 1.vRBCvHBB13PG - 1.vRBCvMGB13PG - 1.vRBCvPGK \quad (A.6.38)$$

$$b13pgRBCi'(t) = -1.vRBCivBPGSP1 + 1.vRBCivGAPDH - 1.vRBCivHBB13PG - 1.vRBCivMGB13PG - 1.vRBCivPGK \quad (A.6.39)$$

$$b23pgRBC'(t) = 1.vRBCvBPGSP7 - 1.vRBCvHBB23PG - 1.vRBCvMGB23PG \quad (A.6.40)$$

$$b23pgRBCi'(t) = 1.vRBCivBPGSP7 - 1.vRBCivHBB23PG - 1.vRBCivMGB23PG \quad (A.6.41)$$

$$bpgspRBC'(t) = -1.vRBCvBPGSP1 + 1.vRBCvBPGSP7 + 1.vRBCvBPGSP9 \quad (A.6.42)$$

$$bpgspRBCi'(t) = -1.vRBCivBPGSP1 + 1.vRBCivBPGSP7 + 1.vRBCivBPGSP9 \quad (A.6.43)$$

$$\begin{aligned} \text{bpgspb13pgRBC}'(t) &= 1.v\text{RBCvBPGSP1} - 1.v\text{RBCvBPGSP2} & (\text{A.6.44}) \\ \text{bpgspb13pgRBCi}'(t) &= 1.v\text{RBCivBPGSP1} - 1.v\text{RBCivBPGSP2} & (\text{A.6.45}) \\ \text{bpgspb23pgRBC}'(t) &= 1.v\text{RBCvBPGSP5} + 1.v\text{RBCvBPGSP6} - 1.v\text{RBCvBPGSP7} & (\text{A.6.46}) \\ \text{bpgspb23pgRBCi}'(t) &= 1.v\text{RBCivBPGSP5} + 1.v\text{RBCivBPGSP6} - 1.v\text{RBCivBPGSP7} & (\text{A.6.47}) \\ \text{bpgsppRBC}'(t) &= 1.v\text{RBCvBPGSP2} - 1.v\text{RBCvBPGSP3} \\ &\quad - 1.v\text{RBCvBPGSP4} - 1.v\text{RBCvBPGSP8} & (\text{A.6.48}) \\ \text{bpgsppRBCi}'(t) &= 1.v\text{RBCivBPGSP2} - 1.v\text{RBCivBPGSP3} \\ &\quad - 1.v\text{RBCivBPGSP4} - 1.v\text{RBCivBPGSP8} & (\text{A.6.49}) \\ \text{bpgsppp2gRBC}'(t) &= 1.v\text{RBCvBPGSP4} - 1.v\text{RBCvBPGSP6} & (\text{A.6.50}) \\ \text{bpgsppp2gRBCi}'(t) &= 1.v\text{RBCivBPGSP4} - 1.v\text{RBCivBPGSP6} & (\text{A.6.51}) \\ \text{bpgsppp3gRBC}'(t) &= 1.v\text{RBCvBPGSP3} - 1.v\text{RBCvBPGSP5} & (\text{A.6.52}) \\ \text{bpgsppp3gRBCi}'(t) &= 1.v\text{RBCivBPGSP3} - 1.v\text{RBCivBPGSP5} & (\text{A.6.53}) \\ \text{bpgsppphosRBC}'(t) &= 1.v\text{RBCvBPGSP8} - 1.v\text{RBCvBPGSP9} & (\text{A.6.54}) \\ \text{bpgsppphosRBCi}'(t) &= 1.v\text{RBCivBPGSP8} - 1.v\text{RBCivBPGSP9} & (\text{A.6.55}) \\ \text{cAMP}'(t) &= -2.\text{Jg10} - 2.\text{Jg11} + 1.v_c1\text{cAMP} - 1.v_c2\text{cAMP} & (\text{A.6.56}) \\ \text{citrate}'(t) &= -1.v_L14 + 1.v_L8 - 1.v_L9 & (\text{A.6.57}) \\ \text{dhapPF}'(t) &= 1.v\text{PFvALD} - 1.v\text{PFvG3PDH} - 1.v\text{PFvTPI} & (\text{A.6.58}) \\ \text{dhapRBC}'(t) &= 1.v\text{RBCvALD} + 1.v\text{RBCvTIM} & (\text{A.6.59}) \\ \text{dhapRBCi}'(t) &= 1.v\text{RBCivALD} + 1.v\text{RBCivTIM} & (\text{A.6.60}) \\ \text{ery4pRBC}'(t) &= 1.v\text{RBCvTA} - 1.v\text{RBCvTK5} & (\text{A.6.61}) \\ \text{ery4pRBCi}'(t) &= 1.v\text{RBCivTA} - 1.v\text{RBCivTK5} & (\text{A.6.62}) \\ \text{f16bpPF}'(t) &= 1.v\text{PFvPFK} - 1.v\text{PFvALD} & (\text{A.6.63}) \\ \text{f16p2RBC}'(t) &= -1.v\text{RBCvALD} - 1.v\text{RBCvMGF16P2} + 1.v\text{RBCvPFK} & (\text{A.6.64}) \\ \text{f16p2RBCi}'(t) &= -1.v\text{RBCivALD} - 1.v\text{RBCivMGF16P2} + 1.v\text{RBCivPFK} & (\text{A.6.65}) \\ \text{f6pPF}'(t) &= 1.v\text{PFvPGI} - 1.v\text{PFvPFK} & (\text{A.6.66}) \\ \text{f6pRBC}'(t) &= -1.v\text{RBCvPFK} + 1.v\text{RBCvPGI} + 1.v\text{RBCvTA} + 1.v\text{RBCvTK6} & (\text{A.6.67}) \\ \text{f6pRBCi}'(t) &= -1.v\text{RBCivPFK} + 1.v\text{RBCivPGI} + 1.v\text{RBCivTA} + 1.v\text{RBCivTK6} & (\text{A.6.68}) \\ \text{g16p2RBC}'(t) &= -1.v\text{RBCvMGG16P2} & (\text{A.6.69}) \\ \text{g16p2RBCi}'(t) &= -1.v\text{RBCivMGG16P2} & (\text{A.6.70}) \\ \text{g3pPF}'(t) &= 1.v\text{PFvG3PDH} - 1.v\text{PFvGLYtr} & (\text{A.6.71}) \\ \text{g6p}'(t) &= 1.v_L1f - 1.v_L1r - 1.v_L2f + 1.v_L2r - 1.v_L3f + 1.v_L3r & (\text{A.6.72}) \\ \text{g6pPF}'(t) &= 1.v\text{PFvHK} - 1.v\text{PFvPGI} & (\text{A.6.73}) \\ \text{g6pRBC}'(t) &= -1.v\text{RBCvG6PDH} + 1.v\text{RBCvHK} - 1.v\text{RBCvPGI} & (\text{A.6.74}) \\ \text{g6pRBCi}'(t) &= -1.v\text{RBCivG6PDH} + 1.v\text{RBCivHK} - 1.v\text{RBCivPGI} & (\text{A.6.75}) \\ \text{gapPF}'(t) &= 1.v\text{PFvALD} - 1.v\text{PFvGAPDH} + 1.v\text{PFvTPI} & (\text{A.6.76}) \\ \text{gapRBC}'(t) &= 1.v\text{RBCvALD} - 1.v\text{RBCvGAPDH} - 1.v\text{RBCvTA} - 1.v\text{RBCvTIM} \\ &\quad + 1.v\text{RBCvTK2} & (\text{A.6.77}) \\ \text{gapRBCi}'(t) &= 1.v\text{RBCivALD} - 1.v\text{RBCivGAPDH} - 1.v\text{RBCivTA} - 1.v\text{RBCivTIM} \\ &\quad + 1.v\text{RBCivTK2} & (\text{A.6.78}) \\ \text{glcPF}'(t) &= 1.v\text{PFvGLCtr} - 1.v\text{PFvHK} & (\text{A.6.79}) \\ \text{glcRBC}'(t) &= 1.v\text{RBCvGLCTRANSPORT} - 1.v\text{RBCvHK} & (\text{A.6.80}) \\ \text{glcRBCi}'(t) &= -1.v\text{PFvGLCtr} + 1.v\text{RBCivGLCTRANSPORT} - 1.v\text{RBCivHK} & (\text{A.6.81}) \\ \text{gluc}'(t) &= -1.v_L1f + 1.v_L1r + 1.v_tL1 & (\text{A.6.82}) \\ \text{glutamate}'(t) &= -1.v_L21f + 1.v_L21r - 1.v_L22 & (\text{A.6.83}) \\ \text{glycgn}'(t) &= 1.v_L2f - 1.v_L2r & (\text{A.6.84}) \\ \text{gshRBC}'(t) &= 2.v\text{RBCvGSSGR} - 2.v\text{RBCvOX} & (\text{A.6.85}) \\ \text{gshRBCi}'(t) &= 2.v\text{RBCivGSSGR} - 2.v\text{RBCivOX} & (\text{A.6.86}) \\ \text{gssgRBC}'(t) &= 1.v\text{RBCvOX} - 1.v\text{RBCvGSSGR} & (\text{A.6.87}) \\ \text{gssgRBCi}'(t) &= 1.v\text{RBCivOX} - 1.v\text{RBCivGSSGR} & (\text{A.6.88}) \end{aligned}$$

$$\begin{aligned} \text{hbRBC}'(t) &= -1.\text{vRBCvHBADP} - 1.\text{vRBCvHBATP} - 1.\text{vRBCvHBB13PG} \\ &\quad - 1.\text{vRBCvHBB23PG} - 1.\text{vRBCvHBMGATP} \end{aligned} \quad (\text{A.6.89})$$

$$\begin{aligned} \text{hbRBCi}'(t) &= -1.\text{vRBCivHBADP} - 1.\text{vRBCivHBATP} - 1.\text{vRBCivHBB13PG} \\ &\quad - 1.\text{vRBCivHBB23PG} - 1.\text{vRBCivHBMGATP} \end{aligned} \quad (\text{A.6.90})$$

$$\text{hbadpRBC}'(t) = 1.\text{vRBCvHBADP} \quad (\text{A.6.91})$$

$$\text{hbadpRBCi}'(t) = 1.\text{vRBCivHBADP} \quad (\text{A.6.92})$$

$$\text{hbatpRBC}'(t) = 1.\text{vRBCvHBATP} \quad (\text{A.6.93})$$

$$\text{hbatpRBCi}'(t) = 1.\text{vRBCivHBATP} \quad (\text{A.6.94})$$

$$\text{hbb13pgRBC}'(t) = 1.\text{vRBCvHBB13PG} \quad (\text{A.6.95})$$

$$\text{hbb13pgRBCi}'(t) = 1.\text{vRBCivHBB13PG} \quad (\text{A.6.96})$$

$$\text{hbb23pgRBC}'(t) = 1.\text{vRBCvHBB23PG} \quad (\text{A.6.97})$$

$$\text{hbb23pgRBCi}'(t) = 1.\text{vRBCivHBB23PG} \quad (\text{A.6.98})$$

$$\text{hbm gatpRBC}'(t) = 1.\text{vRBCvHBMGATP} \quad (\text{A.6.99})$$

$$\text{hbm gatpRBCi}'(t) = 1.\text{vRBCivHBMGATP} \quad (\text{A.6.100})$$

$$\text{ket}'(t) = 1.\text{v_L19} - 1.\text{v_tL3} \quad (\text{A.6.101})$$

$$\text{lac}'(t) = 1.\text{v_L5f} - 1.\text{v_L5r} + 1.\text{v_tL2} \quad (\text{A.6.102})$$

$$\text{lacPF}'(t) = 1.\text{vPFvLDH} - 1.\text{vPFvLACtr} \quad (\text{A.6.103})$$

$$\text{lacRBC}'(t) = -1.\text{vRBCvLACTRANSPORT} + 1.\text{vRBCvLDH} + 1.\text{vRBCvLDHP} \quad (\text{A.6.104})$$

$$\text{lacRBCi}'(t) = 1.\text{vPFvLACtr} - 1.\text{vRBCivLACTRANSPORT} + 1.\text{vRBCivLDH} + 1.\text{vRBCivLDHP} \quad (\text{A.6.105})$$

$$\text{malate}'(t) = 1.\text{v_L10} + 1.\text{v_L11f} - 1.\text{v_L11r} - 1.\text{v_L12} \quad (\text{A.6.106})$$

$$\text{malonyl}'(t) = 1.\text{v_L15} - 7.\text{v_L16} \quad (\text{A.6.107})$$

$$\begin{aligned} \text{mgRBC}'(t) &= -1.\text{vRBCvMGADP} - 1.\text{vRBCvMGATP} - 1.\text{vRBCvMGB13PG} \\ &\quad - 1.\text{vRBCvMGB23PG} - 1.\text{vRBCvMGF16P2} - 1.\text{vRBCvMGG16P2} \\ &\quad - 1.\text{vRBCvMGPHOS} \end{aligned} \quad (\text{A.6.108})$$

$$\begin{aligned} \text{mgRBCi}'(t) &= -1.\text{vRBCivMGADP} - 1.\text{vRBCivMGATP} - 1.\text{vRBCivMGB13PG} \\ &\quad - 1.\text{vRBCivMGB23PG} - 1.\text{vRBCivMGF16P2} - 1.\text{vRBCivMGG16P2} \\ &\quad - 1.\text{vRBCivMGPHOS} \end{aligned} \quad (\text{A.6.109})$$

$$\begin{aligned} \text{mgadpRBC}'(t) &= -1.\text{vRBCvAK} + 1.\text{vRBCvATPASE} + 1.\text{vRBCvHK} + 1.\text{vRBCvMGADP} \\ &\quad + 1.\text{vRBCvPFK} - 1.\text{vRBCvPGK} - 1.\text{vRBCvPK} \end{aligned} \quad (\text{A.6.110})$$

$$\begin{aligned} \text{mgadpRBCi}'(t) &= -1.\text{vRBCivAK} + 1.\text{vRBCivATPASE} + 1.\text{vRBCivHK} + 1.\text{vRBCivMGADP} \\ &\quad + 1.\text{vRBCivPFK} - 1.\text{vRBCivPGK} - 1.\text{vRBCivPK} \end{aligned} \quad (\text{A.6.111})$$

$$\begin{aligned} \text{mgatpRBC}'(t) &= 1.\text{vRBCvAK} - 1.\text{vRBCvATPASE} - 1.\text{vRBCvHBMGATP} \\ &\quad - 1.\text{vRBCvHK} + 1.\text{vRBCvMGATP} - 1.\text{vRBCvPFK} + 1.\text{vRBCvPGK} \\ &\quad + 1.\text{vRBCvPK} \end{aligned} \quad (\text{A.6.112})$$

$$\begin{aligned} \text{mgatpRBCi}'(t) &= 1.\text{vRBCivAK} - 1.\text{vRBCivATPASE} - 1.\text{vRBCivHBMGATP} \\ &\quad - 1.\text{vRBCivHK} + 1.\text{vRBCivMGATP} - 1.\text{vRBCivPFK} + 1.\text{vRBCivPGK} \\ &\quad + 1.\text{vRBCivPK} \end{aligned} \quad (\text{A.6.113})$$

$$\text{mgb13pgRBC}'(t) = 1.\text{vRBCvMGB13PG} \quad (\text{A.6.114})$$

$$\text{mgb13pgRBCi}'(t) = 1.\text{vRBCivMGB13PG} \quad (\text{A.6.115})$$

$$\text{mgb23pgRBC}'(t) = 1.\text{vRBCvMGB23PG} \quad (\text{A.6.116})$$

$$\text{mgb23pgRBCi}'(t) = 1.\text{vRBCivMGB23PG} \quad (\text{A.6.117})$$

$$\text{mgf16p2RBC}'(t) = 1.\text{vRBCvMGF16P2} \quad (\text{A.6.118})$$

$$\text{mgf16p2RBCi}'(t) = 1.\text{vRBCivMGF16P2} \quad (\text{A.6.119})$$

$$\text{m gg16p2RBC}'(t) = 1.\text{vRBCvMGG16P2} \quad (\text{A.6.120})$$

$$\text{m gg16p2RBCi}'(t) = 1.\text{vRBCivMGG16P2} \quad (\text{A.6.121})$$

$$\text{mgphosRBC}'(t) = 1.\text{vRBCvMGPHOS} \quad (\text{A.6.122})$$

$$\text{mgphosRBCi}'(t) = 1.\text{vRBCivMGPHOS} \quad (\text{A.6.123})$$

$$\text{nadPF}'(t) = 1.\text{vPFvG3PDH} - 1.\text{vPFvGAPDH} + 1.\text{vPFvLDH} \quad (\text{A.6.124})$$

$$\text{nadRBC}'(t) = -1.\text{vRBCvGAPDH} + 1.\text{vRBCvLDH} + 1.\text{vRBCvOXNADH} \quad (\text{A.6.125})$$

$$\text{nadRBCi}'(t) = -1.\text{vRBCivGAPDH} + 1.\text{vRBCivLDH} + 1.\text{vRBCivOXNADH} \quad (\text{A.6.126})$$

$$\text{nadhPF}'(t) = -1.\text{vPFvG3PDH} + 1.\text{vPFvGAPDH} - 1.\text{vPFvLDH} \quad (\text{A.6.127})$$

$$\begin{aligned} \text{nadhRBC}'(t) &= 1.v\text{RBCvGAPDH} - 1.v\text{RBCvLDH} - 1.v\text{RBCvOXNADH} & (\text{A.6.128}) \\ \text{nadhRBCi}'(t) &= 1.v\text{RBCivGAPDH} - 1.v\text{RBCivLDH} - 1.v\text{RBCivOXNADH} & (\text{A.6.129}) \\ \text{nadpRBC}'(t) &= -1.v\text{RBCvG6PDH} + 1.v\text{RBCvGSSGR} + 1.v\text{RBCvLDHP} - 1.v\text{RBCvP6GDH} & (\text{A.6.130}) \\ \text{nadpRBCi}'(t) &= -1.v\text{RBCivG6PDH} + 1.v\text{RBCivGSSGR} + 1.v\text{RBCivLDHP} - 1.v\text{RBCivP6GDH} & (\text{A.6.131}) \\ \text{nadphRBC}'(t) &= 1.v\text{RBCvG6PDH} - 1.v\text{RBCvGSSGR} - 1.v\text{RBCvLDHP} + 1.v\text{RBCvP6GDH} & (\text{A.6.132}) \\ \text{nadphRBCi}'(t) &= 1.v\text{RBCivG6PDH} - 1.v\text{RBCivGSSGR} - 1.v\text{RBCivLDHP} + 1.v\text{RBCivP6GDH} & (\text{A.6.133}) \\ \text{oa}_c'(t) &= 1.v_L12 - 1.v_L13 + 1.v_L14 & (\text{A.6.134}) \\ \text{oa}_m'(t) &= -1.v_L11f + 1.v_L11r + 1.v_L6 - 1.v_L8 & (\text{A.6.135}) \\ \text{p2gPF}'(t) &= 1.v\text{PFvPGM} - 1.v\text{PFvENO} & (\text{A.6.136}) \\ \text{p2gRBC}'(t) &= -1.v\text{RBCvBPGSP4} - 1.v\text{RBCvENO} + 1.v\text{RBCvPGM} & (\text{A.6.137}) \\ \text{p2gRBCi}'(t) &= -1.v\text{RBCivBPGSP4} - 1.v\text{RBCivENO} + 1.v\text{RBCivPGM} & (\text{A.6.138}) \\ \text{p3gPF}'(t) &= 1.v\text{PFvPGK} - 1.v\text{PFvPGM} & (\text{A.6.139}) \\ \text{p3gRBC}'(t) &= 1.v\text{RBCvBPGSP2} - 1.v\text{RBCvBPGSP3} + 1.v\text{RBCvPGK} - 1.v\text{RBCvPGM} & (\text{A.6.140}) \\ \text{p3gRBCi}'(t) &= 1.v\text{RBCivBPGSP2} - 1.v\text{RBCivBPGSP3} + 1.v\text{RBCivPGK} - 1.v\text{RBCivPGM} & (\text{A.6.141}) \\ \text{p6gRBC}'(t) &= 1.v\text{RBCvPGLHYDROLYSIS} - 1.v\text{RBCvP6GDH} & (\text{A.6.142}) \\ \text{p6gRBCi}'(t) &= 1.v\text{RBCivPGLHYDROLYSIS} - 1.v\text{RBCivP6GDH} & (\text{A.6.143}) \\ \text{p6glRBC}'(t) &= 1.v\text{RBCvG6PDH} - 1.v\text{RBCvPGLHYDROLYSIS} & (\text{A.6.144}) \\ \text{p6glRBCi}'(t) &= 1.v\text{RBCivG6PDH} - 1.v\text{RBCivPGLHYDROLYSIS} & (\text{A.6.145}) \\ \text{palm}'(t) &= 1.v_L16 - 1.v_L17 + 1.v_tL5 & (\text{A.6.146}) \\ \text{palmCoA}'(t) &= 1.v_L17 - 1.v_L18 & (\text{A.6.147}) \\ \text{pep}'(t) &= 1.v_L13 + 2.v_L3f - 2.v_L3r - 1.v_L4 & (\text{A.6.148}) \\ \text{pepPF}'(t) &= 1.v\text{PFvENO} - 1.v\text{PFvPK} & (\text{A.6.149}) \\ \text{pepRBC}'(t) &= 1.v\text{RBCvENO} - 1.v\text{RBCvPK} & (\text{A.6.150}) \\ \text{pepRBCi}'(t) &= 1.v\text{RBCivENO} - 1.v\text{RBCivPK} & (\text{A.6.151}) \\ \text{phosRBC}'(t) &= 1.v\text{RBCvATPASE} - 1.v\text{RBCvBPGSP8} + 2.v\text{RBCvBPGSP9} - 1.v\text{RBCvGAPDH} \\ &\quad - 1.v\text{RBCvMGPHOS} - 1.v\text{RBCvPHOSTRANSPORT} & (\text{A.6.152}) \\ \text{phosRBCi}'(t) &= 1.v\text{RBCivATPASE} - 1.v\text{RBCivBPGSP8} + 2.v\text{RBCivBPGSP9} - 1.v\text{RBCivGAPDH} \\ &\quad - 1.v\text{RBCivMGPHOS} - 1.v\text{RBCivPHOSTRANSPORT} & (\text{A.6.153}) \\ \text{pyr}'(t) &= 1.v_L20 - 1.v_L21f + 1.v_L21r + 1.v_L4 - 1.v_L5f + 1.v_L5r - 1.v_L6 \\ &\quad - 1.v_L7 & (\text{A.6.154}) \\ \text{pyrPF}'(t) &= -1.v\text{PFvLDH} + 1.v\text{PFvPK} - 1.v\text{PFvPYRtr} & (\text{A.6.155}) \\ \text{pyrRBC}'(t) &= -1.v\text{RBCvLDH} - 1.v\text{RBCvLDHP} + 1.v\text{RBCvPK} - 1.v\text{RBCvPYRTRANSPORT} & (\text{A.6.156}) \\ \text{pyrRBCi}'(t) &= 1.v\text{PFvPYRtr} - 1.v\text{RBCivLDH} - 1.v\text{RBCivLDHP} + 1.v\text{RBCivPK} \\ &\quad - 1.v\text{RBCivPYRTRANSPORT} & (\text{A.6.157}) \\ \text{rib5pRBC}'(t) &= 1.v\text{RBCvR5PI} - 1.v\text{RBCvTK3} & (\text{A.6.158}) \\ \text{rib5pRBCi}'(t) &= 1.v\text{RBCivR5PI} - 1.v\text{RBCivTK3} & (\text{A.6.159}) \\ \text{ru5pRBC}'(t) &= 1.v\text{RBCvP6GDH} - 1.v\text{RBCvR5PI} - 1.v\text{RBCvRu5PE} & (\text{A.6.160}) \\ \text{ru5pRBCi}'(t) &= 1.v\text{RBCivP6GDH} - 1.v\text{RBCivR5PI} - 1.v\text{RBCivRu5PE} & (\text{A.6.161}) \\ \text{sed7pRBC}'(t) &= 1.v\text{RBCvTK4} - 1.v\text{RBCvTA} & (\text{A.6.162}) \\ \text{sed7pRBCi}'(t) &= 1.v\text{RBCivTK4} - 1.v\text{RBCivTA} & (\text{A.6.163}) \\ \text{tkRBC}'(t) &= -1.v\text{RBCvTK1} + 1.v\text{RBCvTK4} + 1.v\text{RBCvTK6} & (\text{A.6.164}) \\ \text{tkRBCi}'(t) &= -1.v\text{RBCivTK1} + 1.v\text{RBCivTK4} + 1.v\text{RBCivTK6} & (\text{A.6.165}) \\ \text{tkgRBC}'(t) &= 1.v\text{RBCvTK2} - 1.v\text{RBCvTK3} - 1.v\text{RBCvTK5} & (\text{A.6.166}) \\ \text{tkgRBCi}'(t) &= 1.v\text{RBCivTK2} - 1.v\text{RBCivTK3} - 1.v\text{RBCivTK5} & (\text{A.6.167}) \\ \text{tkgery4pRBC}'(t) &= 1.v\text{RBCvTK5} - 1.v\text{RBCvTK6} & (\text{A.6.168}) \\ \text{tkgery4pRBCi}'(t) &= 1.v\text{RBCivTK5} - 1.v\text{RBCivTK6} & (\text{A.6.169}) \\ \text{tkgrib5pRBC}'(t) &= 1.v\text{RBCvTK3} - 1.v\text{RBCvTK4} & (\text{A.6.170}) \\ \text{tkgrib5pRBCi}'(t) &= 1.v\text{RBCivTK3} - 1.v\text{RBCivTK4} & (\text{A.6.171}) \end{aligned}$$

$$\text{tkxu5pRBC}'(t) = 1.\text{vRBCvTK1} - 1.\text{vRBCvTK2} \quad (\text{A.6.172})$$

$$\text{tkxu5pRBCi}'(t) = 1.\text{vRBCivTK1} - 1.\text{vRBCivTK2} \quad (\text{A.6.173})$$

$$\text{xu5pRBC}'(t) = 1.\text{vRBCvRu5PE} - 1.\text{vRBCvTK1} \quad (\text{A.6.174})$$

$$\text{xu5pRBCi}'(t) = 1.\text{vRBCivRu5PE} - 1.\text{vRBCivTK1} \quad (\text{A.6.175})$$

Appendix B

Publication

The paper in this Appendix has been accepted for publication in the Biochemical Society Transactions journal.

Quantitative analysis of drug effects at the whole-body level: a case study for glucose metabolism in malaria patients

Jacky L. Snoep*†‡¹, Kathleen Green*, Johann Eicher*, Daniel C. Palm*, Gerald Penkler*, Francois du Toit*, Nicolas Walters*, Robert Burger*, Hans V. Westerhoff†‡ and David D. van Niekerk*

*Department of Biochemistry, Stellenbosch University, Private Bag X1, Matieland 7602, South Africa

†Molecular Cell Physiology, Vrije Universiteit Amsterdam, 1081 HV Amsterdam, The Netherlands

‡MIB, University of Manchester, M1 7EN Manchester, U.K.

Abstract

We propose a hierarchical modelling approach to construct models for disease states at the whole-body level. Such models can simulate effects of drug-induced inhibition of reaction steps on the whole-body physiology. We illustrate the approach for glucose metabolism in malaria patients, by merging two detailed kinetic models for glucose metabolism in the parasite *Plasmodium falciparum* and the human red blood cell with a coarse-grained model for whole-body glucose metabolism. In addition we use a genome-scale metabolic model for the parasite to predict amino acid production profiles by the malaria parasite that can be used as a complex biomarker.

Multi-scale hierarchical modelling of disease states

Diseases manifest as phenotypic changes in whole-body physiology that are experienced as illness and can be caused by external factors (e.g. infectious diseases caused by bacteria) or by internal dysfunction (e.g. type II diabetes, cancer). Medical treatment of a disease can be in the form of medication, such as a pharmaceutical drug that affects specific reactions in target cells. In the case of a so-called ‘magic bullet’ drug, displaying complete specificity and complete inhibition of an essential reaction in a parasite or diseased cell, the outcome of the drug effect is direct and simple to predict and no detailed analysis is required. However, most drugs affect more than one reaction step, do not lead to complete inhibition and have side effects [1]. The response to such a drug is more complicated and a quantitative analysis of the combined effects on the whole-body physiology is necessary to evaluate the treatment. Analysis of whole-body responses to partial inhibition of one or more reaction steps is challenging; typically, mathematical models at the whole-body level are not fine-grained and do not include individual chemical reaction steps. We propose a hierarchical approach where parts of a system are resolved with sufficient detail to analyse drug effects at the individual reaction step, whereas for other parts of the system coarse-grained models are used. This approach is illustrated with a multi-scale hierarchical model for glucose metabolism in malaria patients (Figure 1).

From diagnosis to drug

Medical treatment usually starts with a diagnosis and classification of a disease. Typically these are initially made on the basis of simple phenotypic descriptions. Relating these symptoms to a mechanistic interpretation of the disease is not a trivial task and will involve a systems based approach [2], especially when multiple molecular aetiologies with patient-dependent contributions are involved. Biomarkers play an important role in such a diagnosis and are likely to be found at the metabolomics level [3]. A mechanistic, systems level interpretation of a disease could point to multiple drug targets, moving away from the single drug single target paradigm [4]. Such systems approaches to pharmacology [5] and toxicology [6] could lead to more effective drug development strategies [7].

Genome-scale network analysis of metabolism

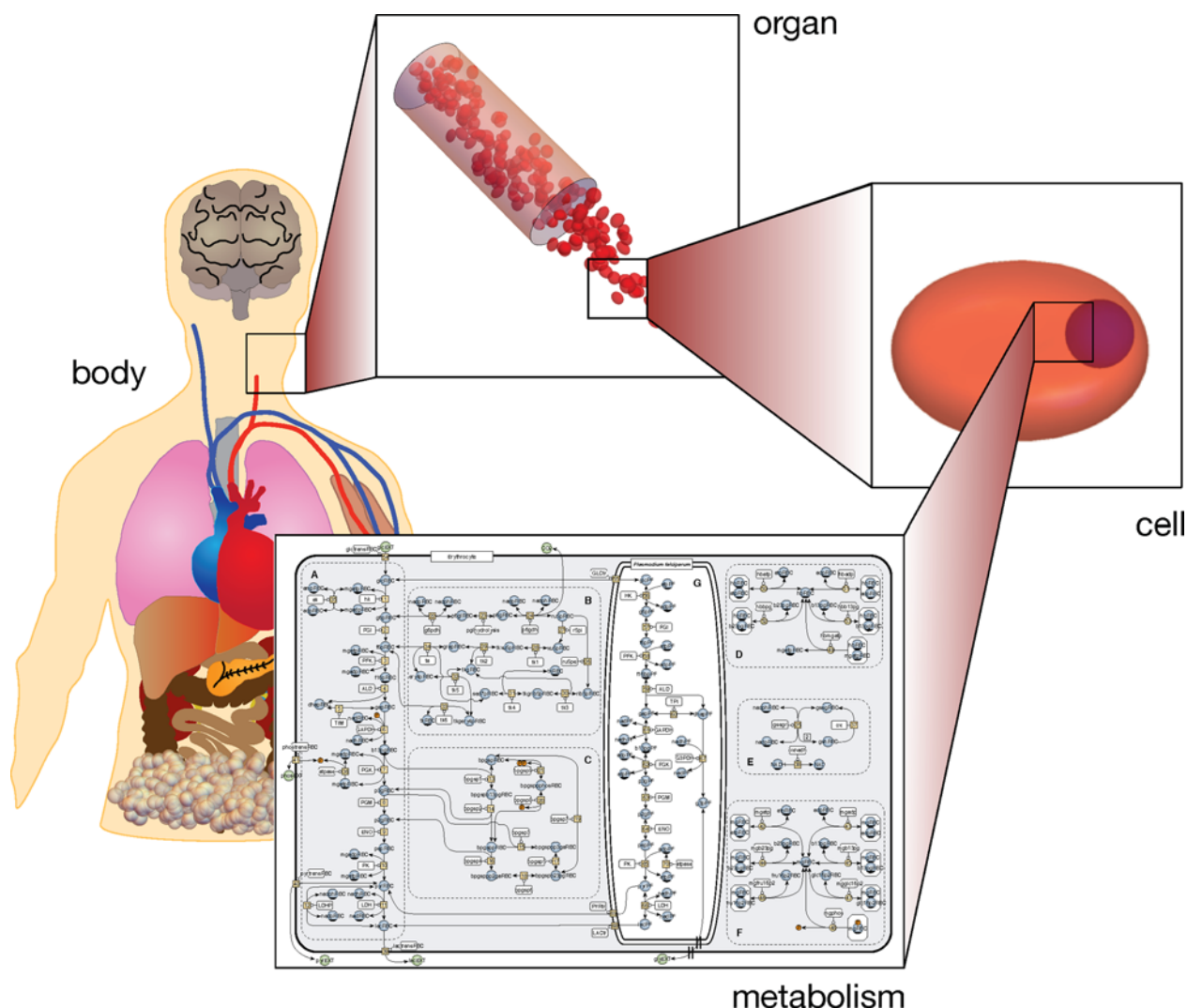
Metabolomics and metabolic modelling are important tools in following and predicting disease progress and understanding drug efficacy and mode of action [3,8]. In the last decade, enormous progress has been made in the genome-scale analysis of metabolic networks for a large number of species ranging from bacteria (e.g. *E. coli* [9]), to eukaryotes (e.g. *S. cerevisiae* [10]) to humans [11,12] and includes important human pathogens (e.g. *Haemophilus influenzae* [13], *Mycobacterium tuberculosis* [14] and *Plasmodium falciparum* [15–18]). These networks are very large, up to several thousands of reactions and the analyses are restricted to topological and constraint based modelling techniques,

Key words: glucose metabolism, malaria, multi-scale hierarchical model, *Plasmodium falciparum*.

¹ To whom correspondence should be addressed (email jls@sun.ac.za).

Figure 1 | Hierarchical multi-scale model for malaria patients

The whole-body model consists of several modules at the organ level, each described with input-output functions. The red blood cell compartment is modelled at the cellular and detailed metabolic level, including *P. falciparum* metabolism.



such as flux balance analysis [19,20]. Such models have been very useful for calculating metabolic phenotypes [21], such as the prediction of changes in metabolite biomarkers for inborn errors of metabolism [12] or, for instance, in analysing medium composition requirements for bacterial growth [22]. The models are typically analysed for steady state conditions and optimization criteria (e.g. growth rate) are used to minimize the solution space. Choosing suitable constraints on exchange reactions, biomass composition and maintenance reactions can have important effects on model predictions and should be done carefully.

Why study metabolism in malaria patients?

Malaria is a dreaded disease that is widespread across tropical and sub-tropical regions and responsible for the death of

between 500000 and 1000000 people per year, mostly children in sub-Saharan countries. One might not immediately think of malaria as a metabolic disease; the classic symptom of 48-h cyclical fever attacks and diagnosis via blood smears has no relation to metabolism. However, the key-diagnostics for poor chances of survival, lactic acidosis and hypoglycaemia [23] are clearly linked to metabolism. In addition, in malaria patients, blood concentrations of glycerol [24] and alanine are increased and arginine concentration is decreased [25], indicating more general metabolic changes [26].

To what extent can these metabolic changes be related to metabolic activity of the parasite? *Plasmodium* cannot synthesize its own amino acids and is dependent on the host's haemoglobin for protein biosynthesis and on the host's glucose for its free energy production. As such, the metabolic activity of the parasite has a direct effect on the host, but, in addition, the parasites cause indirect damage by lysis of red

blood cells and sequestration of parasitized red blood cells in the vasculature leading to reduced blood perfusion [27].

Although the pathophysiology used to be attributed to two main syndromes, cerebral malaria and severe anaemia malaria, it has become clear that severe malaria is complicated and involves several syndromes [27–29]. Ultimately, the goal is to delineate the individual contributions of these syndromes to the pathophysiology of malaria. Such an analysis would point at the best points of intervention to relieve the burden of the disease. In an attempt to estimate the direct contribution of *Plasmodium* activity we set out to analyse its amino acid and carbohydrate metabolism.

***Plasmodium* biomass production from haemoglobin**

The genome of *P. falciparum* was sequenced in 2002 and several genome-scale metabolic maps have been reconstructed [30]. *Plasmodium* is severely limited in its biosynthetic reactions and is largely dependent on the host's supply of amino acids for protein synthesis, for which the parasite degrades almost all haemoglobin in the red blood cell during its 48-h growth cycle. The specific condition of *Plasmodium* growing in the red blood cell and using the available haemoglobin for protein synthesis, leads to an elegant set of constraints that can be used in a genome-scale analysis. We used an existing genome-scale model [18] with a set rate of haemoglobin consumption (assuming a 75% consumption of total haemoglobin in 48-h [31]) and optimized for biomass production, only allowing uptake of the amino acids isoleucine and arginine. Isoleucine is not present in haemoglobin and must be taken up from the blood. *P. falciparum* is known to convert arginine to ornithine [32], leading to hypoargininaemia [25]. Under these conditions, a specific growth rate of 0.049 h^{-1} was calculated for *P. falciparum*, which is close to the expected value of 0.058 h^{-1} (calculated on the basis of 16 merozoites formed in 48-h). A glucose consumption rate of $1.6 \text{ mmol}\cdot\text{h}^{-1}\cdot\text{gDW}^{-1}$ was obtained which is somewhat lower than the experimentally measured value of $2.1 \text{ mmol}\cdot\text{h}^{-1}\cdot\text{gDW}^{-1}$ [33].

The complete set of reactions for the genome-scale network is shown in Figure 2(A), where the red lines indicate the fluxes through the reactions. In Figure 2(B), a subset of reactions involved in amino acid metabolism is shown. These reactions fall in three classes: (1) degradation of haemoglobin, (2) the synthesis of biomass and (3) export and inter-conversion of amino acids. The export fluxes for the amino acids are indicated in Figure 2(C).

The relative amino acid production rates compare well with rates observed in *P. falciparum* culture [32]. Note that the arginine to ornithine conversion was part of the objective and is therefore not a validation for the model. One cannot immediately compare these amino acid product formation rates to changes in blood amino acid concentrations in malaria patients since these concentrations are also dependent on the consumption rates in the body. However, the high capacity of the network to consume arginine and the high alanine

production rates are in good agreement with the observed hypoargininaemia and high alanine blood concentrations in malaria patients. Interestingly, a high alanine blood concentration in malaria patients is usually attributed to a reduced alanine to glucose conversion in the liver [26], but our network analysis shows that a high alanine production by *Plasmodium* could contribute to this symptom. For an accurate prediction of blood concentration changes of amino acids a full body implementation of a model is required. However, high production rates (e.g. alanine) or consumption rates (e.g. arginine) due to *Plasmodium* activity can point to potential metabolic biomarkers for malaria progression. In addition, one can simulate the effect of a drug by setting a constraint on a metabolic flux in the network. If such an inhibition is complete then the network analysis can be accurate and the effect is dependent on whether the inhibited step is essential or not. If the inhibition is not complete, which is the likely scenario, it is better to analyse the effect in a kinetic model.

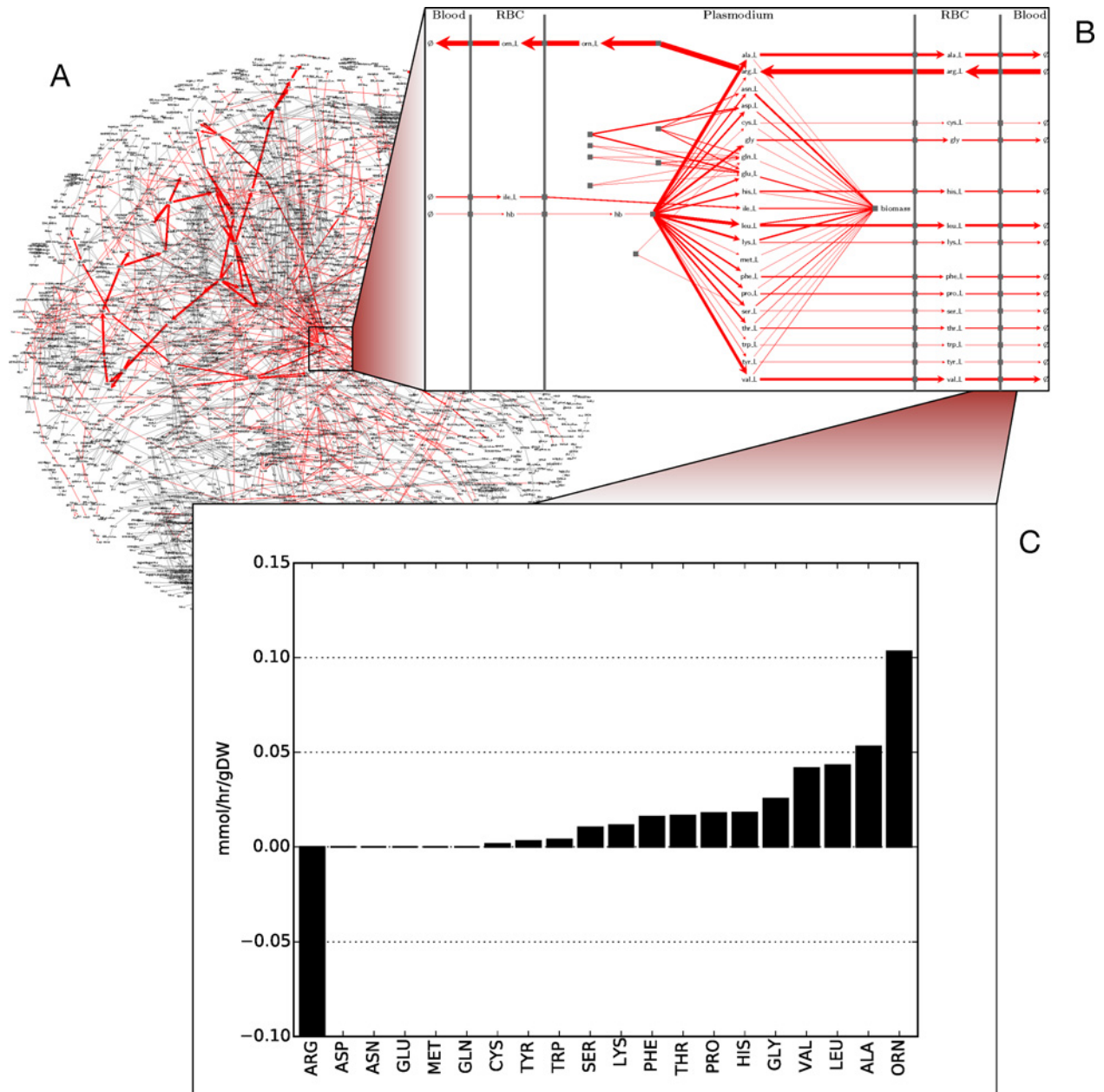
Kinetic modelling of *Plasmodium* glucose metabolism in malaria patients

Currently no detailed kinetic models exist for genome-scale networks, mostly due to limited kinetic information. Kinetic models do exist for smaller systems, such as central carbon metabolism and in a more coarse-grained form for organ and organism level metabolism. To analyse the effect of increased glycolytic activity of *Plasmodium* infected red blood cells in malaria patients, we merged three existing kinetic models: a detailed kinetic model for glycolysis of *P. falciparum* [34], a detailed kinetic model for central carbon metabolism of the red blood cell [35–37] and a coarse grained kinetic model for whole-body glucose metabolism [38]. The models were obtained from the JWS Online [39] and Biomodels [40] model repositories, corrected for units and shared-variable-names inconsistencies and integrated. No adaptations were made to the *P. falciparum* and red blood cell model and for the whole-body model only the fixed metabolites alanine and non-esterified fatty acids were changed. A detailed description of the merged model will be published elsewhere (K. Green, D.C. Palm, F. du Toit and D.D. van Niekerk and Snoep, manuscript in preparation).

Figure 3(A) shows a schema for the combined model with the compartmentalized whole-body model and the added *Plasmodium* infected red blood model. A simulation of the effect of increased parasitaemia on blood glucose concentration is given in Figure 3(B), together with patient data (and rat model data) obtained from the literature. The patient data show a lot of scatter, which is indicative of large intermittent variance (no longitudinal data for a patient followed over time was available). Most papers make reference to hypoglycaemia in severe malaria patients, but then do not report both parasitaemia and blood glucose levels. The model prediction does simulate the reference state and the few patient data with hypoglycaemia, for which data were

Figure 2 | *P. falciparum* genome-scale network analysis

The steady state solution space for the genome-scale metabolic network for *P. falciparum* [18] with a set influx rate of $0.83 \mu\text{mol haemoglobin}\cdot\text{h}^{-1}\cdot\text{gDW}^{-1}$ was optimized for biomass formation and ornithine production. Fluxes are indicated in red on the complete network structure in (A). A subset of reactions for amino acid metabolism, indicating the haemoglobin degradation, biomass formation and the amino acid inter-conversion and export are indicated in (B). The export fluxes of the different amino acids are indicated in (C).



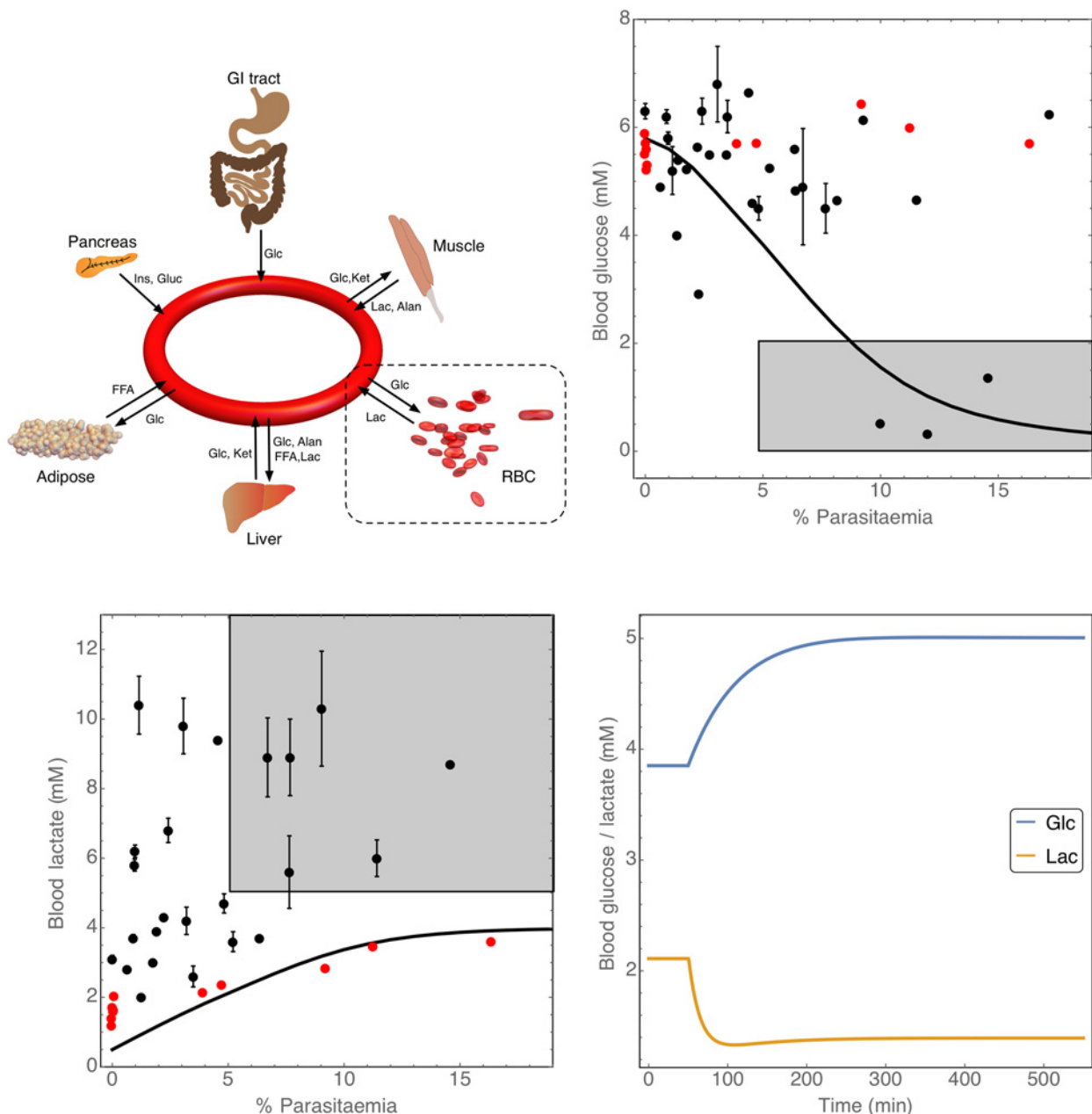
available, quite well. Similarly, the lactate data for malaria patients shows a lot of scatter (Figure 3C) and much more consistent data for the longitudinal rat study was obtained. The model prediction of lactate is low for the reference state but seems to follow the trend of lactate increase (and the rat data) reasonably well. In Figure 3(D), the results of an inhibition of the glucose transporter (to 50% of non-inhibited lactate flux) in *P. falciparum* are simulated.

Discussion and conclusion

To understand the pathophysiology of complex diseases, whole-body mathematical models can be strong tools to integrate and analyse the numerous effects that lead to the disease state. Specifically, when personal parameters can be added to such a model, they can be instrumental in choosing a correct treatment. Currently only very few molecularly informed models exist for the whole-body level

Figure 3 | Modelling glucose and lactate metabolism in malaria patients

(A) kinetic model for whole-body glucose metabolism [38] was merged with two detailed kinetic models for glucose metabolism in *P. falciparum* [34] and the red blood cell [35–37] (A). The effect of increasing levels of parasitaemia on steady state blood glucose and lactate concentrations was analysed and shown in (B and C) respectively, together with concentrations measured in malaria patients (black symbols, calculated from [41–52]) and rat data (red symbols, calculated from [53]). The shaded boxes indicate the severe malaria (> 5% parasitaemia) and hypoglycaemia (<2 mM glucose, B) and lactic acidosis (>5 mM lactate, C) areas. (D) The effect of inhibition of the glucose transport step (starting at $t = 50$ min, resulting in 50% reduction in glycolytic flux in the parasite) on blood glucose and lactate concentrations in a malaria patient (5% parasitaemia) was simulated.



that are detailed enough to be useful in medical applications (e.g. <http://www.entelos.com>). Specifically for the simulation of pharmacological drug effects on the disease state there is a big challenge in terms of modelling at the correct

level of detail. To simulate the drug effect at the reaction step, a high level of detail is needed at the drug target level, which cannot be sustained up to the whole-body level.

In the present paper, we illustrated how a hierarchical model, with a high level of detail at the drug target site and more coarse-grained for the whole-body level, can be used to simulate the effect of a pharmaceutical drug on blood glucose concentration. Clearly, the model is still in a very rudimentary stage; we only simulate the direct metabolic effect of parasite activity and have ignored any effects on blood perfusion or reduced red blood cell contents due to cell lysis or any of the large number of secondary effects caused by the malaria parasites. In addition, we simulated the drug effect by simply assuming a constant inhibitor concentration in the blood, a much more realistic simulation would have to include a full PK/PD (pharmacokinetics/pharmacodynamics) model to evaluate the drug efficacy [5,54].

The aim to mechanistically simulate drug effects (inhibiting a specific target reaction) at the whole-body level (physiological disease state) is very ambitious. However, we feel the time is right for this. Some large-scale projects have existed for quite some time and produced detailed kinetic models at the organ level that can be extended to the whole-body level (e.g. the physiome project, <http://physiomeproject.org> [55]; the virtual liver, <http://www.virtual-liver.de> [56]). In addition, a much stronger adherence to modelling standards, such as description in standard formats [systems biology markup language (SBML) and CellML]) and storage in curated model databases (JWS Online, Biomodels and CellML), makes model reuse much easier. For our initial model construction, we merged three existing models and this enabled us to make some preliminary simulations at different hierarchical levels. Of course, one cannot simply merge all existing models; they must be compatible and constructed for similar physiological conditions [57]. After merging of existing models, one can start a number of iterative cycles to improve the integral model and adapt it to specific disease states.

With the present concept paper, we hope to have illustrated the approach we follow towards whole-body modelling of blood glucose and lactate metabolism in malaria patients. Clearly, much work is still needed and especially at the whole-body level the model needs to be validated more thoroughly. For this, we will first work in a rat model system for which it is much easier to obtain longitudinal data. Although the specific model for malaria patients is still very preliminary, the suggested approach of a hierarchical model structure with a high level of detail at the drug target level and more coarse-grained models at the whole-body physiological level, is generic and could be applied to other complex metabolic diseases such as type II diabetes.

Acknowledgements

We thank Gunnar Cedersund and Brett Olivier, who were involved in the initial stages of the construction of the dynamic and structural model respectively and Barbara Bakker for discussing potential modelling strategies at the whole-body disease state.

Funding

This work was supported by the National Research Foundation, South Africa [grant numbers SARCHI 82813 (to J.L.S.) and TTK14051967526 (to D.D.v.N.)].

References

- Xie, L., Xie, L., Kinnings, S. and Bourne, P. (2012) Novel computational approaches to polypharmacology as a means to define responses to individual drugs. *Annu. Rev. Pharmacol. Toxicol.* **52**, 361–379 [CrossRef PubMed](#)
- Fryburg, D., Song, D., Laifenfeld, D. and de Graaf, D. (2014) Systems diagnostics: anticipating the next generation of diagnostic tests based on mechanistic insight into disease. *Drug Discov. Today* **19**, 108–112 [CrossRef PubMed](#)
- Kell, D.B. and Goodacre, R. (2014) Metabolomics and systems pharmacology: why and how to model the human metabolic network for drug discovery. *Drug Discov. Today* **19**, 171–182 [CrossRef PubMed](#)
- Hopkins, A. (2008) Network pharmacology: the next paradigm in drug discovery. *Nat. Chem. Biol.* **4**, 682–690 [CrossRef PubMed](#)
- Zhao, S. and Iyengar, R. (2012) Systems pharmacology: network analysis to identify multiscale mechanisms of drug action. *Annu. Rev. Pharmacol. Toxicol.* **52**, 505–521 [CrossRef PubMed](#)
- Bai, J. and Abernethy, D. (2013) Systems pharmacology to predict drug toxicity: integration across levels of biological organization. *Annu. Rev. Pharmacol. Toxicol.* **53**, 451–473 [CrossRef PubMed](#)
- Butcher, E., Berg, E. and Kunkel, E. (2004) Systems biology in drug discovery. *Nat. Biotechnol.* **22**, 1253–1259 [CrossRef PubMed](#)
- Kell, D. (2006) Systems biology, metabolic modelling and metabolomics in drug discovery and development. *Drug Discov. Today* **11**, 1085–1092 [CrossRef PubMed](#)
- Edwards, J. and Palsson, B. (2000) The *Escherichia coli* mg1655 *in silico* metabolic genotype: its definition, characteristics, and capabilities. *Proc. Natl. Acad. Sci. U.S.A.* **97**, 5528–5533 [CrossRef PubMed](#)
- Forster, J., Famili, I., Fu, P., Palsson, B. and Nielsen, J. (2003) Genome-scale reconstruction of the *Saccharomyces cerevisiae* metabolic network. *Genome Res.* **13**, 244–253 [CrossRef PubMed](#)
- Duarte, N.C., Becker, S.A., Jamshidi, N., Thiele, I., Mo, M.L., Vo, T.D., Srivas, R. and Palsson, B.O. (2007) Global reconstruction of the human metabolic network based on genomic and bibliomic data. *Proc. Natl. Acad. Sci. U.S.A.* **104**, 1777–1782 [CrossRef PubMed](#)
- Thiele, I., Swainston, N., Fleming, R.M., Hoppe, A., Sahoo, S., Aurich, M.K., Haraldsdottir, H., Mo, M.L., Rolfsson, O., Stobbe, M.D. et al. (2013) A community-driven global reconstruction of human metabolism. *Nat. Biotechnol.* **5**, 419–425 [CrossRef](#)
- Fleischmann, R.D., Adams, M.D., White, O., Clayton, R.A., Kirkness, E.F., Kerlavage, A.R., Bult, C.J., Tomb, J.F., Dougherty, B.A. and Merrick, J.M. (1995) Whole-genome random sequencing and assembly of *Haemophilus influenzae* Rd. *Science* **269**, 496–512 [CrossRef PubMed](#)
- Jamshidi, N. and Palsson, B. (2007) Investigating the metabolic capabilities of *Mycobacterium tuberculosis* h37rv using the *in silico* strain inj661 and proposing alternative drug targets. *BMC Syst. Biol.* **1**, 26 [CrossRef PubMed](#)
- Yeh, I., Hanekamp, T., Tsoka, S., Karp, P. and Altman, R. (2004) Computational analysis of *Plasmodium falciparum* metabolism: organizing genomic information to facilitate drug discovery. *Genome Res.* **14**, 917–924 [CrossRef PubMed](#)
- Fatumo, S., Plaimas, K., Mallm, J.P., Schramm, G., Adebisi, E., Oswald, M., Eils, R. and Konig, R. (2009) Estimating novel potential drug targets of *Plasmodium falciparum* by analysing the metabolic network of knock-out strains *in silico*. *Infect. Genet. Evol.* **9**, 351–358 [CrossRef PubMed](#)
- Huthmacher, C., Hoppe, A., Bulik, S. and Holzhutter, H.G. (2010) Antimalarial drug targets in *Plasmodium falciparum* predicted by stage-specific metabolic network analysis. *BMC Syst. Biol.* **4**, 120 [CrossRef PubMed](#)
- Plata, G., Hsiao, T.L., Olszewski, K., Llinas, M. and Vitkup, D. (2010) Reconstruction and fluxbalance analysis of the *Plasmodium falciparum* metabolic network. *Mol. Syst. Biol.* **6**, 408 [CrossRef PubMed](#)
- Fell, D. and Small, J. (1986) Fat synthesis in adipose tissue. An examination of stoichiometric constraints. *Biochem. J.* **238**, 781–786 [CrossRef PubMed](#)

- 20 Orth, J., Thiele, I. and Palsson, B. (2010) What is flux balance analysis? *Nat. Biotechnol.* **28**, 245–248 [CrossRef PubMed](#)
- 21 McCloskey, D., Palsson, B. and Feist, A. (2013) Basic and applied uses of genome-scale metabolic network reconstructions of *Escherichia coli*. *Mol. Syst. Biol.* **9**, 661 [CrossRef PubMed](#)
- 22 Teusink, B., Wiersma, A., Molenaar, D., Francke, C., de Vos, W.M., Siezen, R.J. and Smid, E.J. (2006) Analysis of growth of *Lactobacillus plantarum* wcf51 on a complex medium using a genome-scale metabolic model. *J. Biol. Chem.* **281**, 40041–40048 [CrossRef PubMed](#)
- 23 Krishna, S., Waller, D.W., ter Kuile, F., Kwiatkowski, D., Crawley, J., Craddock, C.F., Nosten, F., Chapman, D., Brewster, D., Holloway, P.A. and White, N.J. (1994) Lactic acidosis and hypoglycaemia in children with severe malaria: pathophysiological and prognostic significance. *Trans. R. Soc. Trop. Med. Hyg.* **88**, 67–73 [CrossRef PubMed](#)
- 24 Pukrittayakamee, S., White, N.J., Davis, T.M., Supanaranond, W., Crawley, J., Nagachinta, B. and Williamson, D.H. (1994) Glycerol metabolism in severe falciparum malaria. *Metabolism* **43**, 887–892 [CrossRef PubMed](#)
- 25 Lopansri, B.K., Anstey, N.M., Weinberg, J.B., Stoddard, G.J., Hobbs, M.R., Levesque, M.C., Mwaikambo, E.D. and Granger, D.L. (2003) Low plasma arginine concentrations in children with cerebral malaria and decreased nitric oxide production. *Lancet* **361**, 676–678 [CrossRef PubMed](#)
- 26 Planche, T., Dzeing, A., Ngou-Milama, E., Kombila, M. and Stacpoole, P. (2005) Metabolic complications of severe malaria. *Curr. Top. Microbiol. Immunol.* **295**, 105–136 [PubMed](#)
- 27 Mackintosh, C., Beeson, J. and Marsh, K. (2004) Clinical features and pathogenesis of severe malaria. *Trends Parasitol* **20**, 597–603 [CrossRef PubMed](#)
- 28 Clark, I. and Cowden, W. (2003) The pathophysiology of falciparum malaria. *Pharmacol. Ther.* **99**, 221–260 [CrossRef PubMed](#)
- 29 Maitland, K. and Marsh, M. (2004) Pathophysiology of severe malaria in children. *Acta Trop.* **90**, 131–140 [CrossRef PubMed](#)
- 30 Tymoshenko, S., Oppenheim, R., Soldati-Favre, D. and Hatzimanikatis, V. (2013) Functional genomics of *Plasmodium falciparum* using metabolic modelling and analysis. *Brief Funct. Genomics* **12**, 316–327 [CrossRef PubMed](#)
- 31 Esposito, A., Tiffert, T., Mauritz, J.M., Schlachter, S., Bannister, L.H., Kaminski, C.F. and Lew, V.L. (2008) FRET imaging of hemoglobin concentration in *Plasmodium falciparum*-infected red cells. *PLoS One* **3**, e3780 [CrossRef PubMed](#)
- 32 Olszewski, K.L., Morrisey, J.M., Wilinski, D., Burns, J.M., Vaidya, A.B., Rabinowitz, J.D. and Llinas, M. (2009) Host-parasite interactions revealed by *Plasmodium falciparum* metabolomics. *Cell Host Microbe* **5**, 191–199 [CrossRef PubMed](#)
- 33 Jensen, M.D., Conley, M. and Helstowski, L.D. (1983) Culture of *Plasmodium falciparum*: the role of pH, glucose, and lactate. *J. Parasitol.* **69**, 1060–1067 [CrossRef PubMed](#)
- 34 Penkler, G., du Toit, F., Adams, W., Rautenbach, M., Palm, D.C., van Niekerk, D.D. and Snoep, J.L. (2015) Construction and validation of a detailed kinetic model of glycolysis in *Plasmodium falciparum*. *FEBS J.* **282**, 1481–1511 [CrossRef PubMed](#)
- 35 Mulquiney, P.J., Bubb, W.A. and Kuchel, P.W. (1999) Model of 2,3-bisphosphoglycerate metabolism in the human erythrocyte based on detailed enzyme kinetic equations: *in vivo* kinetic characterization of 2,3-bisphosphoglycerate synthase/phosphatase using ¹³C and ³¹P NMR. *Biochem. J.* **342**, 567–580 [CrossRef PubMed](#)
- 36 Mulquiney, P.J. and Kuchel, P.W. (1999) Model of 2,3-bisphosphoglycerate metabolism in the human erythrocyte based on detailed enzyme kinetic equations: computer simulation and metabolic control analysis. *Biochem. J.* **342**, 597–604 [CrossRef PubMed](#)
- 37 Mulquiney, P.J. and Kuchel, P.W. (1999) Model of 2,3-bisphosphoglycerate metabolism in the human erythrocyte based on detailed enzyme kinetic equations: equations and parameter refinement. *Biochem. J.* **342**, 581–596 [CrossRef PubMed](#)
- 38 Xu, K., Morgan, K.T., Gehris, A.T., Elston, T. and Gomez, S. (2011) A whole-body model for glycogen regulation reveals a critical role for substrate cycling in maintaining blood glucose homeostasis. *PLoS Comput. Biol.* **7**, e1002272 [CrossRef PubMed](#)
- 39 Olivier, B. and Snoep, J. (2004) Web-based kinetic modelling using JWS online. *Bioinformatics* **20**, 2143–2144 [CrossRef PubMed](#)
- 40 Le Novere, N., Bornstein, B., Broicher, A., Courtot, M., Donizelli, M., Dhururi, H., Li, L., Sauro, H., Schilstra, M., Shapiro, B. et al. (2006) Biomodels database: a free, centralized database of curated, published, quantitative kinetic models of biochemical and cellular systems. *Nucleic Acids Res.* **34**, D689–D691 [CrossRef PubMed](#)
- 41 White, N.J., Marsh, K., Turner, R.C., Miller, K.D., Berry, C.D., Williamson, D.H. and Brown, J. (1987) Hypoglycaemia in African children with severe malaria. *Lancet* **329**, 708–711 [CrossRef](#)
- 42 Taylor, T.E., Molyneux, M.E., Wirima, J.J., Fletcher, K.A. and Morris, K. (1988) Blood glucose levels in Malawian children before and during the administration of intravenous quinine for severe falciparum malaria. *N. Engl. J. Med.* **319**, 1040–1047 [CrossRef PubMed](#)
- 43 Davis, T.M., Looareesuwan, S., Pukrittayakamee, S., Levy, J.C., Nagachinta, B. and White, N.J. (1993) Glucose turnover in severe falciparum malaria. *Metabolism* **42**, 334–340 [CrossRef PubMed](#)
- 44 Taylor, T.E., Borgstein, A. and Molyneux, M.E. (1993) Acid-base status in paediatric *Plasmodium falciparum* malaria. *Q. J. Med.* **86**, 99–109 [PubMed](#)
- 45 Waller, D., Krishna, S., Crawley, J., Miller, K., Nosten, F., Chapman, D., ter Kuile, F.O., Craddock, C., Berry, C., Holloway, P.A. et al. (1995) Clinical features and outcome of severe malaria in Gambian children. *Clin. Infect. Dis.* **21**, 577–587 [CrossRef PubMed](#)
- 46 Allen, S.J., O'Donnell, A., Alexander, N.D. and Clegg, J.B. (1996) Severe malaria in children in Papua New Guinea. *QJM* **89**, 779–788 [CrossRef PubMed](#)
- 47 Day, N.P., Phu, N.H., Mai, N.T., Chau, T.T., Loc, P.P., Chuong, L.V., Sinh, D.X., Holloway, P., Hien, T.T. and White, N.J. (2000) The pathophysiology and prognostic significance of acidosis in severe adult malaria. *Crit. Care Med.* **28**, 1833–1840 [CrossRef PubMed](#)
- 48 Planche, T., Agbenyega, T., Bedu-Addo, G., Ansong, D., Owusu-Ofori, A., Micah, F., Anakwa, C., Asafo-Agyei, E., Hutson, A., Stacpoole, P.W. and Krishna, S. (2003) A prospective comparison of malaria with other severe diseases in African children: prognosis and optimization of management. *Clin. Infect. Dis.* **37**, 890–897 [CrossRef PubMed](#)
- 49 Dzeing-Ella, A., Nze Obiang, P.C., Tchoua, R., Planche, T., Mboza, B., Borrmann, S., Muller-Roemer, U., Jarvis, J., Kendjo, E., Ngou-Milama, E. et al. (2005) Severe falciparum malaria in Gabonese children: clinical and laboratory features. *Malar. J.* **4**, 1 [CrossRef PubMed](#)
- 50 Jarvis, J.N., Planche, T., Bicanic, T., Dzeing-Ella, A., Kombila, M., Issifou, S., Dissanjany, F.A., Kremsner, P.G. and Krishna, S. (2006) Lactic acidosis in Gabonese children with severe malaria is unrelated to dehydration. *Clin. Infect. Dis.* **42**, 1719–1725 [CrossRef PubMed](#)
- 51 Issifou, S., Kendjo, E., Missinou, M.A., Matsigui, P.B., Dzeing-Ella, A., Dissanjany, F.A., Kombila, M., Krishna, S. and Kremsner, P.G. (2007) Differences in presentation of severe malaria in urban and rural Gabon. *A. J. Trop. Med. Hyg.* **77**, 1015–1019
- 52 Seydel, K.B., Kampondeni, S.D., Valim, C., Potchen, M.J., Milner, D.A., Muwalo, F.W., Birbeck, G.L., Bradley, W.G., Fox, L.L., Glover, S.J. et al. (2015) Brain swelling and death in children with cerebral malaria. *N. Engl. J. Med.* **372**, 1126–1137 [CrossRef PubMed](#)
- 53 Holloway, P.A., Knox, K., Bajaj, N., Chapman, D., White, N.J., O'Brien, R., Stacpoole, P.W. and Krishna, S. (1995) *Plasmodium berghei* infection: dichloroacetate improves survival in rats with lactic acidosis. *Exp. Parasitol.* **80**, 624–632 [CrossRef PubMed](#)
- 54 van der Graaf, P. and Benson, B. (2011) Systems pharmacology: bridging systems biology and pharmacokinetics-pharmacodynamics (PKPD) in drug discovery and development. *Pharm. Res.* **28**, 1460–1464 [CrossRef PubMed](#)
- 55 Hunter, P., Crampin, E. and Nielsen, P. (2008) Bioinformatics, multiscale modeling and the IUPS physiome project. *Brief. Bioinform.* **9**, 333–343 [CrossRef PubMed](#)
- 56 Holzthutter, H., Drasdo, D., Preusser, T., Lippert, J. and Henney, A. (2012) The virtual liver: a multidisciplinary, multilevel challenge for systems biology. *Wiley Interdiscip. Rev. Syst. Biol. Med.* **4**, 221–235 [CrossRef PubMed](#)
- 57 Snoep, J.L., Bruggeman, F., Olivier, B.G. and Westerhoff, H.V. (2006) Towards building the silicon cell: a modular approach. *Biosystems* **83**, 207–216 [CrossRef PubMed](#)

Received 23 June 2015
doi:10.1042/BST20150145

Bibliography

- [1] Gerald Penkler, Francois Du Toit, Waldo Adams, Marina Rautenbach, Daniel C. Palm, David D. Van Niekerk, and Jacky L. Snoep. Construction and validation of a detailed kinetic model of glycolysis in *Plasmodium falciparum*. *FEBS Journal*, 282(8):1481–1511, 2015.
- [2] F. Du Toit. Modeling glycolysis in *Plasmodium*-infected erythrocytes. (March):1–202, 2015.
- [3] Ke Xu, Kevin T. Morgan, Abby Todd Gehris, Timothy C. Elston, and Shawn M. Gomez. A whole-body model for glycogen regulation reveals a critical role for substrate cycling in maintaining blood glucose homeostasis. *PLoS Computational Biology*, 7(12):1–13, 2011.
- [4] Robert W Snow. Sixty years trying to define the malaria burden in Africa: have we made any progress? *BMC medicine*, 12(1):227, 2014.
- [5] WHO | Fact Sheet: World Malaria Report 2015. *WHO*, 2016.
- [6] WHO | Overview of malaria treatment. <http://www.who.int/malaria/areas/treatment/overview/en/>, 2016.
- [7] R Price, M van Vugt, L Phaipun, C Luxemburger, J Simpson, R McGready, F ter Kuile, a Kham, T Chongsuphajaisiddhi, N J White, and F Nosten. Adverse effects in patients with acute *falciparum* malaria treated with artemisinin derivatives. *The American journal of tropical medicine and hygiene*, 60(4):547–555, 1999.
- [8] Robert W Snow. Global malaria eradication and the importance of *Plasmodium falciparum* epidemiology in Africa. *BMC medicine*, 13(1):23, 2015.
- [9] P J Mulquiney, W A Bubb, and P W Kuchel. Model of 2,3-bisphosphoglycerate metabolism in the human erythrocyte based on detailed enzyme kinetic equations: in vivo kinetic characterization of 2,3-bisphosphoglycerate synthase/phosphatase using ¹³C and ³¹P NMR. *The Biochemical journal*, 342 Pt 3:567–580, 1999.
- [10] Peter J Mulquiney and Philip W Kuchel. Model of 2,3-bisphosphoglycerate metabolism in the human erythrocyte based on detailed enzyme kinetic equations: equations and parameter refinement. *The Biochemical journal*, 342 Pt 3(1999):581–596, 1999.

- [11] Peter J Mulquiney and Philip W Kuchel. Model of 2,3-bisphosphoglycerate metabolism in the human erythrocyte based on detailed enzyme kinetic equations: computer simulation and Metabolic Control Analysis. *The Biochemical journal*, 342 Pt 3:597–604, 1999.
- [12] Yau H. and Stacpoole P. The Pathophysiology of Hypoglycemia and Lactic Acidosis in Malaria. *Encyclopedia of Malaria*, 2014.
- [13] S. Krishna, D. W. Wailer, F. Ter Kuile, D. Kwiatkowski, J. Crawley, C. F C Craddock, F. Nosten, D. Chapman, D. Brewster, P. A. Holloway, N. J. White, D W Waller, F. Ter Kuile, D. Kwiatkowski, J. Crawley, C. F C Craddock, F. Nosten, D. Chapman, D. Brewster, P. A. Holloway, and N. J. White. Lactic acidosis and hypoglycaemia pathophysiological and prognostic in children with severe malaria: pathophysiological and prognostic significance. *Transactions of the Royal Society of Tropical Medicine and Hygiene*, 88(1):67–73, 1994.
- [14] Claire L. MacKintosh, James G. Beeson, and Kevin Marsh. Clinical features and pathogenesis of severe malaria. *Trends in Parasitology*, 20(12):597–603, 2004.
- [15] Judith G. Voet Donald Voet. *Biochemistry: Biomolecules, Mechanisms of Enzyme Action, and Metabolism*. Wiley, 3rd edition.
- [16] Jeremy M Berg, John L Tymoczko, and Lubert Stryer. Each Organ Has a Unique Metabolic Profile. chapter 30.2. W H Freeman, 5th edition, 2002.
- [17] Maciej Swat, Szymon M Kiełbasa, Sebastian Polak, Brett Olivier, Frank J Bruggeman, Mark Quinton Tulloch, Jacky L Snoep, Arthur J Verhoeven, and Hans V Westerhoff. What it takes to understand and cure a living system: computational systems biology and a systems biology-driven pharmacokinetics-pharmacodynamics platform. *Interface focus*, 1(1):16–23, 2011.
- [18] Peter J. Hunter, Edmund J. Crampin, and Poul M F Nielsen. Bioinformatics, multiscale modeling and the IUPS Physiome Project. *Briefings in Bioinformatics*, 9(4):333–343, 2008.
- [19] E Zeynep Erson and M C Cenk. A Software Framework for Multiscale and Multilevel Physiological Model Integration and Simulation. In *2008 30th Annual International Conference of the IEEE Engineering in Medicine and Biology Society*, pages 5449—5453, 2008.
- [20] Aarash Bordbar, Adam M Feist, Renata Usaite-Black, Joseph Woodcock, Bernhard O Palsson, and Iman Famili. A multi-tissue type genome-scale metabolic network for analysis of whole-body systems physiology. *BMC systems biology*, 5(1):180, 2011.
- [21] Woochang Hwang, Yongdeuk Hwang, Sunjae Lee, and Doheon Lee. Rule-based multi-scale simulation for drug effect pathway analysis. *BMC medical informatics and decision making*, 13(Suppl 1):S4, 2013.

- [22] Markus Krauss, Stephan Schaller, Steffen Borchers, Rolf Findeisen, Jörg Lipfert, and Lars Kuepfer. Integrating Cellular Metabolism into a Multiscale Whole-Body Model. *PLoS Computational Biology*, 8(10), 2012.
- [23] John H. Gennari, Maxwell L. Neal, Michal Galdzicki, and Daniel L. Cook. Multiple ontologies in action: Composite annotations for biosimulation models. *Journal of Biomedical Informatics*, 44(1):146–154, 2011.
- [24] Falko Krause, Jannis Uhlendorf, Timo Lubitz, Marvin Schulz, Edda Klipp, and Wolfram Liebermeister. Annotation and merging of SBML models with semanticSBML. *Bioinformatics*, 26(3):421–422, 2009.
- [25] M. Ginkel, A. Kremling, T. Nutsch, R. Rehner, and E. D. Gilles. Modular modeling of cellular systems with ProMoT/Divi. *Bioinformatics*, 19(9):1169–1176, 2003.
- [26] Tom Bulatewicz, J. Cuny, and M. Warman. The Potential Coupling Interface: Metadata for Model Coupling. *Proceedings of the 2004 Winter Simulation Conference, 2004.*, 1:175–182, 2004.
- [27] Physiome Project: The Virtual Physiological Human. <http://physiomeproject.org/about/the-virtual-physiological-human>.
- [28] SM Rapoport, TA; Heinrich, R; Rapaport. The Regulatory Principles of Glycolysis in Erythrocytes in vivo and in vitro. *Biochemical Journal*, 154:449–469, 1976.
- [29] Ronny Schuster, Hermann Georg Holzhütter, and Gisela Jacobasch. Interrelations between glycolysis and the hexose monophosphate shunt in erythrocytes as studied on the basis of a mathematical model. *BioSystems*, 22(1):19–36, 1988.
- [30] Ayako Kinoshita. Simulation of Human Erythrocyte Metabolism. In *E-Cell System: Basic Concepts and Applications*, chapter 3, pages 89–104. Springer New York, 2013.
- [31] Yoichi Nakayama, Ayako Kinoshita, and Masaru Tomita. Dynamic simulation of red blood cell metabolism and its application to the analysis of a pathological condition. *Theoretical biology & medical modelling*, 2:18, 2005.
- [32] A Friedman and E M Lungu. Can malaria parasite pathogenesis be prevented by treatment with tumor necrosis factor-alpha? *Math Biosci Eng*, 10(3):609–624, 2013.
- [33] C Chiyaka, W Garira, and S Dube. Using Mathematics to Understand Malaria Infection During Erythrocytic Stages. 5:1–11, 2010.
- [34] Monika Mehta, Haripalsingh M. Sonawat, and Shobhona Sharma. Malaria parasite-infected erythrocytes inhibit glucose utilization in uninfected red cells. *FEBS Letters*, 579(27):6151–6158, 2005.

- [35] Monika Mehta, Haripalsingh M. Sonawat, and Shobhona Sharma. Glycolysis in *Plasmodium falciparum* results in modulation of host enzyme activities. *Journal of Vector Borne Diseases*, 43(3):95–103, 2006.
- [36] Leslie L. McKnight, Secundino Lopez, Anna Kate Shoveller, and James France. Models for the Study of Whole-Body Glucose Kinetics: A Mathematical Synthesis. *ISRN Biomathematics*, 2013:1–16, 2013.
- [37] Yin Hoon Chew, Yoke Lin Shia, Chew Tin Lee, Fadzilah Adibah Abdul Majid, Lee Suan Chua, Mohamad Roji Sarmidi, and Ramlan Abdul Aziz. Modeling of glucose regulation and insulin-signaling pathways. *Molecular and Cellular Endocrinology*, 303(1):13–24, 2009.
- [38] Jaeyeon Kim, Gerald M. Saidel, and Marco E. Cabrera. Multi-scale computational model of fuel homeostasis during exercise: Effect of hormonal control. *Annals of Biomedical Engineering*, 35(1):69–90, 2006.
- [39] Chiara Dalla Man, Robert A. Rizza, and Claudio Cobelli. Meal simulation model of the glucose-insulin system. *IEEE Transactions on Biomedical Engineering*, 54(10):1740–1749, 2007.
- [40] Athena Makroglou, Jiayu Li, and Yang Kuang. Mathematical models and software tools for the glucose-insulin regulatory system and diabetes: An overview. *Applied Numerical Mathematics*, 56(3-4 SPEC. ISS.):559–573, 2006.
- [41] Matthias König, Sascha Bulik, and Hermann-Georg Holzhütter. Quantifying the Contribution of the Liver to Glucose Homeostasis: A Detailed Kinetic Model of Human Hepatic Glucose Metabolism. *PLoS Computational Biology*, 8(6):e1002577, 2012.
- [42] Hyuk Kang, Kyungreem Han, and MooYoung Choi. Mathematical model for glucose regulation in the whole-body system. *Islets*, 4(2):84–93, 2012.
- [43] V W Bolie. Coefficients of normal blood glucose regulation. *Journal of applied physiology*, 16(5):783–788, sep 1961.
- [44] R N Bergman and C Cobelli. Minimal modeling, partition analysis, and the estimation of insulin sensitivity. *Federation proceedings*, 39(1):110–5, jan 1980.
- [45] Claudio Cobelli, G. Federspil, G. Pacini, A. Salvan, and C. Scandellari. An integrated mathematical model of the dynamics of blood glucose and its hormonal control. *Mathematical Biosciences*, 58(1):27–60, 1982.
- [46] Andrea De Gaetano and Ovide Arino. Mathematical modelling of the intravenous glucose tolerance test. *Journal of Mathematical Biology*, 40(2):136–168, 2000.
- [47] Roman Hovorka, Fariba Shojaei-Moradie, Paul V Carroll, Ludovic J Chassin, Ian J Gowrie, Nicola C Jackson, Romulus S Tudor, a Margot Umpleby, and Richard H Jones. Partitioning glucose distribution/transport, disposal, and endogenous production during IVGTT. *American journal of physiology. Endocrinology and metabolism*, 282(5):E992–E1007, 2002.

- [48] Anirban Roy and Robert S Parker. Dynamic modeling of free fatty acid, glucose, and insulin: an extended "minimal model". *Diabetes Technol Ther*, 8(6):617–626, 2006.
- [49] Haiyan Wang, Jiaxu Li, and Yang Kuang. Enhanced modelling of the glucose–insulin system and its applications in insulin therapies. *Journal of Biological Dynamics*, 3(1):22–38, 2009.
- [50] Mary C. Hill, Dmitri Kavetski, Martyn Clark, Ming Ye, Mazdak Arabi, Dan Lu, Laura Foglia, and Steffen Mehl. Practical Use of Computationally Frugal Model Analysis Methods. *Groundwater*, 54(2):159–170, 2016.
- [51] A Saltelli. Sensitivity analysis for importance assessment. *Risk Analysis*, 22:579–590, 2002.
- [52] David D. van Niekerk, Gerald Penkler, Francois du Toit, and Jacky L. Snoep. Targeting glycolysis in the malaria parasite *Plasmodium Falciparum*. *FEBS Journal*, 283(4):634–646, 2016.
- [53] R Heinrich and T a Rapoport. A linear steady-state treatment of enzymatic chains. General properties, control and effector strength. *European journal of biochemistry / FEBS*, 42(1):89–95, 1974.
- [54] JA Kacser, H and and Burns. No Title. In *Symp. SOC. Exp*, pages 65–104, 1973.
- [55] Gerald Patrick Penkler. A kinetic model of glucose catabolism in *Plasmodium falciparum*. (March 2013), 2013.
- [56] Marta Cascante, Laszlo G Boros, Begoña Comin-Anduix, Pedro de Atauri, Josep J Centelles, and Paul W Lee. Metabolic control analysis in drug discovery and disease. *Nature Biotechnology*, 20(3):243–249, 2002.
- [57] Brett G. Olivier and Jacky L. Snoep. Web-based kinetic modelling using JWS Online. *Bioinformatics*, 20(13):2143–2144, 2004.
- [58] C E McLaren, G M Brittenham, and V Hasselblad. Statistical and graphical evaluation of erythrocyte volume distributions. *The American journal of physiology*, 252(4):H857–H866, apr 1987.
- [59] Hermann Georg Holzhütter. The principle of flux minimization and its application to estimate stationary fluxes in metabolic networks. *European Journal of Biochemistry*, 271(14):2905–2922, 2004.
- [60] Philip W. Potts, Jennifer R., Kuchel. Anomeric preference of fluoroglucose exchange across human red-cell membranes. ¹⁹F-nmr studies. *Biochemical Journal*, 281(3):753–759, 1992.
- [61] Edward L King and C Altman. A Schematic Method of Deriving the Rate Laws for Enzyme-Catalyzed Reactions. *Journal of Physical Chemistry*, 60(10):1375–1378, 1956.

- [62] Robert C Neuman. Organic Chemistry. In *Chapter 20: Carbohydrates*, page 12.
- [63] James S Hutchison, Roxanne E Ward, Jacques Lacroix, Paul C Hébert, Marcia A Barnes, Desmond J Bohn, Peter B Dirks, Steve Doucette, Dean Ferguson, Ronald Gottesman, Ari R Joffe, Haresh M Kirpalani, Philippe G Meyer, Kevin P Morris, David Moher, Ram N Singh, Peter W Skippen, and Hypothermia Pediatric Head Injury Trial Investigators and the Canadian Critical Care Trials Group. Hypothermia therapy after traumatic brain injury in children. *The New England journal of medicine*, 358(23):2447–56, 2008.
- [64] Henry M Staines, Stephanie Ashmore, Hannah Felgate, Jessica Moore, Trevor Powell, and J Clive Ellory. Solute transport via the new permeability pathways in *Plasmodium falciparum*-infected human red blood cells is not consistent with a simple single-channel model. *Blood*, 108(9):3187–94, nov 2006.
- [65] Eva Bianconi, Allison Piovesan, Federica Facchin, Alina Beraudi, Raffaella Casadei, Flavia Frabetti, Lorenza Vitale, Maria Chiara Pelleri, Simone Tassani, Francesco Piva, Soledad Perez-Amodio, Pierluigi Strippoli, and Silvia Canaider. An estimation of the number of cells in the human body. *Annals of Human Biology*, 40(6):463–471, nov 2013.
- [66] P. Alberts, B., Johnson, A., Lewis, J., Raff, M., Roberts, K., & Walter. Leukocyte functions and percentage breakdown. *Molecular biology of the cell. NCBI Bookshelf*, 2005.
- [67] Virtual Liver SEEK. <http://seek.virtual-liver.de/>.
- [68] Guido Freckmann, Sven Hagenlocher, Annette Baumstark, Nina Jendrike, Ralph C Gillen, Katja Rössner, and Cornelia Haug. Continuous glucose profiles in healthy subjects under everyday life conditions and after different meals. *Journal of diabetes science and technology (Online)*, 1(5):695–703, 2007.
- [69] J. L. Snoep, K. Green, J. Eicher, D. C. Palm, G. Penkler, F. du Toit, N. Walters, R. Burger, H. V. Westerhoff, and D. D. van Niekerk. Quantitative analysis of drug effects at the whole-body level: a case study for glucose metabolism in malaria patients. *Biochemical Society Transactions*, 43(6):1157–1163, 2015.
- [70] M Kasahara and Peter C Hinkle. Reconstitution and Purification of the {D}-Glucose Transporter from Human Erythrocytes. *Journal of Biological Chemistry*, 252(20):7384–7390, 1977.
- [71] David C Sogin and Peter C Hinkle. Binding of Cytochalasin B to Human Erythrocyte Glucose Transporter. 19(23):5417–5420, 1980.
- [72] Jacky L. Snoep, Frank Bruggeman, Brett G. Olivier, and Hans V. Westerhoff. Towards building the silicon cell: A modular approach. *BioSystems*, 83(2-3 SPEC. ISS.):207–216, 2006.
- [73] Project Overview | The Virtual Physiological Rat Project. <http://www.virtualrat.org/>.